Fraunhofer-Institut für Angewandte Polymerforschung

Biofunctional Polymers for Medical Applications

Kumulative Dissertation

Zur Erlangung des akademischen Grades
“doctor rerum naturalium”
(Dr. rer. nat.)
in der Wissenschaftsdisziplin Polymerchemie

eingereicht an der
Mathematisch-Naturwissenschaftlichen Fakultät
Institut für Chemie
der Universität Potsdam
von

Jo Sing Julia Tang

Potsdam, Oktober 2022

1. Gutachter/in: Prof. Dr. Alexander Boker
2. Gutachter/in: Prof. Dr. Helmut Schlaad
3. Gutachter/in: Prof. Dr. Rainer Haag

Published online on the
Publication Server of the University of Potsdam:
https://doi.org/10.25932/publishup-56363
https://nbn-resolving.org/urn:nbn:de:kobv:517-opus4-563639

Abstract

Carbohydrates are found in every living organism, where they are responsible for numerous, essential biological functions and processes. Synthetic polymers with pendant saccharides, called glycopolymers, mimic natural glycoconjugates in their special properties and functions. Employing such biomimetics furthers the understanding and controlling of biological processes. Hence, glycopolymers are valuable and interesting for applications in the medical and biological field. However, the synthesis of carbohydrate-based materials can be very challenging. In this thesis, the synthesis of biofunctional glycopolymers is presented, with the focus on aqueous-based, protecting group free and short synthesis routes to further advance in the field of glycopolymer synthesis.

A practical and versatile precursor for glycopolymers are glycosylamines. To maintain biofunctionality of the saccharides after their amination, regioselective functionalization was performed. This frequently performed synthesis was optimized for different sugars. The optimization was facilitated using a design of experiment (DoE) approach to enable a reduced number of necessary experiments and efficient procedure. Here, the utility of using DoE for optimizing the synthesis of glycosylamines is discussed.

The glycosylamines were converted to glycomonomers which were then polymerized to yield biofunctional glycopolymers. Here, the glycopolymers were aimed to be applicable as layer-by-layer (LbL) thin film coatings for drug delivery systems. To enable the LbL technique, complimentary glycopolymer electrolytes were synthesized by polymerization of the glycomonomers and subsequent modification or by post-polymerization modification. For drug delivery, liposomes were embedded into the glycopolymer coating as potential cargo carriers. The stability as well as the integrity of the glycopolymer layers and liposomes were investigated at physiological pH range.

Different glycopolymers were also synthesized to be applicable as anti-adhesion therapeutics by providing advanced architectures with multivalent presentations of saccharides, which can inhibit the binding of pathogene lectins. Here, the synthesis of glycopolymer hydrogel particles based on biocompatible poly(*N*-isopropylacrylamide) (NiPAm) was established using the free-radical precipitation polymerization technique. The influence of synthesis parameters on the sugar content in the gels and on the hydrogel morphology is discussed. The accessibility of the saccharides to model lectins and their enhanced, multivalent interaction were investigated.

At the end of this work, the synthesis strategies for the glycopolymers are generally discussed as well as their potential application in medicine.

Kurzfassung

Kohlenhydrate sind in jedem Lebewesen zu finden, wo sie für zahlreiche, essenzielle biologische Funktionen und Prozesse verantwortlich sind. Synthetische Polymere, die Saccharide tragen, werden Glykopolymere genannt und können natürliche Glykokonjugate in ihren besonderen Eigenschaften und Funktionen nachahmen. Der Einsatz solcher Biomimetika fördert das Verständnis und die Kontrolle biologischer Prozesse. Daher sind Glykopolymere besonders interessant für Anwendungen im medizinischen und biologischen Bereich. Die Synthese von Materialien auf Kohlenhydratbasis kann jedoch eine große Herausforderung darstellen. In dieser Arbeit wird die Synthese biofunktioneller Glykopolymere vorgestellt, wobei der Schwerpunkt auf wässrigen, schutzgruppenfreien und kurzen Synthesewegen liegt, um weitere Fortschritte auf dem Gebiet der Glykopolymersynthese zu erzielen.

Ein praktisches und vielseitiges Ausgangsmaterial für Glykopolymere sind Glykosylamine. Um die Biofunktionalität der Saccharide nach deren Aminierung zu erhalten, wurde eine regioselektive Funktionalisierung durchgeführt. Diese häufig durchgeführte Synthese wurde für verschiedene Zucker optimiert. Die Optimierung wurde durch die Anwendung von statistischer Versuchsplanung (*Design of Experiments*, DoE) vereinfacht, um die Anzahl der erforderlichen Experimente zu reduzieren und ein effizientes Verfahren zu ermöglichen. Hier wird der Nutzen des DoE-Ansatzes für die Optimierung der Synthese von Glykosylaminen diskutiert.

Die Glykosylamine wurden in Glykomonomere umgewandelt, die daraufhin polymerisiert wurden, um biofunktionelle Glykopolymere zu erhalten. Die Glykopolymere sollten als Layer-by-Layer (LbL)-Beschichtungen für *Drug-Delivery*-Systeme anwendbar sein. Um die LbL-Technik zu ermöglichen, wurden komplementäre Glykopolymerelektrolyte durch Polymerisation der Glykomonomere mit anschließender Modifkation oder durch Postpolymerisationsglykosylierung hergestellt. Für die Verabreichung von Arzneimitteln wurden Liposomen als potenzielle Wirkstoffcarrier in die Glykopolymerbeschichtung eingebettet. Die Stabilität sowie die Unversehrtheit der Glykopolymerschichten und Liposomen wurden im physiologischen pH-Bereich nachgewiesen.

Abschließend wurden verschiedene Glykopolymere synthetisiert, die als Anti-Adhäsions-Therapeutika anwendbar sein könnten, indem sie komplexe Architekturen mit multivalenter Präsentation von Sacchariden bereitstellen, welche die Bindung von Pathogenenlektinen hemmen können. Hier wurde die Synthese von Glykopolymer-Hydrogelpartikeln auf der Basis von biokompatiblem Poly(*N*-isopropylacrylamid) (NiPAm) mit Hilfe einer radikalischen Fällungspolymerisation etabliert. Der Einfluss der Syntheseparameter auf den Zuckergehalt in den Gelen und auf die Hydrogelmorphologie wurde diskutiert. Die Zugänglichkeit der Saccharide für Modell-Lektine und ihre verstärkte, multivalente Interaktion wurden untersucht.

Zum Abschluss dieser Arbeit werden die Synthesestrategien für die Glykopolymere sowie deren mögliche Anwendung in der Medizin allgemein diskutiert.

Table of Content

List of Abbreviations

ABCVA	4,4'-Azobis(4-cyanovaleric acid)
AFM	Atomic force microscopy
CRD	Carbohydrate recognition domain
d	Doublet
D_h	Hydrodynamic diameter
DLS	Dynamic light scattering
DMSO	Dimethyl sulfoxide
DoE	Design of experiment
E. coli	*Escherischia coli*
ECL	*Erythrina cristagalli* lectin
EGDMA	Ethylene glycol dimethacrylate
ESI-MS	Electrospray ionization mass spectrometry
EtOH	Ethanol
FRP	Free radical polymerization
Fuc	Fucose
Gal	Galactose
GalNAc	*N*-Acetylgalactosamine
GPC	Gelpermeation chromatography
HPLC	High performance liquid chromatography
Hz	Hertz
IC_{50}	Half-maximal inhibitory concentration
IR	Infrared
J	Coupling constant
K_D	Dissociation constant
Lac	Lactose
LbL	Layer-by-layer
LCST	Lower critical solution temperature
m	Multiplet
Mal	Maltose
MAm	Methacrylamide
MBA	*N*,*N*'-methylenebis(acrylamide)

Mel	Melibiose
MeOH	Methanol
MS	Mass spectrometry
NiPAm	*N*-Isopropylacrylamide
NiPMAm	*N*-Isopropylmethacrylamide
NMR	Nuclear magnetic resonance spectroscopy
PBS	Phosphate-buffered saline
PDI	Polydispersity index
PEI	Polyethyleneimine
pH	Negative common logarithm of the hydrogen ion activity
QCM-D	Quartz crystal microbalance with dissipation
rpm	Rounds per minute
s	Singlet
SEC	Size exclusion chromatography
SEM	Scanning electron microscopy
t	Triplet
TGA	Thermogravimetric analysis
THF	Tetrahydrofuran
UV	Ultraviolet light
Vis	Visible light
WGM	Whispering gallery mode
λ	Wavelength

1 Introduction

1.1 Carbohydrates

Carbohydrates are an essential class of natural compounds as well as the most abundant one on earth. They are found in all organisms in various compositions, structures, and sizes with assorted classifications (Figure 1.1).[1]

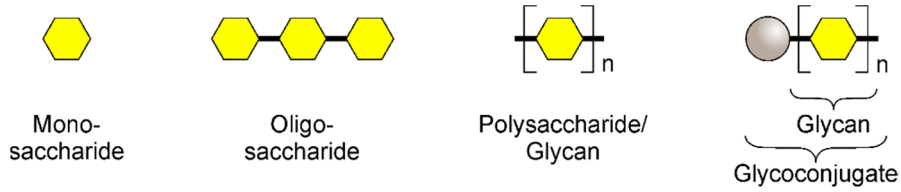

Figure 1.1. General classifications of carbohydrate compounds: monosaccharide (1 unit), oligosaccharide (3-10 units), polysaccharide/glycan (>10 units), glycoconjugate with saccharides (>3 units) covalently bound to other molecules.

The vast ubiquity and complexity of saccharides in nature indicate their tremendous significance for living beings. In the past, the function of carbohydrates was thought to be limited to energy storage and structural composition, like starch and glycogen serving as energy sources for plants or humans, as well as cellulose and chitin functioning as skeletal components for plants, fungi, or insects. In the 1960s, it was discovered that isolated plant proteins can interact with erythrocytic carbohydrates.[1–3] Such saccharide binding proteins are termed lectins and indicated that saccharides may exhibit more functions than previously assumed. After the first animal lectin was identified in the 1980s, interest in the biological role of carbohydrates and their utilization in the medical field started to rise. Over the years, the study of carbohydrates has gathered immense attention with the realization that various, fundamental biological processes are mediated by carbohydrate compounds. As the biological role of carbohydrate has been reevaluated, the term glycobiology was coined in 1988. The field of glycobiology combines the disciplines carbohydrate chemistry and biochemistry describing the structures as well as functions of carbohydrates in biological environments and holds immense relevance to this day.[4] Especially the utilization of carbohydrates in biology and medicine is of great interest since glycans take vital roles in human health and disease development. Industrial utilization of carbohydrate-based compounds is found in the fields of food, pharmaceutics, cosmetics, agricultural products, adhesives, fermentation, fuel, paper, and textile.

1.1.1 Carbohydrates and Glycobiology

In plants, animals and humans, saccharides are typically covalently bound as glycoconjugates such as glycoproteins and -lipids on cell surfaces. The glycans in vertebrates are typically composed of nine specific monosaccharides (Figure 1.2).[4]

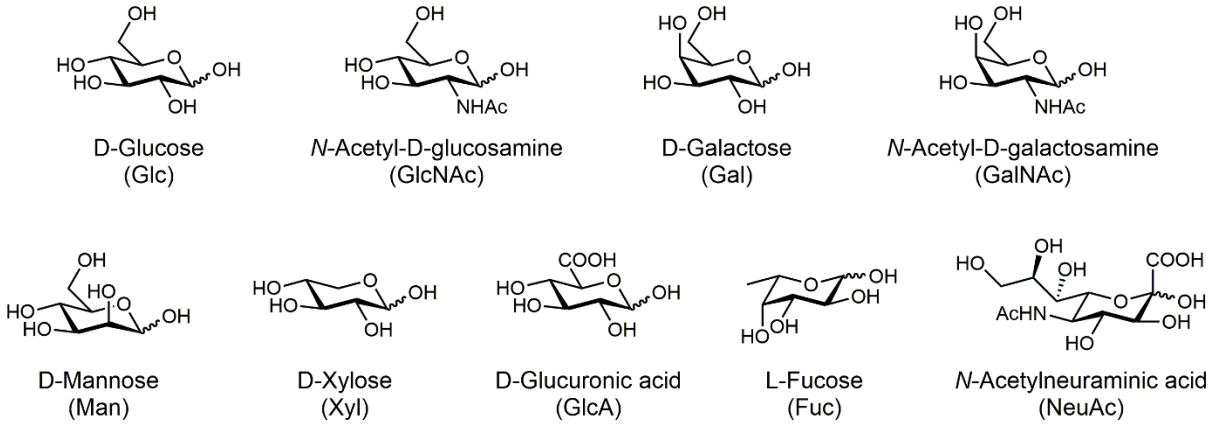

Figure 1.2. The nine common monosaccharides found in the glycoconjugates of vertebrates.

Carbohydrates can carry coded information which relays specific biological messages. Saccharides come in numerous forms with a variety of branching patterns, sequences, chemical structures and conformations. Thus, this structural complexity allows already a small number of monosaccharides to code a high density of information in contrast to nucleotides or amino acids which encode less information content by sequencing only.[5]

Carbohydrates mediate various biological functions and events like energy storage, structural composition, lubrication, and cellular recognition processes for fertilization, cell growth, cell migration, cell adhesion, immune response, cancer metastasis, bacterial and viral infections.[1,6–12] For example, the blood group specificity is solely determined by small modifications of the oligosaccharides bound to the glycolipids on the surface of red blood cells (Figure 1.3a). The body can recognize and decode these glycans and cause blood agglutination or clotting when foreign glycans of other blood types are detected.[13] The glycans on cell surfaces and glycoproteins are also altered depending on physiological and pathological states like cell differentiation or cancer.[2,5] This occurrence can be utilized in (early) cancer diagnostics.[14,15] Pathogens use cell surface glycans for adhesion onto the host cells. By employing saccharides with high affinity for pathogenic lectins, pathogens bind the saccharides due to competitive inhibition, and thus, can be prevented from infiltrating host cells.[2] For instance, D-mannose is used as an anti-adhesion therapeutic for urinary tract infections induced by *Escherichia coli* (E. coli) whose surface lectins can bind to mannosylated lining cells of the bladder (Figure 1.3b).[16-19] Natural anti-infective carbohydrates can be found in human breast milk, like 2'-fucosyl-lactose and lacto-*N*-neotetraose, which support the new and weak immune system of infants.[1,9]

Another example for carbohydrate compounds in nature that bind to pathogens by their lectins are a class of glycoproteins, called mucins. Mucins are constructed from a polypeptide backbone with heavily glycosylated branches (Figure 1.3c). They are of high molecular weight whereof up to 90% originates from the glycans.[20,21] In the human body, mucins can be found in saliva, ocular tears, synovial fluids and the mucous membrane of e.g. lungs, intestines, stomach, genital tract, and ear canal.[22] Due to their branched architecture, mucins can form network-like structures and hold large amounts of water which allows functions such as hydration, lubrication, protection, and antimicrobial activity. For instance, they prevent desiccation of the eye, friction and tearing of tissues during swallowing or sexual intercourse, and permeation of larger foreign objects, such as fungi, into the network. Smaller foreign objects like pathogens can be bound to the glycans and transported out of the body by the clearance of mucus.

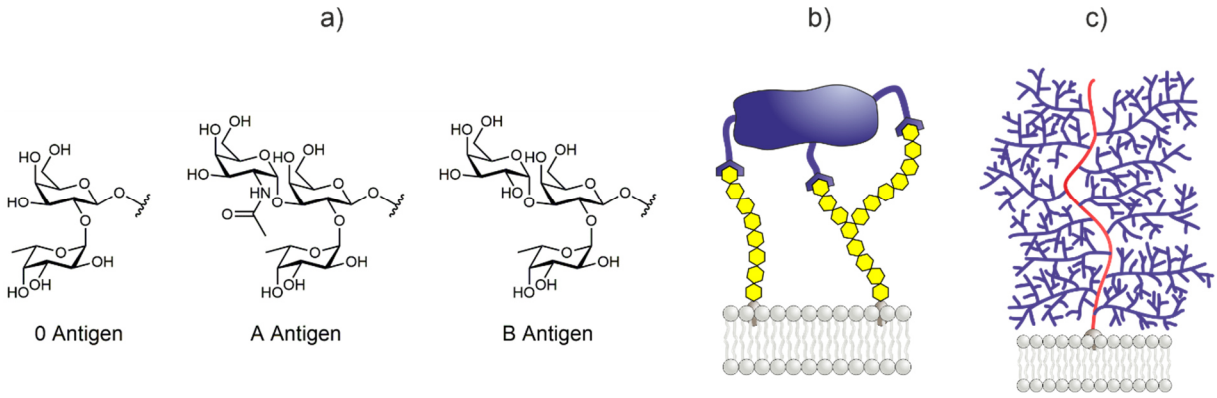

Figure 1.3. Examples of glycans in humans: a) blood type specific antigens of glycolipids on red blood cells, b) pathogen interaction with cell surface glycans, c) hyper branched mucin.

In conclusion, carbohydrates are a crucial class of natural compounds with immense biological relevance. Studying and utilizing their remarkable properties and biofunctionalities is of tremendous significance to biological and medical applications. To further advance the comprehension of the biological role and effect of carbohydrates as well as their industrial utilization, more research needs to be conducted on these biomolecules or, alternatively, their analogue biomimetics.

1.1.2 Carbohydrates and Lectin Binding

Lectins are a diverse group of proteins that can recognize and bind carbohydrates. Hence, they decode the biological information carried by glycans and mediate essential biological processes involving carbohydrates like cell-cell recognition and cell growth.[2,6] They naturally occur in animals, plants, fungi, viruses, and bacteria. Most lectins can only bind certain saccharides, namely mannose,

glucose, galactose, *N*-acetylglucosamine, *N*-acetylgalactosamine, fucose and *N*-acetylneuraminic acid. These sugars are all typical constituents of the glycans in vertebrates (Figure 1.2).[2]

The binding site of this protein group consists of a limited sequence segment of polypeptides which allows interactions with carbohydrates and is therefore termed carbohydrate recognition domain (CRD). Lectins typically carry two or more binding sites rendering them di- or polyvalent.[2] Unlike enzymes or carbohydrate-binding antibodies, they neither catalyze modifications of ligands nor do they originate from the immune system. Lectins are able to recognize both covalently bound glycans as well as free small saccharides. Particularly, the terminal, non-reducing part of carbohydrates is bound by the CRD.[23,24] This interaction can be highly specific to carbohydrates and their isomers. An example for specific binding is *E. coli* whose lectins bind glycans of glycolipids containing *N*-glycolylneuraminic acid but not those that contain N-acetylneuraminic acid which only differs by a single hydroxy group.[25] *Sambucus nigra* agglutinin (SNA) has a binding affinity to α(2,6)-linked sialic acid, and *Maackia amurensis* leukoagglutinin (MAL) preferably binds to α(2,3)-linked sialic acid.[26,27] Moreover, lectins can also exhibit anomeric specificity towards α- and β-glycosides like Concanavalin A (Con A) which binds α-configurations of mannose and glucose but not their β-anomers.[28] However, if a lectin does bind different isomers, the affinity for each ligand can differ by magnitudes.[24,29,30] For instance, the binding strength of the lectin *Erythrina cristagalli* agglutinin to *N*-dansylacetylgalactosamine is 62 times stronger than its affinity to *N*-acetylgalactosamine (GalNAc).[30]

This non-covalent interaction is reversable and primarily relies on hydrogen bonds and hydrophobic interactions.[2] In addition, lectins and carbohydrates form hydrogen bonds with the surrounding water molecules which are then broken upon lectin binding where new hydrogen bonds between carbohydrate and lectin are formed. The monovalent lectin binding of mono- and oligosaccharides is therefore relatively weak with a dissociation constant (K_D) in the order of micromolar to millimolar range.[31,32] In nature, this carbohydrate-lectin interaction is strengthened by a so-called 'cluster glycoside effect' (also named 'glycoside cluster effect').[2,5,33] This effect depends on clusters of CRDs and the multivalent presentation of ligands with suitable orientation and spacing (Figure 1.4). Multivalent ligand presentation can be found in oligosaccharide branches on cell surfaces or in glycoproteins that carry several identical glycans, for example. Thus, they can interact with several binding sites of the lectin enhancing their affinity by magnitudes and gaining a K_D in nanomolar range.

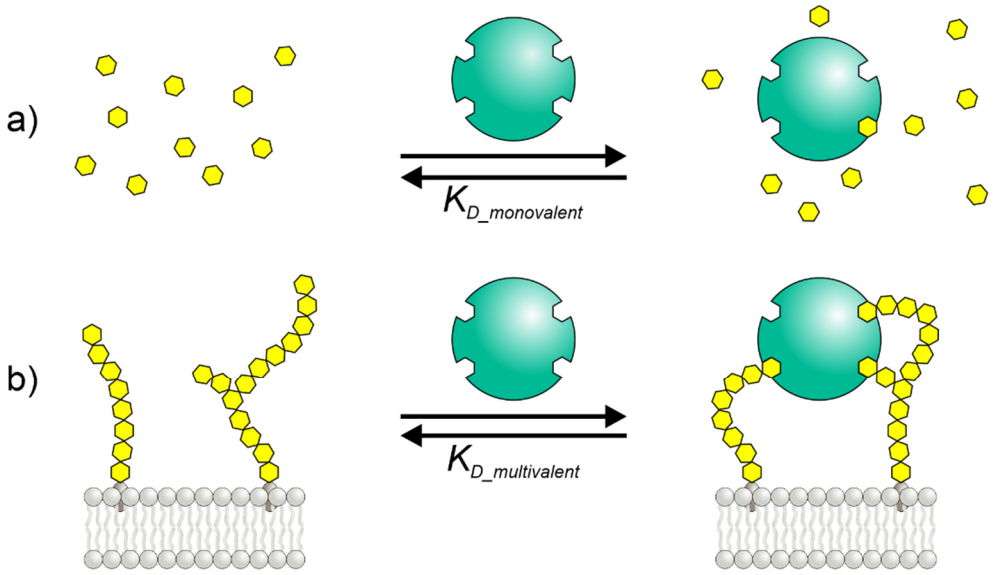

$$K_{D\_monovalent} > K_{D\_multivalent}$$

Figure 1.4. Schematic illustration of a) monovalent and b) multivalent carbohydrate-lectin binding. Binding strength is enhanced by multivalency. Lectin is depicted in green and sugars in yellow.

There are several mechanisms involved in this multivalent effect. A prominent one is chelation (Figure 1.5). Here, the cost of translational and rotational entropy is paid by the binding of the first ligand. Thus, the reduction of entropy is lower for binding of additional ligands from the same molecule as opposed to monovalent carbohydrates paying the same entropic cost individually.[34] Another mechanism is the statistical rebinding. After the first binding event of multivalent carbohydrates, the saccharides concentration in close vicinity of the binding sites is consequently high. This proximity effect causes statistical rebinding.[28,35] If a ligand dissociates from a lectin due to the weak interaction, another ligand in close proximity can immediately bind to the protein. Furthermore, the effective concentration of saccharides around the lectin increases the probability of additional ligand binding to other CRDs of the protein.[36] For multivalent proteins and ligands, a clustering effect can occur where intermolecular interactions lead to crosslinking and, therefore, formation of large aggregates with reduced solubility. This irreversible precipitation contributes to the carbohydrate-protein interaction.[34,36] Steric hindrance of an already bound multivalent ligand prevents the binding of other molecules to the same protein. This steric stabilization inhibits the dissociation of the ligand by competitive binding.[34,37,38] Hence, one will find numerous multivalent carbohydrates compounds in nature.

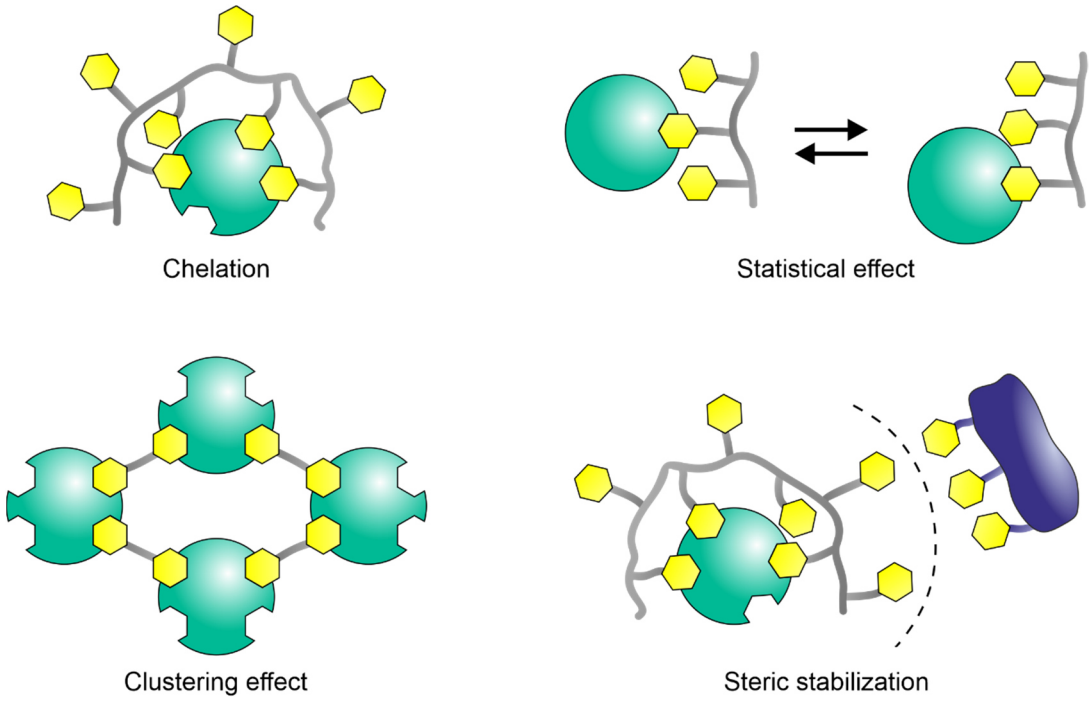

Figure 1.5. Multivalent effect caused by chelation, statistical effect, clustering, and effect steric stabilization.

1.2 Glycopolymers as Biomimetics

Glycopolymers are synthetic polymers that carry pendant saccharides. The biofunctionality of the carbohydrates render them as biomimetics. Generally, biomimetics are of great interest as they can mimic or even surpass their natural examples. For instance, biomimicking glycopolymers can exhibit biocompatibility, enhanced stability, and stronger lectin binding in comparison to their natural counterparts. Carbohydrates in nature, such as hyaluronic acid, are biodegradable and produced via extraction from animal materials and biotechnological recovery from plant materials which is costly and laborious.[39] Therefore, glycopolymers are practical alternatives to natural products since glycans can be difficult to obtain or synthesize due to their complex nature. Fundamental studies of more readily available biomaterials forward research of biological functions and processes involving carbohydrates, especially when they are specifically designed for these purposes. Hence, these biomimetics are desired materials for biological research.

The first glycopolymer was synthesized with pendant saccharides in 1978 by Hořejší *et. al.* and was found to present similar lectin binding abilities to those of natural biopolymers.[40] Here, the lactose-based polymer revealed interactions with lectins similar to natural polysaccharides. Other reports indicate that the spatial distance between sugar moieties influences binding of the CRD of the lectin.[41,42] These pioneer works demonstrated the possibility of utilizing biomimicking glycopolymers

to gain better comprehension of biological processes and raised interest in employing synthetic glycopolymers for fundamental research as well as biomedical applications.

Since then, reports about glycopolymers steadily increased and remained of great interest to this day. Glycopolymers of diverse compositions, structures and functions have been synthesized from various sugar alcohols, sugars and oligosaccharides including *N,N'*-diacetylchitobiose, fructose, galactose, *N*-acetylgalactosamine, glucose, *N*-acetylglucosamine, gluconolactone, glucuronic acid, glucosamine, glucitol, mannitol, mannose, lactose, *N*-acetallactosamine, lactobionic acid, maltose, maltoheptaose, glucofuranose, 3'-sialyllactose, 2'-fucosyllactose, and trehalose.[43–61] The glycopolymers have been investigated in fields like drugs, drug delivery systems, cell culturing, biosensors, surface modification, catalytic and responsive hydrogels, artificial tissues and organ substrates.[38,55,62–90]

In conclusion, the properties and biofunctionalities of glycopolymers render them as a desirable biomaterial for studying, understanding, and controlling biological processes for biomedical applications.

1.2.1 Glycopolymer Synthesis Strategies and Architectures

For the chemical synthesis of glycopolymers, two general strategies are applied: 1) the (co-)polymerization of carbohydrate-based monomers, known as glycomonomers, and 2) the post-polymerization modification with saccharides (Scheme 1.1). Both approaches offer their own benefits as well as drawbacks.

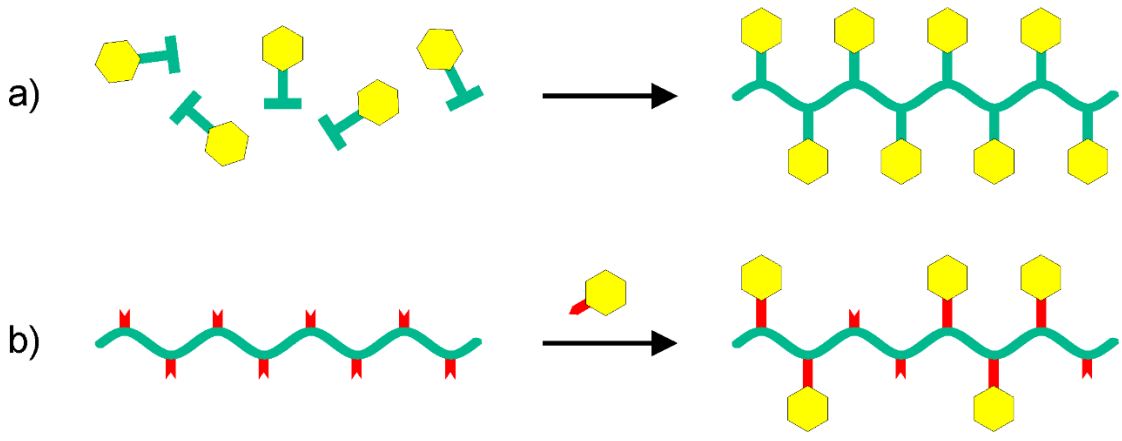

Scheme 1.1. Schematic presentation of general synthesis strategies for glycopolymers: a) polymerization of glycomonomers, b) post-polymerization glycosylation.

The advantage of polymerizing glycomonomers is the high density and homogeneous distribution of carbohydrates on the resulting glycopolymers. The molecular weight, distribution of molecular weight, composition, end group functionality, structure, and architecture of polymer can be

tailored with various polymerization techniques.[91] However, the synthesis of necessary glycomonomers for polymerization can be complex, laborious, and cost intensive. Further challenges lie in the tolerance of polymerization techniques towards the functional groups of monomers as well as in the control and reproducibility of specific molecular weights and polydispersities.

The post-polymerization modification is an efficient method as it typically relies on simple and efficient reactions such as click-reactions.[92] In addition, readily available starting materials can be employed without prior complex syntheses. However, post-functionalization can lead to not fully glycosylated polymers and/or inhomogeneous distribution of glycans. Properties like molecular weight and distribution are pre-determined by the initial polymers available for post-glycosylation and are not feasible for precise tailoring.

For extended control of polymer properties, both synthesis strategies can be applied in combination where the polymer backbone is synthesized and tailored as required by polymerization before post-glycosylation is conducted.[93]

The first reported glycopolymer synthesis in 1978 applied the traditional free radical polymerization (FRP) technique and yielded a linear copolymer with pendant galactose moieties. Most studied glycopolymers are of linear structure due to their facile and efficient syntheses. However, the simple structure showed reduced lectin-carbohydrate binding strength compared to glycopolymers with complex architectures. Even if linear glycopolymers constitute multivalent presentation of ligands, their hydroxy groups form intramolecular hydrogen bonds causing clustering of glycopolymers.[94,95] Thus, glycopolymers of advanced macromolecular architectures which offer specific and strong recognition binding are desired. Numerous polymerization techniques for glycopolymers have been investigated including traditional free radical, anionic, cationic, ring-opening, coordination, stable free radical, nitroxide-mediated, reversible addition fragmentation transfer and atom transfer radical polymerization.[44,96–104] Consequently, a variety of well-defined glycopolymer architectures were explored such as dendrimers, linear block copolymers, nanoparticles, networks, brush and star polymers and many more (Figure 1.6).[60,61,105–111]

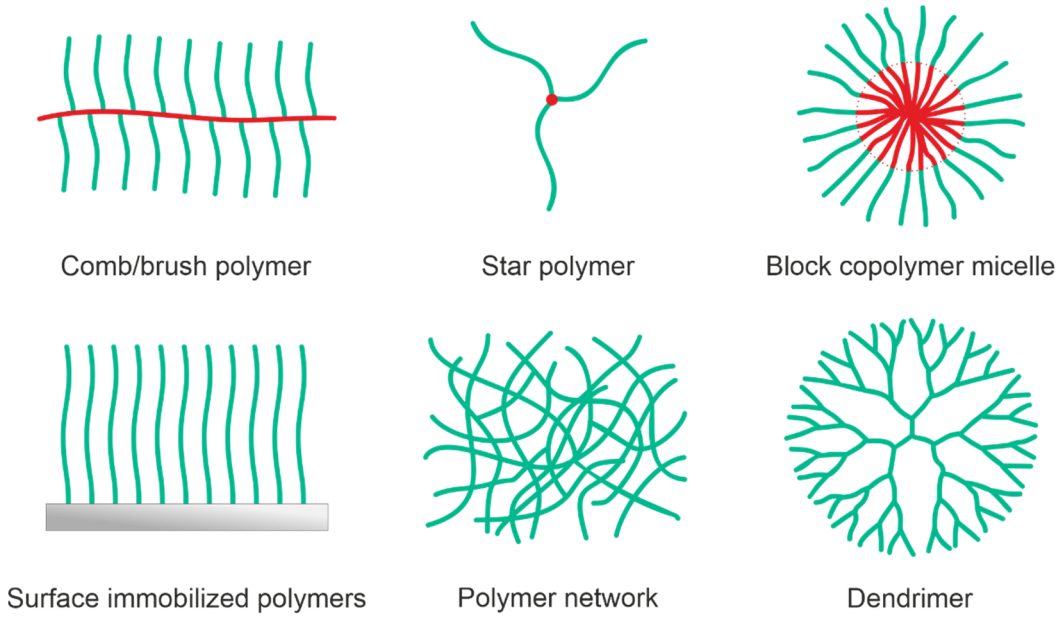

Figure 1.6. Examples of different glycopolymer architectures.

By tailoring features like glycosylation pattern, polymer structure and architecture, the properties and functionalities of biomimicking glycopolymers can be tuned. For example, tandem post-polymerization glycosylation allowed the preparation of glycopolymers based on methacrylate and galactose with varied linker length, galactose density and polymer chain length.[93] The inhibition of different lectins were tested in dependance of the glycopolymer properties. Nonlinear dependence was partially observed which indicates the complexity of biomolecular interactions. Strong inhibition potentials were achieved if the glycopolymers met structural conditions such as depths and spacing of binding sites of the lectin. Therefore, glycopolymers specifically designed with high affinity for a certain lectin do not necessarily show strong inhibition potential for other proteins. Studies have shown that glycopolymers of complex macromolecular architectures enable improved biofunctionality such as enhanced lectin interactions. An example for the utilization of non-linear glycopolymers are surface grafted glycopolymers for studying carbohydrate-lectin interactions as a model system for biosensors.[112] Thermoresponsive, glycosylated hydrogels were synthesized for temperature-controlled binding of lectins.[113]

Thus, optimizing the architectures of glycopolymers and their syntheses for specific applications is worthwhile and adjuvant for fundamental research in glycobiology.

1.2.2 Glycopolymers via Free Radical Polymerization

Since the first synthesis of glycopolymers in 1978, many glycopolymers have been synthesized by the traditional FRP method as it offers efficacy, versatility in choice of solvent, temperature, as well as initiator, and does not require additional reactants.[40,114–119] Moreover, this polymerization

technique is moderately tolerant to impurities, scalable, of low costs and, thus, a well-established synthesis method as well as the most common polymerization type in industry.[44,91] As free radicals are highly reactive, conventional FRP leads to broad distribution of molecular weight and little control over architecture as well as end group functionality. However, these challenges can be circumvented by employing polymerization techniques like emulsion, precipitation or controlled radical polymerization. Emulsion and precipitation polymerizations depend on heterogeneous polymerization processes. Such systems enable the fabrication of advanced architectures and functions like magnetic nanoparticles or thermoresponsive microgels of high monodispersity.[120,121]

The reaction mechanism of a typical FRP involves initiation, propagation, termination and chain transfer, which are depicted in Figure 1.7a.[91] The kinetic essentials in Figure 1.7b are described under the assumptions that 1) a steady state concentration of propagating species dominates the majority of polymerization process, 2) rate constants are independent of chain lengths, 3) no chain transfer reactions take place, and 4) no gel-effect occurs.

Initiation step starts with the generation of radicals by initiator decomposition with the rate constant k_d. Depending on the initiation type, this can occur by thermal decomposition, photolysis, redox reaction, ionizing radiation, electrolysis, or plasma, for example. As generated radicals can undergo side reactions such as recombination, only a fraction of the initiator concentration generates radicals effective for polymerization. The efficacy of an initiator to generate effective radicals for polymerization is described by the initiator efficiency factor f which typically lies below its maximum value of 1. The generated radicals start polymerization with the initiating rate constant k_i by reaction with monomers and formation of propagating molecules. As $k_d < k_i$, the initiator decomposition is the rate determining step of the initiation process, hence, the initiation rate depends on k_d and the initiator concentration. Since the initiator generates two radicals, the initiation rate has a double dependence on the initiator concentration (Figure 1.7b).

The propagation step constitutes the main part of the polymerization process. Here, monomers add to the growing radicals increasing their chain lengths with the rate constant k_p until termination occurs. The propagation rate constant is assumed to be independent of the chain lengths. Thus, the propagation rate essentially equals the conversion of monomer.

Termination of polymer chains occurs due to the high reactivity of radicals. Hence, the termination step is influenced by the concentration of radical molecules. This bimolecular step involves recombination or disproportionation of two propagating chains with the termination rate constants k_{tc} and k_{td}, respectively. The sum of k_{tc} and k_{td} equals k_t which is used in the kinetic expression for convenience. Under the steady state approximation, the rates of radical formation and termination are equal. Thus, the concentration of radicals remains constant during the majority of a FRP process.

The unknown concentration of active molecules can be substituted by a function of monomer and initiator concentrations which is used to further express the rate of propagation (Figure 1.7b).

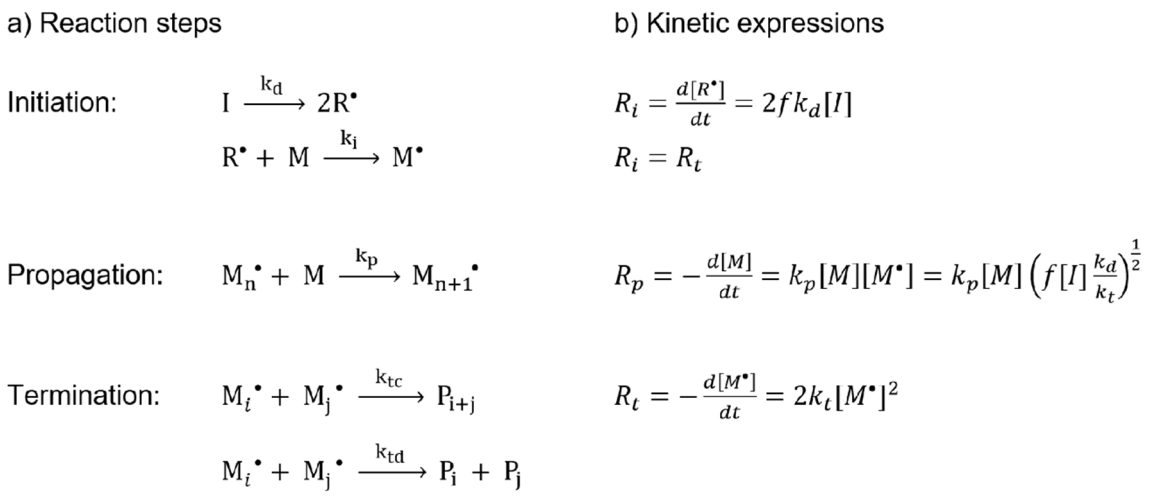

Figure 1.7. a) Reaction steps of free radical polymerization and b) its kinetic expressions. I = Initiator; R = radical; M = monomer; P = polymer; f = initiator efficiency factor; k = rate constant; R_x = reaction rate.[91]

FRP is a chain growth polymerization with rapid monomer conversion in the beginning. The kinetic chain length *v* represents the average number of monomers added to a growing chain before termination occurs. Therefore, the ratio of propagation rate to termination rate is regarded in Equation 1. The degree of polymerization X_n describes the number of monomer units in a polymer. If chain transfer reactions are disregarded, X_n can be determined from *v* (Equation 2).

$$v = \frac{R_p}{R_t} = \frac{k_p[M]}{2(fk_dk_t[I])^{\frac{1}{2}}} \quad (1)$$

$$X_n = \alpha * v = \alpha \frac{k_p[M]}{2(fk_dk_t[I])^{\frac{1}{2}}} \quad (2)$$

$$a = 1 \quad for\ termination\ by\ disproportionation$$

$$a = 2 \quad for\ termination\ by\ recombination$$

During polymerization, side reactions of highly reactive radicals can occur. Impurities such as oxygen can inhibit polymerization as it reacts with radicals and the resulting oxygen radicals are less reactive than monomers which slows down the polymerization rate (Scheme 1.2a). Chain transfer can take place at any time where the radical of a propagating chain is transferred to another molecule and an atom is abstracted (Scheme 1.2b). This leads to a decrease of average molecular weight. If chain transfer occurs to a polymer, branched architectures can be formed (Scheme 1.2c).

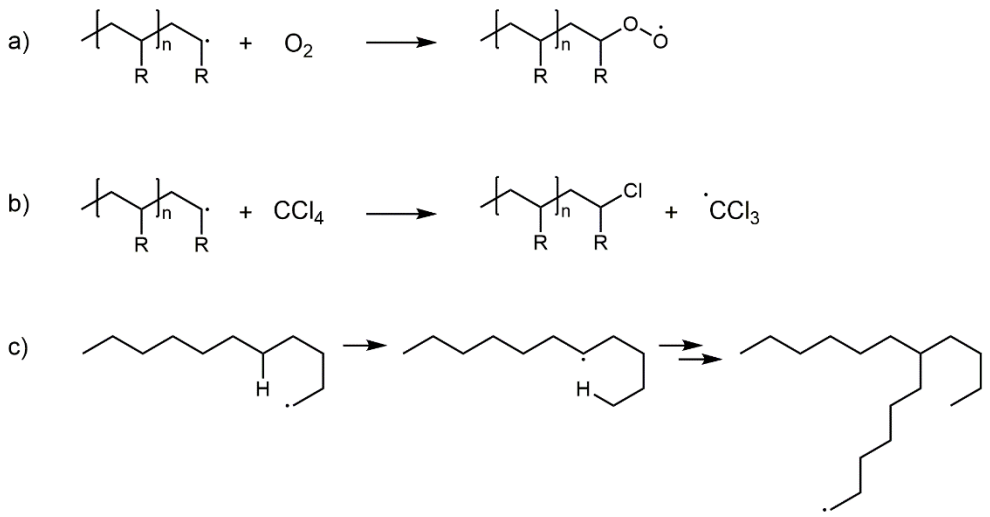

Scheme 1.2. Side reactions of free radical polymerization: a) inhibition by oxygen, b) chain transfer to solvent results in decreased molecular weights, c) chain transfer to polymer results in branched architectures.

1.2.3 Glycomonomers for Free Radical Polymerization

To achieve glycopolymers with high sugar densities, glycomonomers are polymerized. Glycopolymers are often prepared by radical polymerization, hence, glycomonomers with radical polymerizable moieties have been widely researched. Typically, glycomonomers are synthesized by glycosylation of vinyl compounds, either chemically or enzymatically.[94,122] Depending on the application, biomimetic glycopolymers must be biofunctional. The challenge in maintaining the biofunctionality of carbohydrates is the regio- and stereoselective functionalization of saccharides. For example, lectins generally bind the non-reducing part of carbohydrates. Thus, studies often reported synthesis strategies of regio- and/or stereoselective functionalization at the anomeric C1-position of saccharides.[59,123,124] Numerous published synthesis routes of glycomonomers involve protection groups to ensure selectivity, however, in recent years reports of protecting group free synthesis strategies for glycomonomers have increased due to their compatibility with aqueous conditions and the elimination of harmful organic solvents as well as several synthesis steps.[119,125,126] In case of protected glycomonomers, deprotection can be performed before or after polymerization which changes consecutive reaction conditions like choice of solvents due to the immense difference in hydrophilicity before and after deprotection. If deprotection is performed on the glycopolymer, it can lead to incomplete deprotection and, hence, to ill-defined glycopolymers.[127]

Studies presented a variety of glycomonomers often based on (meth)acrylates, (meth)acrylamides, and allyl and styrenic monomers (Figure 1.8).[43,46,47,52,104,118,125,126,128–131] Saccharides can be glycosydically O-, N-, C-, or S-linked to the polymerizable moiety.[48,118,132,133] Some reactions open the sugar ring on the reducing end. In these cases, saccharides of 2 or more units can

be employed to retain biofunctionality.[125,130,131,134,135] The linker length between saccharide and polymerizable moiety can vary and influence the biofunctionality of resulting polymer. For example, longer linkers can lead to enhanced lectin binding as the saccharides can reach into deeper binding pockets of lectins.

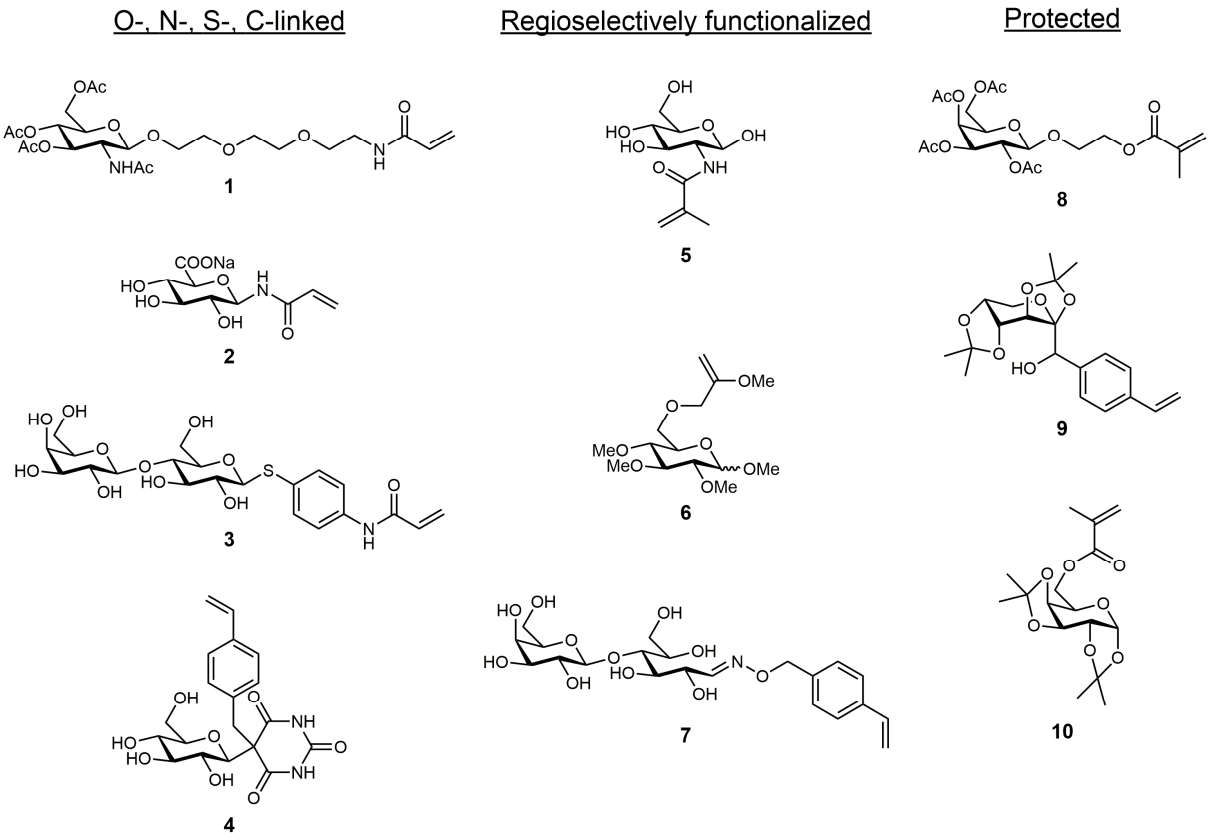

Figure 1.8. Examples of glycomonomers with different glycosidic bonds, positions of glycosidic bonds and protecting groups.

Since amines can undergo various reactions, glycosylamines present a practical precursor for glycomonomers.[48,136–140] For instance, reactions of glycosylamines with carboxylic acid chlorides, iso(thio)cyanates or epoxides yield the respective N-linked glycomonomers.[132] Synthesis routes for the regioselective amination of saccharides were reported which are protecting group free, straightforward, and inexpensive.[141–144] The regioselective modification of the C1-position allows the perpetuation of biofunctionality. The amination reactions simply involve saccharides suspended or dissolved in a solvent in the presence of an excess of ammonium salt (Scheme 1.3). Studies have used water, methanol, and dimethyl sulfoxide as solvents. Drawbacks of these reactions are the slow reaction rate and the enormous excess amount of ammonium salts. By applying microwave irradiation, the long reaction time of days can be remarkably reduced to 90 min and the 50-fold excess of salts can be decreased by 90% to a 5-fold amount.[145] However, studies have shown that the yield of glycosylamines can differ tremendously depending on the saccharide itself. For instance, amination of

GlcNAc and GalNAc led to 24% and 77% amination yield, respectively, even though solely the configuration of one hydroxy group at the C4-position differs.[146] This indicates the complexity of carbohydrate chemistry.

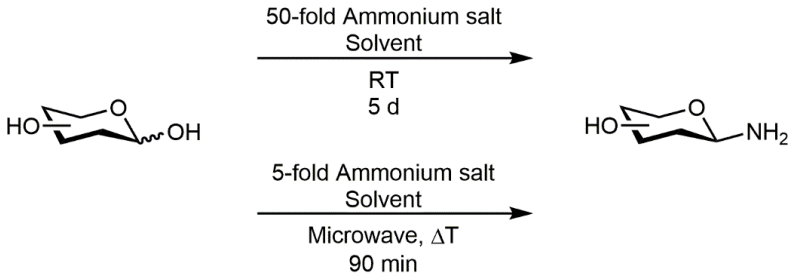

Scheme 1.3. Synthesis of glycosylamines by conventional Kochetkov-amination reaction and microwave-assisted amination.

As there are nine common monosaccharides in vertebrates, which are all essential for biological processes and functions, the fabrication of glycopolymers based on these sugars is of great interest and necessitate synthesis routes and reaction conditions suitable for each saccharide.

1.2.4 Glycopolymer Immobilization

Glycopolymers gained great attention due to their ability to mimic biological functions of carbohydrates.[147–149] Over the years, different synthesis strategies for glycopolymers have been researched and enabled the fabrication of various architectures including surface immobilized glycopolymers. Glycopolymers attached to various surfaces have been studied for applications such as drug delivery, affinity chromatography, mucosa mimetics, cell culturing, lectin-based biosensors, pathogen detection, model systems for studying biological processes, modification of surface chemistry, antifogging, antifouling and antimicrobial coatings.[150–157]

They can be immobilized on surfaces by chemical reactions or physical interactions. Covalently bound glycopolymers offer great stability, whereas immobilization methods based on electrostatic interactions allow mild preparation conditions, for example. Protected as well as deprotected saccharides are employed for fabricating glycopolymer coatings. However, if deprotection of sugar groups is required after immobilization, this reaction needs be suitable to the chemistry of the polymer coating to avoid any damage or loss of coating.

For the covalent immobilization of polymers, there are two general strategies: 1) direct polymerization from the surface and 2) grafting polymers onto the surface. The syntheses of glycopolymers are performed either by polymerization of glycomonomers or post-polymerization

glycosylation (Chapter 1.2.2). Hence, the overall preparation of surface bound glycopolymers can involve different combinations of these strategies (Figure 1.9).

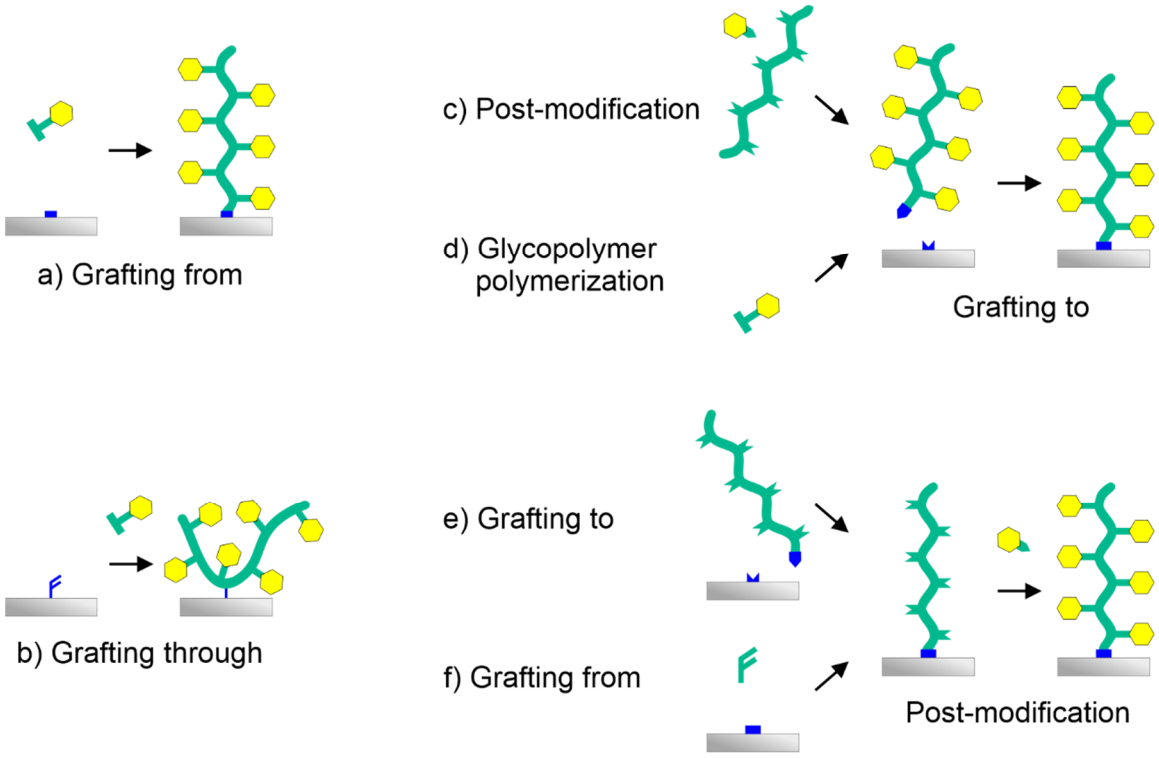

Figure 1.9. Strategies for covalently immobilized glycopolymers: a) glycopolymer via grafting from, b) glycopolymer via grafting through, c) grafting to of glycopolymers prepared by post-modification, d) grafting to of glycopolymers prepared by polymerization, e) glycosylation of grafted to polymers, f) glycosylation of grafted from polymers.

Non-covalent immobilization is based on e.g., electrostatic, hydrophobic, or protein interactions. For instance, complimentary polyelectrolytes can be deposited on a surface in alternating layers leading to multilayer thin films (Figure 1.10a). Functional groups that enable this layer-by-layer (LbL) technique can be incorporated into the glycopolymer by copolymerization or post-functionalization.[45,57] For example, positively charged glycopolymers have been synthesized by glycosylating cationic polyethyleneimine (PEI) which was assembled with anionic heparin or polyacrylic acid for drug delivery and biosensor applications. In this case, branched PEI was functionalized via reductive amination. As the reductive amination opens the first sugar ring, the disaccharide maltose was employed to retain one closed biofunctional sugar moiety. This aqueous-based synthesis offers facile and efficient functionalization of amines with various oligosaccharides and eliminates the necessity of prior modification or protection of both polymer and saccharide. To synthesize negatively charged glycopolymers, poly(ethylene-*alt*-maleic anhydride) was functionalized with various amino-terminated saccharides to gain a glycopolymer with carboxylic acid groups on the backbone. It was deposited on a layer of cationic poly(diallyldimethylammonium chloride) to detect shiga toxins of

pathogenic *E. coli* bacteria.[158,159] Other glycosylated polyanions were prepared by glycosylating copolymers of acrylic acid and vinylbenzene or hydroxyethyl acrylate with galactose or glucose moieties. Gold nanoparticles were coated with PEI, polyacrylic acid and finally the anionic glycopolymer by the LbL approach.[160]

Hydrophobic interactions between polymers and substrate surfaces can lead to the self-assembly of polymer films on the surface. To utilize this interaction, amphiphilic glyco-homopolymers were prepared by free radical polymerization and formed stable layers on hydrophobic octadecyltrimethoxysilane functionalized surfaces (Figure 1.10b).[115] The polymer backbones were based on hydrophobic polystyrene or poly(1-ethenyl decanedioate) which adsorbed to the hydrophobic surface while the pendant sugar groups were oriented in the opposite direction. Thus, the sugar moieties formed the outermost layer. By applying lithography techniques on hydrophobic templates prior to the glycopolymer adsorption, micropatterned carbohydrate displays could be achieved. Additionally, micropatterned proteins could be fabricated by binding lectins to the carbohydrate displays.

Glycopolymer films based on protein interactions were prepared from glycopolymers with biotin incorporated into the side chains or at the terminal position. Biotin strongly binds to the protein streptavidin which can be functionalized on surfaces to immobilize biotinylated glycopolymers (Figure 1.10c).[161] This method was used to fabricate glycocalyx-mimetic surfaces by immobilizing biotin-terminated glycopolymers on polymeric lipid membranes functionalized with streptavidin. Another example is the immobilization of biotin end-functionalized polymers that carry pendant chondroitin sulfate groups to mimic chondroitin sulfate proteoglycans.[148]

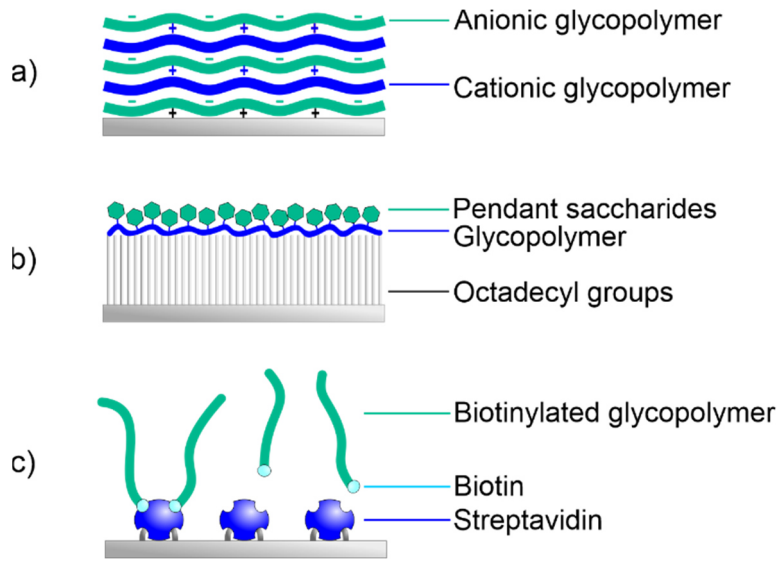

Figure 1.10. Strategies for surface immobilizing glycopolymers via physical interactions: a) layer-by-layer self-assembly of complementary charged glycopolymers, b) protein interaction between immobilized streptavidin and biotinylated glycopolymers, c) hydrophobic interactions between glycopolymer backbone and modified, hydrophobic surface.

1.2.5 Glycopolymer Hydrogels

Hydrogels are polymeric three-dimensional networks that absorb and swell in water without dissolving. The network is formed by chemically crosslinked polymer chains or physical interactions like tangling or hydrogen bonds. The large water uptake is enabled by hydrophilic moieties in the network as well as its deformability and swellabilty.[162] Many studies about hydrogels have been conducted on colloidal hydrogels, also called nanogels (100 nm) or microgels (>100 nm). It has to be noted, that the classification in literature is inconsistent as hydrogel particles up to 1000 nm are sometimes termed as nanogels while particles in the micrometer range are called microgels. Generally, the biocompatibility of hydrogels makes them of great interest for biomedical applications.[163] Due to the properties and structure of hydrogels, they have been used as scaffolds for saccharides to investigate biological and medical applications such as drug delivery or biosensors (Figure 1.11). For example, lectin binding studies with glycosylated hydrogels for biosensor applications have shown enhanced carbohydrate-lectin interaction.[164] Surface immobilized glycopolymeric hydrogels were reported to mimic the mucoadhesion of natural mucosa.[151] Ionic, thermoresponsive glycol-nanogels were synthesized using the RAFT polymerization approach for siRNA and drug delivery.[134,165,166] Temperature-controlled adhesion of lectins to thermoresponsive, glycosylated microgels were studied as a platform to capture and release pathogens.[113] Compared to other glycosylated nanoparticles, e.g. gold nanoparticles, microgels exhibit a soft and deformable structure which could allow reaching into CRDs to a greater degree and, therefore, enhance the lectin binding. Furthermore, lectins could potentially enter the hydrogel network and be trapped inside. Even though these glycopolymers present remarkable properties and functions, only a limited number of glycosylated hydrogel particles have been reported.

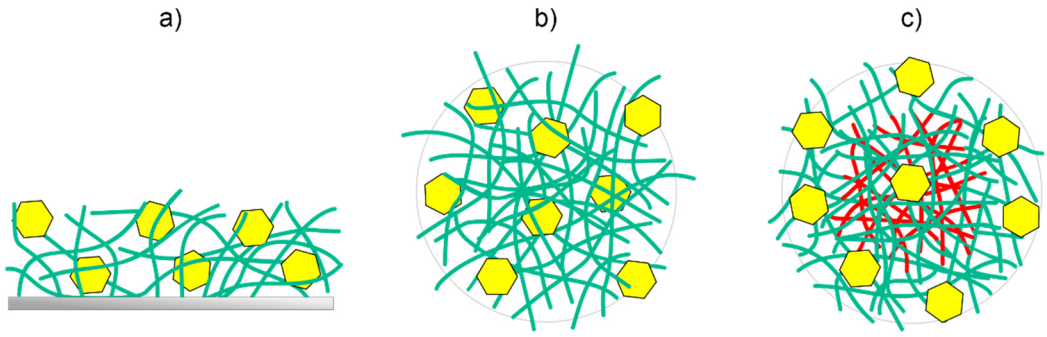

Figure 1.11. Examples of glycosylated hydrogels: a) hydrogel network with pendant saccharides, b) glycosylated hydrogel particles, c) core-shell hydrogel particles with glycosylated shell.

One of the most extensively studied microgels are based on poly(*N*-isoproypacrylamide) (PNiPAm).[167] Due to its biocompatibility, it has been investigated for biomedical applications and could present a suitable multivalent scaffold for saccharides to research carbohydrate-protein

interactions.[168] PNiPAM microgels are commonly synthesized via free-radical precipitation polymerization which can be performed with comonomers in aqueous media.[169] It is a facile and efficient method to synthesize copolymeric hydrogel colloids with multivalent presentation of glycans and, furthermore, allows fabrication of microgels with excellent monodispersity, uniformity, tailored sizes and properties like temperature- or pH-responsitivity. PNiPAm exhibits thermoresponsivity due to its lower critical solution temperature (LCST) which also enables its use in the precipitation polymerization method.

The synthesis of microgels via precipitation polymerization is illustrated in Scheme 1.4. The polymerization system starts as a homogenous phase where all reagents are soluble in the reaction medium. After initiation, the propagating polymer chains exceed their solubility in high temperature and precipitate. Crosslinkers like *N,N'*-methylenebis(acrylamide) (MBA) react with the propagating chains and cause the formation of a hydrogel network. As the system is stabilized by surfactants or electrostatic repulsion of ionic initiators, colloidal hydrogels are formed. Since MBA is known to exhibit a higher reaction rate than NiPAm, the crosslinks are concentrated in the center of the microgel.[170] Thus, a core-shell like morphology is achieved where the core is denser than the outer layer while the microgel surface appears softer and fuzzy.

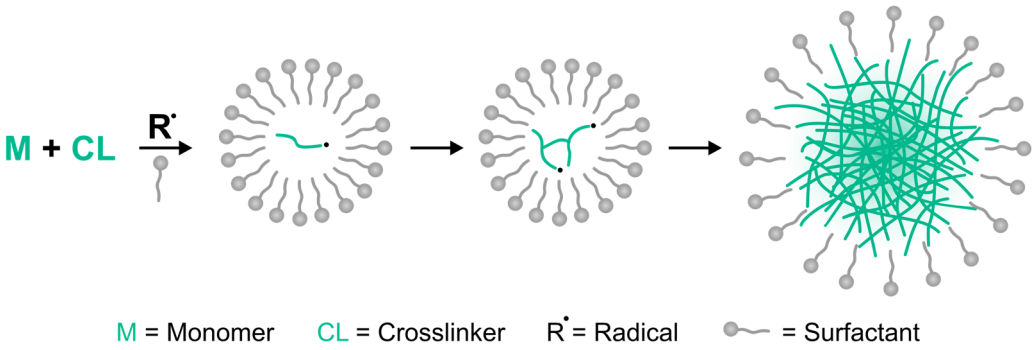

Scheme 1.4. Free-radical precipitation polymerization of micro-/nanogels stabilized by surfactants.

1.3 Motivation and Outline

Carbohydrates are essential organic compounds for every living being as they mediate various, crucial biological processes. Hence, glycopolymers that mimic the remarkable functions and properties of carbohydrates are of great importance and interest for various applications in the biological and medical field. Moreover, they are desired biomaterials in biological research for studying, understanding, and controlling biological processes. However, syntheses of biofunctional materials based on carbohydrates can be complex and challenging.

This work deals with the syntheses of sugar-based materials using different synthesis routes to further advance in the field of glycopolymer synthesis. Synthesis strategies which enable efficient, aqueous-based, protecting group free and short synthesis routes were focused on. In addition, a method for facilitating optimization of reactions was investigated to improve frequently performed synthesis steps for glycopolymers. Furthermore, the aim is to present synthesis strategies for glycopolymers that are applicable for enhanced lectin binding and thin film coatings for medical applications. For enhanced carbohydrate-lectin interactions, multivalent presentations of suitable carbohydrates must be achieved. Thin films based on electrostatic interactions and prepared by the LbL approach require complimentary charged materials with homogenous distribution of charges and sufficient charge density. In this thesis, the glycopolymers were investigated for their syntheses and their required functions in dependance of their properties.

In Chapter 2, the optimization of the regioselective synthesis of glycomonomer precursors is presented. For this, optimization was performed using the design of experiments (DoE) approach to efficiently optimize reactions with a limited number of experiments. The chapter discusses the results and, therefore, the utility of using DoE for optimizing the amination of sugars. Chapter 3 describes the synthesis of complementary charged glycopolymers for thin film coatings. Applicability of glycopolymer polyelectrolytes on LbL self-assembly technique was investigated in the physiological pH range. In addition, the glycopolymers were studied as scaffolds for liposomes as potential cargo carriers. In chapter 4, the synthesis of glycosylated hydrogel particles via free-radical precipitation polymerization is discussed. Specifically, the influence of synthesis parameters on the hydrogel morphology and carbohydrate content is investigated. The enhanced interactions between their multivalent presentation of carbohydrates and lectins are studied in dependance on the hydrogel morphology and sugar content. Chapter 5 discusses the overall results of this thesis. Finally, chapter 6 and 7 present the conclusion and outlook of this work.

1.4 Contribution Statement of Publications

This doctoral thesis is based on published work listed below. Numbering of chapters, schemes, figures, and tables of published work as well as font styles, paragraph and page settings are adapted to this thesis. Minor spelling errors are corrected in this work.

- **Chapter 2**

  "Optimization of the Microwave Assisted Glycosylamines Synthesis Based on a Statistical Design of Experiments Approach"

  Jo Sing Julia Tang, Kristin Schade, Lucas Tepper, Sany Chea, Gregor Ziegler and Ruben R. Rosencrantz

  Molecules **2020**, *25*, 5121
  DOI: 10.3390/molecules25215121

  Statistical design of experiment and analysis were executed by Jo Sing Tang. Conceptualization, writing (excluding some parts of the introduction) and revision of the manuscript were done by Jo Sing Tang with the consultation of Dr. Ruben R. Rosencrantz.

- **Chapter 3**

  "Glycopolymer Based LbL Multilayer Thin Films with Embedded Liposomes"

  Jo Sing Julia Tang, Aline Debrassi Smaczniak, Lucas Tepper, Sophia Rosencrantz, Mina Aleksanyan, Lars Dähne and Ruben R. Rosencrantz

  Macromol. Biosci. **2022**, 2100461
  DOI: 10.1002/mabi.202100461

  Synthesis of GalNAcMAm and glycopolymers as well as characterization via NMR and IR spectroscopy and MS spectrometry were done by Jo Sing Tang. Writing (excluding the experimental sections of layer-by-layer coating of sensor particles, whispering gallery modes and quartz crystal microbalance with dissipation measurements in Chapter 3.4) and revision of the manuscript were done by Jo Sing Tang with the consultation of Dr. Ruben R. Rosencrantz and Dr. Lars Dähne.

- **Chapter 4**

  “Functional Glyco-Nanogels for Multivalent Interaction with Lectins”

  Jo Sing Julia Tang, Sophia Rosencrantz, Lucas Tepper, Sany Chea, Stefanie Klöpzig, Anne Krüger-Genge, Joachim Storsberg and Ruben R. Rosencrantz

  Molecules **2019**, *24*, 1865
  DOI: 10.3390/molecules24101865

  Design and synthesis of glycopolymers as well as characterization via NMR spectroscopy, mass spectrometry and dynamic light scattering were done by Jo Sing Tang. Jo Sing Tang wrote chapters 4.2.1-4.2.2 (results and discussion about the synthesis of glycopolymers), 4.3.1-4.3.4 (materials, methods, and synthesis procedures) and 4.4 (conclusion). Jo Sing Tang took active part in the revision of the manuscript.

1.5 References

[1] H. M. I. Osborn, *Carbohydrates*, **2003**.
[2] N. Sharon, H. Lis, *Lectins*, **2007**.
[3] G. P. Espino-Solis, *Vitae* **2015**, *22*, 9.
[4] A. Varki, *Essentials of Glycobiology*, **2002**.
[5] Y. C. Lee, R. T. Lee, *Society* **1995**, *28*, 950182.
[6] N. Sharon, H. Lis, *Sci. Am.* **1993**, *268*, 82.
[7] M. N. Hatton, R. E. Loomis, M. J. Levine, L. A. Tabak, *Biochem. J.* **1985**, *230*, 817.
[8] L. A. Tabak, M. J. Levine, *Arch. Oral Biol.* **1981**, *26*, 315.
[9] Y. Vandenplas, B. Berger, V. P. Carnielli, J. Ksiazyk, H. Lagström, M. S. Luna, N. Migacheva, J. M. Mosselmans, J. C. Picaud, M. Possner, A. Singhal, M. Wabitsch, *Nutrients* **2018**, *10*.
[10] V. Ladmiral, E. Melia, D. M. Haddleton, *Eur. Polym. J.* **2004**, *40*, 431.
[11] R. A. Dwek, *Biochem. Soc. Trans.* **1995**, *23*, 1.
[12] S. Defaus, M. Aviles, D. Andreu, R. Gutierrez-Gallego, *Mol. Cell. Proteomics* **2016**, *15*, 2236.
[13] S. L. Flitsch, R. V. Ulijn, *Nature* **2003**, *421*, 219.
[14] M. J. Kailemia, D. Park, C. B. Lebrilla, *Anal. Bioanal. Chem.* **2017**, *409*, 395.
[15] D. H. Dube, C. R. Bertozzi, *Nat. Rev. Drug Discov.* **2005**, *4*, 477.
[16] C. De Nunzio, R. Bartoletti, A. Tubaro, A. Simonato, V. Ficarra, *Antibiotics* **2021**, *10*, 1.
[17] Y. T. Pan, B. Xu, K. Rice, S. Smith, R. Jackson, A. D. Elbein, *Infect. Immun.* **1997**, *65*, 4199.
[18] C. H. Jones, J. S. Pinkner, R. Roth, J. Heuser, A. V. Nicholes, S. N. Abraham, S. J. Hultgren, *Proc. Natl. Acad. Sci. U. S. A.* **1995**, *92*, 2081.
[19] D. Scribano, M. Sarshar, C. Prezioso, M. Lucarelli, A. Angeloni, C. Zagaglia, A. T. Palamara, C. Ambrosi, *Molecules* **2020**, *25*.
[20] J. Perez-Vilar, R. L. Hill, *J. Biol. Chem.* **1999**, *274*, 31751.
[21] M. Kesimer, J. K. Sheehan, *Methods Mol. Biol.* **2012**, *842*, 67.
[22] C. Werlang, G. Cárcarmo-Oyarce, K. Ribbeck, *Nat. Rev. Mater.* **2019**, *4*, 134.
[23] R. Mody, S. H. antara. Joshi, W. Chaney, *J. Pharmacol. Toxicol. Methods* **1995**, *33*, 1.
[24] H. Lis, N. Sharon, *Annu. Rev. Biochem.* **1986**, *VOL. 55*, 35.
[25] N. Sharon, *Biochim. Biophys. Acta - Gen. Subj.* **2006**, *1760*, 527.
[26] N. Shibuya, I. J. Goldstein, W. F. Broekaert, M. Nsimba-Lubaki, B. Peeters, W. J. Peumans, *J. Biol. Chem.* **1987**, *262*, 1596.
[27] W. C. Wang, R. D. Cummings, *J. Biol. Chem.* **1988**, *263*, 4576.
[28] R. J. Pieters, *Org. Biomol. Chem.* **2009**, *7*, 2013.
[29] M. S. Shet, M. Madaiah, M. I. Khan, *Biochim. Biophys. Acta (BBA)/Protein Struct. Mol.* **1988**, *954*, 44.
[30] H. De Boeck, F. G. Loontiens, H. Lis, N. Sharon, *Arch. Biochem. Biophys.* **1984**, *234*, 297.
[31] E. Laigre, C. Tiertant, D. Goyard, O. Renaudet, *ACS Omega* **2018**, *3*, 14013.
[32] R. T. Lee, Y. C. Lee, *Glycoconj. J.* **2000**, *17*, 543.
[33] Y. C. Lee, R. T. Lee, K. Rice, Y. Ichikawa, T. Wong, **1991**, *63*, 499.
[34] J. J. Lundquist, E. J. Toone, *Chem. Rev.* **2002**, *102*, 555.
[35] J. E. Gestwicki, C. W. Cairo, L. E. Strong, K. A. Oetjen, L. L. Kiessling, *J. Am. Chem. Soc.* **2002**, *124*, 14922.
[36] D. Deniaud, K. Julienne, S. G. Gouin, *Org. Biomol. Chem.* **2011**, *9*, 966.
[37] P. I. Kitov, D. R. Bundle, *J. Am. Chem. Soc.* **2003**, *125*, 16271.
[38] L. L. Kiessling, J. E. Gestwicki, L. E. Strong, *Curr. Opin. Chem. Biol.* **2000**, *4*, 696.
[39] Z. Y. Yao, J. Qin, J. S. Gong, Y. H. Ye, J. Y. Qian, H. Li, Z. H. Xu, J. S. Shi, *Carbohydr. Polym.* **2021**, *264*, 118015.
[40] V. Hořejší, O. Chaloupecká, J. Kocourek, *BBA - Gen. Subj.* **1978**, *539*, 287.
[41] S. Nishimura, K. Matsuoka, T. Furuike, S. Ishii, K. Kurita, **1991**, 4236.
[42] S. I. Nishimura, N. Nagahori, *Compr. Glycosci.* **2007**, 453.
[43] M. Nasiri Oskooie, M. Pooresmaeil, H. Namazi, *J. Polym. Res.* **2019**, *26*.

[44] M. Arcos-Hernandez, P. Naidjonoka, S. J. Butler, T. Nylander, H. Stålbrand, P. Jannasch, *Biomacromolecules* **2021**, *22*, 2338.
[45] S. Salem, M. Müller, B. Torger, A. Janke, K. J. Eichhorn, B. Voit, D. Appelhans, *Macromol. Chem. Phys.* **2015**, *216*, 182.
[46] A. Ghadban, L. Albertin, *Polymers (Basel).* **2013**, *5*, 431.
[47] M. R. Bockman, R. J. Dalal, R. Kumar, T. M. Reineke, *Polym. Chem.* **2021**, *12*, 4063.
[48] A. Ghadban, L. Albertin, R. W. Moussavou Mounguengui, A. Peruchon, A. Heyraud, *Carbohydr. Res.* **2011**, *346*, 2384.
[49] P. Kiran, S. Kumari, J. Dernedde, R. Haag, S. Bhatia, *New J. Chem.* **2019**, *43*, 16012.
[50] S. R. S. Ting, E. H. Min, P. Escalé, M. Save, L. Billon, M. H. Stenzel, *Macromolecules* **2009**, *42*, 9422.
[51] Y. Chen, G. Wulff, *Macromol. Chem. Phys.* **2001**, *202*, 3426.
[52] S.-I. Nishimura, K. Matsuoka, K. Kurita, *Macromolecules* **1990**, *23*, 4182.
[53] J. Tanaka, A. S. Gleinich, Q. Zhang, R. Whitfield, K. Kempe, D. M. Haddleton, T. P. Davis, S. Perrier, D. A. Mitchell, P. Wilson, *Biomacromolecules* **2017**, *18*, 1624.
[54] K. Godula, D. Rabuka, K. T. Nam, C. R. Bertozzi, *Angew. Chemie Int. Ed.* **2009**, *48*, 4973.
[55] Z. C. Chia, L. X. Yang, T. Y. Cheng, Y. J. Chen, H. L. Cheng, F. T. Hsu, Y. J. Wang, Y. Y. Chen, T. C. Huang, Y. S. Fang, C. C. Huang, *ACS Appl. Mater. Interfaces* **2021**, *13*, 52295.
[56] S. Lou, X. Zhang, M. Zhang, S. Ji, W. Wang, J. Zhang, C. Li, D. Kong, *Int. J. Nanomedicine* **2017**, *12*, 3653.
[57] D. Appelhans, H. Komber, M. A. Quadir, S. Richter, S. Schwarz, J. Van Der Vlist, A. Aigner, M. Müller, K. Loos, J. Seidel, K. F. Arndt, R. Haag, B. Voit, *Biomacromolecules* **2009**, *10*, 1114.
[58] V. Ladmiral, L. Monaghan, G. Mantovani, D. M. Haddleton, *Polymer (Guildf).* **2005**, *46*, 8536.
[59] K. Kurita, N. Masuda, S. Aibe, K. Murakami, S. Ishii, S. I. Nishimura, *Macromolecules* **1994**, *27*, 7544.
[60] S. Woerly, S. Fort, A. Heyraud, *Macromol. Rapid Commun.* **2007**, *28*, 1045.
[61] Y. Abdouni, G. Yilmaz, A. Monaco, R. Aksakal, C. R. Becer, *Biomacromolecules* **2020**, *21*, 3756.
[62] X. C. Liu, J. S. Dordick, *J. Polym. Sci. Part A Polym. Chem.* **1999**, *37*, 1665.
[63] C. Culture, **1999**, *23*, 881.
[64] M. G. García-Martín, C. Jiménez-Hidalgo, S. S. J. Al-Kass, I. Caraballo, M. V. De Paz, J. A. Galbis, *Polymer (Guildf).* **2000**, *41*, 821.
[65] M. G. Baek, R. Roy, *Biomacromolecules* **2000**, *1*, 768.
[66] R. Roy, M. G. Baek, *Rev. Mol. Biotechnol.* **2002**, *90*, 291.
[67] T. Miyata, T. Uragami, K. Nakamae, *Adv. Drug Deliv. Rev.* **2002**, *54*, 79.
[68] A. David, P. Kopecková, J. Kopeček, A. Rubinstein, *Pharm. Res.* **2002**, *19*, 1114.
[69] A. C. Roche, I. Fajac, S. Grosse, N. Frison, C. Rondanino, R. Mayer, M. Monsigny, *Cell. Mol. Life Sci.* **2003**, *60*, 288.
[70] Y. H. Yun, D. J. Goetz, P. Yellen, W. Chen, *Biomaterials* **2004**, *25*, 147.
[71] A. S. Gambaryan, E. Y. Boravleva, T. Y. Matrosovich, M. N. Matrosovich, H. D. Klenk, E. V. Moiseeva, A. B. Tuzikov, A. A. Chinarev, G. V. Pazynina, N. V. Bovin, *Antiviral Res.* **2005**, *68*, 116.
[72] E. Palomino, *Adv. Drug Deliv. Rev.* **1994**, *13*, 311.
[73] C. Fleming, A. Maldjian, D. Da Costa, A. K. Rullay, D. M. Haddleton, J. St John, P. Penny, R. C. Noble, N. R. Cameron, B. G. Davis, *Nat. Chem. Biol.* **2005**, *1*, 270.
[74] D. Grande, V. Fr, S. Baskaran, F. City, **2007**, *2*.
[75] Y. Wang, X. Zhang, Y. Han, C. Cheng, C. Li, *Carbohydr. Polym.* **2012**, *89*, 124.
[76] E. H. Song, M. J. Manganiello, Y. H. Chow, B. Ghosn, A. J. Convertine, P. S. Stayton, L. M. Schnapp, D. M. Ratner, *Biomaterials* **2012**, *33*, 6889.
[77] E. A. Vogler, **2016**, *105*, 1.
[78] F. Liu, Y. Wu, L. Bai, X. Peng, H. Zhang, Y. Zhang, P. An, S. Wang, G. Ma, X. Ba, *Polym. Chem.* **2018**, *9*, 5024.
[79] L. Liu, F. Zhou, J. Hu, X. Cheng, W. Zhang, Z. Zhang, G. Chen, N. Zhou, X. Zhu, *Macromol. Rapid Commun.* **2019**, *40*, 1.

[80] T. D. Young, W. T. Liau, C. K. Lee, M. Mellody, G. C. L. Wong, A. M. Kasko, P. S. Weiss, *ACS Appl. Mater. Interfaces* **2020**, *12*, 35767.
[81] S. Saxena, B. Kandasubramanian, *Int. J. Polym. Mater. Polym. Biomater.* **2021**, *0*, 1.
[82] H. Cai, Y. Xiang, Y. Zeng, Z. Li, X. Zheng, Q. Luo, H. Zhu, Q. Gong, Z. Gu, Y. Liu, H. Zhang, K. Luo, *Acta Pharm. Sin. B* **2021**, *11*, 544.
[83] M. S. Wadhwa, K. G. Rice, *J. Drug Target.* **1995**, *3*, 111.
[84] K. Bhattacharya, U. Kalita, N. K. Singha, *Polym. Chem.* **2022**, *13*, 1458.
[85] G. Wulff, J. Schmid, T. P. Venhoff, *Macromol. Chem. Phys.* **1996**, *197*, 1285.
[86] G. Wulff, L. Zhu, H. Schmidt, *Macromolecules* **1997**, *30*, 4533.
[87] S. K. Choi, M. Mammen, G. M. Whitesides, *J. Am. Chem. Soc.* **1997**, *119*, 4103.
[88] S. J. Novick, J. S. Dordick, *Chem. Mater.* **1998**, *10*, 955.
[89] E. J. Gordon, L. E. Strong, L. L. Kiessling, *Bioorganic Med. Chem.* **1998**, *6*, 1293.
[90] G. Wulff, H. Schmidt, L. Zhu, *Macromol. Chem. Phys.* **1999**, *200*, 774.
[91] J. M. G. Cowie, V. Arrighi, **2007**, 520.
[92] P. Theato, H.-A. Klok, *Functional Polymers by Post-Polymerization Modification*, **2013**.
[93] S. J. Richards, M. W. Jones, M. Hunaban, D. M. Haddleton, M. I. Gibson, *Angew. Chemie - Int. Ed.* **2012**, *51*, 7812.
[94] I. Pramudya, H. Chung, *Biomater. Sci.* **2019**, *7*, 4848.
[95] L.-C. You, F.-Z. Lu, Z.-C. Li, W. Zhang, F.-M. Li, *Macromolecules* **2003**, *36*, 1.
[96] K. Aoi, K. Tsutsumiuchi, E. Aoki, M. Okada, *Macromolecules* **1996**, *29*, 4456.
[97] T. Taguchi, A. Kishida, N. Sakamoto, M. Akashi, *J. Biomed. Mater. Res.* **1998**, *41*, 386.
[98] J. Wang, I. Tomita, **2001**, 4294.
[99] D. Grande, S. Baskaran, E. L. Chaikof, *Macromolecules* **2001**, *34*, 1640.
[100] W. Ye, S. Wells, J. M. Desimone, *J. Polym. Sci. Part A Polym. Chem.* **2001**, *39*, 3841.
[101] F. D'Agosto, M. T. Charreyre, C. Pichot, B. Mandrand, *Macromol. Chem. Phys.* **2002**, *203*, 146.
[102] A. B. Lowe, B. S. Sumerlin, C. L. McCormick, *Polymer (Guildf).* **2003**, *44*, 6761.
[103] K. Ohno, Y. Tsujii, T. Fukuda, *J. Polym. Sci. Part A Polym. Chem.* **1998**, *36*, 2473.
[104] S. R. S. Ting, G. Chen, M. H. Stenzel, *Polym. Chem.* **2010**, *1*, 1392.
[105] K. C. Sheng, M. Kalkanidis, D. S. Pouniotis, S. Esparon, C. K. Tang, V. Apostolopoulos, G. A. Pietersz, *Eur. J. Immunol.* **2008**, *38*, 424.
[106] J. Ishii, M. Chikae, M. Toyoshima, Y. Ukita, Y. Miura, Y. Takamura, *Electrochem. commun.* **2011**, *13*, 830.
[107] M. Ahmed, P. Wattanaarsakit, R. Narain, *Polym. Chem.* **2013**, *4*, 3829.
[108] J. Lazar, H. Park, R. R. Rosencrantz, A. Böker, L. Elling, U. Schnakenberg, *Macromol. Rapid Commun.* **2015**, *36*, 1472.
[109] H. Park, S. Walta, R. R. Rosencrantz, A. Körner, C. Schulte, L. Elling, W. Richtering, A. Böker, *Polym. Chem.* **2016**, *7*, 878.
[110] T. J. Paul, S. Rübel, M. Hildebrandt, A. K. Strzelczyk, C. Spormann, T. K. Lindhorst, S. Schmidt, *ACS Appl. Mater. Interfaces* **2019**, *11*, 26674.
[111] J. Li, Y. Zhang, C. Cai, X. Rong, M. Shao, J. Li, C. Yang, G. Yu, *Biomater. Sci.* **2020**, *8*, 189.
[112] S. R. Salem, J. L. Sullivan, P. D. Topham, B. J. Tighe, *Polym. Bull.* **2020**, *77*, 3143.
[113] T. J. Paul, A. K. Strzelczyk, S. Schmidt, *Macromol. Biosci.* **2021**, *21*, 1.
[114] Y. Miura, T. Ikeda, K. Kobayashi, *Biomacromolecules* **2003**, *4*, 410.
[115] Y. Miura, H. Sato, T. Ikeda, H. Sugimura, O. Takai, K. Kobayashi, *Biomacromolecules* **2004**, *5*, 1708.
[116] E. W. Pugh, L. R. Johnson, J. H. Palmer, *IBM's 360 Early 370 Syst.* **2020**, 906.
[117] Y. Miura, T. Ikeda, N. Wada, H. Sato, K. Kobayashi, *Green Chem.* **2003**, *5*, 610.
[118] G. Wulff, G. Clarkson, *Macromol. Chem. Phys.* **1994**, *195*, 2603.
[119] R. Roy, F. D. Tropper, A. Romanowska, *Bioconjug. Chem.* **1992**, *3*, 256.
[120] V. S. Zaitsev, D. S. Filimonov, I. A. Presnyakov, R. J. Gambino, B. Chu, *J. Colloid Interface Sci.* **1999**, *212*, 49.
[121] N. Pimpha, S. Chaleawlert-Umpon, P. Sunintaboon, *Polymer (Guildf).* **2012**, *53*, 2015.

[122] W. M. J. Kloosterman, S. Roest, S. R. Priatna, E. Stavila, K. Loos, *Green Chem.* **2014**, *16*, 1837.
[123] K. Matsuoka, H. Yamaguchi, T. Koyama, K. Hatano, D. Terunuma, *Tetrahedron Lett.* **2010**, *51*, 2529.
[124] Y. Zhao, Y. Zhang, C. Wang, G. Chen, M. Jiang, *Biomacromolecules* **2017**, *18*, 568.
[125] W. J. Zhou, M. E. Wilson, M. J. Kurth, Y. Lo Hsieh, J. M. Krochta, C. F. Shoemaker, *Macromolecules* **1997**, *30*, 7063.
[126] T. Tanaka, G. Inoue, S. I. Shoda, Y. Kimura, *J. Polym. Sci. Part A Polym. Chem.* **2014**, *52*, 3513.
[127] M. Ambrosi, A. S. Batsanov, N. R. Cameron, B. G. Davis, J. A. K. Howard, R. Hunter, *J. Chem. Soc. Perkin Trans. 1* **2002**, 45.
[128] A. Adharis, D. Vesper, N. Koning, K. Loos, *Green Chem.* **2018**, *20*, 476.
[129] J. Bernard, X. Hao, T. P. Davis, C. Barner-Kowollik, M. H. Stenzel, *Biomacromolecules* **2006**, *7*, 232.
[130] R. Narain, S. P. Armes, *Biomacromolecules* **2003**, *4*, 1746.
[131] K. Kobayashi, H. Sumitomo, Y. Ina, **1985**, *17*, 567.
[132] T. Tanaka, *Trends Glycosci. Glycotechnol.* **2016**, *28*, E101.
[133] X. Jiang, A. Housni, G. Gody, P. Boullanger, M. T. Charreyre, T. Delair, R. Narain, *Bioconjug. Chem.* **2010**, *21*, 521.
[134] S. Quan, Y. Wang, A. Zhou, P. Kumar, R. Narain, *Biomacromolecules* **2015**, *16*, 1978.
[135] K. Ohno, T. Fukuda, H. Kitano, *Macromol. Chem. Phys.* **1998**, *199*, 2193.
[136] J. Kim, Y. K. Pak, K. H. Chun, J. E. N. Shin, **2001**, *22*, 758.
[137] S. A. Chambers, S. D. Townsend, *MethodsX* **2020**, *7*.
[138] J. Tang, E. Ozhegov, Y. Liu, D. Wang, X. Yao, X. L. Sun, *ACS Macro Lett.* **2017**, *6*, 107.
[139] J. Li, Y. Zhang, C. Cai, X. Rong, M. Shao, J. Li, C. Yang, G. Yu, *Biomater. Sci.* **2020**, *8*, 189.
[140] K. K. Chan, Q. Lei, J. Tang, X. L. Sun, *RSC Adv.* **2020**, *10*, 38561.
[141] L. M. Likhosherstov, O. S. Novikova, V. A. Derevitskaja, N. K. Kochetkov, *Carbohydr. Res.* **1986**, *146*, 8.
[142] L. M. Likhosherstov, O. S. Novikova, V. N. Shibaev, *Dokl. Akad. Nauk* **2002**, *383*, 500.
[143] L. M. Likhosherstov, O. S. Novikova, V. N. Shibaev, *Dokl. Chem.* **2003**, *389*, 73.
[144] L. M. Likhosherstov, O. S. Novikova, A. O. Zheltova, V. N. Shibaev, *Russ. Chem. Bull.* **2004**, *53*, 709.
[145] M. Bejugam, S. L. Flitsch, *Org. Lett.* **2004**, *6*, 4001.
[146] M. A. Brun, M. D. Disney, P. H. Seeberger, *ChemBioChem* **2006**, *7*, 421.
[147] S. Muthukrishnan, M. Nitschke, S. Gramm, Z. Özyürek, B. Voit, C. Werner, A. H. E. Müller, *Macromol. Biosci.* **2006**, *6*, 658.
[148] S. G. Lee, J. M. Brown, C. J. Rogers, J. B. Matson, C. Krishnamurthy, M. Rawat, L. C. Hsieh-Wilson, *Chem. Sci.* **2010**, *1*, 322.
[149] F. Jacobi, A. C. De La Calle, S. Boden, A. Grafmüller, L. Hartmann, S. Schmidt, *Biomacromolecules* **2018**, *19*, 3479.
[150] T. Maver, T. Mohan, L. Gradišnik, M. Finšgar, K. S. Kleinschek, U. Maver, *Front. Chem.* **2019**, *7*.
[151] M. T. Cook, S. L. Smith, V. V. Khutoryanskiy, *Chem. Commun.* **2015**, *51*, 14447.
[152] S. Rosencrantz, J. S. J. Tang, C. Schulte-Osseili, A. Böker, R. R. Rosencrantz, *Macromol. Chem. Phys.* **2019**, *220*, 1.
[153] Q. Yang, C. Kaul, M. Ulbricht, *Langmuir* **2010**, *26*, 5746.
[154] S. P. Authimoolam, A. L. Vasilakes, N. M. Shah, D. A. Puleo, T. D. Dziubla, *Biomacromolecules* **2014**, *15*, 3099.
[155] S. P. Authimoolam, T. D. Dziubla, *Polymers (Basel).* **2016**, *8*.
[156] K. Feng, L. Peng, L. Yu, Y. Zheng, R. Chen, W. Zhang, G. Chen, G. Chen, *ACS Appl. Mater. Interfaces* **2020**, *12*, 27632.
[157] C. Von Der Ehe, C. Weber, M. Gottschaldt, U. S. Schubert, *Prog. Polym. Sci.* **2016**, *57*, 64.
[158] H. Uzawa, H. Ito, M. Izumi, H. Tokuhisa, K. Taguchi, N. Minoura, *Tetrahedron* **2005**, *61*, 5895.
[159] H. Uzawa, H. Ito, P. Neri, H. Mori, Y. Nishida, *ChemBioChem* **2007**, *8*, 2117.
[160] C. Boyer, A. Bousquet, J. Rondolo, M. R. Whittaker, M. H. Stenzel, T. P. Davis, *Macromolecules*

2010, *43*, 3775.
[161] K. Godula, C. R. Bertozzi, *J. Am. Chem. Soc.* **2010**, *132*, 9963.
[162] A. Pich, W. Richtering, *Chemical Design of Responsive Microgels*, Vol. 53, **2010**.
[163] M. E. SantosMiranda, C. Marcolla, C. A. Rodriguez, H. M. Wilhelm, M. R. Sierakowski, T. M. BelleBresolin, R. Alves de Freitas, *Polym Int* **2006**, *55*, 961.
[164] Z. Cai, A. Sasmal, X. Liu, S. A. Asher, *ACS Sensors* **2017**, *2*, 1474.
[165] M. Ahmed, B. F. L. Lai, J. N. Kizhakkedathu, R. Narain, *Bioconjug. Chem.* **2012**, *23*, 1050.
[166] M. Ahmed, P. Wattanaarsakit, R. Narain, *Eur. Polym. J.* **2013**, *49*, 3010.
[167] Z. Dai, T. Ngai, *J. Polym. Sci. Part A Polym. Chem.* **2013**, *51*, 2995.
[168] Y. Guan, Y. Zhang, *Soft Matter* **2011**, *7*, 6375.
[169] R. H. Pelton, P. Chibante, *Colloids and Surfaces* **1986**, *20*, 247.
[170] X. Wu, R. H. Pelton, a E. Hamielec, D. R. Woods, W. McPhee, *Colloid Polym. Sci.* **1994**, *272*, 467.

2 Optimization of the Microwave Assisted Glycosylamines Synthesis Based on a Statistical Design of Experiments Approach

Abstract

Glycans carry a vast range of functions in nature. Utilizing their properties and functions in form of polymers, coatings or glycan derivatives for various applications makes the synthesis of modified glycans crucial. Since amines are easy to modify for subsequent reactions, we investigated regioselective amination conditions of different saccharides. Amination reactions were performed according to Kochetkov and Likhoshertov and accelerated by microwave irradiation. We optimized the synthesis of glycosylamines for *N*-acetyl-d-galactosamine, D-lactose, D-glucuronic acid and L-(−)-fucose using the design of experiments (DoE) approach. DoE enables efficient optimization with limited number of experimental data. A DoE software generated a set of experiments where reaction temperature, concentration of carbohydrate, nature of aminating agent and solvent were investigated. We found that the synthesis of glycosylamines significantly depends on the nature of the carbohydrate and on the reaction temperature. There is strong indication that high temperatures are favored for the amination reaction.

2.1 Introduction

Glycosylation is a crucial modification of biomolecules involved in almost all biological processes [1–5]. Glycans may act as scaffolds for mechanical stabilization, as cell-surface coating, enabling cellular crosstalk and have various functions including in diseases [6–11]. Especially for the latter, potent inhibitors of glycan-binding proteins (lectins) are sought after as well as glycan scaffolds for trapping pathogens [12–14]. For all examples, the glycans may be chemically modified and presented in polymers [15–17], on surfaces [18–22], on nanoparticles [23–25] or as (multivalent) glycan derivatives [26–29] with increased binding affinity [30–32]. Prerequisites for this are straight forward chemical processes that yield regioselective modifications of glycans without hampering the natural recognition processes. For this, very diverse chemical routes have been employed which can be roughly distinguished between protecting group dependent and protecting group free or even enzymatic routes [33–36]. Protecting group free routes in general require less synthesis steps, but the

reaction conditions and purification must be elaborated carefully. However, we utilized a protecting group free process to regioselectively insert an amino group into saccharides at the C1-position which was subsequently modified into a methacrylamide to generate glycopolymers [37,38]. From literature and our work, amination seems a rather robust process, but it turned out that chosen reaction conditions influence the yield substantially. Interestingly, this effect was diverse for different carbohydrates. This amination was introduced by Kochetkov and later modified by Likhoshertov [39–42]. The Kochetkov reaction is performed with ammonium carbonate whereas the amination according to Likhoshertov employs ammonium carbamate as the aminating agent. Significant advantages of these methods are enabling of protecting group free synthesis routes, the regioselectivity and the applicability on various oligosaccharides with only few and cost-efficient reagents. Essentially, a saccharide is stirred in solvent with an excess amount of amination agent. It is a straightforward approach to regioselectively insert a single functional group into various glycans and enables subsequent coupling to generate glycoconjugates. The Kochetkov amination is further facilitated by employing the advantageous features of microwave assisted synthesis. The reaction can be tremendously accelerated by microwave irradiation, shortening the initial reaction time of 5 d to 90 min [18,43]. Moreover, the use of microwave irradiation allows the tenfold reduction of the amount of ammonium salt, facilitating homogeneous suspending of starting material and purification [43]. To the best of our knowledge, the amination according to Likhoshertov has not been performed under microwave irradiation yet. Here, we investigate this synthesis using microwave irradiation as well. As the syntheses have a broad substrate scope and are only a one-step procedure, they seem a very worthwhile approach to yield glycan derivatives for follow-up functionalization to achieve glycomonomers, biosensor coatings and others. We chose a statistical approach to efficiently determine the optimal amination conditions of saccharides and to study the use of design of experiment (DoE) for optimization of glycochemistry reactions.

Design of experiments is a valuable tool to limit the amount of data needed to find optimal experimental conditions. Any method to optimize a synthesis of interest starts by identifying the parameters of the reaction, namely, temperature, concentration or reaction time. In a classical optimization setting, all but one parameter are kept constant at a time, and the result of the experiment, such as yield or purity, is improved. This strategy, referred to as “one-variable-at-a-time” (OVAT), can be unnecessarily labor-intensive and fails to capture correlations between the input parameters. If these input factors influence each other strongly, OVAT might not find the true optimum of the experimental conditions and the result depends on the initial reaction conditions selected [44]. To circumvent this obstacle, we use a statistical design of experiments approach as an alternative to the OVAT method. DoE aims to evenly sample all possible values for the input parameters and find a mathematical relationship between them and the outcome of the experiment. Although it has been

known since the early 1900s, it has only recently found wide-spread application [45–51]. DoE was previously employed to optimize synthetic procedures with a small number of experiments [50–55]. A successful application of DoE guides the selection of further experiments and allows the localization of most promising sets of features. It has become increasingly accessible to researchers through the advent of user-friendly software options such as MODDE or JMP.

Contrary to former studies, where amination was mostly optimized for one specific carbohydrate [18,43,56], we show the significance of and possible interactions between selected parameters for each respective saccharide as the yield and optimal reaction conditions are strongly determined by the nature of chosen saccharide [18,40,43,56–58]. For instance, Likhoshertov et al. yielded 81% aminated d-glucuronic acid, while the amination of l-fucose resulted in a yield of 52% with the same reaction conditions [40]. By utilizing the DoE software MODDE, we optimized the reaction conditions for four selected saccharides: *N*-acetyl-D-galactosamine (GalNAc), D-lactose (Lac), D-glucuronic acid (GlcA) and L-(−)fucose (Fuc). These saccharides are important for biomolecular interactions on the one hand and, on the other, they resemble an overview of the most common chemical properties of non-modified glycans such as *N*-acetyl glycans, disaccharides, uronic acids and desoxy-glycans.

2.2 Results and Discussion

2.2.1 Optimizing the Amination of Oligosaccharides

We optimized the synthesis of glycosylamines using a statistical DoE approach. As our synthesis route, we chose the amination methods of Kochetkov and Likhoshertov assisted by microwave irradiation (Scheme 2.1).

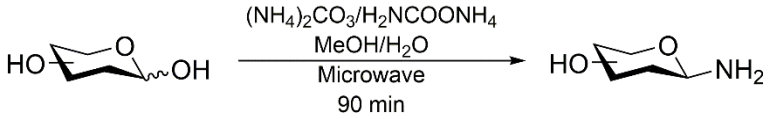

Scheme 2.1. Protecting group free and microwave-assisted synthesis route for amination of free saccharides according to Kochetkov and Likhoshertov in methanol or water with a 5-fold excess of ammonium salt.

To promote an equal distribution of microwave irradiation for all experiments, the volume of solvent was kept constant. We chose to vary reaction temperature, concentration of starting material, solvent and ammonium salt as our quantitative and qualitative parameters (Table 2.1). Ranges of

temperature and concentration were set to 30–60 °C and 10–100 mg/mL, respectively, as the conditions of previous studies mostly lie within these ranges. Former studies showed successful amination of saccharides in water, dimethyl sulfoxide and methanol [18,39,43,56,58–61]. We tested water and methanol as solvent, since they are more readily removed by evaporation than dimethyl sulfoxide. In addition, ammonium salts and unmodified oligosaccharides generally dissolve better in water than in organic solvents, which might be beneficial for reaction and yield. The other qualitative parameters are the aminating agents ammonium carbonate and ammonium carbamate.

Table 2.1. Reaction conditions and yields of amination. Highest yields are indicated by underscores.

Exp No	T (°C)	(mg/mL)	Salt	Solvent	Yield (%)			
					Am-I $GalNAcNH_2$	Am-II $LacNH_2$	Am-III $GlcANH_2$	Am-IV $FucNH_2$
01	60	10	$(NH_4)_2CO_3$	MeOH	<u>64.2</u>	<u>83.6</u>	7	60.5
02	30	100	$(NH_4)_2CO_3$	MeOH	53.7	33	0.9	12.4
03	60	100	$(NH_4)_2CO_3$	MeOH	42.2	68	33.6	21.8
04	30	40	$(NH_4)_2CO_3$	MeOH	43.1	46.4	2.1	45
05	40	10	$(NH_4)_2CO_3$	MeOH	30.9	20.8	1.6	25
06	30	10	$H_2NCOONH_4$	MeOH	33.6	11.8	3.3	42.6
07	60	10	$H_2NCOONH_4$	MeOH	51.6	81.4	12	<u>69.8</u>
08	30	100	$H_2NCOONH_4$	MeOH	44.9	27.4	3	32.4
09	60	100	$H_2NCOONH_4$	MeOH	41.9	79.2	23.6	38.8
10	45	55	$H_2NCOONH_4$	MeOH	57.4	79.7	53.1	26
11	30	10	$(NH_4)_2CO_3$	H_2O	39.1	16.7	16.8	16.2
12	60	10	$(NH_4)_2CO_3$	H_2O	27.3	26.2	35.7	18.2
13	30	100	$(NH_4)_2CO_3$	H_2O	26.5	11.5	37.3	9
14	60	70	$(NH_4)_2CO_3$	H_2O	37.8	42.4	54.6	10.3
15	50	100	$(NH_4)_2CO_3$	H_2O	20.4	44.3	51.9	8.4
16	30	10	$H_2NCOONH_4$	H_2O	41.2	8.8	18.3	6.9
17	60	100	$H_2NCOONH_4$	H_2O	50.5	30.2	46.8	12.4
18	30	70	$H_2NCOONH_4$	H_2O	29.4	13.5	47.8	8.7
19	60	40	$H_2NCOONH_4$	H_2O	44.2	21.5	44.4	17.1
20	50	10	$H_2NCOONH_4$	H_2O	30	20.1	46.1	11.1
21	40	100	$H_2NCOONH_4$	H_2O	34.4	24.7	40.3	8.7
22a	45	55	$H_2NCOONH_4$	H_2O	17	32.5	77.7	33.3
22b	45	55	$H_2NCOONH_4$	H_2O	20.4	74.1	77	41.8
22c	45	55	$H_2NCOONH_4$	H_2O	18	62.5	<u>81.6</u>	31.2

We tested the optimization conditions on four chosen saccharides: (I) *N*-acetyl-D-galactosamine (GalNAc), (II) D-lactose (Lac), (III) D-glucuronic acid (GlcA) and (IV) L-(−)-fucose (Fuc) (Figure 2.1).

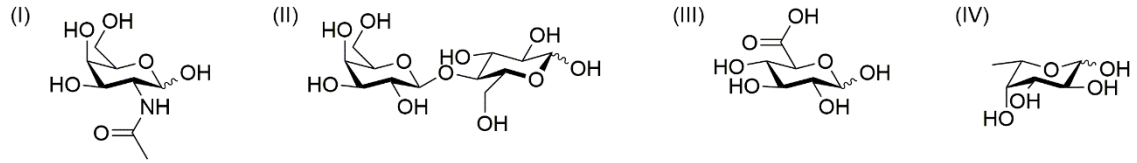

Figure 2.1. Mono- and disaccharides chosen for the optimization of amination reactions.

The products were not isolated but solvents were fully and ammonium salts were partially or mostly removed under high vacuum. We determined the yields by ^{1}H-NMR spectroscopy in deuterium oxide. Here, the peak of the anomeric proton of glycosylamine was analyzed in relation to a known peak that both starting material and glycosylamine share, for example, the methyl moiety of GalNAc/GalNAcNH$_2$. NMR spectroscopy offers fast and easy analysis without requiring the isolation of products and is sufficient for the optimization process. However, it is known that glycosylamines can hydrolyze in D_2O which could distort the actual yield. The hydrolysis rate is decreased with higher pH value [59]. Experiments performed with high amounts of aminating agents can lead to residuals of them after drying and therefore to higher pH values. Due to the basic conditions, less hydrolysis might occur which does not distort the yield as much as experiments performed with low amounts of ammonium salts.

We used the DoE software MODDE to design a set of experiments with varied reaction parameters for optimization. MODDE provides a summary of fit with four values which estimate how well the respective model works. R^2 indicates how well the model fits the data and should be of large value for a good model. An R^2 of 0.5 presents a model with rather low significance. The prediction value Q^2 estimates the predictive power of the model and is the most sensitive indication. Here, a value above 0.1 represents a significant model whereas a value above 0.5 expresses a good model. However, Q^2 should not deviate from R^2 by more than 0.3. A model validity of 1.0 represents a perfect model. If the model validity is below 0.25, there are indications of statistically significant problems with the model. Values above 0.25 show that the model error is in the same range as the pure experimental error. The reproducibility value represents the experimental error according to the deviation of responses of repeated experiments and should be above 0.25. MODDE displays a coefficient plot where the significance of chosen factors and their interactions is shown (Supporting Information). We removed non-significant terms from the model.

2.2.2 Design of Experiment Approach

The amination of GalNAc was investigated as this saccharide is not only a model compound for 2-*N*-acetylated sugars, but also an important saccharide in mucin-like *O*-glycosylation. In the

experimental set for GalNAc, we recognized the data of the experiments Am-I-06 and Am-I-10 (Table **2.1**) as outliers and removed them from the model. The summary of fits of GalNAc (Figure 2a) presents an R^2 value of 0.80 and a Q^2 value of 0.50, which indicates a good model. The model validity of 0.27 is rather low; the reproducibility displays a very good value of 0.98. The model validity might be low due to the great reproducibility value. Overall, this model of GalNAc is significant. Significant terms according to MODDE are temperature, concentration, both aminating agents ammonium carbonate and carbamate, the solvents methanol and water and the quadratic term of temperature × temperature, concentration × concentration, ammonium carbonate × water, ammonium carbamate × methanol and ammonium carbamate × water (Figure 2.2b). The 4D contour plot represents predicted response values as a function of chosen (and significant) factors. Figure 2.2c shows the yield as a function of concentration (Y-axis) and temperature (X-axis) for both ammonium salts and both solvents, respectively. According to this, temperature and concentration greatly influence the yield. Ammonium carbonate affects the yield only when different solvents are compared. Amination with ammonium carbamate is similar in both water and methanol. We found that the highest yield (64.2%) is achieved at the highest chosen temperature (60 °C) and at the lowest tested concentration (10 mg/mL) with ammonium carbonate and methanol. MODDE calculated optimized conditions with exactly the same reaction conditions and a predicted yield of 54.7%. The predicted yield differs from the achieved one by more than the error deviation; additionally, the calculated optimized yield is lower than the highest yield achieved. This indicates statistical problems of this model. Considering the quantity of varied parameters, a rather small set of experiments has been conducted. A larger number of experiments can improve the model. Since the experimental conditions with methanol and ammonium carbonate proved to be superior, we suggest the collecting of additional data for mentioned condition to further improve the model and optimize the amination conditions for GalNAc.

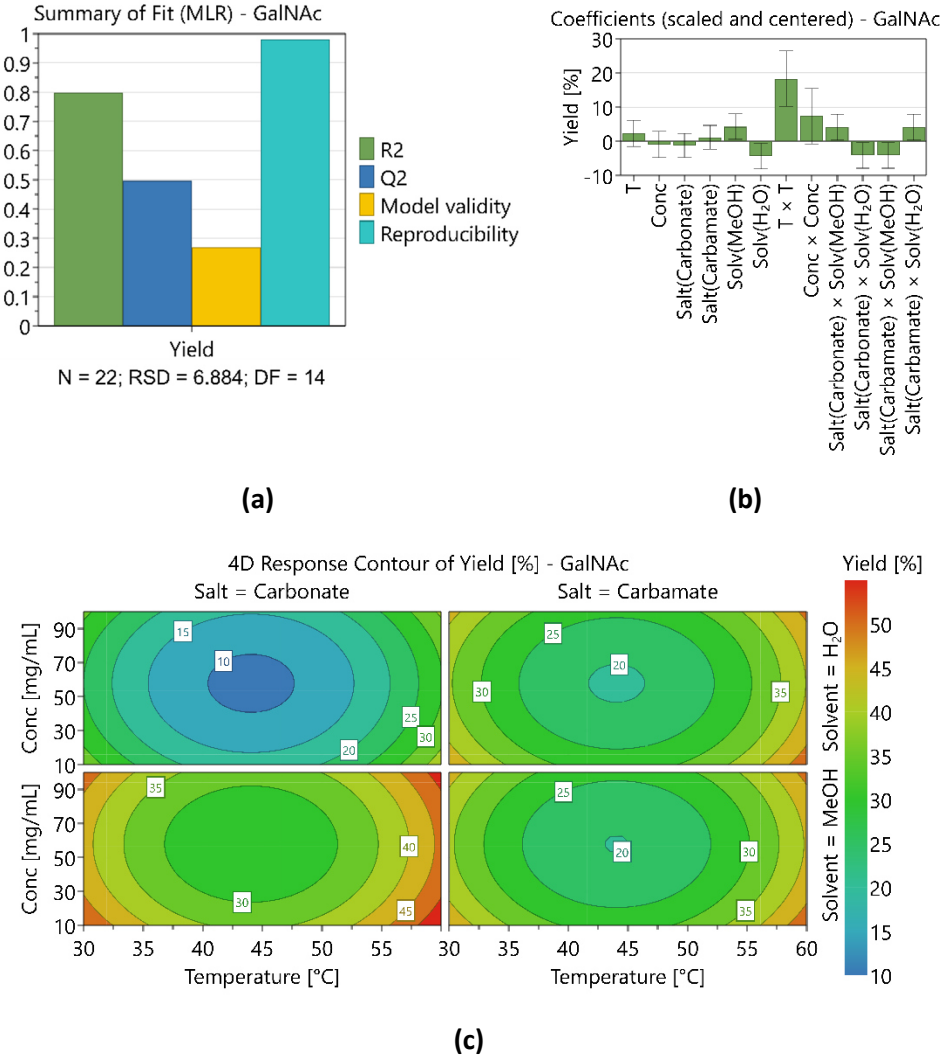

Figure 2.2. Plots of the model for GalNAc generated by MODDE: (**a**) Summary of fit shows a rather low significance of the model; (**b**) plot of coefficient values for scaled and centered factors shows significant factors according to the model; (**c**) the 4D response contour plot of yield predicts yields of amination in dependence on qualitative and quantitative factors.

Next, we investigated the reaction of Lac, which is our model compound for disaccharides and also an important ligand for lectins, mostly due to the terminal Gal residue. The summary of fits of the model for Lac shows good values with R^2 = 0.75 and Q^2 = 0.59 (Figure 3a). It has an excellent model validity of 0.97 and a low reproducibility of 0.29. Thus, we understand the model for Lac has high significance. Significant terms are temperature, concentration, the solvents methanol and water, the quadratic term of concentration × concentration, temperature × methanol and temperature × water (Figure 2.3b). Hence, the amination of Lac is less dependent on the nature of ammonium salt than on the other factors. The 4D response contour plot for Lac shows that the yield increases with rising temperature and with a concentration converging at 58.3 mg/mL (Figure 2.3c). We can clearly observe a strong dependence of the yield on temperature and less on concentration. Furthermore, the plot indicates that temperatures above 60 °C may lead to even better yields. Surprisingly, the solvent

methanol is by far superior to water even though the solubility of Lac is poor in methanol. We conclude that the solubility of a saccharide is not a determining factor for the amination according to Kochetkov and Likhoshertov. As well as for GalNAc, we obtained the highest yield for Lac (83.6%) at the highest temperature (60 °C) and the lowest concentration (10 mg/mL) with ammonium carbonate and methanol. Calculated optimized conditions for Lac are a temperature of 60 °C and a concentration of 58 mg/mL with ammonium carbonate and methanol. After conducting the optimized experiment, we could indeed increase the yield to 91.1%. The deviation from the predicted yield of 100.4% lies within the experimental error. The prediction lies above 100% as solely the target was set to 100% and not the maximum (the maximum cannot equal the target in MODDE). Overall, the DoE approach successfully improved the yield of aminated Lac.

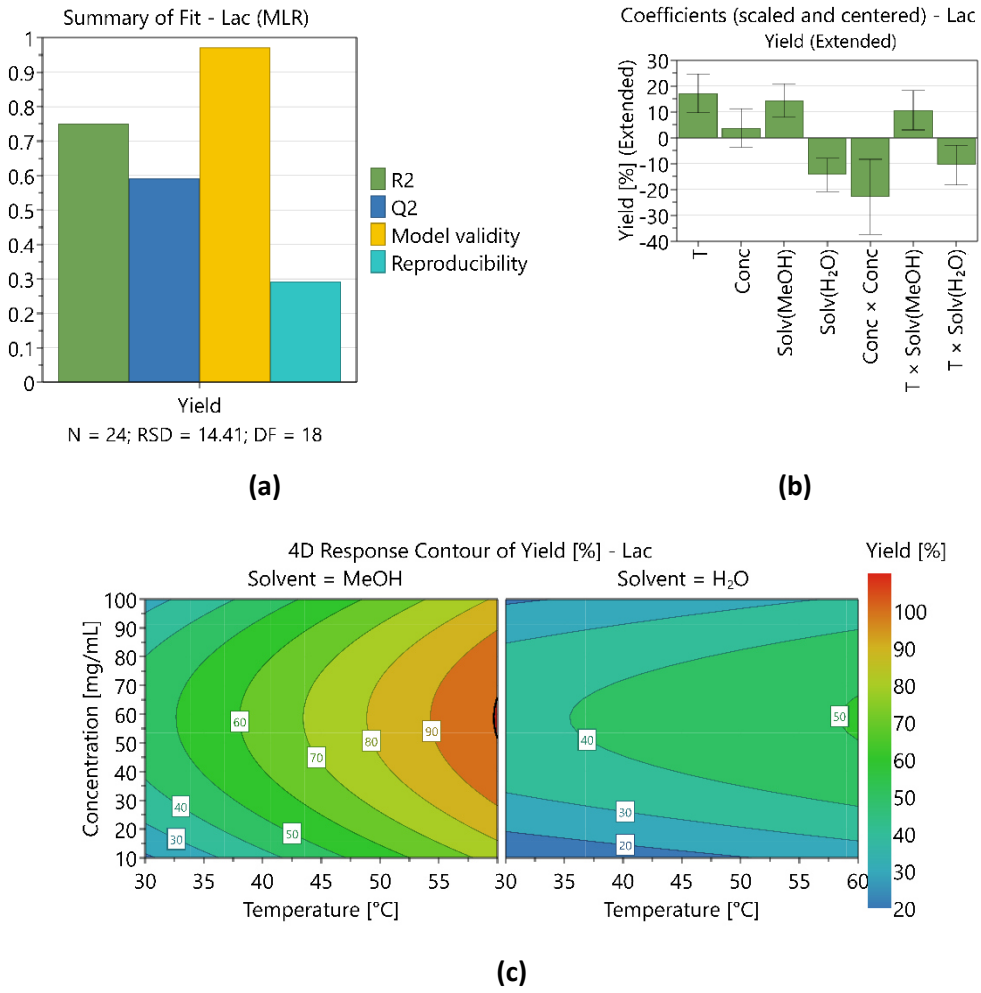

Figure 2.3. Plots of the model for Lac generated by MODDE: (**a**) Summary of fit represents a good model; (**b**) plot of coefficient values for scaled and centered factors shows significant factors according to the model; (**c**) the 4D response contour plot of yield predicts yields of amination in dependence on qualitative and quantitative factors.

GlcA is a uronic acid and therefore our model compound for this class of saccharides. After amination a zwitter-ionic compound is produced. In humans, GlcA is mostly found in

glucosaminoglycans. The summary of fits for GlcA displays excellent values of R^2 = 0.94 and Q^2 = 0.84 (Figure 2.4a). In comparison, the model validity is rather low (0.39) which may be due to the high reproducibility value of 0.99 and not due to a real lack of fit. Significant terms for GlcA are temperature, concentration, both aminating agents ammonium carbonate and ammonium carbamate, the solvents methanol and water, the quadratic term of temperature × temperature, concentration × concentration, temperature × methanol, temperature × water, concentration × ammonium carbonate and concentration × ammonium carbamate (Figure 2.4b). The amination of GlcA seems strongly dependent on temperature, concentration and choice of solvent. Interestingly, for GlcA further factors are significant including the nature of ammonium salt and its dependency on the concentration. From the 4D contour plot (Figure 2.4c), it is evident that water works better than methanol for the amination of GlcA. Regarding the aminating agent, ammonium carbamate appears to be the preferred choice. In experiments, the highest yield (81.6%) was achieved at 45 °C, 55 mg/mL with ammonium carbamate in water. Optimized reactions conditions are 47 °C, 59 mg/mL, ammonium carbamate and water with a predicted yield of 73.8%. The optimized experimental conditions resulted in a yield of 60.3%. The predicted yield is lower than the highest yield found in previous experiments and, furthermore, does not correlate to the yield found. This hints at statistical problems of the model even though the prediction value Q^2 was very good. Moreover, in this model yields above 73.8% are not achievable although Ghadban et al. did attain yields of up to 89% [56]. We suggest a larger set of experiments and a wider range of reaction parameters for the reaction conditions with water and ammonium carbamate to improve the model.

Our model compound for desoxy-sugars is 6-desoxy galactose, better known as Fuc. Fuc-based derivatives could, for example, be important for inhibiting the formation of *Pseudomonas aeruginosa* biofilms. Additionally, it is a very abundant sugar in human milk oligosaccharides. The summary of fits for Fuc presents a good R^2 value of 0.67 and a Q^2 value of 0.40 (Figure 2.5a). The model validity is 0.57 and the reproducibility has a high value of 0.90. Thus, this is a model of lower significance. Although the histogram of the Fuc experiments exhibits positive skewness (Supplementary Materials), no transformation was performed as the model for Fuc produced better values than without transformation. MODDE displays the significant terms temperature, concentration, both salts ammonium carbonate and carbamate, the solvents methanol and water, the square term of temperature × concentration, temperature × methanol, temperature × water, concentration × methanol and concentration × water (Figure 2.5b). Thus, the amination of Fuc greatly depends on temperature, concentration and nature of solvent. Furthermore, the choice of ammonium salt and the influence of temperature and concentration on the solvents affect the yield, too. In the 4D contour plot of yield (Figure 2.5c), when comparing the solvents, we see that overall methanol leads to higher yields. Water seems to work poorly for the amination of Fuc. Regarding the aminating agent, the

highest yield is obtained with ammonium carbamate. Yield increases with rising temperature and decreasing concentration. Hence, a further increase of the temperature and decrease of the concentration might improve the yield. We obtained the highest yield of 69.8% at 60 °C and 10 mg/mL with ammonium carbamate and methanol. Optimized amination conditions for Fuc are the exact reaction conditions with a predicted yield of 63.4%. The predicted yield is lower than the already obtained yield but lies within the experimental error. This still indicates a flawed model, which correlates to the rather low prediction value Q^2. However, the optimized reaction conditions coincide with the performed conditions with the best result. To further optimize the amination of Fuc, the model should be improved by producing more data of experiments where methanol is used as the solvent.

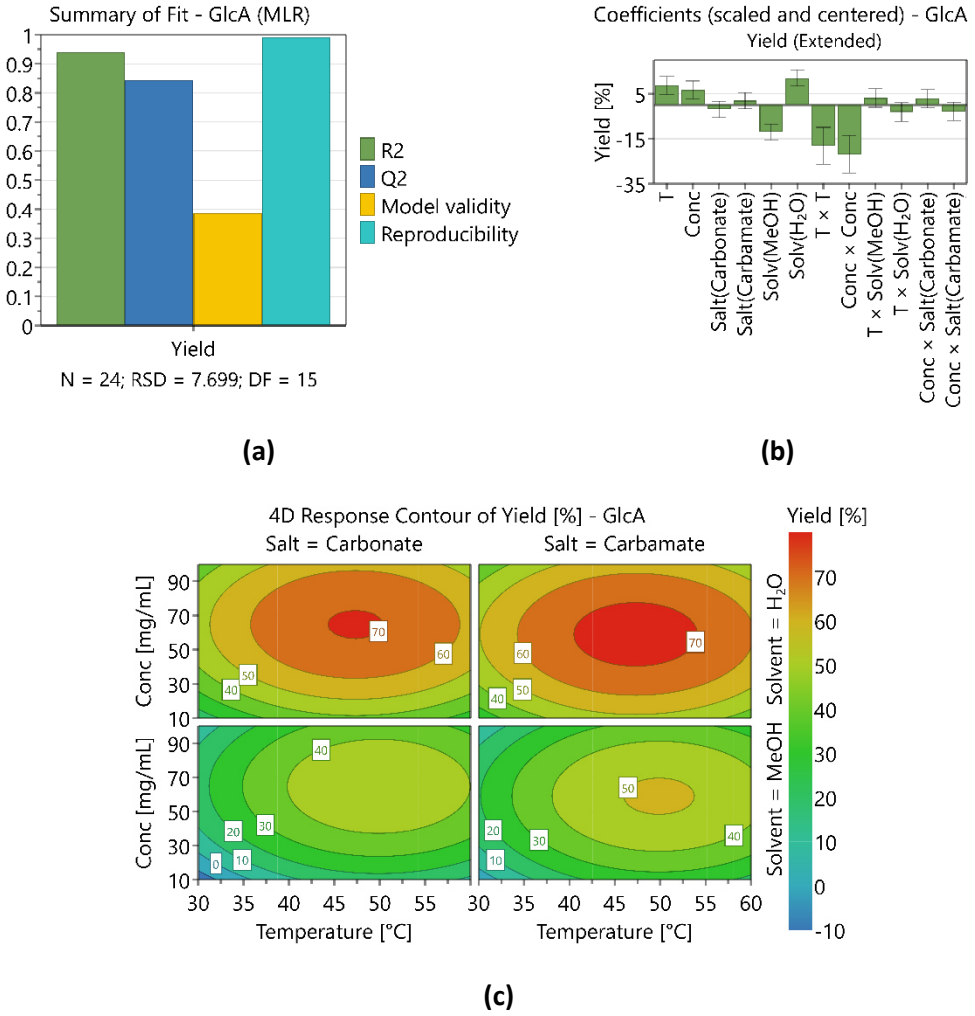

Figure 2.4. Plots of the model for GlcA generated by MODDE: (a) Summary of fit represents a good model; (b) plot of coefficient values for scaled and centered factors show significant factors according to the model; (c) the 4D response contour plot of yield predicts yields of amination in dependence on qualitative and quantitative factors.

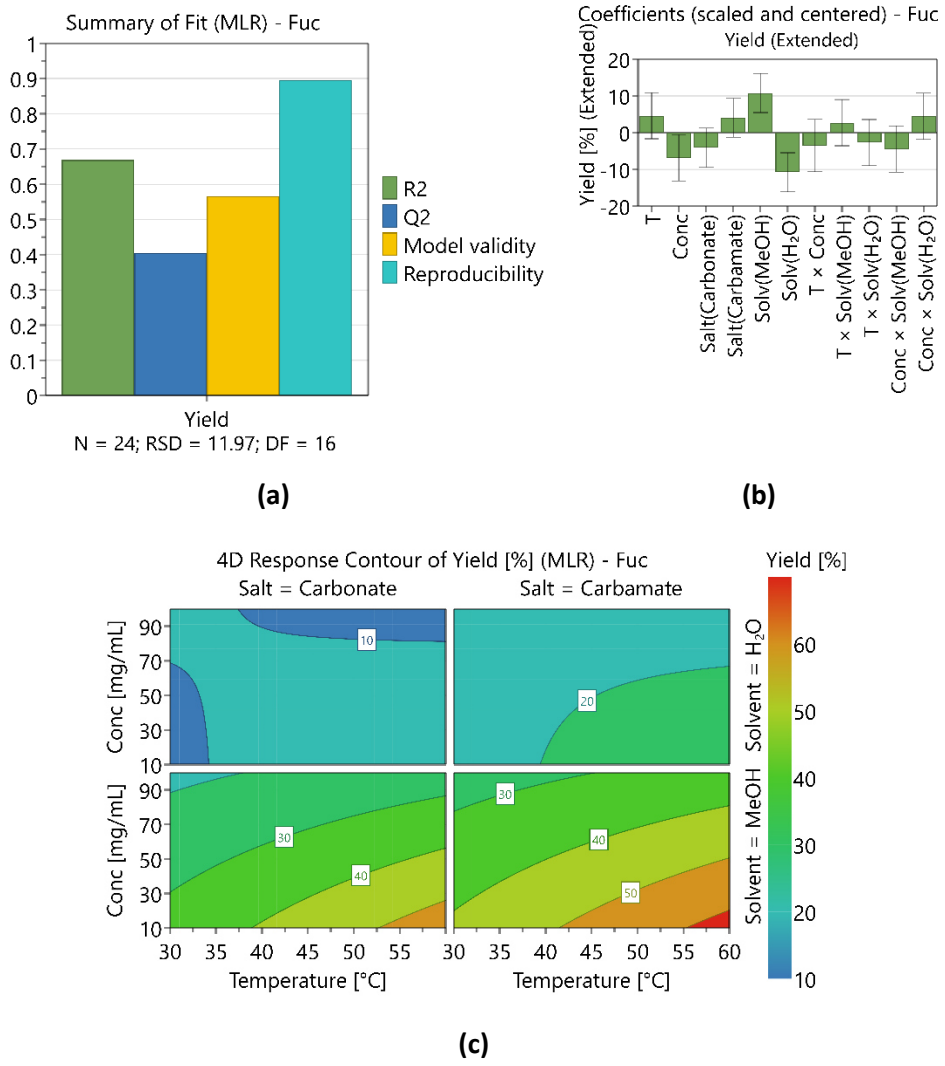

Figure 2.5. Plots of the model for Fuc generated by MODDE: (**a**) Summary of fit shows a lower significance of the model; (**b**) plot of coefficient values for scaled and centered factors show significant factors according to the model; (**c**) the 4D response contour plot of yield predicts yields of amination in dependence on qualitative and quantitative factors.

Overall, for the amination of carbohydrates according to the Kochetkov and Likhoshertov method, the reaction temperature has the most significant influence on the yield. The contour plots of MODDE indicate that higher yields are achievable at temperatures above 60 °C. In contrast, according to Bejugam et al. higher temperatures generally lead to an increased formation of side products and, therefore, lower yields [43]. Side products such as dimers were not analyzed but as such would usually not disturb subsequent reactions like, for example, (meth-)acrylations [37,38]. Though colorations of yellow and reddish brown were observed after reaction at temperatures above 50 °C, this did not seem to diminish the yield of glycosylamines. Concentration of saccharide does affect the yield but not strongly. Surprisingly, suspension of highly concentrated reactions did not necessarily decrease the yield even though thorough stirring was not always possible; microwave irradiation and excess amount of ammonium salt was enough to aminate the saccharides in the suspension. Choice of

solvent also influences the yield and depends on the nature of saccharide. Contrary to our expectation, methanol seems to be the superior solvent for amination of saccharides except for GlcA. The poor solubility of saccharides and aminating agents in methanol shows no negative influence on the yield. In conclusion, the solubility of starting material does not seem to affect the amination. A possible explanation is that the temperature and microwave irradiation are enough to dissolve, aminate, or both, the saccharides in methanol. Moreover, water can lead to hydrolysis and hence decrease the actual yield during purification or analysis. Regarding the first-time use of microwave assisted amination according to Likhoshertov, good yields of up to 81.6% could be obtained within 90 min as opposed to the 4–48 h from the traditional procedure [40]. Thus, microwave irradiation allows a great reduction of reaction time for the amination according to Likhoshertov, too. Generally, the nature of aminating agent can have an influence depending on selected saccharide, solvent, or both. This shows that both microwave-assisted syntheses work equally well as amination reaction for oligosaccharides and is not surprising since both ammonium salts are volatile and generate ammonia. Furthermore, we repeated experiment Am-I-01 (Table 2.1) with a 33-fold batch size in a 1 L PTFE vessel as its reaction conditions lead to the highest yield achieved. In this way we investigated the scalability of the process in principle. The initial yield of 64% dropped significantly even if the reaction time was doubled. No amine was found in NMR spectrum and only little amine was found by TLC. This may be due to different distribution of microwave irradiation in the larger volume, which could be another parameter for future investigations. However, we can also conclude that alterations of microwave distribution can be one of the reasons why yields from different publications and our yields may differ.

The DoE approach enabled a reduced number of experiments; however, if the model is insufficient, more experiments have to be conducted to improve the model. Predictions of the software support the direction of future experiments, namely, which solvent or aminating agent to use. We suggest additional experiments with higher reaction temperatures to further optimize the amination of saccharides. We consider investigating the reaction time to be worthwhile as well.

2.3 Materials and Methods

2.3.1 Materials

All chemicals were purchased from commercial sources. Water was double deionized by a Milli-Q purification system (18.2 MΩ·cm, Millipore Quantum TEX, Darmstadt, Germany). *N*-Acetyl-D-galactosamine (GalNAc; ≥99%, Carbosynth, Comptun, UK), D-lactose monohydrate (Lac; ≥96%, Carbosynth), D-glucuronic acid (GlcA; ≥98%, Carbosynth), L-(−)-fucose (Fuc; ≥98%, Carbosynth), ammonium carbamate ($H_2NCOONH_4$; 99%, Aldrich, Steinheim, Germany), ammonium carbonate

($(NH_4)_2CO_3$; ≥30.5% NH_3, extra pure, Carl Roth, Karlsruhe, Germany), methanol (MeOH; ≥98.8%, VWR, Darmstadt, Germany), deuterium oxide (D_2O; 99.9%, Deutero, Kastellaun, Germany) were used as received.

2.3.2 Methods

2.3.2.1 Design of Experiments (DoE)

The software MODDE version 12.1 (Sartorius Stedim Data Analytics AB, Malmö, Sweden) for generation and evaluation of statistical experimental designs was used to optimize synthesis conditions. We selected concentration of saccharide (Conc) and reaction temperature (T) as quantitative factors. The aminating agents (Salt) and solvents (Solv) represented our qualitative factors. We investigated the yield of the respective glycosylamine as response and set 100% yield as target. We chose the D-optimal design (with highest G-efficiency) and quadratic model to generate a set of experiments for optimization. This set includes two replicates for testing reproducibility. The models were fitted with multiple linear regression (MLR) analysis.

2.3.2.2 Nuclear Magnetic Resonance (NMR)

^{1}H-NMR spectra were recorded on a Bruker Neo Avance 400 MHz spectrometer (Bruker, Ettlingen, Germany) to identify the glycosylamines and determine their yields. We measured all spectra in D_2O. Yields of the respective glycosylamines were determined by evaluating the ratio between the integral of proton signals, that both starting material and glycosylamine share, and the integral that is solely specific to the respective glycosylamine. In case of $GalNAcNH_2$, we examined the ratio between the integral of the methyl group proton signal of GalNAc/$GalNAcNH_2$ (H-7; 3 H) and the integral of the anomeric proton signal of the $GalNAcNH_2$ (n H; yield of glycosylamine = n × 100%). For $LacNH_2$, the ratio between the integral of the proton peak H-7 (1 H) and the integral of the anomeric proton signal of $LacNH_2$ (n H). As peaks of the anomeric proton of GlcA and its amination product overlap, we performed global spectral deconvolution (GSD) for analysis. The integral of the peaks of the protons H-2 to H-5 (4 H) were compared with the integral of the anomeric proton signal of $GlcANH_2$ (n H). The yield of $FucNH_2$ was determined by analyzing the ratio between the integral of the methyl group proton signal H-6 (3 H) and the integral of the anomeric proton peak of $FucNH_2$ (n H).

2.3.2.3 Electrospray Ionization Mass Spectrometry (ESI-MS)

ESI-MS spectra were recorded on a PerkinElmer Flexar SQ 300 MS (Rodgau, Germany). We dissolved samples in acetonitrile/water mixture (50:50) with 0.1% formic acid. The measurements were performed at 300 °C with a flow rate of 15 µL min^{-1}.

2.3.2.4 Synthesis of Glycosylamines

Amination of saccharides were performed in a START 1500 rotaPREP microwave reactor (MLS GmbH, Leutrich, Germany). The respective saccharide is charged in a 50 mL-glass vessel and stirred with solvent. Afterwards, the ammonium salt is added under stirring and the reaction vessel is transferred to the microwave reactor. We set the reaction time to 90 min. The heating phase to our desired reaction temperature was set to 5 min. Volume of solvent was constantly 8 mL to ensure equal distribution of microwave irradiation for every experiment. We varied reaction temperature, concentration of saccharide, solvent and aminating agent according to Table 2.1. The last experiment is repeated three times in total for testing reproducibility. After reaction, samples prepared in MeOH were first concentrated by rotary evaporation at 40 °C and 300 mbar, followed by complete drying under high vacuum over several days or until most of the ammonium salt is removed. Aqueous reaction mixtures were lyophilized after reaction for several days or until most of the ammonium salt is removed. We yielded (hygroscopic) β-glycosylamines and stored them in nitrogen atmosphere at 4 °C.

The numbering of experiments starts with “Am” for amination, followed by the designated roman numeral of saccharide, GalNAc (I), Lac (II), GlcA (III)and Fuc (IV), and ends with the number of experiment. For example, Am-IV-03 refers to the amination of Fuc with the reaction conditions of experiment number 03. Experiments with optimized reaction conditions generated by MODDE carry the experiment number 0 (Table 2.2).

Table 2.2. Optimized reaction conditions and yields generated by MODDE.

Exp No	T (°C)	(mg/mL)	Salt	Solvent	Predicted Yield (%)	Found Yield (%)
Am-I-0/-01	60	10	$(NH_4)_2CO_3$	MeOH	54.7	64.2
Am-II-0	60	58	$(NH_4)_2CO_3$	MeOH	100.4	91.1
Am-III-0	47	59	$H_2NCOONH_4$	H_2O	73.8	60.3
Am-IV-0/-07	60	50	$H_2NCOONH_4$	MeOH	63.4	69.8

2.4 Conclusions

We optimized amination conditions for *N*-acetyl-D-galactosamine, D-lactose, D-glucuronic acid and L-(−)-fucose using DoE approach. Additionally, we showed that the acceleration of the amination according to Likhoshertov is possible by microwave irradiation. It is very apparent that optimized reaction conditions for one saccharide do not apply in the same way for other saccharides. Due to the relatively small number of experiments most models were lacking to some extent. However, the DoE approach supported the direction of which reaction parameters are worth further testing, including their quantitative and qualitative ranges or properties, respectively. The model for the amination of Lac provided a great improvement of yield. We observed strong indication that high temperatures are preferable for the amination. For future experiments, we suggest additional data of experiments with our found, most beneficial conditions to improve the models, testing of reaction time and of elevated temperatures.

2.5 Acknowledgements

We thank Angela Krtitschka from the University of Potsdam for enabling measurements of NMR spectra and Sophia Rosencrantz from Fraunhofer IAP for reviewing the manuscript.

2.6 References

1. Reily, C.; Stewart, T.J.; Renfrow, M.B.; Novak, J. Glycosylation in health and disease. *Nat. Rev. Nephrol.* **2019**, *15*, 346–366, doi:10.1038/s41581-019-0129-4.
2. Krasnova, L.; Wong, C.-H. Understanding the Chemistry and Biology of Glycosylation with Glycan Synthesis. *Annu. Rev. Biochem.* **2016**, *85*, 599–630, doi:10.1146/annurev-biochem-060614-034420.
3. Gabius, H.-J. *The Sugar Code*, 2nd ed.; John Wiley & Sons: Hoboken, NJ, USA, 2011; ISBN 9783527320899.
4. Varki, A.; Lowe, J.B. Biological Roles of Glycans. In *Essentials of Glycobiology*, 2nd ed.; Varki, A., Cummings, R.D., Esko, J.D., Freeze, H.H., Stanley, P., Bertozzi, C.R., Hart, G.W., Etzler, M.E., Eds.; Cold Spring Harbor: New York, NY, USA, 2009; ISBN 9780879697709.
5. Varki, A.; Cummings, R.D.; Esko, J.D.; Freeze, H.H.; Stanley, P.; Bertozzi, C.R.; Hart, G.W.; Etzler, M.E. (Eds.) *Essentials of Glycobiology,* 2nd ed.; Cold Spring Harbor: New York, NY, USA, 2009; ISBN 9780879697709.
6. van Breedam, W.; Pöhlmann, S.; Favoreel, H.W.; de Groot, R.J.; Nauwynck, H.J. Bitter-sweet symphony: Glycan-lectin interactions in virus biology. *FEMS Microbiol. Rev.* **2014**, *38*, 598–632, doi:10.1111/1574-6976.12052.
7. Ielasi, F.S.; Alioscha-Perez, M.; Donohue, D.; Claes, S.; Sahli, H.; Schols, D.; Willaert, R.G. Lectin-Glycan Interaction Network-Based Identification of Host Receptors of Microbial Pathogenic Adhesins. *mBio* **2016**, *7*, doi:10.1128/mBio.00584-16.
8. Rambaruth, N.D.S.; Dwek, M.V. Cell surface glycan-lectin interactions in tumor metastasis. *Acta Histochem.* **2011**, *113*, 591–600, doi:10.1016/j.acthis.2011.03.001.

9. Möckl, L. The Emerging Role of the Mammalian Glycocalyx in Functional Membrane Organization and Immune System Regulation. *Front. Cell Dev. Biol.* **2020**, *8*, 253, doi:10.3389/fcell.2020.00253.
10. Puri, A.; Neelamegham, S. Understanding glycomechanics using mathematical modeling: A review of current approaches to simulate cellular glycosylation reaction networks. *Ann. Biomed. Eng.* **2012**, *40*, 816–827, doi:10.1007/s10439-011-0464-5.
11. Bojarová, P.; Rosencrantz, R.R.; Elling, L.; Křen, V. Enzymatic glycosylation of multivalent scaffolds. *Chem. Soc. Rev.* **2013**, *42*, 4774–4797, doi:10.1039/c2cs35395d.
12. Wagner, S.; Hauck, D.; Hoffmann, M.; Sommer, R.; Joachim, I.; Müller, R.; Imberty, A.; Varrot, A.; Titz, A. Covalent Lectin Inhibition and Application in Bacterial Biofilm Imaging. *Angew. Chem. Int. Ed. Engl.* **2017**, *56*, 16559–16564, doi:10.1002/anie.201709368.
13. Ebrahim, A.H.; Alalawi, Z.; Mirandola, L.; Rakhshanda, R.; Dahlbeck, S.; Nguyen, D.; Jenkins, M.; Grizzi, F.; Cobos, E.; Figueroa, J.A.; et al. Galectins in cancer: Carcinogenesis, diagnosis and therapy. *Ann. Trans. Med.* **2014**, *2*, 88, doi:10.3978/j.issn.2305-5839.2014.09.12.
14. Ng, S.; Lin, E.; Kitov, P.I.; Tjhung, K.F.; Gerlits, O.O.; Deng, L.; Kasper, B.; Sood, A.; Paschal, B.M.; Zhang, P.; et al. Genetically encoded fragment-based discovery of glycopeptide ligands for carbohydrate-binding proteins. *J. Am. Chem. Soc.* **2015**, *137*, 5248–5251, doi:10.1021/ja511237n.
15. Luo, Y.; Gu, Y.; Feng, R.; Brash, J.; Eissa, A.M.; Haddleton, D.M.; Chen, G.; Chen, H. Synthesis of glycopolymers with specificity for bacterial strains via bacteria-guided polymerization. *Chem. Sci.* **2019**, *10*, 5251–5257, doi:10.1039/c8sc05561k.
16. von der Ehe, C.; Buś, T.; Weber, C.; Stumpf, S.; Bellstedt, P.; Hartlieb, M.; Schubert, U.S.; Gottschaldt, M. Glycopolymer-Functionalized Cryogels as Catch and Release Devices for the Pre-Enrichment of Pathogens. *ACS Macro Lett.* **2016**, *5*, 326–331, doi:10.1021/acsmacrolett.5b00856.
17. Filipová, M.; Bojarová, P.; Rodrigues Tavares, M.; Bumba, L.; Elling, L.; Chytil, P.; Gunár, K.; Křen, V.; Etrych, T.; Janoušková, O. Glycopolymers for Efficient Inhibition of Galectin-3: In Vitro Proof of Efficacy Using Suppression of T Lymphocyte Apoptosis and Tumor Cell Migration. *Biomacromolecules* **2020**, *21*, 3122–3133, doi:10.1021/acs.biomac.0c00515.
18. Brun, M.A.; Disney, M.D.; Seeberger, P.H. Miniaturization of microwave-assisted carbohydrate functionalization to create oligosaccharide microarrays. *ChemBioChem* **2006**, *7*, 421–424, doi:10.1002/cbic.200500361.
19. Puvirajesinghe, T.M.; Turnbull, J.E. Glycoarray Technologies: Deciphering Interactions from Proteins to Live Cell Responses. *Microarrays* **2016**, *5*, 3, doi:10.3390/microarrays5010003.
20. Mateescu, A.; Ye, J.; Narain, R.; Vamvakaki, M. Synthesis and characterization of novel glycosurfaces by ATRP. *Soft Matter* **2009**, *5*, 1621–1629, doi:10.1039/B817487C.
21. Pacholski, C.; Rosencrantz, S.; Rosencrantz, R.R.; Balderas-Valadez, R.F. Plasmonic biosensors fabricated by galvanic displacement reactions for monitoring biomolecular interactions in real time. *Anal. Bioanal. Chem.* **2020**, *412*, 3433–3445, doi:10.1007/s00216-020-02414-0.
22. Schulte-Osseili, C.; Kleinert, M.; Keil, N.; Rosencrantz, R.R. Rapid Drop-Test for Lectin Binding with Glycopolymer-Coated Optical Ring Resonators. *Biosensors* **2019**, *9*, 24, doi:10.3390/bios9010024.
23. Barras, A.; Martin, F.A.; Bande, O.; Baumann, J.-S.; Ghigo, J.-M.; Boukherroub, R.; Beloin, C.; Siriwardena, A.; Szunerits, S. Glycan-functionalized diamond nanoparticles as potent E. coli anti-adhesives. *Nanoscale* **2013**, *5*, 2307–2316, doi:10.1039/c3nr33826f.
24. Poonthiyil, V.; Nagesh, P.T.; Husain, M.; Golovko, V.B.; Fairbanks, A.J. Gold Nanoparticles Decorated with Sialic Acid Terminated Bi-antennary N-Glycans for the Detection of Influenza Virus at Nanomolar Concentrations. *ChemistryOpen* **2015**, *4*, 708–716, doi:10.1002/open.201500109.
25. Witten, K.G.; Rech, C.; Eckert, T.; Charrak, S.; Richtering, W.; Elling, L.; Simon, U. Glyco-DNA-gold nanoparticles: Lectin-mediated assembly and dual-stimuli response. *Small* **2011**, *7*, 1954–1960, doi:10.1002/smll.201100492.
26. Böcker, S.; Laaf, D.; Elling, L. Galectin Binding to Neo-Glycoproteins: LacDiNAc Conjugated BSA as Ligand for Human Galectin-3. *Biomolecules* **2015**, *5*, 1671–1696, doi:10.3390/biom5031671.
27. Böcker, S.; Elling, L. Biotinylated N-Acetyllactosamine- and N,N-Diacetyllactosamine-Based Oligosaccharides as Novel Ligands for Human Galectin-3. *Bioengineering* **2017**, *4*, 31, doi:10.3390/bioengineering4020031.

28. Bhatia, S.; Dimde, M.; Haag, R. Multivalent glycoconjugates as vaccines and potential drug candidates. *Med. Chem. Commun.* **2014**, *5*, 862–878, doi:10.1039/C4MD00143E.
29. Kiran, P.; Kumari, S.; Dernedde, J.; Haag, R.; Bhatia, S. Synthesis and comparison of linear and hyperbranched multivalent glycosides for C-type lectin binding. *New J. Chem.* **2019**, *43*, 16012–16016, doi:10.1039/C9NJ02018G.
30. Lundquist, J.J.; Toone, E.J. The cluster glycoside effect. *Chem. Rev.* **2002**, *102*, 555–578, doi:10.1021/cr000418f.
31. Lee, R.T.; Lee, Y.C. Affinity enhancement by multivalent lectin-carbohydrate interaction. *Glycoconj. J.* **2000**, *17*, 543–551, doi:10.1023/a:1011070425430.
32. Ginsburg, V. *Complex. Carbohydrates;* Academic Press: Orlando, FL, USA, 1987; ISBN 9780121820381.
33. Hoffmann, M.; Gau, E.; Braun, S.; Pich, A.; Elling, L. Enzymatic Synthesis of 2-(β-Galactosyl)-ethyl Methacrylate by β-Galactosidase from Pyrococcus woesei and Application for Glycopolymer Synthesis and Lectin Studies. *Biomacromolecules* **2020**, *21*, 974–987, doi:10.1021/acs.biomac.9b01647.
34. Adharis, A.; Loos, K. Green Synthesis of Glycopolymers Using an Enzymatic Approach. *Macromol. Chem. Phys.* **2019**, *220*, 1900219, doi:10.1002/MACP.201900219.
35. Kwase, Y.A.; Cochran, M.; Nitz, M. *Protecting-Group-Free Glycoconjugate Synthesis: Hydrazide and Oxyamine Derivatives in N-Glycoside Formation*; Wiley: Hoboken, NJ, USA, 2013; ISBN 9783527658947.
36. Vidal, S. (Ed.) *Protecting Groups. Strategies and Applications in Carbohydrate Chemistry*; Wiley-VCH: Weinheim, Germany, 2019; ISBN 3527697012.
37. Tang, J.S.J.; Rosencrantz, S.; Tepper, L.; Chea, S.; Klöpzig, S.; Krüger-Genge, A.; Storsberg, J.; Rosencrantz, R.R. Functional Glyco-Nanogels for Multivalent Interaction with Lectins. *Molecules* **2019**, *24*, 1865, doi:10.3390/molecules24101865.
38. Rosencrantz, S.; Tang, J.S.J.; Schulte-Osseili, C.; Böker, A.; Rosencrantz, R.R. Glycopolymers by RAFT Polymerization as Functional Surfaces for Galectin-3. *Macromol. Chem. Phys.* **2019**, *220*, 1900293, doi:10.1002/macp.201900293.
39. Likhoshertov, L.M.; Novikova, O.S.; Derevitskaja, V.A.; Kochetkov, N.K. A new simple synthesis of amino sugar b-D-glycosylamines. *Carbohydr. Res.* **1986**, *146*, C1–C5.
40. Likhoshertov, L.M.; Novikova, O.S.; Shibaev, V.N. New Efficient Synthesis of b-Glucosylamines of Mono- and Disaccharides with the Use of Ammonium Carbamate. *Dokl. Chem.* **2002**, *4*, 500–503.
41. Likhoshertov, L.M.; Novikova, O.S.; Shibaev, V.N. New Synthesis of b-Glycosylamines of D-Mannose, 2- and 6-Deoxysugars, and D-Glucuronic Acid with the Use of Ammonium Carbamate. *Dokl. Chem.* **2003**, *4*, 482–485.
42. Likhoshertov, L.M.; Novikova, O.S.; Zheltova, A.O.; Shibaev, V.N. An improved procedure for the synthesis of N-bromoacetyl-b-glycopyranosylamines, derivatives of mono- and disaccharides. *Russ. Chem. Bull.* **2004**, *3*, 709–713.
43. Bejugam, M.; Flitsch, S.L. An efficient synthetic route to glycoamino acid building blocks for glycopeptide synthesis. *Org. Lett.* **2004**, *6*, 4001–4004, doi:10.1021/ol048342n.
44. Dejaegher, B.; Heyden, Y.V. Experimental designs and their recent advances in set-up, data interpretation, and analytical applications. *J. Pharm. Biomed. Anal.* **2011**, *56*, 141–158, doi:10.1016/j.jpba.2011.04.023.
45. Montgomery, D.C. *Design and Analysis of Experiments*, 6th ed.; John Wiley & Sons: Hoboken, NJ, USA, 2004; ISBN 978-0-471-48735-7.
46. Yates, F. *The Design and Analysis of Factorial Experiments;* Imperial Bureau of Soil Science: Harpenden, UK, 1937.
47. Tye, H. Application of statistical 'design of experiments' methods in drug discovery. *Drug Discov. Today* **2004**, *9*, 485–491, doi:10.1016/S1359-6446(04)03086-7.
48. Lendrem, D.; Lendrem, B.C.; Woods, D.; Rowland-Jones, R.C.; Burke, M.; Chatfield, M.J.; Isaacs, J.; Owen, M. Lost in space: Design of experiments and scientific exploration in a Hogarth Universe. *Drug Discov. Today* **2015**, doi:10.1016/j.drudis.2015.09.015.

49. Leardi, R. Experimental design in chemistry: A tutorial. *Anal. Chim. Acta* **2009**, *652*, 161–172, doi:10.1016/j.aca.2009.06.015.
50. Bowden, G.D.; Pichler, B.J.; Maurer, A. A Design of Experiments (DoE) Approach Accelerates the Optimization of Copper-Mediated 18F-Fluorination Reactions of Arylstannanes. *Sci. Rep.* **2019**, *9*, 11370, doi:10.1038/s41598-019-47846-6.
51. Murray, P.M.; Bellany, F.; Benhamou, L.; Bučar, D.-K.; Tabor, A.B.; Sheppard, T.D. The application of design of experiments (DoE) reaction optimisation and solvent selection in the development of new synthetic chemistry. *Org. Biomol. Chem.* **2016**, *14*, 2373–2384, doi:10.1039/c5ob01892g.
52. Tye, H.; Whittaker, M. Use of a Design of Experiments approach for the optimisation of a microwave assisted Ugi reaction. *Org. Biomol. Chem.* **2004**, *2*, 813–815, doi:10.1039/B400298A.
53. Liu, Z.; Zhu, Y.; Gao, P.; Zhang, Z. Application of the factorial design of experiments to hydrothermal synthesis of lithium iron phosphate. *Int. J. Appl. Ceram. Technol.* **2020**, *17*, 1231–1240, doi:10.1111/ijac.13453.
54. Hemmati, S.; Barkey, D.P. Parametric Study, Sensitivity Analysis, and Optimization of Polyol Synthesis of Silver Nanowires. *ECS J. Solid State Sci. Technol.* **2017**, *6*, P132, doi:10.1149/2.0141704jss.
55. Karim, M.R.; Ferrandon, M.; Medina, S.; Sture, E.; Kariuki, N.; Myers, D.J.; Holby, E.F.; Zelenay, P.; Ahmed, T. Coupling High-Throughput Experiments and Regression Algorithms to Optimize PGM-Free ORR Electrocatalyst Synthesis. *ACS Appl. Energy Mater.* **2020**, *3*, 9083–9088, doi:10.1021/acsaem.0c01466.
56. Ghadban, A.; Albertin, L.; Moussavou Mounguengui, R.W.; Peruchon, A.; Heyraud, A. Synthesis of β-D-glucopyranuronosylamine in aqueous solution: Kinetic study and synthetic potential. *Carbohydr. Res.* **2011**, *346*, 2384–2393, doi:10.1016/j.carres.2011.08.018.
57. Chambers, S.A.; Townsend, S.D. Bioorthogonal human milk oligosaccharide probes for antimicrobial target identification within Streptococcus agalactiae. *Carbohydr. Res.* **2020**, *488*, 107895, doi:10.1016/j.carres.2019.107895.
58. Vetter, D.; Gallop, M.A. Strategies for the Synthesis and Screening of Glycoconjugates. 1. A Library of Glycosylamines. *Bioconj. Chem.* **1995**, *6*, 316–318.
59. Ghadban, A.; Albertin, L.; Condamine, E.; Mounguengui, R.W.M.; Heyraud, A. NMR and MS study of the formation of β-D-glucopyranosylamine uronic acid in aqueous solution. *Can. J. Chem.* **2011**, *89*, 987–1000, doi:10.1139/v11-064.
60. Hackenberger, C.P.R.; O'Reilly, M.K.; Imperiali, B. Improving glycopeptide synthesis: A convenient protocol for the preparation of b-glycosylamines and the synthesis of glycopeptides. *J. Org. Chem.* **2005**, *70*, 3574–3578, doi:10.1021/jo047801v.
61. Liu, X.; Zhang, G.; Chan, K.; Li, J. Microwave-assisted Kochetkov amination followed by permanent charge derivatization: A facile strategy for glycomics. *Chem. Commun.* **2010**, *46*, 7424–7426, doi:10.1039/c0cc01732a.

3 Glycopolymer Based LbL Multilayer Thin Films with Embedded Liposomes

Abstract

Layer-by-layer (LbL) self-assembly emerged as an efficient technique for fabricating coating systems for, e.g., drug delivery systems with great versatility and control. In this work, protecting group free and aqueous-based syntheses of bioinspired glycopolymer electrolytes are described. Thin films of the glycopolymers are fabricated by LbL self-assembly and function as scaffolds for liposomes, which potentially can encapsulate active substances. The adsorbed mass, pH stability, and integrity of glycopolymer coatings as well as the embedded liposomes are investigated via whispering gallery mode (WGM) technology and quartz crystal microbalance with dissipation (QCM-D) monitoring, which enable label-free characterization. Glycopolymer thin films, with and without liposomes, are stable in the physiological pH range. QCM-D measurements verify the integrity of lipid vesicles. Thus, the fabrication of glycopolymer-based surface coatings with embedded and intact liposomes is presented.

3.1 Introduction

Since its emergence in the 1990s, the layer-by-layer (LbL) self-assembly of films has gained tremendous interest worldwide due to its numerous advantages.[1,2] The LbL technique offers facile, inexpensive, versatile, and aqueous-based preparations of thin films, where the film thickness and permeability can be controlled in the nanometer scale.[3–8] Furthermore, substrates can vary in their material, size and geometry which makes the precise coating of e.g. implants and micro needles possible.[9–12] The mild and versatile preparation conditions allow a vast variety of coating materials such as colloids and sensitive biomolecules. Hence, a large array of compounds like small molecules, RNAs, proteins, enzymes and cells are enabled as coating components.[2,13,14] Typically, there are three different approaches to incorporate substances: 1) the substance is non-covalently incorporated into the LbL coating; 2) the substance is covalently bound to the coating material; 3) the substance is encapsulated into an additional carrier that is incorporated in the LbL film.[3,8] The first two methods are limited to the properties of substance as they can only be incorporated into the coating with suitable functional groups such as charged or linker moieties.. The third approach allows a wide variety of substances to be encapsulated in appropriate carriers and enables even poorly water-soluble drugs

to be incorporated in thin films. This is a crucial advantage since for example numerous FDA approved drugs are not or poorly water-soluble.[4,15]

We prepared the LbL self-assembly based on electrostatic interactions and, thus, selected complementary polyelectrolytes for the thin films. Therefor, we employed bioinspired glycopolymers as coating material, which mimic a natural glycoprotein, called mucin. In nature, mucins are responsible for protecting organs from desiccation, foreign bodies, pathogens and harsh pH environments like for example in nasal, gastric and respiratory mucosa.[16–19] These properties are advantageous for applications like implant coatings or wound healing, for instance.[20,21] However, natural carbohydrates such as chitosan, are not stable due to enzymatic, acidic, oxidative or thermal degradation.[22] Bioinspired synthetic glycopolymers exhibit high hydrophilicity, high stability and can result in improved biocompatibility due to the basis of natural carbohydrate components which makes them possibly suitable for e.g. biological or medical applications.[23–28] We synthesized positively and negatively charged glycopolymers, carrying *N*-acetylgalactosamine (GalNAc), lactose (Lac) or maltose (Mal), using two protecting group free and aqueous-based synthesis routes. We chose these three saccharides as GalNAc and the monomeric components of lactose as well as maltose, namely galactose and glucose, are found in natural mucins.[29] As mucins are naturally negatively charged by sulfate and mainly sialic acid groups, our artificial glycopolymers gain negative charges by a one-step chemical sulfation. For the positively charged glycopolymers, branched polyethyleneimine (PEI) has been used as polymer backbone as its high number of amines offers sufficient positive charges for the LbL-process in addition to facile functionalization with saccharides. The coupling was performed as an aqueous-based one-step synthesis of glycosylated branched PEI via reductive amination.

Since LbL self-assembly allows the facile embedment of particles, we integrated charged liposomes as potential substance carriers into the LbL thin films (Scheme 3.1). Liposomes are aqueous phase filled vesicles composed of lipid bilayers. They are great for the delivery of compounds due to their biocompatibility and ability to encapsulate a range of sensitive substances like RNAs, proteins as well as poorly water-soluble drugs for example, whereas the latter are incorporated into the liposomal membrane due their hydrophobicity.[30–32] Studies have shown that their embedment in LbL coatings can provide protection to the liposomes and control of substance release.[33,34]

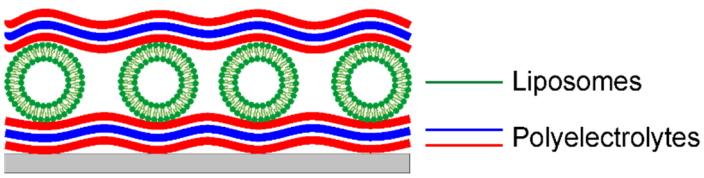

Scheme 3.1. Schematic illustration of a general LbL coating with complimentary polyelectrolytes and embedded charged liposomes.

In this work, we present a general approach on surface coatings based on bioinspired glycopolymers with embedded liposomes as potential cargo carriers, fabricated by LbL self-assembly.

3.2 Results and Discussion

We synthesized glycopolymer electrolytes as scaffolds for liposomes and investigated the LbL self-assembly of glycopolymers and liposomes regarding stability, thickness, and integrity.

3.2.1 Synthesis and Characterization of charged Glycopolymers

For the preparation of all glycopolymers, we generally utilize protecting group free and aqueous based synthesis routes where the biological functionality of the saccharides is retained. GalNAc, Lac and Mal were chosen as starting material as they or their components appear in natural mucins, are inexpensive and/or easily accessible.

3.2.1.1 Glycopolymers

The preparation of negatively charged glycopolymers comprises the synthesis of glycomonomer, the polymerization of latter and the sulfation of resulting glycopolymer (Scheme 3.2).

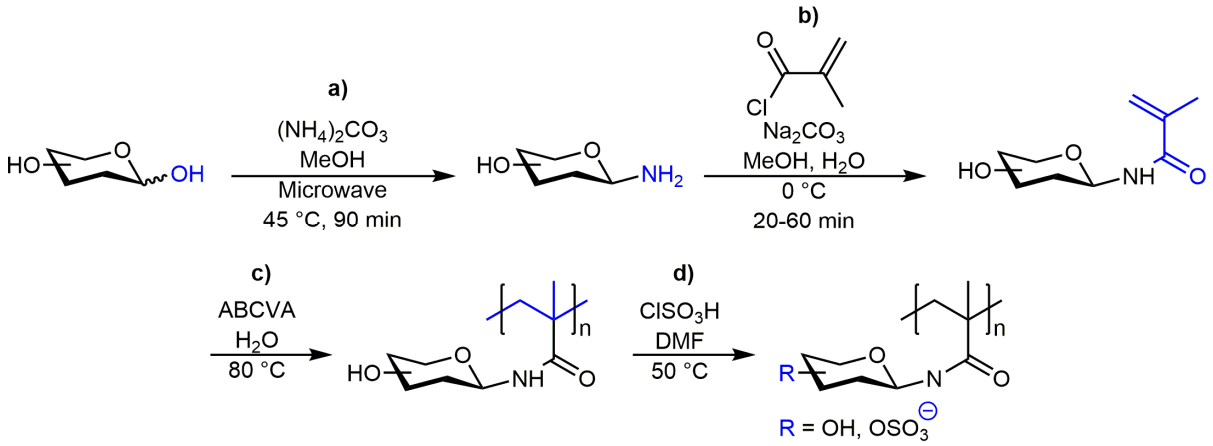

Scheme 3.2. Synthesis route of sulfated glycopolymers: a) Kochetkov amination, b) methacrylation, c) free radical polymerization, d) chemical sulfation.

The glycomonomer is synthesized from GalNAc and Lac, respectively. The procedure is adapted and modified from previous publications.[35,36] First, a glycosylamine is formed from the starting material via microwave-assisted Kochetkov amination, followed by the conversion to a methacrylamide (MAm) which constitutes our final glycomonomers GalNAcMAm and LacMAm. We

confirmed the formation of glycomonomers via NMR spectroscopy. In the ^{1}H NMR spectrum of GalNAcMAm, the signals of the glycoside are found at 5.13 ppm, 4.21-3.78 ppm and at 2.0 ppm and are attributed to the anomeric proton, saccharide ring and acetyl group, respectively (Figure 3.S3, Supporting Information). Singlets typical of methacrylamides are detected at 5.73 ppm, 5.56 ppm and 2.08 ppm. LacMAm and both glycosylamines have been characterized in previous studies.[35,36]

The respective glycomonomer is polymerized by a thermally initiated, free radical polymerization in water. We utilized ^{1}H NMR spectroscopy to verify the glycopolymers and to investigate the conversion and polymerization kinetic of glycomonomers. Comparing the spectra of glycopolymers and glycomonomers, the proton signals of the olefins disappeared which indicates their conversion to polymers. Both monomers showed rapid reaction in the first hour before the polymerization rate slowed down significantly (Figure 3.S1). LacMAm lead to higher and faster conversion of 90% after 2 h, whereas GalNAcMAm yielded a conversion of 86% after 4 h. Afterwards, no further significant conversion was detected for both monomers.

Last, we performed a chemical sulfation of the obtained glycopolymers to yield the negatively charged glycopolymers S-GalNAc and S-Lac. We adopted a reported one-step, direct inhomogeneous sulfation procedure .[37] The sulfation reaction is regioselective and favors the C-2 and C-6 positions of saccharides. Due to its regioselectivity, this method ensures homogeneous distribution of the charges and is therefore beneficial for the LbL self-assembly as opposed to, for example, asymmetric copolymerizations with charged comonomers like e.g. acrylic acid.[37] It has to be noted that modified sugars may exhibit altered biofunctionalities. Former reports demonstrated that modified glycans could improve their interactions with proteins in comparison to the unmodified analogues.[38–41] As not all sugars are sulfated in this case, the glycopolymers may retain the original biofunctionality of the saccharides. We confirmed the sulfated glycopolymers by ^{1}H NMR and IR spectroscopy (Figures 3.S6, 3.S8, and 3.S13, Supporting Information). Both spectra show that the sugar moieties remain on the polymer after sulfation. The IR spectra present a new signal at ~1200 cm^{-1} which can be assigned to sulfate groups. We determined the sulfation degree (sulfate group per monomer unit) by elemental analysis. Thus, for the respective sulfated polymers, we found a functionalization degree of 0.9 out of 1.0 possible sulfate moiety per GalNAc and 1.7 out of 4 sulfate groups per Lac. These charge densities are very suitable for LbL self-assemblies. Additional sulfation reactions with sulfur trioxide pyridine complex in place of chlorosulfonic acid were performed for easier handling of chemicals, though, they resulted in a decrease of sulfation degree for both glycopolymers and were not further investigated (results not shown).

3.2.1.2 PEI-based Glycopolymers

We utilized branched PEI as a glycopolymer backbone since its amino groups offer the desired positive charges and facile chemical glycosylation. The known cytotoxicity of PEI can be inhibited or greatly decreased by glycosylation and immobilization.[42,43] Here, PEI is functionalized via reductive amination according to a modified procedure of previously published work (Scheme 3.3).[44,45] The pH was adjusted to acidic conditions to ensure protonation of the targeted aldehyde and the forming iminium. As the reductive amination leads to opening of the saccharide ring, we employed disaccharides like Lac and Mal to retain one closed, biofunctional sugar ring and obtained lactose functionalized PEI (Lac-PEI) as well as maltose functionalized PEI (Mal-PEI), respectively.

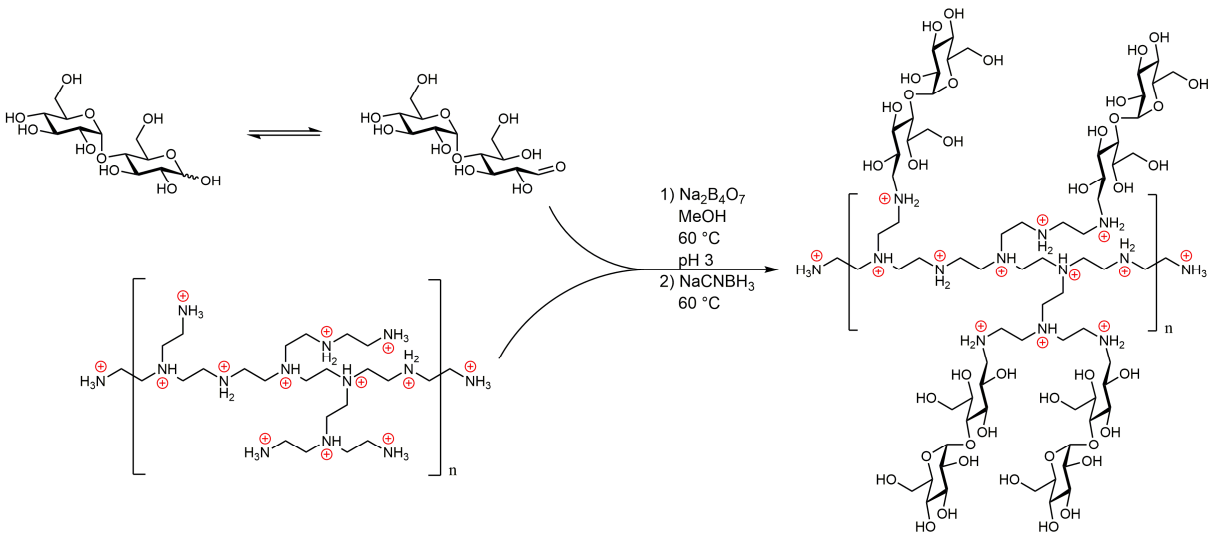

Scheme 3.3. Synthesis of glycosylated PEI via reductive amination with disaccharides (on the example of maltose).

We verified the formation of glycosylated PEIs via ^{1}H NMR and IR spectroscopy (Figures 3.S9, 3.S10, and 3.S14, Supporting Information). However, boron residues were found by ^{11}B NMR spectroscopy (Figures 3.S11 and 3.S12, Supporting Information). We attribute them to the boric reagents which probably formed boronate esters with the hydroxyl groups of the glycosides. Studies have shown that coatings solely based on boronate ester formation are viable and stable.[46–49] Therefore, the boron residues might be of advantage for the stability of our glycopolymer thin films, if they further stabilize the integrity of glycopolymer coatings by intermolecular interactions. To quantify the boron compounds, inductively coupled plasma optical emission spectrometry (ICP-OES) measurements were performed, and we found a boron content of 1.47 wt% in Lac-PEI and 1.30 wt% in Mal-PEI. For further characterization, the sugar content of glycosylated PEIs was determined by phenol-sulfuric acid assay and elemental analysis. According to the results of the phenol-sulfuric acid assay and in respect to the primary amines of PEI, the functionalization degree of Lac-PEI is 7%

(0.5 µmol Lac/mg Lac-PEI) and of Mal-PEI is 18% (1.0 µmol Mal/mg Mal-PEI). However, elemental analysis indicates complete functionalization of the primary amines (Experimental Section). ^{1}H NMR spectroscopy indicates similar sugar content for both glycosylated PEIs (Figures 3.S9 and 3.S10, Supporting Information). We explain these findings with the probable boronate ester formation with the glycosides which could block the saccharides from reaction with sulfuric acid and phenol. Furthermore, the efficacy of the assay might be disturbed by bound sugars as this assay was developed for free, unbound carbohydrates. GPC characterization supports these results as Lac-PEI presents a very high polydispersity of 242 while Mal-PEI has a low polydispersity of 2.2. Boronate esters are formed with vicinal diols and Lac exhibit more possible donor sites for borates than Mal.[50] Hence, Lac-PEI leads to an increased possibility of intramolecular and intermolecular boron carbohydrate interactions which, in turn, results in crosslinked polymers and therefore high polydispersity. This explanation coincides with Lac-PEI showing a lower sugar content via phenol-sulfuric acid assay. Nevertheless, we confirm the formation of glycosylated PEI. This possibly decreases or inhibits the cytotoxicity of PEI, which is essential for medical applications, and due to their numerous amino groups, the polymers are applicable for LbL self-assembly.

3.2.2 Layer-by-Layer Self-Assembly

3.2.2.1 Layer-by-Layer Self-Assembly of Glycopolymers

Different glycopolymers with complementary charges were coated in alternating layers via LbL self-assembly. Here, negatively charged glycopolymers carry either sulfated GalNAc (S-GalNAc) or sulfated Lac (S-Lac) moieties; positively charged glycopolymers are functionalized with Mal (Mal-PEI) or Lac (Lac-PEI), respectively (Scheme 3.4).

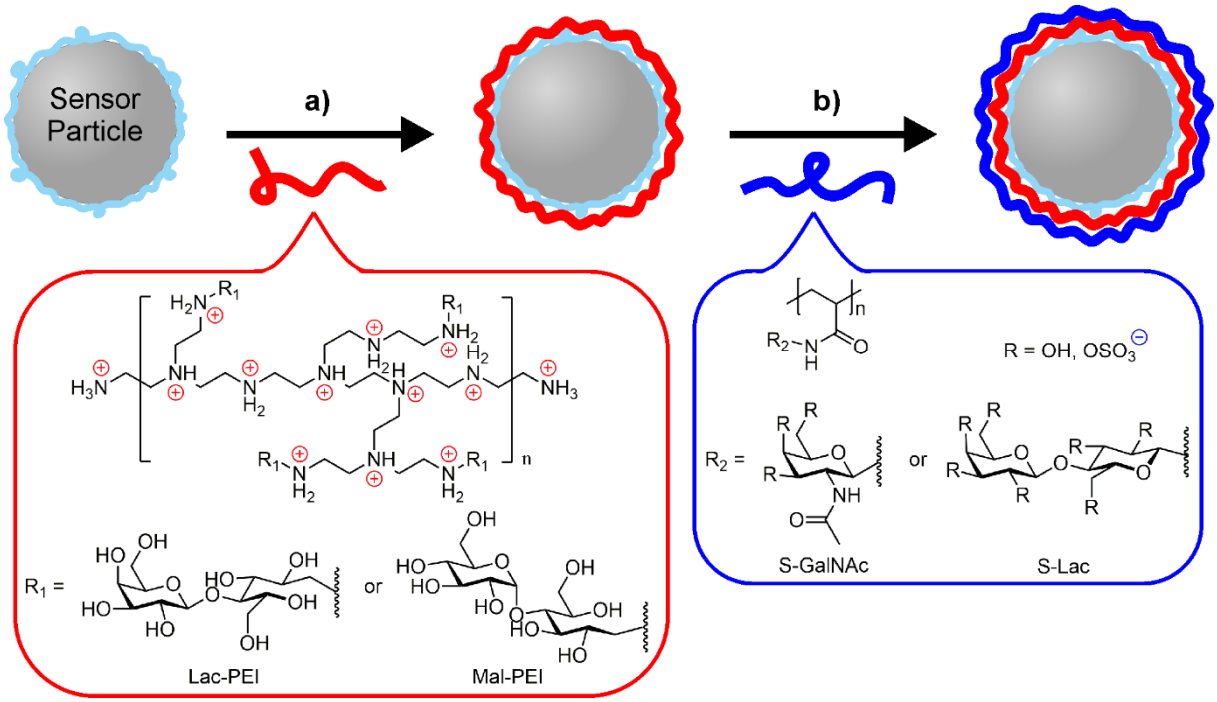

Scheme 3.4. Schematic illustration of deposition of a) cationic glycopolymers and b) anionic glycopolymers on polystyrene sulfonate and polyallylamine hydrochloride (PSS/(PAH/PSS)$_2$) precoated WGM sensor particles via LbL self-. Step a) and b) can be repeated consecutively.

We investigated the formation, mass and (pH) stability of coating layers on 10 µm sensor particles using whispering gallery mode (WGM) technology for every complimentary polyelectrolyte combination.[51] The adsorbed polyelectrolyte changes the refractive index on the sensor particle surface, which results in a wavelength shift of the emitted WGM-peaks. This WGM shift is measured during the LbL self-assembly and yield a sensitive, label-free online detection of the adsorbed mass (Figure 3.1).[51,52] Although the mass of deposited polymer is proportional to the shift, we could not transform the shift into exact mass, because the exact refractive index of the polymers was not known.

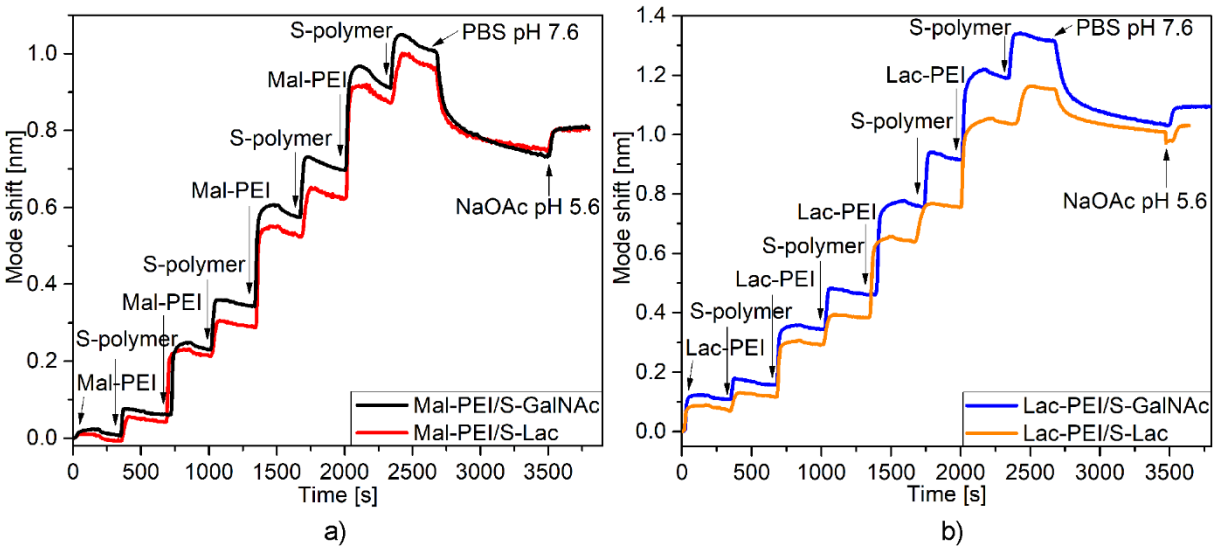

Figure 3.1. WGM shift response for LbL coating with a) Mal-PEI and S-GalNAc (black) or S-Lac (red) and b) Lac-PEI and S-GalNAc (blue) or S-Lac (orange). LbL coating with glycopolymers was performed in NaOAc buffer at pH 5.6 and stability of the layers was tested with PBS buffer at pH 7.6. The change of mode shift upon buffer change stems from the change of refractive index of the different buffers.

Experiments were carried out in NaOAc buffer at pH 5.6 and each coating step was followed by washing with the same buffer. The thin film remains stable after each washing step. LbL self-assemblies based on electrostatic interactions require adequate charge densities of the coating material. As PEI is less protonated with increasing pH, we tested the coating stability with PBS buffer at pH 7.6 to approximate physiological pH to investigate the suitability for biological or medical applications.[53]

Generally, every glycopolymer thin film behaved similarly. After a total of 8 glycopolymer layers, we washed with PBS buffer at pH 7.6 and only a small portion of the total film was washed away. Finally, washing with pH of 5.6 yielded a completely stable film. Therefore, we achieved stable glycopolymer thin films of different compositions within the physiological pH range.

We investigated the layer thickness of the total coating and of each single layer which are presented in Figure 3.2. The adsorbed mass of the total LbL thin film consistently increases with each layer, here, up to the eighth one and indicates no limit yet (Figure 3.2a). When the individual layers are examined, the adsorbed mass of respective glycopolymer noticeably increases with further coating steps (Figure 3.2b). Such exponential growth behavior is typical for many LbL assemblies and takes place preferentially with biopolymers.[1] Exponential growth is explained by partly diffusion of each outermost layer inside in the already formed film due to the high hydration of glycopolymers and the resulting high permeability. With increasing film thickness more polymers can be taken up at each assembling step.

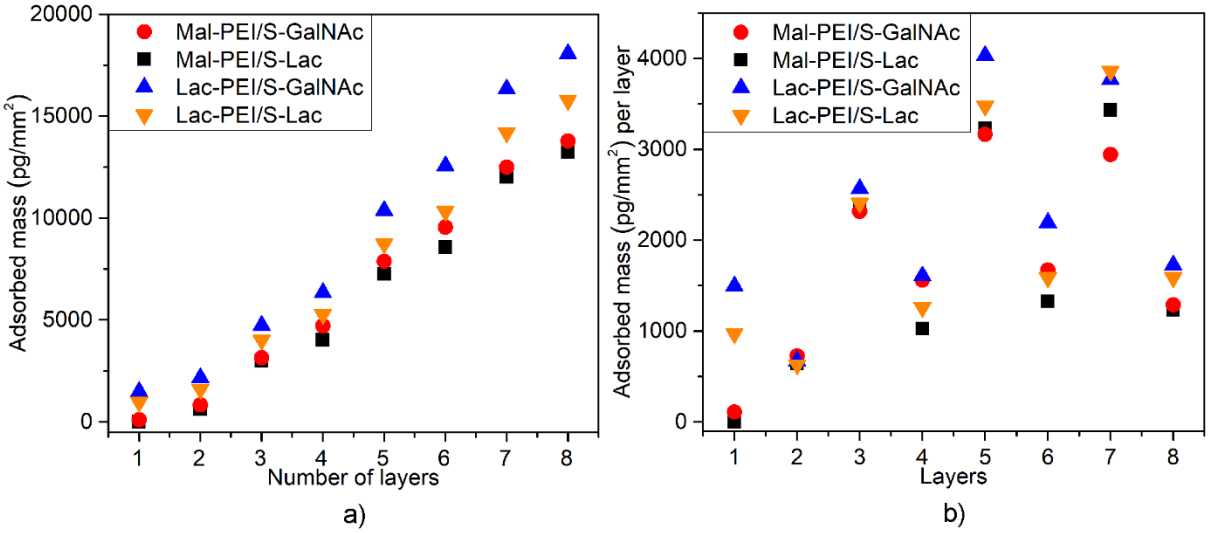

Figure 3.2. WGM characterization of the total mass of adsorbed glycopolymer a) after each coating step of different LbL films and b) of each single layer. Glycosylated PEIs form the first layer of every LbL coating.

Comparing the different glycopolymers, glycosylated PEI generally reaches higher adsorbed masses than sulfated glycopolymers, while Lac-PEI and S-GalNAc lead to thicker layers than Mal-PEI and S-Lac, respectively. A possible explanation for the difference between PEI-based and sulfated glycopolymers are boronate esters that possibly lead to intramolecular crosslinking with the glycosides and, therefore, higher molecular weight. For further investigation, we replaced glycosylated PEI with unmodified PEI and alternatingly coated it with S-GalNAc (Figure 3.3).

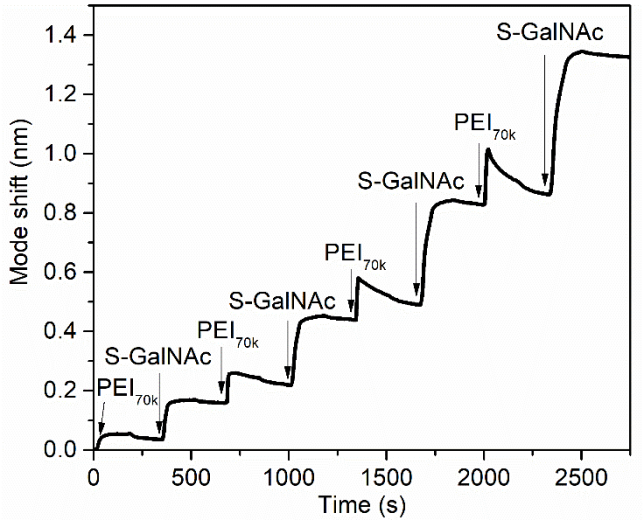

Figure 3.3. WGM shift response for LbL coating with unmodified PEI_{70k} and S-GalNAc in NaOAc buffer at pH 5.6.

Here, the contrary to the previous results is found where the sulfated glycopolymer lead to higher adsorbed masses than PEI. Moreover, the layer of unmodified PEI is very unstable during the washing steps at pH 5.6 and majority of adsorbed PEI is washed away whereas the thin films with

glycosylated PEI stayed stable at even higher pH. This supports our explanation that either boronate esters or interactions between the glycosides contribute to the thickness and stability of glycopolymer based LbL thin films where sole electrostatic interactions are not sufficient to reach the same quality of coating. Previous studies presented thin films of carbohydrates or other hydroxy rich polymers solely based on boronate ester formation.[46–49] However, their coating formation and stability are pH and carbohydrate sensitive whereas our system is based on electrostatic interactions and stable in the physiological pH range, which makes them more suitable for applications in for example medicine or biology. An additional explanation is the difference in mass-to-charge ratio of unmodified PEI and glycosylated PEI. A defined number of charges is needed to reach charge saturation. As functionalized PEI exhibit significantly increased mass-to-charge ratio, a higher amount of this polycation is adsorbed until charge saturation in comparison to unmodified PEI. Therefore, we can achieve thicker and stable coatings with glycosylated PEI than with commercial PEI.

3.2.2.2 Immobilization of Liposomes in LbL Glycopolymer Coating

After establishing stable glycopolymer coatings, further LbL self-assembly experiments were performed at physiological pH with liposomes as potential vehicles for active substances. Basic layers of glycopolymer coatings consisting of (Lac-PEI/S-Lac) or (Mal-PEI/S-Lac) were prepared and finished with the respective cationic, glycosylated PEI. In the next step, we attempted the adsorption of negatively charged liposomes followed by three glycosylated layers (Lac-PEI/S-Lac/Lac-PEI) or (Mal-PEI/S-Lac/Mal-PEI). To achieve a dense film of liposomes this sequence was repeated. The LbL self-assembly was followed on sensor particles by the WGM technology (Figure 3.4). In case of the liposomes only the lipid bilayer of ~5 nm contributes to the change of refractive index. In contrast to measurements with quartz crystal microbalance (QCM), the aqueous interior of the liposomes gives no signal. If the liposomes are larger than around 100 nm as in our case, the upper part of the lipid film is already outside of the evanescent field of the sensor and can also not be measured. If the liposomes do not form a densely packed monolayer, an average layer thickness of less than 5 nm will be observed.

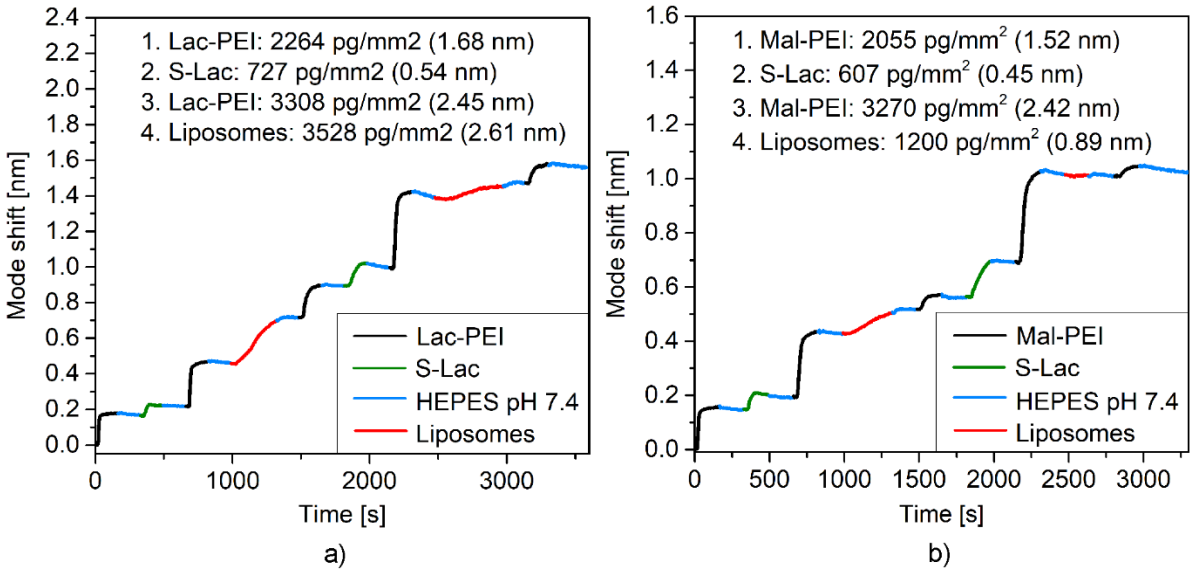

Figure 3.4. WGM shift response for LbL coating with liposomes, S-Lac and a) Lac-PEI or b) Mal-PEI in HEPES buffer at pH 7.4. Diameter of the liposomes is 100 nm ± 20 nm.

The first liposome layer was immobilized on three preceding glycopolymer layers. It showed good adsorption on Lac-PEI with an average layer thickness of 2.61 nm and was very stable after washing (Figure 3.4a). Liposome adsorption on Mal-PEI also resulted in a stable film, however, the layer thickness was almost three times as thin (0.89 nm) as the one with Lac-PEI, although the preceding glycopolymer coatings were similar in thickness (Figure 3.4b). Hence, the difference in liposome loading stems from the materials Lac-PEI and Mal-PEI. A possible explanation is the different configuration of the glycosides where the terminal non-reducing sugar in Lac is □-configurated and Mal □-configurated. This might sterically hinder the liposomes from adsorbing onto the positively charged PEI polymer backbone. The liposome layer remained stable as well as the three consecutive glycopolymer layers. The glycosylated PEI layer (layer 5) following the liposome layer (layer 4) is thinner than the preceding glycosylated PEI layer (layer 3), which again coincides with the observation that the presence of glycosides is beneficial for a stable and thick glycopolymer coating. Three further glycopolymer layers (layer 5-7) were coated onto the first liposome layer for the second liposome layer (layer 8). When the liposomes were assembled a second time, Lac-PEI enabled only little adsorption of the liposomes and Mal-PEI showed no liposome adsorption at all. As the size of the liposomes (~100 nm) is quite large in relation to the glycopolymer thin films of a few nanometers, the immobilization of liposomes onto uneven glycopolymer coatings is impeded. In this case, the adsorption of one stable liposome layer is possible. One additional layer of glycosylated PEIs was tested and both experiments showed very little increase of adsorbed mass in comparison to all other glycopolymer layers as there are only little or no positive charges to interact with.

To investigate the integrity of the immobilized liposomes, we monitored the LbL self-assembly in parallel via QCM-D measurements. The frequency shift describes the adsorption or desorption of substance mass, independent on the refractive index of the material. In combination with the dissipation shift, information about the mechanical properties of the adsorbed layer is delivered and indicates if the liposomes disintegrate as lipid monolayer or bilayer, or stay intact. Results display increased dissipation and decreased frequency for the liposome assembly, thus, present the increase of adsorbed mass and no desorption (Figure 3.5). In this method, the adsorption of the liposomes yields a remarkably larger shift than the thin polyelectrolyte films due to the high mass of water in the liposomes. This confirms the adsorption and intact integrity of the liposomes in the LbL film. Hence, a common loading of the liposomes with active substances, such as drugs or proteins, could enable an advanced drug delivery system on surfaces, for example. In conclusion, we established a stable LbL coating system out of bioinspired glycopolymers with intact liposomes.

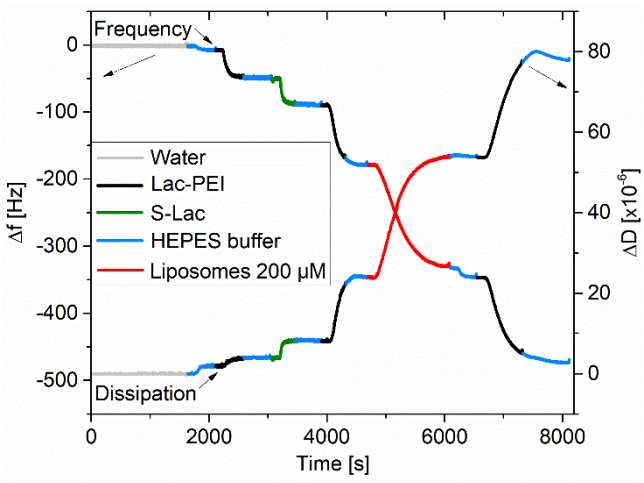

Figure 3.5. LbL coating with Lac-PEI and S-Lac and immobilization of liposomes in the LbL films monitored by QCM-D curves of frequency (left axis) and dissipation (right axis) (5th overtone).

3.3 Conclusion

We successfully synthesized glycomonomers and negatively charged, sulfated glycopolymers based on GalNAc and Lac, as well as Lac and Mal functionalized glycopolymers with positive charges that were suitable for LbL self-assembly. Each glycopolymer LbL multilayer film of every possible pairing was stable in physiological pH range and indicated strong interactions between the glycopolymers. Here, glycosylated PEIs were superior to unmodified PEI. Adsorption of one liposome layer in between the glycopolymer layers was successful. WGM and QCM-D measurements verified stable immobilization of liposomes and their intact integrity. Thus, we present a general approach on

the fabrication of stable LbL surface coatings out of bioinspired glycopolymer electrolytes with embedded liposomes.

3.4 Experimental Section

Materials: All chemicals were purchased from commercial sources and used as received if not stated otherwise. *N*-Acetyl-D-galactosamine (GalNAc; ≥99%) and d-lactose monohydrate (Lac; ≥96%) were obtained from Carbosynth (UK). Methacryloyl chloride (purum, dist., ≥97%), polyethyleneimine solution (branched, 50 wt.%, average Mn 60,000 by GPC, average Mw 750,000 by LS), silica gel (high-purity grade, pore size 60 Å, N,N,-dimethylformamide (≥99%), phenol, poly(sodium-4-styrenesulfate) (PSS, 70,000 Da), sodium thioglycolate, (4-(2-hydroxyethyl)-1-piperazineethanesulfonic acid) (HEPES), sodium acetate and 4,4'-azobis(4-cyanovaleric acid) (≥98%) were purchased from Sigma-Aldrich (Germany). Poly(allylamine hydrochloride) (PAH, 40,000 Da) was purchased from Beckmann-Kenko (Germany) and further purified by dialysis before use. Sodium chloride, ammonium carbonate ($(NH_4)_2CO_3$; ≥30.5% NH_3, extra pure), sodium carbonate (Na_2CO_3; ≥99%, anhydrous), acetonitrile (ACN; ≥99.8%, for preparative HPLC) were purchased from Carl Roth (Germany). Methanol (MeOH; ≥98.8%) and deuterium oxide were purchased from VWR (Germany). Diethyl ether (Et_2O; p. a.) and tetrahydrofuran (THF) were purchased from Chemsolute (Germany). Sulfuric acid (95%) was purchased from Th. Geyer (Germany). 4-Methoxyphenol (98+%) was purchased from Alfa Aesar (Germany). Chlorosulfonic acid (97%) was purchased from Acros Organics (Germany). Dimethylsulfoxide-d_6 (DMSO-d_6; 99.8%) was purchased from Deutero GmbH (Germany). Water was double deionized by a Milli-Q purification system (18.2 MW_cm, Millipore Quantum TEX, Darmstadt, Germany). WGM sensor particles (10 µm diameter) were prepared by Surflay Nanotec GmbH. Liposomes composed of 1-palmitoyl-2-oleoyl-glycero-3-phosphocholine (POPC, 90%) and 1-palmitoyl-2-oleoyl-sn-glycero-3-phospho-L-serine (sodium salt) (POPS, 10%) were provided by Dr. Peter Müller, from the Group of Molecular Biophysics (Humboldt-Universität zu Berlin, Germany).

Methods: Nuclear magnetic resonance (NMR) spectra were recorded on a Bruker Avance 300 MHz Spectrometer (Germany). We dissolved ^1H NMR samples in D2O and ^{13}C NMR samples in DMSO-d_6. For the kinetic study of the free radical polymerization, samples were taken from the reaction mixture and immediately frozen and lyophilized before measurements. Mass spectra were recorded on FlexarTM SQ 300 MS Detector (PerkinElmer, Germany) and obtained in electrospray ionization (ESI) mode. We prepared the samples in acetonitrile/water (50:50) with formic acid (0.1%). Measurements were performed at 300 °C with a flow rate of 15 µL min^{-1}. IR spectra were recorded on a Thermo Nicolet Nexus FT-IR spectrometer (Thermo Fisher Scientific, Germany) by an attenuated total reflectance method. Elemental analysis was carried out using a FlashEA 1112 CHNS/O Automatic Elemental

Analyser (Thermo Scientific, Bremen, Germany). Inductively coupled plasma optical emission spectrometry (ICP-OES) was carried out using an ICP-OES Optima 2100 DV (PerkinElmer; Germany). Gel permeation chromatography (GPC) was performed using a WGE SEC-3010 system (Dr. Bures, equipped) with an RI detector and the chromatography columns TSK Gel and PSS Suprema, respectively. Flow rate was 1 mL min^{-1}. For neutral and anionic polymers, the eluent was 0.07 M disodium phosphate buffer and calibration was performed with polyacrylic acid standards. For cationic polymers, the eluent was aqueous potassium chloride (0.2 mol L^{-1}) with formic acid (0.02 mol L^{-1}) and calibration was conducted with dextran standards.

Phenol-Sulfuric Acid Assay for Determination of total Sugar Content: The phenol-sulfuric acid assay was performed as described elsewhere.[35] Briefly, three different concentrations of glycopolymer (0.3, 0.6 and 1 mg mL^{-1} for Lac-PEI; 0.15, 0.3 and 0.6 mg mL^{-1} for Mal-PEI) were prepared in water. 50 µL of sample was thoroughly mixed with sulfuric acid (150 µL). Subsequently, phenol (30 µL, 5%) was added and mixed. After incubation at 90 °C for 5 min and cooling in a water bath for further 5 min, the solution was transferred into a 96-well plate (Carl Roth, Germany) and the absorption at 490 nm was measured. Calibration with lactose and maltose were used for calculating the total sugar amount.

Synthesis of the Glycomonomers GalNAcMAm and LacMAm: The GalNAc based monomer was synthesized in a two-step reaction similar to previous published procedure.[35] The first step was performed in START 1500 rotaPREP microwave reactor (MLS GmbH, Germany). Here, GalNAc (4.424 g, 20 mmol), MeOH (246 mL, 18 mg mL^{-1}) and $(NH)_4CO_3$ (22.12 g, 5 equiv wt) were charged in a 1 L-polytetrafluoroethylene vessel. The reaction mixture was heated to 41 °C over 10 min under microwave irradiation and stirring. Then the reaction was allowed to proceed for further 90 min at 41 °C. Afterwards, the excess ammonium salt was removed by rotary evaporation at 45 °C and 400 mbar. Methanol was removed at lower pressures. The product was completely dried under high vacuum and stored in nitrogen atmosphere. We yielded a hygroscopic glycosylamine, $GalNAcNH_2$, with an amine conversion of 72% (determined by ^1H NMR analysis).

For the second synthesis step, $GalNAcNH_2$ (1.321 g, 6 mmol) and Na_2CO_3 (3.180 g, 5 equiv) were charged in a round bottom flask and stirred in an ice water bath. MeOH (24 mL) and Milli-Q water (24 mL) were added subsequently. We diluted methacryloyl chloride (2.3 mL, 4 equiv) in THF (mL) before dropwise adding this solution to the reaction mixture over 5 min. After further 20 min, we added Milli-Q water (30 mL) and MeHQ (0.74 mg, 250 ppm) for stabilization of monomer. The solvents were removed by rotary evaporation at 40 °C. A part of this reaction mixture was purified via preparative HPLC (Knauer Azura ASM 2.1L; column: Luna 5 µm C18 100A, 100 x 30.0 mm) with ACN/H_2O (97:3) as eluent and a flow rate of 7 mL min^{-1}. The resulting monomer GalNAcMAm was obtained as white solid. ^1H NMR (300 MHz, D_2O, δ): 5.65 (s, 1H, CH_2), 5.47 (s, 1H, CH_2), 4.99 (d, J =

9.7 Hz, 1H, CH), 5.02-3.97 (m, 6H), 1.93 (s, 3H, CH_3), 1.85 (s, 3H, CH_3); ^{13}C NMR (100 MHz, DMSO-d_6, δ): 171.35 (C_{quart}), 167.35 (C_{quart}), 139.24 (C_{quart}), 120.33 (CH_2), 80.50 (CH), 76.76 (CH), 71.05 (CH), 67.36 (CH), 60.35 (CH_2), 51.02 (CH), 22.76 (CH_3), 18.25 (CH_3); MS (ESI) *m/z*: $[M + H]^+$ calcd for $C_{12}H_{20}N_2O_6$, 289.14; found $[M + H]^+$, 289.37.

The synthesis of the glycomonomer LacMAm is described in our previous published procedure.[35]

Synthesis of the Glycopolymers PGalNAcMAm and PLacMAm: The glycopolymers were prepared by free radical polymerization. Here, GalNAcMAm (240 mg, 0.832 mmol) and ABCVA (4.7 mg, 2 mol%) were dissolved in Milli-Q water (2085 µL, 0.4 mmol mL^{-1}) and purged with nitrogen for at least 30 min. Afterwards, the reaction vessel was submerged in an 80 °C oil bath to start the polymerization. The reaction was allowed to proceed for 54.5 h. The polymer was purified by dialysis against deionized water before freeze-drying. We obtained a white fluffy solid (PGalNAcMAm) (186.8 mg, 76%).

For the preparation of PLacMAm, we dissolved LacMAm (114.6 mg) and ABCVA (1.6 mg, 2 mol%) in Milli-Q water (933.0 µL, 0.3 mmol mL^{-1}) and followed the same procedure as above for the synthesis of PGalNAcMAm. We yielded a white fluffy solid (95.7 mg, 82%).

Sulfation of the sulfated Glycopolymers to S-GalNAc and S-Lac: We performed the sulfation according to a modified procedure of a previously published work.[35] For the sulfation of PGalNAcMAm, GalNAcMAm (155 mg) and dry DMF (7.75 mL, 20 mg mL^{-1}) were charged in a dried Schlenk flask under nitrogen atmosphere. The suspension was stirred for 18 h before we added chlorosulfonic acid (160.8 µL, 1.5 equiv per OH). The reaction mixture was heated to 50 °C and stirred for further 5 h. Afterwards, saturated NaOAc-EtOH solution (15 mL) was added and the precipitate was centrifuged (14,000 rpm, 10 min). The sediment was washed and centrifuged with EtOH again. Then it was dissolved in little deionized water and dialyzed against deionized water. After freeze-drying, a white fluffy solid is obtained as our product S-GalNAc (127 mg). The sulfation degree is 0.91 sulfate group per monomer unit. Anal. found: C 33.84, H 5.54, N 6.91, O 38.45, S 7.23.

For the synthesis of S-Lac, we followed the same procedure as for S-GalNAc. Here, PLacMAm (90 mg) were suspended in dry DMF (4.50 mL, 20 mg/mL) and chlorosulfonic acid (409 µL, 4 eq. per OH) were added. A white fluffy solid (117 mg) was obtained. The sulfation degree of S-Lac is 1.68 sulfate moiety per monomer unit. Anal. found: C 28.18, H 4.63, N 2.43, O 43.74, S 9.34.

Synthesis of Glycofunctionalized PEIs Lac-PEI and Mal-PEI: For the synthesis of Lac-PEI, 10 g PEI solution (50 wt%), lactose monohydrate (27 g, 75 mmol, 7 equiv per monomer unit), MeOH (35 mL) and $Na_2B_4O_7$ solution (50 mL, 50 mM) were stirred at 60 °C until completely dissolved. Subsequently, the reaction mixture was allowed to cool, and the pH was adjusted to pH 3 with formic acid. We suspended $NaCNBH_3$ (16.6 g, 264 mmol, 3.5 eq per lactose) in MeOH (15 mL, 1.1 g mL^{-1}) before adding it to the reaction mixture in portions. We allowed the reaction to proceed at 60 °C for 16-17 h. Any

precipitate was filtered with a Kimtech Science® precision wipes (Germany). The yellow solution was dialyzed against deionized water and freeze-dried. We obtained a white solid (12.1 g). Anal. found: C 40.05, H 7.11, N 7.44, O 31.94; ICP-OES: 1.47 wt% B.

The preparation of Mal-PEI was conducted according to the procedure above. After reaction, MeOH was removed by rotary evaporation. The reaction mixture was then dialyzed without prior filtering. We obtained a white solid (6.6 g). Anal. found: C 40.45, H 7.14, N 7.12, O 32.11; ICP-OES: 1.30 wt% B.

Layer-by-Layer (LbL) Coating of Sensor Particles: A basic LbL coating of WGM sensor particles was performed by alternating deposition of polyelectrolytes of opposite charge on the particles. Polyelectrolyte solutions were prepared in acetate buffer (50 mM, pH 5.6) with sodium chloride (200 mM) and a polyelectrolyte concentration of 1 mg mL^{-1} . For coating, sensor particles were washed three times with ultrapure water, dispersed in the respective polyelectrolyte solution, and incubated for 1 h at room temperature. Particles were washed again three times with ultrapure water and the coating process was repeated (incubation time of 20 min for each subsequent layer) until the particles were coated with a base film of $PSS/(PAH/PSS)_2$. The polyelectrolytes noted in the brackets describe the alternating layers of polyelectrolytes and the index presents the number of electrolyte pairs; the base film starts with one PSS layer.

Whispering Gallery Modes (WGM) Measurements: S-Lac (0.5 mg mL^{-1}), S-GalNAc, Lac-PEI, and Mal-PEI (1 mg mL^{-1}) solutions for WGM measurements were prepared either in sodium acetate buffer (50 mM, pH 5.6) with sodium chloride (200 mM) or in HEPES buffer (10 mM, pH 7.4) with sodium chloride (150 mM) for the experiments with liposomes. Liposome solutions (200 μM) were prepared in HEPES (10 mM, pH 7.4) with sodium chloride (150 mM). The set-up of the WGM device and the microfluidic array system were described in a previously published work.[51] WGM sensor particles coated with $PSS/(PAH/PSS)_2$ were injected in the microfluidic chip and allowed to sediment into microwells of 12 μm in diameter. The chip containing the sensor particles was connected to the microfluidic system and the WGM instrument and rinsed with ultrapure water for approximately 10 min. Afterwards, the particles in the chip were equilibrated with the measuring buffer (same type of buffer and sodium chloride concentration of the glycopolymer solutions to be tested) for approximately 5 min. For the measurements, the fluorescent WGM sensors were excited for 25 milliseconds by a 405 nm diode laser. Emitted fluorescence was filtered from the excitation light by means of a dichroic beamsplitter, dispersed onto a spectrograph (focal length = 200 mm), and collected by a CCD-line camera with an optical resolution of 10 pm. The solutions to be tested (glycopolymers or liposomes) were alternately injected in the microfluidic system with a flow rate of 80 μL min^{-1} while measuring the WGM response of a selected sensor every 5.5 s. The sensors in the chip were rinsed with measuring buffer between each step to remove any non-adsorbed material.

Quartz Crystal Microbalance with Dissipation (QCM-D) measurements: QCM-D measurements were performed using a QSense E4 QCM-D instrument from Biolin Scientific (Sweden) at 18 °C and Cr/Au-coated quartz crystals (5 MHz) from Quartz Pro (Sweden). Chips were UV treated for 10 min on each side, then immersed for 15 min in a 5:1:1 solution of ultrapure water, ammonia (25%), and hydrogen peroxide (30%) at 70 °C. The chips were extensively rinsed with water, dried, and UV treated for additional 10 min on each side. The chips were immersed in 1 mM sodium thioglycolate in ethanol overnight at room temperature, rinsed with ethanol, ultrapure water, and dried. Before the experiments, the chips were rinsed overnight with ultrapure water inside the instrument at a flow rate of 20 µL min^{-1}. Flow rate was increased to 80 µL min^{-1}, frequency and dissipation were monitored until they were stable, and the measurement was started. In the beginning of the experiment, the chips were rinsed with a buffer (10 mM HEPES, pH 7.4 and 150 mM sodium chloride. For each layer, S-Lac (0.5 mg mL^{-1}), Lac-PEI (1 mg mL^{-1}) or liposome (200 µM) solutions in the buffer were flown over the sensors in the chip while monitoring frequency and dissipation. The sensors were rinsed with the buffer between each step to remove any non-adsorbed material.

3.5 Acknowledgements

This research was funded by Bundesministerium für Bildung und Forschung (BMBF) (FKZ 01IO1803). The authors thank Dr. Peter Müller from the Group ofMolecular Biophysics (Humboldt-Universität zu Berlin, Germany) for providing the liposomes. The authors thank Angela Krtitschka from the University of Potsdam for enabling the measurements of NMR spectra. The authors would also like to thank Dr. Erik Wischerhoff and Dr. Hendrik Wetzel from Fraunhofer IAP for GPC and EA measurements.

Open access funding enabled and organized by Projekt DEAL.

3.6 References

[1] J. Campbell, A. S. Vikulina, *Polymers (Basel).* **2020**, *12*, 1.
[2] M. Keeney, X. Y. Jiang, M. Yamane, M. Lee, S. Goodman, F. Yang, *J. Mater. Chem. B* **2015**, *3*, 8757.
[3] D. Alkekhia, P. T. Hammond, A. Shukla, *Annu. Rev. Biomed. Eng.* **2020**, *22*, 1.
[4] K. Ariga, M. McShane, Y. M. Lvov, Q. Ji, J. P. Hill, *Expert Opin. Drug Deliv.* **2011**, *8*, 633.
[5] Y. He, J. Li, M. E. Turvey, M. L. T. Funkenbusch, C. Hong, Di. S. S. M. Uppu, H. He, D. J. Irvine, P. T. Hammond, *ACS Macro Lett.* **2017**, *6*, 1320.
[6] B. S. Kim, R. C. Smith, Z. Poon, P. T. Hammond, *Langmuir* **2009**, *25*, 14086.
[7] B. Kim, S. W. Park, P. T. Hammond, *ACS Nano* **2008**, *2*, 386.
[8] B. M. Wohl, J. F. J. Engbersen, *J. Control. Release* **2012**, *158*, 2.
[9] S. Chen, Y. Shi, Y. Luo, J. Ma, *Colloids Surfaces B Biointerfaces* **2019**, *179*, 121.
[10] A. Escobar, N. Muzzio, S. E. Moya, *Pharmaceutics* **2021**, *13*, 1.

[11] P. C. Demuth, X. Su, R. E. Samuel, P. T. Hammond, D. J. Irvine, *Adv. Mater.* **2010**, *22*, 4851.
[12] S. Sunny, N. Vogel, C. Howell, T. L. Vu, J. Aizenberg, *Adv. Funct. Mater.* **2014**, *24*, 6658.
[13] J. Hong, B. S. Kim, K. Char, P. T. Hammond, *Biomacromolecules* **2011**, *12*, 2975.
[14] A. N. Zelikin, *ACS Nano* **2010**, *4*, 2494.
[15] T. Loftsson, M. E. Brewster, *J. Pharm. Pharmacol.* **2010**, *62*, 1607.
[16] H. Nordman, J. R. Davies, G. Lindell, C. De Bolós, F. Real, I. Carlstedt, *Biochem. J.* **2002**, *364*, 191.
[17] S. P. Authimoolam, T. D. Dziubla, *Polymers (Basel).* **2016**, *8*.
[18] G. Petrou, T. Crouzier, *Biomater. Sci.* **2018**, *6*, 2282.
[19] A. Sharma, B. Thongrom, S. Bhatia, B. von Lospichl, A. Addante, S. Y. Graeber, D. Lauster, M. A. Mall, M. Gradzielski, R. Haag, *Macromol. Rapid Commun.* **2021**, *2100303*, 1.
[20] J. Y. Co, T. Crouzier, K. Ribbeck, *Adv. Mater. Interfaces* **2015**, *2*, 1.
[21] M. U. Adikwu, B. U. Alozie, *Sci. Res. Essays* **2009**, *4*, 453.
[22] E. Szymanska, K. Winnicka, *Mar. Drugs* **2015**, 1819.
[23] M. Ahmed, B. F. L. Lai, J. N. Kizhakkedathu, R. Narain, *Bioconjug. Chem.* **2012**, *23*, 1050.
[24] Y. Chen, D. Diaz-Dussan, Y. Y. Peng, R. Narain, *Biomacromolecules* **2019**, *20*, 2068.
[25] Y. X. Wang, J. L. Robertson, W. B. Spillman, R. O. Claus, *Pharm. Res.* **2004**, *21*, 1362.
[26] M. R. Tavares, M. Bláhová, L. Sedláková, L. Elling, H. Pelantová, R. Konefał, T. Etrych, V. Křen, P. Bojarová, P. Chytil, *Biomacromolecules* **2020**, *21*, 641.
[27] M. Filipová, P. Bojarová, M. Rodrigues Tavares, L. Bumba, L. Elling, P. Chytil, K. Gunár, V. Křen, T. Etrych, O. Janoušková, *Biomacromolecules* **2020**, *21*, 3122.
[28] S. Bhatia, D. Lauster, M. Bardua, K. Ludwig, S. Angioletti-Uberti, N. Popp, U. Hoffmann, F. Paulus, M. Budt, M. Stadtmüller, T. Wolff, A. Hamann, C. Böttcher, A. Herrmann, R. Haag, *Biomaterials* **2017**, *138*, 22.
[29] A. Guzman-Aranguez, P. Argüeso, *Ocul. Surf.* **2010**, *8*, 8.
[30] W. M. Merritt, Y. G. Lin, W. A. Spannuth, M. S. Fletcher, A. A. Kamat, L. Y. Han, C. N. Landen, N. Jennings, K. De Geest, R. R. Langley, G. Villares, A. Sanguino, S. K. Lutgendorf, G. Lopez-Berestein, M. M. Bar-Eli, A. K. Sood, *J. Natl. Cancer Inst.* **2008**, *100*, 359.
[31] S. Kalepu, V. Nekkanti, *Acta Pharm. Sin. B* **2015**, *5*, 442.
[32] A. M. Bapolisi, C. I. Nkanga, R. B. Walker, R. W. M. Krause, *J. Drug Deliv. Sci. Technol.* **2020**, *58*, 101751.
[33] Y. A. Brito Barrera, G. Hause, M. Menzel, C. E. H. Schmelzer, E. Lehner, K. Mäder, C. Wölk, T. Groth, *Mater. Today Bio* **2020**, *7*.
[34] Y. A. Brito Barrera, C. Husteden, J. Alherz, B. Fuhrmann, C. Wölk, T. Groth, *Mater. Sci. Eng. C* **2021**, *131*, 112516.
[35] J. S. J. Tang, S. Rosencrantz, L. Tepper, S. Chea, S. Klöpzig, A. Krüger-Genge, J. Storsberg, R. R. Rosencrantz, *Molecules* **2019**, *24*, 1.
[36] J. S. J. Tang, K. Schade, L. Tepper, S. Chea, G. Ziegler, R. R. Rosencrantz, *Molecules* **2020**, *25*.
[37] K. Zhang, E. Brendler, A. Geissler, S. Fischer, *Polymer (Guildf).* **2011**, *52*, 26.
[38] S. Böcker, L. Elling, *Bioengineering* **2017**, *4*.
[39] H. Ideo, A. Seko, T. Ohkura, K. L. Matta, K. Yamashita, *Glycobiology* **2002**, *12*, 199.
[40] H. Ideo, T. Matsuzaka, T. Nonaka, A. Seko, K. Yamashita, *J. Biol. Chem.* **2011**, *286*, 11346.
[41] M. L. Talaga, N. Fan, A. L. Fueri, R. K. Brown, P. Bandyopadhyay, T. K. Dam, *Biochemistry* **2016**, *55*, 4541.
[42] S. J. Kim, H. Ise, M. Goto, K. Komura, C. S. Cho, T. Akaike, *Biomaterials* **2011**, *32*, 3471.
[43] M. Ratanajanchai, S. Soodvilai, N. Pimpha, P. Sunintaboon, *Mater. Sci. Eng. C* **2014**, *34*, 377.
[44] K. Kunath, A. Von Harpe, D. Fischer, T. Kissel, *J. Control. Release* **2003**, *88*, 159.
[45] M. A. Zanta, O. Boussif, A. Adib, J. P. Behr, *Bioconjug. Chem.* **1997**, *8*, 839.
[46] B. Wang, K. Yoshida, K. Sato, J. Anzai, *Polymers (Basel).* **2017**, 1.
[47] G. B. Sukhorukov, B. T. Levy, C. De, *Adv. Funct. Mater.* **2008**, 1586.
[48] X. Zhang, Y. Guan, Y. Zhang, *Biomacromolecules* **2012**.
[49] K. Sato, K. Awaji, M. Ito, J. Anzai, *Colloid Polym. Sci.* **2017**, 877.
[50] R. van den Berg, J. A. Peters, H. van Bekkum, *Carbohydr. Res.* **1994**, *253*, 1.

[51] M. Olszyna, A. Debrassi, C. Üzüm, L. Dähne, *Adv. Funct. Mater.* **2019**, *29*, 1.
[52] R. Bischler, M. Olszyna, M. Himmelhaus, L. Dähne, *Eur. Phys. J. Spec. Top.* **2014**, *223*, 2041.
[53] J. Suh, B. K. Hwang, *Ionization of PEI and PAA at various pH's*, Vol. 22, **1994**, pp. 318–327.

4 Functional Glyco-Nanogels for Multivalent Interaction with Lectins

Abstract

Interactions between glycans and proteins have tremendous impact in biomolecular interactions. They are important for cell–cell interactions, proliferation and much more. Here, we emphasize the glycan-mediated interactions between pathogens and host cells. *Pseudomonas aeruginosa*, responsible for a huge number of nosocomial infections, is especially the focus when it comes to glycan-derivatives as pathoblockers. We present a microwave assisted protecting group free synthesis of glycomonomers based on lactose, melibiose and fucose. The monomers were polymerized in a precipitation polymerization in the presence of NiPAm to form crosslinked glyco-nanogels. The influence of reaction parameters like crosslinker type or stabilizer amount was investigated. The gels were characterized in lectin binding studies using model lectins and showed size and composition-dependent inhibition of lectin binding. Due to multivalent presentation of glycans in the gel, the inhibition was clearly stronger than with unmodified saccharides, which was compared after determination of the glycan loading. First studies with *Pseudomonas aeruginosa* revealed a surprising influence on the secretion of virulence factors. Functional glycogels may be in the future potent alternatives or adjuvants for antibiotic treatment of infections based on glycan interactions between host and pathogen.

4.1 Introduction

A vast number of pathogens utilize glycan-mediated interactions for cell invasion and their actual pathogenicity [1,2]. Well known examples are enterohemorrhagic *E. coli* (EHEC) with its shiga-like toxin [3], *Clostridium difficile* with its glycan binding Toxin A [4,5], *Vibrio cholera* [6] and others. Several small molecules based on sugars as well as larger glycoclusters have been synthesized as patho-blocking agents for fighting these microbes or their toxins [7,8,9].

A key point for strong glycan-mediated interactions is the multivalent presentation of glycan ligands inducing the ‘cluster glycoside effect’ [10,11,12]. Good choices for multivalent glycostructures are so called glycopolymers [13,14,15,16]. These are polymers with pendent glycan groups attached to a polymeric backbone. Glycopolymers have been shown to enable very high binding avidities with lectins resulting in K_D values in the nanomolar range [17]. Multivalency is crucial for good interactions

between glycans and lectins and may increase binding strength in orders of magnitude. Examples of the usage of glycopolymers are biosensor surfaces for lectin binding studies or as mannose-based scavenging material for *E. coli* [17,18,19,20,21].

Recently, polymeric gels containing glycans were synthesized [22] via a microfluidic set-up to yield lactose containing gels with good binding to appropriate lectins [23]. Micro-, nano- or hydrogels in general can be considered as very promising systems for lectin binding. This is mainly due to their swollen "waterlike" state, their biocompatibility, the large internal volume and their potential multivalent presentation mode with incorporated glycans [24,25]. A very often used monomer for nanogel synthesis is NiPAm (*N*-isopropylacrylamide), which yields thermoresponsive polymers and enables precipitation polymerization of uniform gel particles [26,27]. PNiPAm (Poly(N-isopropylacrylamide)) shows a lower critical solution temperature (LCST) of about 32 °C. Below this temperature, gel particles are considered swollen and rather fuzzy, whereas above the LCST the particles become more defined, smaller and more rigid due to denser packaging. While NiPAm itself is considered cytotoxic, PNiPAm is reported to be biocompatible and non-toxic to cells [28,29,30]. The thermoresponsive properties of PNiPAm enable the batch synthesis of gels via precipitation polymerization preventing the usage of organic solvents compared to, e.g., emulsion polymerization.

Pseudomonas aeruginosa (PA) is an opportunistic pathogen rated as critical by the WHO list indicating for which strain new antibiotics are urgently needed [31,32]. Interestingly, PA utilizes two lectins (LecA and LecB) as virulence factors [33,34]. Many glycan derivatives were synthesized as patho-blocking agents [35,36]. However, the number of reports on glycopolymeric multivalent structures for lectin inhibition is rather limited. Potent glycomaterials must comprise a sufficient multivalent mode of ligand presentation. For PA, it was shown that multivalent ligands based on glycooligomers, dendrimers or as peptide derivatives are superior to the monovalent species [37,38,39,40,41]. This stands also for other lectins: Here, increase of affinity over several orders of magnitude by multivalent ligand presentation is known [13].

We here describe for the first time the synthesis of different glycogel species containing either lactose (Galβ1,4Glc-), melibiose (Galα1,6Glc-) or fucose. The glycans were chosen as readily available, naturally occurring structures, with the latter two known to act as ligand for LecA and LecB [42,43]. By enabling multivalent presentation in the gel, we expect to circumvent the necessity of introducing modifications to monovalent glycans increasing their affinity. The gels were synthesized in a batch process via precipitation polymerization utilizing NiPAm and lactose, melibiose or fucose glycomonomers in the presence of crosslinker and surfactant for stabilization. In this study, we focus on the influence of synthesis parameters on the inhibition potential of the gels and determined the presence or absence of a multivalent effect compared to monovalent, soluble sugars. Ability of lectin

inhibition was screened by an ELISA-type approach with fluorescently labeled plant lectins as model lectins. Ultimately, we tested in a preliminary study the influence of the gels on the growth of PA.

In the future, glycan-based soft matter can be a good way to yield biocompatible yet strong pathoblockers for medical applications. Glycoscavengers can be used for numerous different pathogens and be a promising alternative to antibiotic treatment with minimal selection pressure avoiding acquirement of resistances.

4.2 Results and Discussion

4.2.1 Synthesis of Glycomonomers

For the synthesis of glycomonomers with a polymerizable moiety at the C1-position we chose a protecting group free microwave-assisted Kochetkov-amination with subsequent reaction with methacryloylchloride (Scheme 4.1) [44,45,46,47].

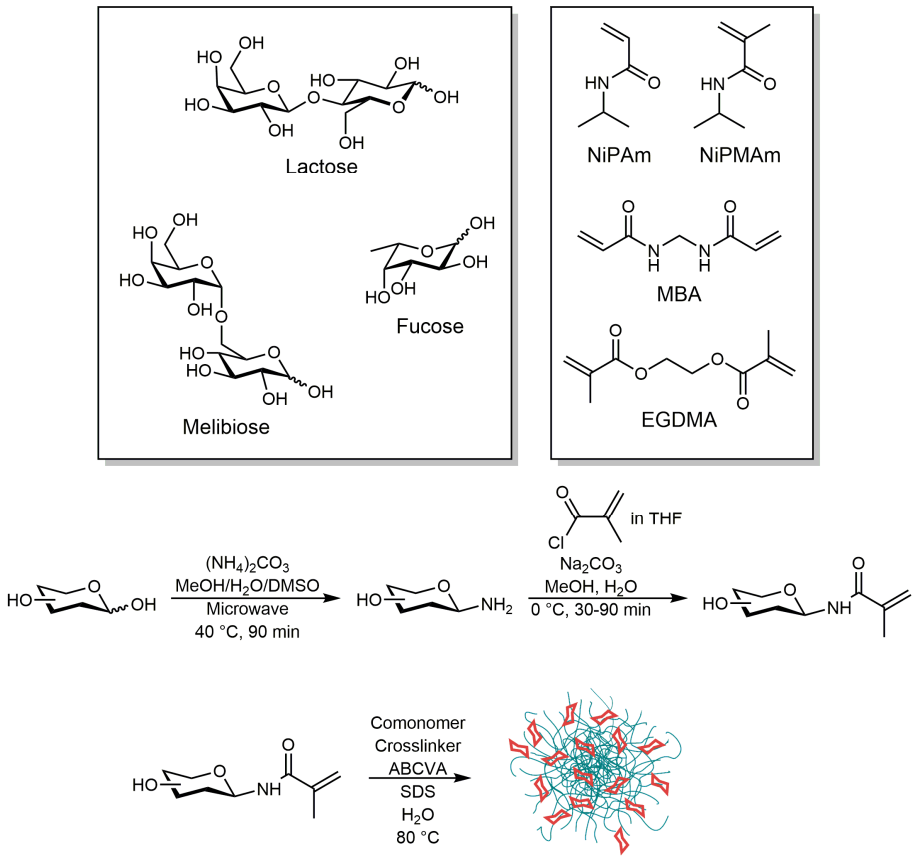

Scheme 4.1. Lactose, melibiose and fucose were converted via a protecting group free synthesis utilizing microwave irradiation to the respective methacrylamides. The monomers were used for the synthesis of glyco-nanogels in a precipitation polymerization in the presence of comonomer N-isopropylacrylamide (NiPAm) or *N*-isopropylmethacrylamide (NiPMAm) and crosslinker methylenebis(acrylamide) (MBA) or ethylene glycol dimethacrylate (EGDMA).

Modification of the saccharides at C1-postion should not affect the biological recognition of the sugar by lectins. The disaccharides lactose and melibiose as well as the monosaccharide fucose were used as starting material and converted to the respective methacrylamides MelMAm (melibiose-methacrylamide), LacMAm (lactose-methacrylamide) and FucMAm (fucose-methacrylamide) (Scheme 4.1). The overall yields ranged from 18% to 75%, which is sufficient for the production of nanogels. The compounds were identified by NMR spectroscopy and ESI MS (Figures 4.S1–4.S9, Supporting Information). Advantages of the synthesis are the usage of cheap starting materials, the intact cyclisation of the reducing sugar and the regioselectivity for the C1-position. However, it must be noted that the β-anomer is strongly favored as reaction product. For melibiose and lactose, we do not expect any drawbacks regarding this, but β-fucose is a rather rare compound and may not be recognized by typical fucose binding lectins like *Ulex europaeus* agglutinin I (UEA I). However, it is reported that LecB binding can be inhibited to some extent by fucosylamine, which is in fact 1-amino-β-L-fucose and the intermediate of our synthesis route [35,43,48].

4.2.2 Synthesis of Glycogels

4.2.2.1 Free-Radical Precipitation Polymerization

We evaluated two different procedures for the preparation of the glycogels: Inverse emulsion polymerization and free-radical precipitation polymerization with NiPAm and NiPMAm. The yields of the emulsion polymerization turned out to be not sufficient for subsequent analysis in lectin-assays or tests with PA (yields were below 5%, data not shown). We assume a slow propagation and deactivation by the glycomonomers resulting in these low yields. The syntheses via free-radical precipitation polymerization in contrast gave a sufficient yield of up to 75% compared to the initially used amount of monomer and crosslinker. Furthermore, conducting the reaction in water gives the advantage of bypassing the poor solubility of the unprotected glycomonomers in organic solvents and enabling a “green” route avoiding potentially toxic solvents. Hence, we synthesized all gels presented here by free-radical precipitation polymerization in water. The reaction temperature was chosen to be 80 °C as this is above the LCST of PNiPAm/PNiPMAm as well as above the 10 h half-life decomposition temperature of the water soluble azoinitiator 4,4’-azobis(4-cyanovaleric acid) (ABCVA). The freeze-dried glycogels were hygroscopic and TGA analysis revealed an equilibrium water content of about 10%. Throughout the text the gels carrying melibiose are labeled “MG”, gels with lactose are labeled “LG” and fucose containing gels are labelled “FG”. Gels without sugar serve as comparative sample and negative control for the bioassays and are labelled with “G”.

4.2.2.2 Comonomer and Crosslinker

Since the glycopolymer itself does not precipitate in water upon chain propagation, we required comonomers which are water soluble and exhibit a LCST as a polymer. Furthermore, the different monomers should have similar reaction kinetics in order to form a hydrogel with evenly distributed glycosides to the greatest extent possible. As the glycomonomers are methacrylamides, we selected the methacrylamide NiPMAm and ethylene glycol dimethacrylate (EGDMA) and compared the performance to the acrylamide NiPAm and *N*,*N*'-methylenebis(acrylamide) (MBA) as comonomer and crosslinker, respectively. Interestingly, PNiPMAm glycogels (MG-7) proved to be unsuitable for binding assays, as the pure PNiPMAm nanogel (G-3) itself seems to influence the lectin binding (see Section 4.2.3). Hence, no reliable lectin binding data can be produced with PNiPMAm gels and we omitted these gels. Gels containing PNiPAm showed clearly better suitability for the lectin assays. The type of crosslinker (MBA vs. EGDMA) had no significant influence on the yield but for glycogels synthesized with NiPAm and EGDMA (MG-8), binding studies with lectins showed less inhibition potentials (see Section 4.2.3) than glycogels produced with NiPAm and MBA. Thus, we chose for the syntheses of glycogels NiPAm as the comonomer enabling the precipitation polymerization, and MBA as crosslinker. We assume that for good inhibition performance, a core-shell-like gel morphology is appreciated where the core is built up by the non-glycosylated monomers, surrounded by a glycan-shell. This can be achieved most likely by using the fast polymerizing acrylamides NiPAm and MBA together with the rather slow methacrylamide glycomonomers.

4.2.2.3 PNiPAm Glycogels

Typically, when PNiPAm nanogels particles are formed by precipitation polymerization, the reaction solution turns turbid. The turbidity depends on the concentration and size of the particles. For the glycogels, we observed a strikingly lower turbidity during reaction. This indicates that the gels were not only consisting of NiPAm but the glycomonomer could be incorporated into the polymers as well. We assume that the glyco-comonomer interferes with the complete collapse of PNiPAm and forms a fuzzy shell-like structure around a PNiPAm core. In scanning electron microscopy (SEM) as well as in atomic force microscopy (AFM) images, we can find spherical particles (see Supporting Information). Hence, we achieved glycogel particles and not free polymers. From dynamic light scattering (DLS) measurements and SEM images, we observe high polydispersity in contrast to the excellent monodispersity of pure PNiPAm nanogels (Figure 4.1). Due to the hydrophobic propyl moiety of NiPAm, the polymer precipitates above its LCST when the hydrophobic interactions dominate. The glycomonomers exhibit a high hydrophilicity. This property may counteract the hydrophobic interactions of NiPAm which could explain the high polydispersity. As the gels do not dissolve in water

independently of the surrounding temperature, we can assume that the products are crosslinked networks and not free copolymer chains.

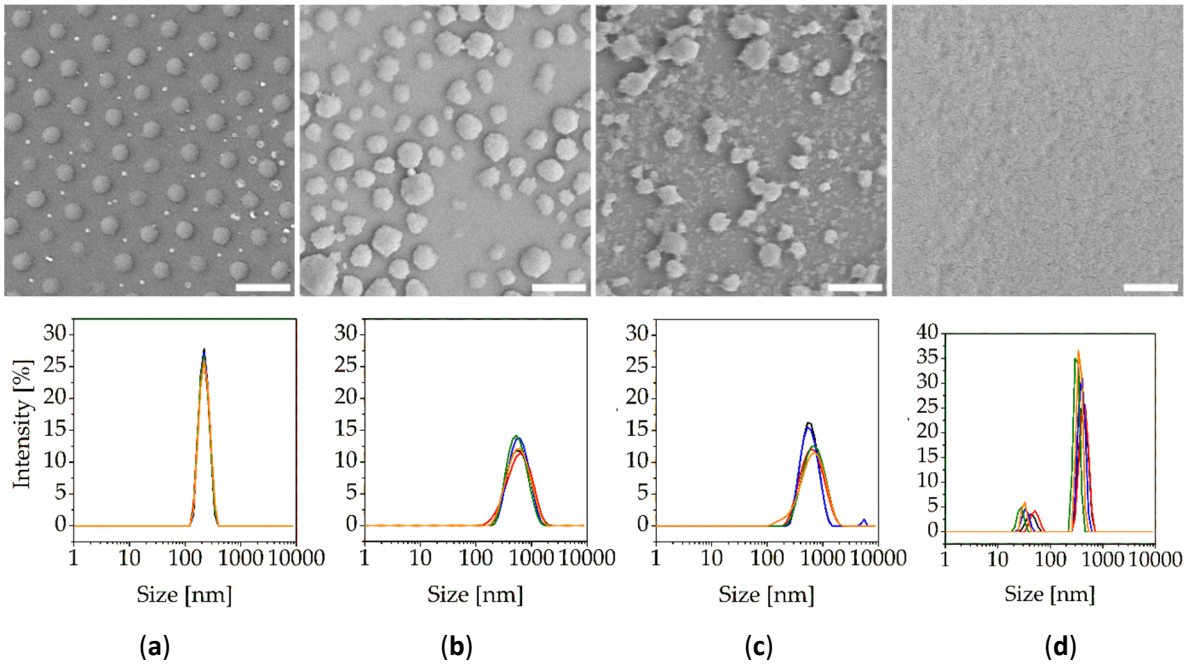

Figure 4.1. Scanning electron microscopy (SEM) images and dynamic light scattering (DLS) size distribution by intensity (at 50 °C) of different nanogels: (**a**) monodisperse PNiPAm nanogel particles G-1 synthesized with 0.2 mM SDS; (**b**) glycogel MG-1 synthesized with 0.4 mM SDS; (**c**) MG-2 synthesized with 2.0 mM SDS; (**d**) glycogel MG-3 synthesized with 4.0 mM SDS. Scale bars represent 1 µm.

We used SDS in order to stabilize the gels during reaction. At similar surfactant concentrations, the sizes of the glycogels are larger than the size of the PNiPAm nanogels (Figure 4.1), which may be related to the fuzzy glyco-shell, which tends to swell in aqueous media independent of the surrounding temperature. Furthermore, with increasing surfactant concentration, the size of the glycogels do not evidently become smaller and their monodispersity does not increase either (Table 4.1). Typically, increased concentrations of stabilizer in precipitation polymerizations lead to smaller diameters [49]. The effect of SDS seems to be diminished in the case of glycogels. Surprisingly, high concentrations of SDS appear to even increase the polydispersity. We assume that the hydrophilic property of the glycomonomers counteracts the formation of monodisperse and uniform particles. A possible explanation is that the hydrophilic part of the surfactant and the hydrophilic glycomonomer repell each other, which disturbs the formation of stabilizing SDS-corona around the growing gel particles. Therefore, a high amount of SDS may cause the glycosyl moiety to distribute and scatter in the water instead of letting formed polymer chains immediately collapse into a coil in between the surfactants.

Table 4.1. Gels synthesized with varied sodium dodecyl sulfate (SDS) concentrations.

Gel	c(SDS) [mM]	Yield [%]	D_h(50 °C) [nm]	PDI [%]
G-1	0.2	-	218	2.54
MG-1	0.4	67	507	21.2
MG-2	2.0	67	554	26.4
MG-3	4.0	43	1084	56.6

Temperature-dependent DLS measurements show that some glycogels still retain some of the thermoresponsiveness of PNiPAm. It has to be noted that the hydrodynamic diameter (D_h) of the glycogels are not reliable as the polydispersity index (PDI) is quite high. However, we can observe a trend where the PDI decreases at 50 °C as well as the averaged hydrodynamic diameter (Table 4.2).

Table 4.2. Hydrodynamic diameters (D_h) and polydispersity index (PDI) of nanogels.

Gel	D_h(20 °C) [nm]	PDI [%]	D_h(50 °C) [nm]	PDI [%]
G-1	406	4.30	218	2.54
G-2	101	9.10	54.2	12.9
MG-0	143	30.3	103	23.0
MG-1	669	29.7	507	21.2
MG-2	678	40.7	554	26.4
MG-3	1084	56.6	1084	56.6
MG-4	474	31.5	488	20.4
MG-5	651	22.4	569	18.7
MG-6	436	66.6	328	27.9

This comes in agreement with the typical behavior of PNiPAm nanogels. Their hydrodynamic diameter decreases with increasing temperature as they collapse. Their PDI usually improves at temperatures above the LCST since the collapsed particles with the defined surface border are easier to measure via DLS than swollen, soft nanogels with their fuzzy surface and dangling polymer chains. Though, we do not observe a defined LCST for the glycogels (see Figure 4.2).

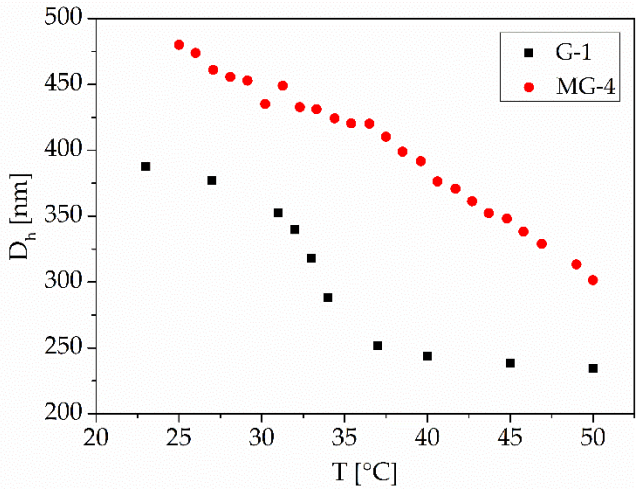

Figure 4.2. Temperature-dependent analysis of the hydrodynamic diameter of PNiPAm nanogel G-1 and melibiose glycogel MG-4 using DLS. While still thermoresponsive to some extent, no distinct lower critical solution temperature (LCST) can be detected for the glycogels (MG-4).

4.2.2.4 Initiation of the Polymerization

Generally, the synthesis of pure PNiPAm nanogels require only little amounts of initiator (0.25 mol%) [50]. By using a mixture of NiPAm and MelMAm, 0.25 mol% of initiator seems to be insufficient as the reaction mixture stays clear. This is even the case with the fourfold amount of ABCVA (1 mol%). This indicates that no crosslinked networks are formed or that the polymerization is not taking place or being inhibited somehow. Therefore, we fed an additional amount initiator after two hours to the reaction mixture (Table 4.3, MG-1). It is also possible to use an even higher amount of the initiator from the beginning to start the reaction (MG-4). For better comparison with previously synthesized gels, we continued with the method mentioned first with an initiator feed. Preceding equilibration of the reaction mixture at the reaction temperature, as often executed for PNiPAm nanogels [49], does not lead to significantly better binding performance (MG-5). The method of reaction start does not significantly affect the yield, hydrodynamic diameter nor the polydispersity. Thus, we synthesized the rest of the glycogels without temperature equilibration.

Table 4.3.Glycogels synthesized with three different methods of reaction start.

Glycogel	X_1(ABCVA) [mol%]	X_2(ABCVA) [mol%]	Yield [%]	D_h(50 °C) [nm]	PDI [%]
MG-1	1.0	2.0	67	507	21.2
MG-4	3.0	-	61	488	20.4
MG-5	3.0	-	66	569	18.7

4.2.2.5 Glycogels with Various Crosslinking Densities

The crosslinking density generally influences the morphology of PNiPAm nanogels such as deformability, softness and swelling ability [50]. Here, we compare glycogels based on different saccharides and the influence of the crosslinker amount. The highest yield of 75% related to the initial amount of total monomer was achieved with LacMAm and 5 mol% crosslinker resulting in glycogel LG-1 (Table 4.4). Similar synthesis with MelMAm and 5 mol% crosslinker gained 29% less yield (MG-6; 46%). For melibiose glycogels, the highest yield was achieved with 10 mol% of crosslinker (MG-2; 67%). Comparable synthesis with FucMAm and 5 mol% crosslinker also achieved lower yields of 56% (FG-1). When changing the crosslinking density from 5 to 10 mol% (FG-2), the yields dropped to 33%. It has to be noted that during synthesis the fucose glycogels precipitated more readily than the other glycogels and tend to aggregate during reaction. Here, we filtered off the large, aggregated sediments before freeze-drying. We assume that higher amounts of crosslinker lead to more aggregation. This is consistent with the low yield of FG-2. It is strongly evident how differently various crosslinker amounts and various saccharides influence the precipitation polymerization, even though LacMAm and MelMAm are both disaccharides. Melibiose exhibits a higher water solubility than lactose, indicating a stronger negative influence on the precipitation behavior of the gels. Therefore, in case of melibiose glycogels, higher amounts of crosslinker might be necessary in order to gain higher yields since MBA reacts faster than NiPAm and, thus, does not slow down the reaction. Fucose, however, carries a non-polar methyl-group which can reestablish a more PNiPAm-like precipitation behavior, hence, the reaction solution turned turbid faster. Besides, the higher hydrophobicity of fucose might be a cause for the aggregation during synthesis.

Table 4.4. Comparison of glycogels with different saccharides and crosslinker amounts.

Glycogel	X(MBA) [mol%]	Yield [%]	D_h(50°C) [nm]	PDI [%]
LG-1	5.0	67	507	21.2
MG-6	5.0	46	488	20.4
MG-2	10	66	569	18.7
FG-1	5.0	56	643	51.7
FG-2	10	33	548	65.0

4.2.2.6 Amount of incorporated Carbohydrates in Glycogels

We determined the amount of incorporated glycomonomer by a phenol-sulfuric acid assay and studied how it is influenced by synthesis parameters and type of sugar (Table 4.5). The assay revealed

the total carbohydrate content of the gel and was calibrated with the free sugars. When the same type of glycomonomer is used, the amount of incorporated sugar is not strongly influenced by different synthesis parameters such as the amount of stabilizer, crosslinker and initiator, the type of comonomer and crosslinker and the method of initiation. Hence, the sugar content is very similar, independent of glycogel size and crosslinking density. This means that the incorporation of the glycan is solely controlled by the polymerization kinetics of the monomer and not dramatically affected by the actual reaction parameters. On the other hand, a striking difference in sugar content is observed when different glycomonomers are examined. On average, the fucose glycogel contains the highest sugar amount with a calculated incorporation of up to 70% of the initially used glycomonomer, followed by lactose (up to 40%) and melibiose (up to 25%) glycogel. This coincides with the aforementioned fast reaction of FucMAm as it is more hydrophobic and therefore might react similar to and with NiPAm in contrast to the very hydrophilic lactose and melibiose glycomonomers.

Table 4.5. Amount of incorporated glycomonomer in the glycogels.

Glycogel	Sugar Content [µmol/mg]	Averaged Sugar Content for Each Glycomonomer Type [µmol/mg]	Theoretical Sugar Content [a] [µmol/mg]	Yield of Incorporated Glycomonomer [b] [%]
LG-1	0.43 ± 0.03	0.41 ± 0.03	1.12	38.3 ± 2.7
LG-2	0.39 ± 0.01		1.16	33.7 ± 0.9
MG-0	0.24 ± 0.02	0.26 ± 0.05	1.16	20.8 ± 1.7
MG-1	0.29 ± 0.06		1.14	25.4 ± 5.3
MG-2	0.28 ± 0.02		1.14	24.5 ± 1.8
MG-3	0.23 ± 0.04		1.14	22.8 ± 3.5
MG-4	0.20 ± 0.05		1.14	18.1 ± 4.5
MG-5	0.26 ± 0.05		1.11	23.5 ± 4.5
MG-6	0.26 ± 0.02		1.12	23.1 ± 1.8
MG-7	0.27 ± 0.02		1.06	25.5 ± 1.9
MG-8	0.28 ± 0.04		1.14	24.5 ± 3.5
FG-1	0.94 ± 0.19	0.98 ± 0.16	1.43	65.6 ± 13
FG-2	1.01 ± 0.13		1.43	70.5 ± 9.1

[a] Theoretical amount of incorporated glycomonomer if complete turn-over of all relevant components is considered. [b] Measured sugar content divided by theoretical sugar content.

4.2.3 Inhibition Studies with Plant Lectins

The aim of this study is to synthesize glycogels with full functionality in means of glycan binding. Therefore, it is important to prove the accessibility of the saccharide units for lectins. For screening the synthesized glycogels, we chose three plant lectins as representatives for melibiose, lactose and fucose binding lectins, respectively—Jacalin [51], *Erythrina cristagalli* lectin (ECL) [52] and *Ulex europaeus* agglutinin I (UEA I) [53]. In ELISA-type inhibition assays, the nanogels were applied as inhibitors for lectin binding to an immobilized ligand.

First of all, we investigated lectin binding to standard glycoproteins asialofetuin (ASF) and thyroglobulin. ECL and Jacalin bind sufficiently to ASF, whereas for UEA I binding α-fucose residues are necessary. This could be found neither on ASF nor on thyroglobulin (data not shown). As mucins contains fucose units, porcine stomach mucin was tested and found to possess ligands for UEA I. The binding curves of UEA I on mucin as well as of the other two lectins on ASF are shown in Figure 4.3a. These binding signals are glycan mediated because inhibition with the appropriate sugar was proven (Figure 4.3b).

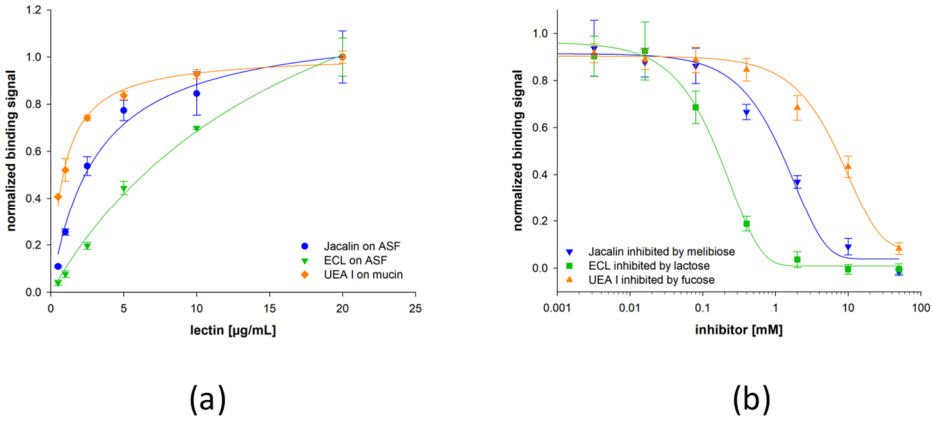

Figure 4.3. Binding and inhibition of chosen plant lectins to immobilized glycoproteins. (**a**) The lectins Jacalin and *Erythrina cristagalli* lectin (ECL) show binding to immobilized asialofetuin (ASF), whereas *Ulex europaeus* agglutinin I (UEA I) binds to immobilized mucin from porcine stomach. (**b**) The three lectins bind glycan mediated and are inhibitable by appropriate saccharides. Typical inhibition curves are shown for Jacalin inhibited by melibiose, ECL inhibited by lactose and UEA I inhibited by fucose.

A set of melibiose containing nanogels was synthesized with different synthesis conditions. The majority of these glycogels inhibited the binding of Jacalin to ASF indicating functional melibiose presentation. The SDS amount during the synthesis had a small influence on the inhibition potential of the glycogels. An increasing amount of SDS seemed to weaken the lectin binding (Figure 4.4a). However, we tested if this is an effect caused by the denaturing properties of SDS and incomplete removal during dialysis. It turned out that the lectin binding is not affected by SDS at concentrations around 0.1% (data not shown), which represents the highest amount used during synthesis. The

initiation method of polymerization is irrelevant for lectin binding, as the inhibition curves for MG-1, MG-4 and MG-5 in Figure 4.4b are nearly identical. The type of crosslinker as well as the monomer type have the strongest influence. If NiPMAm was used for nanogel synthesis, no lectin inhibition was measured but an elevated binding signal occurred (Figure 4.4c). This phenomenon was observed for the NiPMAm control G-3 as well as for the melibiose-NiPMAm gel MG-7. Potentially, the lectin interacts with the nanogel somehow but is further able to bind ASF. In general, PNiPMAm as well as PNiPAm are reported to show rather low unspecific protein adsorption [54]. MG-8 has again a NiPAm backbone but EGDMA as crosslinker instead of MBA. EGDMA and MBA exhibit different reaction kinetics which can lead to different sizes and structures in the gel as shown in previous studies with PNiPAm microgels [55]. The change to EGDMA had a negative influence on the functionality and led to weak inhibitory potency as well as incomplete inhibition (Figure 4.4c and Figure 4.5). Comparing the glycogels, regarding their size, a positive effect was seen with smaller gels (Figure 4.4d). MG-4 with approximately 500 nm D_h showed slightly better inhibition than MG-1 with approximately 700 nm. But the highest inhibitory potency among all melibiose nanogels had MG-0 that was the smallest by far (approximately 150 nm D_h). The smaller the particle, the larger the surface and that means, in this case, a higher density of glycans. We found the highest multivalent effect of these smallest nanogels reaching an IC50 value of 0.05 mg/mL which is a threefold higher inhibition value than the average of all larger nanogels (see Figure 4.5).

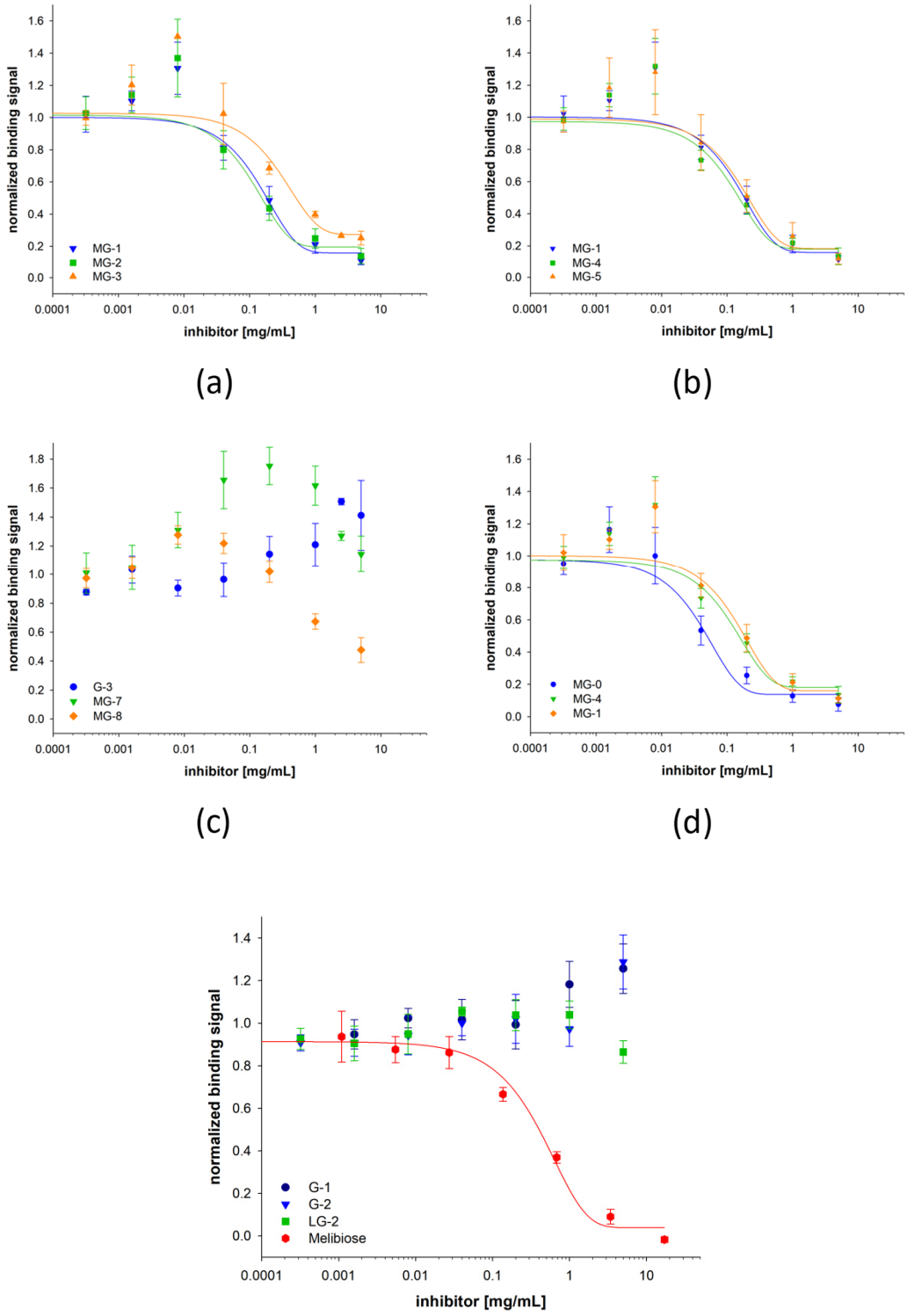

Figure 4.4. Inhibition of Jacalin binding by glyco-nanogels. Melibiose nanogels were investigated in inhibition studies with Jacalin and compared regarding (**a**) SDS amount during the synthesis, (**b**) initiation method of polymerization, (**c**) type of comonomer and crosslinker, and (**d**) the size of the gels. In (**e**), control nanogels without sugar or containing a non-inhibiting sugar show no inhibition. The complete inhibition by the disaccharide melibiose proved the suitability of the assay.

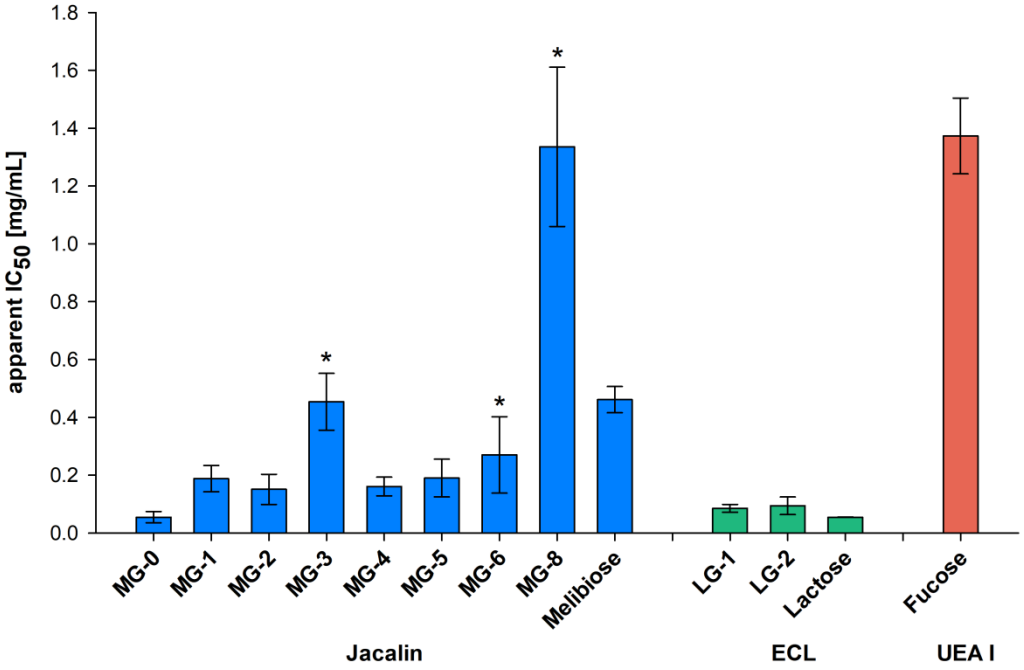

(**a**)

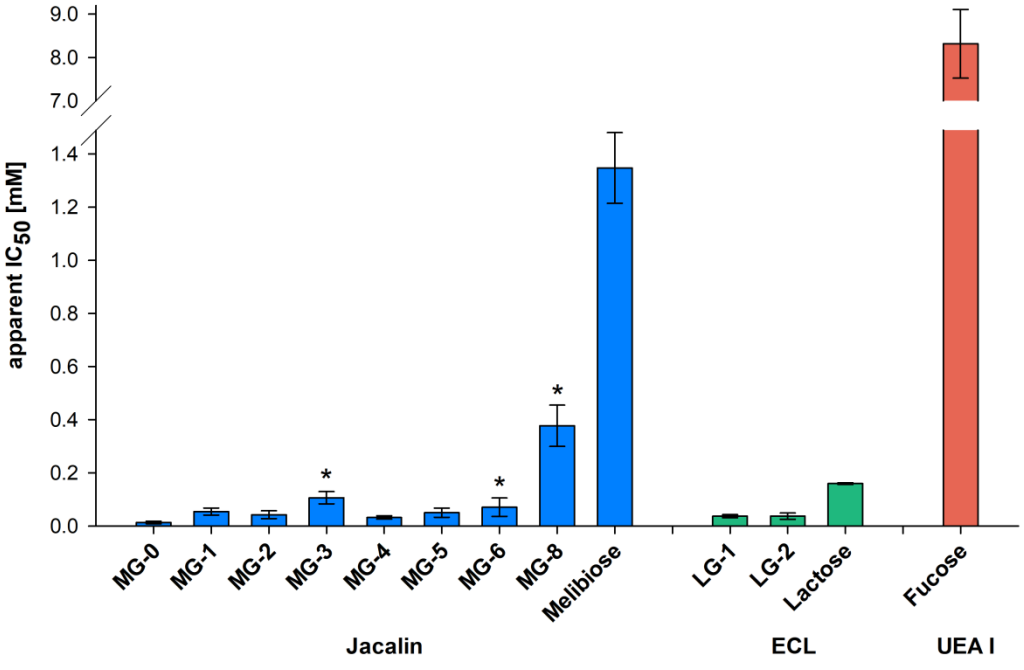

(**b**)

Figure 4.5. Apparent IC_{50} values of glycogels and free saccharides. The concentration (**a**) (mg/mL) glycogel and (**b**) (mM) sugar content that is needed for half maximal inhibition is shown for melibiose nanogels and free melibiose regarding Jacalin binding, lactose nanogels and free lactose regarding ECL binding and fucose regarding UEA I binding. Gels marked with asterisks did not show complete inhibition.

Noticeably, in the presence of glycogels of low concentrations (<0.01 mg/mL) the binding of Jacalin to ASF is enhanced, indicated by a higher fluorescence signal than the value for lectin binding without glycogel. Jacalin is a tetrameric lectin and thus, it is able to crosslink the glycogel with the glycoprotein immobilized on the surface [51,56,57]. In this way, the overall amount of glycans on the surface increases and it is possible that more lectins bind to the crosslinked nanogels, resulting in a higher fluorescence being measured. For calculating the IC50 values, these data points were neglected.

We also included NiPAm controls without sugar content in our binding study. NiPAm nanogels of small size (G-2) as well as of larger size (G-1) did not inhibit the Jacalin binding (Figure 4.4e). The same goes for a lactose containing nanogel—no inhibition was observed. Taking these findings together, the synthesized melibiose nanogels contain melibiose units fully functional for lectin binding. The averaged IC50 value of melibiose nanogels that inhibit Jacalin binding almost completely is 0.15 mg/mL. In comparison, melibiose as free sugar shows an IC50 value of 0.5 mg/mL. In consequence, the glycogels show a multivalent effect that is even higher in consideration of the ratio of sugar monomer during the synthesis of approximately 20% compared to the overall monomer amount. After determining the sugar content of the glycogels and calculating the apparent IC50 values from mg/mL glycogel into mM sugar amount (Figure 4.5b), the multivalent effect of all melibiose nanogels is even more emphasized. Due to the small amount of incorporated melibiose during the synthesis, the IC50 values are in average approximately 15-times lower than for melibiose. MG-0 as most potent inhibitor shows even 100-fold higher inhibition than melibiose. Despite not complete inhibition for MG-3, MG-6 and MG-8, those IC50 values are still lower than melibiose showing again the multivalent character of sugar presentation of the glycogels. The incomplete inhibition of MG-8 might be due to possible differences in the glycogel structure. The lower inhibition strength of MG-3 and MG-6 can also be explained by different structures as we synthesized MG-3 with high concentrations of stabilizer, which influences the size and morphology of the nanogels. The lower crosslinking density in MG-6 determines the morphology of nanogels as well [50]. With regard to one type of glycogel, and therefore the same sugar content, the inhibitory potency seems to be strongly dependent on the morphology of the glycogels.

The synthesized lactose nanogels were analyzed in binding assays using ECL, a lactose binding lectin [52]. LG-1 and LG-2 are two lactose-containing NiPAm nanogels of very similar syntheses. Both glycogels show complete inhibition of ECL binding to ASF with identical IC50 values (Figure 4.5 and Figure 4.6a). For ECL, no binding enhancement at low glycogel concentrations is visible. Due to the dimeric structure of ECL, crosslinking of the glycogel with the immobilized glycoprotein is less pronounced and not enough to yield an increased fluorescence signal. G-1, a control PNiPAm nanogel without sugar, as well as MG-0, a melibiose containing nanogel, did not inhibit ECL binding proving the binding specificity to lactose. Moreover, free lactose is a potent inhibitor for ECL with IC50 in the same

range as the lactose nanogels (Figure 4.5a). However, due to the limited amount of lactose monomer (approximately 20%) during synthesis, both lactose nanogels contain 0.4 µmol lactose per mg nanogel (Table 4.5). With IC50 values that are over four-times lower compared to free lactose, when regarding the sugar content (Figure 4.5b), the lactose nanogel also has a multivalent character and led to good inhibition potency. The multivalent effect of the lactose nanogels, however, is less distinct than that of the melibiose nanogels.

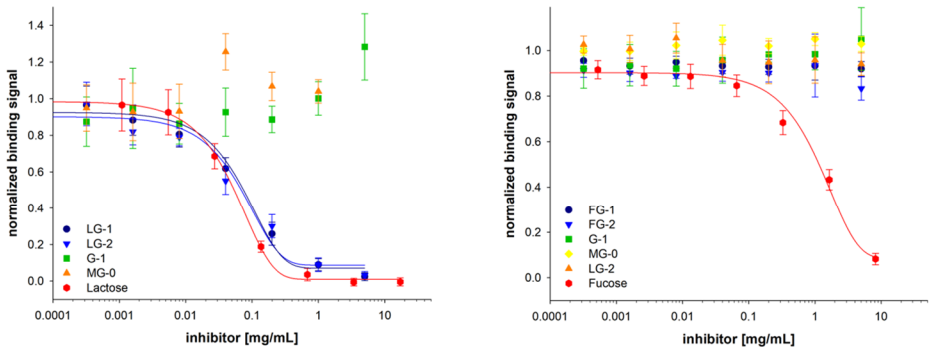

Figure 4.6. Inhibition of ECL and UEA I binding by glyco-nanogels. (**a**) ECL binding is inhibited by lactose containing nanogels and by free lactose, but not by the control nanogel without sugar and by melibiose nanogel. (**b**) UEA I is only inhibited by free fucose; no synthesized glycogel is bound by UEA I.

The third type of glyco-nanogel we synthesized contains fucose. Therefore, the binding assay was performed with UEA I, a fucose binding lectin [53]. Two different fucose nanogels, FG-1 and FG-2, were tested but no inhibition was observed (Figure 4.6b). Our synthesis route led predominantly to β-fucose that is rarely found in nature [58]. Thus, it was no surprise that UEA I did not bind to the glycogel. In addition, UEA I is described to be a lectin binding to α-fucose [53]. As seen in Figure 4.6b, all controls gave the correct results: Nanogel without sugar as well as melibiose and lactose containing nanogels did also not inhibit the UEA I binding, whereas with free fucose selective binding of UEA I to immobilized mucin was proven because it was completely inhibitable. The UEA I binding is the strongest binding to its immobilized glycoprotein among the three tested plant lectins, here. The IC50 value of fucose for UEA I binding is three-times (six-times for mM value) higher than melibiose for Jacalin binding and 25-times (50-times for mM value) higher than lactose for ECL binding (Figure 4.5).

4.2.4 Influence on Pseudomonas aeruginosa

In a small preliminary study, we investigated the influence of the glycogels on the growth of PA. For this, gels were selected by the aforementioned lectin-assay and PA was incubated for 24 h with

MG-0, MG-4, LG-1, FG-1 and G-2. FG-1 was chosen despite the fact no binding was detected in the lectin studies, because reports suggest that LecB is capable of binding β-fucose moieties [35,43,48]. The gel concentration was kept at 2 mg mL^{-1} in the cultivation broth and as additional control, we used unmodified melibiose and fucose (2 mg mL^{-1} each).

In this first study, we focused on the secretion of the fluorescent siderophore pyoverdine, which is an essential virulence factor of PA [59]. Pyoverdine is involved in various processes, including regulation of other virulence factors as well as the enabling the formation of biofilms, which decreases the sensitivity of PA towards antibiotics [60,61]. Figure 4.7 shows a fluorescence image of the 24-well plates with PA and gels.

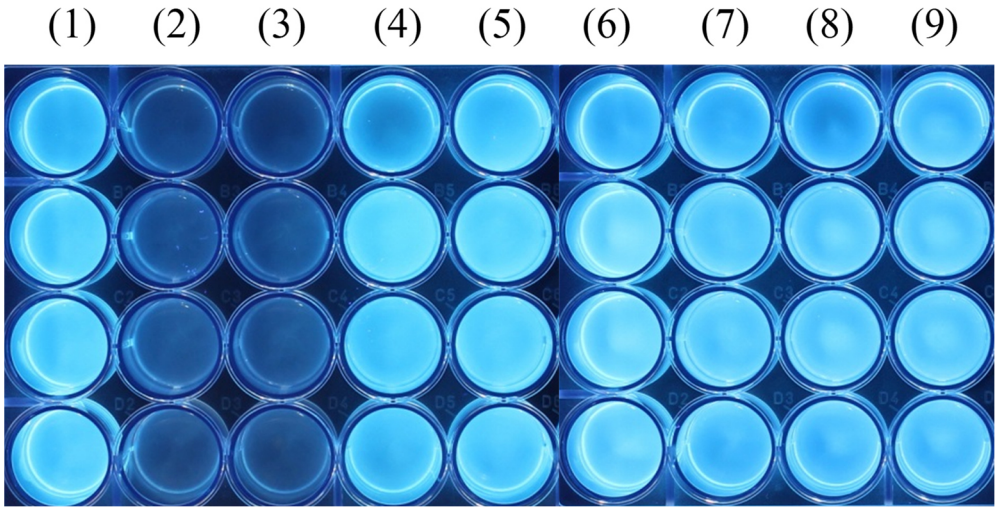

Figure 4.7. Fluorescence images of *Pseudomonas aeruginosa* (PA) incubated with glycogels. The fluorescence is caused by the secreted fluorescent siderophore pyoverdine. Note the strong decrease in fluorescence signal in the wells containing FG-1. All samples were run as quadruples. Each well in a column is treated identically. (1): MG-0; (2): MG-0 and FG-1; (3): FG-1; (4): LG-1; (5): No gel; (6): MG-4; (7): G-2; (8): Unmodified melibiose and fucose; (9): Same as (5).

Surprisingly, FG-1 decreased the detectable fluorescence based on pyoverdine secretion clearly. All other samples showed no effect in this regard. To the best of our knowledge there is no hint reported so far that fucose-derivatives are somehow influencing the secretion status of pyoverdine in PA. To investigate if there is really a change in pyoverdine secretion or just an antimicrobial activity of FG-1, the PA were subsequently plated on petri dishes and cultivated for 24 h. All samples showed the formation of colonies, which proves that the effect was not due to antimicrobial activity of FG-1 (see Figure 4.S20, Supporting Information). As these are the first results on this interesting topic, we will proceed with setting up biofilm assays with PA and our glycogels as well as a more in-depth investigation on the influence of fucose containing gels on the secretion of pyoverdine.

4.3 Materials and Methods

4.3.1 Materials

All chemicals were purchased from commercial sources. We recrystallized *N*-isopropylacrylamide (NiPAm; 97%, Sigma Aldrich, Taufkirchen, Germany) and *N*-isopropylmethacrylamide (NiPMAm; 97%, Sigma Aldrich) from n-hexane. Water was double deionized by a Milli-Q purification system (18.2 MΩ cm, Millipore Quantum® TEX, Darmstadt, Germany). The crosslinkers *N*,*N*'-methylenebis(acrylamide) (MBA; 99%, Sigma Aldrich) and ethylene glycol dimethacrylate (EGDMA; 98%, Sigma Aldrich), the initiator 4,4'-azobis(4-cyanovaleric acid) (ABCVA; ≥98%, Sigma Aldrich), dichloromethane (CH_2Cl_2; for synthesis) and chloroform ($CHCl_3$; extra pure) were redistilled before use. D(+)-Melibiose monohydrate (Mel; ≥99%, Carl Roth, Karlsruhe, Germany), L-(−)-fucose (Fuc; ≥99%, Sigma Aldrich), D-lactose monohydrate (Lac; Carbosynth, Compton, United Kingdom), ammonium carbonate ($(NH_4)_2CO_3$; ≥30.5% NH_3, extra pure, Carl Roth), dimethyl sulfoxide (DMSO; VWR, Darmstadt, Germany), methacryloyl chloride (purum, dist., ≥97%, Sigma Aldrich), sodium carbonate (≥99%, anhydrous, Carl Roth), tetrahydrofuran (THF; p. a., Chemsolute, Renningen, Germany), acetonitrile (≥99.8%, for preparative HPLC, Carl Roth), hydroquinone (99.5%, Acros Organics, Darmstadt, Germany), diethylether (Et_2O; p. a., Chemsolute), methanol (MeOH; extra pure), silica gel (high-purity grade, pore size 60 Å, Sigma Aldrich), sodium dodecyl sulfate (SDS; ≥99.5%, blotting-grade, Carl Roth) were used as received.

4.3.2 Methods

4.3.2.1 Dynamic Light Scattering (DLS)

We investigated the hydrodynamic diameter by using dynamic light scattering (DLS) (Malvern Zetasier Nano-ZS, Kassel, Germany). Measurements were performed in disposable polymethylmethacrylate cuvettes at a backscattering angle of 173° five times. We chose temperatures of 20 and 50 °C. For the measurements at 20 °C, we let the samples equilibrate for 5 min, and for the measurements at 50 °C, the samples were allowed to equilibrate for 10 min to ensure complete collapse of the glycogels. We measured the hydrodynamic diameter of PNiPAm nanogel G-1 and melibiose gel MG-4 as a function of the temperature, ranging from 20 to 50 °C.

4.3.2.2 Scanning Electron Microscopy (SEM)

Diluted samples were dropped onto tilted silicon wafers (CrysTec) to let excess liquid drip off. After letting the wafers dry, the samples were sputtered with platinum (4 nm). Images were taken on a GeminiSEM 300 (Fa. Zeiss, Jena, Germany).

4.3.2.3 Atomic Force Microscopy (AFM)

AFM analysis was performed on a Bruker Dimension Icon using NanoScope 9.1 (Karlsruhe, Germany) for measurements and NanoScope Analysis 1.5 for image processing. We measured in ScanAsyst air mode using a ScanAsyst air tip with a spring constant of ~0.4 N/m and a resonant frequency of 70 Hz.

4.3.2.4 NMR and ESI MS

NMR spectra were recorded on a Bruker Avance 300 MHz Spektrometer (Ettlingen, Germany). Mass spectra were recorded on FlexarTM SQ 300 MS Detector (PerkinElmer, Rodgau, Germany).

4.3.2.5 Thermogravimetric Analysis (TGA)

TGA measurements (TGA 500, TA Instruments, Hüllhorst, Germany) were conducted in nitrogen flow (60 mL/min) with heating rate of 10 K/min up to 200 °C. The water content in the gels was determined to be 5–11 wt.%. For analysis and discussion, we used the wet weight of the gels.

4.3.3 Glycomonomers

The glycomonomers were synthesized in a two-step procedure. For the first step, the respective glycoamines were prepared via Kochetkov amination accelerated by microwave irradiation [44,47]. The second step involves the introduction of a polymerizable moiety following a modified procedure of Ghadban et al. [45].

4.3.3.1 Synthesis of Glycosylamines

The saccharide was dissolved in solvent and ammonium carbonate was added. The respective amounts of reactants and solvents used are listed in Table 4.6. Afterwards the reaction mixture was heated in the microwave reactor (START 1500 rotaPREP, MSL, Leutkirch, Germany) to 40 °C for 90 min under stirring. The mixture was allowed to cool down and the ammonium carbonate and the solvent were removed by rotary evaporation at 40 °C under reduced pressure. In case of $LacNH_2$, the glycosylamine was precipitated with 40 mL of MeOH after reaction and dried. The crude product was dried in high vacuum and stored at 4 °C. We used the glycosylamines for monomer syntheses without

further purification. It has to be noted that residual ammonium carbonate was found in all glycosylamines which could not be removed [46].

Table 4.6. Synthesis details of glycosylamines.

Reactant	**n**	**m**	**V**
	[mmol]	**[g]**	**[mL]**
Lactose monohydrate	8.33	3.3	-
DMSO	-	-	12.0
$(NH_4)_2CO_3$	52.0	5.0	-
Melibiose monohydrate	13.9	5.0	-
H_2O	-	-	100
$(NH_4)_2CO_3$	520	50	-
Fucose	9.14	1.5	-
MeOH	-	-	13.0
$(NH_4)_2CO_3$	78.1	7.5	-

4.3.3.2 Synthesis of Glycosyl Methacrylamides

We dissolved the glycomonomer in a mixture of methanol and Milli-Q water (1:1) and added sodium carbonate. The reaction mixture was cooled in an ice-water bath. Methacryloyl chloride was diluted with THF and dropwise added into the mixture within 10 min under stirring. The reaction was allowed to proceed for further 30–90 min in the ice-water bath (Table 4.7). Then the volatile solvents were removed by rotary evaporation at 30 °C. The products were purified by silica gel column chromatography (LacMAm: acetonitrile/H2O 9:1; MelMAm: acetonitrile/H2O 9:1 → 4:1; FucMAm: CHCl3/MeOH 5:1), followed by the extraction with diethyl ether in the case of LacMAm. We stabilized MelMAm with hydroquinone (3 ppm) as it tends to polymerize spontaneously. FucMAm was hydrolyzed in 30 mL with 106 mg sodium carbonate (1 mmol; 250 mM) overnight as the NMR spectra showed additional methacrylate peaks. Afterwards, we purified FucMAm by a second column chromatography (CHCl3/MeOH 5:1). The products were concentrated and then freeze-dried to obtain white solids (LacMAm: 680 mg, total yield: 57%; MelMAm: 1.12 g, total yield: 18%; FucMAm: 817 mg, total yield: 26%).

Table 4.7. Synthesis details of glycomonomers.

Reactant	n [mmol]	m [g]	V [mL]
$LacNH_2$	3.17	1.0815	-
Sodium carbonate	12.67	1.3434	-
$MeOH/H_2O$ (1:1)	-	-	16.4
Methacryloyl chloride	9.5		0.9141
THF	-	-	6.3373
$MelNH_2$	13.9	5	-
Sodium carbonate	77.8	8.25	-
$MeOH/H_2O$ (1:1)	-	-	150
Methacryloyl chloride	42.6		4.77
THF	-	-	35
$FucNH_2$	12.2	2	-
Sodium carbonate	68.1	7.22	-
$MeOH/H_2O$ (1:1)	-	-	132
Methacryloyl chloride	42.5		4.1
THF	-	-	35

LacMAm. ^{1}H-NMR (D_2O, 300 MHz): δ 5.83 (s, 1 H), 5.53–5.67 (m, 1 H), 5.12 (d, ^3J = 9.2 Hz, 1 H), 4.51 (d, ^3J = 7.7 Hz, 1 H), 3.53–4.01 (m, 12 H), 1.99 (s, 3 H); ^{13}C-NMR (DMSO, 75 MHz): δ 184.23 (C), 140.32 (C), 123.87 (CH_2), 104.46 (CH), 81.09 (CH), 79.40 (CH), 78.02 (CH), 76.94 (CH), 76.70 (CH), 74.09 (CH), 72.91 (CH), 72.52 (CH), 70.13 (CH), 62.62 (CH_2), 61.44 (CH_2), 19.26 (CH_3); ESI MS, *m/z* calcd for $C_{16}H_{28}NO_{11}$: $[M + Na]^+$ 432.38, found: 432.11 $[M + Na]^+$.

MelMAm. ^{1}H-NMR (300 MHz, D_2O): δ = 5.81 (s, 1 H), 5.59 (d, ^3J = 1.6 Hz, 1 H), 5.08 (d, ^3J = 8.9 Hz, 1 H), 5.00 (d, ^3J = 3.5 Hz, 1 H), 3.45–4.05 (m, 12 H), 1.98 (s, 3 H); ^{13}C-NMR (DMSO, 75 MHz): δ 174.27 (C), 140.28 (C), 123.87 (CH_2), 99.70 (CH), 81.38 (CH), 78.24 (CH), 77.73 (CH), 73.04 (CH), 72.42 (CH), 70.99 (CH), 69.95 (CH_2), 62.67 (CH_2), 19.24 (CH_3); ESI MS, calcd for $C_{16}H_{27}NO_{11}$: $[M + Na]^+$ 432.38, found: 432.10 $[M + Na]^+$.

FucMAm. ^{1}H-NMR (300 MHz, D_2O): δ = 5.78 (1 H, s), 5.56 (1 H, s), 4.98 (1 H, d, ^3J = 8.2 Hz), 3.90 (1 H, q, ^3J = 6.4 Hz), 3.79–3.94 (1 H, m), 3.61–3.73 (3 H, m), 1.95 (1 H, s), 1.24 (1 H, d, ^3J = 6.5 Hz); ^{13}C-NMR (DMSO, 75 MHz): *δ* 173.69 (C), 140.22 (C), 123.49 (CH_2), 81.21 (CH), 74.99 (CH), 73.98 (CH), 72.80 (CH), 70.32 (CH), 19.19 (CH_3), 17.17 (CH_3); ESI MS, calcd for $C_{10}H_{17}NO_5$: $[M + Na]^+$ 254.24, found: 254.04 $[M + Na]^+$.

4.3.4 Synthesis of Nanogels via Precipitation Polymerization

4.3.4.1 Synthesis of PNiPAm Nanogel G-1

The reactants, except the initiator, were dissolved in Milli-Q water in a 100 mL-schlenk flask (Table 4.8). We purged the solution with nitrogen and equilibrated at 80 °C in an oil bath for 30 min. Afterwards, the reaction was started by adding the initiator in nitrogen countercurrent. We allowed the turbid mixture to cool down after 4 h of reaction. The nanogels were dialyzed against deionized water for several days and then lyophilized to obtain a white solid.

Table 4.8. Synthesis details of PNiPAm and PNiPMAm nanogels [a].

Nanogel	V(H_2O) [mL]	c(Monomer) [mmol/L]	n(Monomer) [mmol]	X(CL) [mol%]	c(SDS) [mmol/L]	X(ABCVA) [mol%]	t_1 [h]	Yield [%]
G-1	50	100	5	5	0.2	0.25	4.0	-
G-2	50	100	5	10	4.0	2.00	22	86
G-3 [b]	25	100	2.5	5	1.0	2.00	4.5	78

[a] The molfraction X refers to the total monomer amount of substance. Comonomer is NiPMAm if not stated otherwise. Crosslinker is MBA if not stated otherwise. [b] Comonomer is NiPMAm. Crosslinker is EGDMA.

4.3.4.2 Synthesis of PNiPAm Nanogel G-2 and PNiPMAm Nanogel G-3

We dissolved every reactant in Milli-Q water in a 100 mL-schlenk flask or 50 mL-schlenk flask and purged the reaction solution with nitrogen for 30 min (Table 4.8). The reaction was started by submerging the flask into an 80 °C oil bath. After reaction, we let the slightly turbid mixture cool down and purified the product by dialysis against deionized water for several days, followed by lyophilization. We obtained white solids.

4.3.4.3 Synthesis of Melibiose Glycogels MG-1–MG-8

MelMAm (40.9 mg, 0.1 mmol), comonomer (0.4 mmol; 4 eq.), crosslinker, SDS and initiator were dissolved in 5 mL of Milli-Q water (100 mM total monomer concentration) in a 25 mL-schlenk flask. The respective amounts of the chemicals used are listed in Table 4.9. We purged the solution with nitrogen for 30 min, before submerging the flask into an 80 °C oil bath. For some glycogels, we added an additional amount of initiator after approximately 2 h in nitrogen countercurrent (see t_1 in Table 4.9). The reaction was allowed to proceed for a further amount of time (see t_2 in Table 4.9). After cooling down the turbid reaction mixture, we purified the glycogel by dialysis against deionized water for several days and lyophilized the product to obtain a white solid. If large aggregated sediments were

observed after reaction, the product was filtered through Kimtech Science® precision wipes (Darmstadt, Germany) before freeze-drying.

Table 4.9. Synthesis details of melibiose glycogels [a].

Glycogel	n(Comonomer) [mmol]	X(CL) [mol%]	c(SDS) [mmol/L]	X_1(ABCVA) [mol%]	t_1 [h]	X_2(ABCVA) [mol%]	t_2 [h]	Yield [d] [%]
MG-1	0.4	10	0.4	1	2.0	2	17	67
MG-2	0.4	10	2.0	1	1.7	2	16	67
MG-3	0.4	10	4.0	1	2.0	2	20	43
MG-4	0.4	10	0.4	3	22	-	-	61
MG-5	0.4	10	0.4	3	22	-	-	66
MG-6	0.4	5	1.0	2	24	-	-	46
MG-7 [b, c]	0.4	5	0.2	2	23	-	-	37
MG-8 [c]	0.4	10	0.4	1	2	2	17	64

[a] The molfraction X refers to the total monomer amount of substance. Comonomer is NiPMAm if not stated otherwise. Crosslinker is MBA if not stated otherwise. [b] Comonomer is NiPMAm. [c] Crosslinker is EGDMA. [d] Yields were determined once.

In case of MG-5, every reactant was dissolved in Milli Q water with the exception of the initiator. After purging the reaction solution with nitrogen and equilibrating at 80 °C for 30 min, we added the initiator to start the reaction.

4.3.4.4 Synthesis of Melibiose Glycogel MG-0

We first tested the precipitation polymerization with a previously synthesized melibiose monomer that was not stabilized with hydroquinone. We dissolved MelMAm (81.8 mg, 0.2 mmol), NiPAm (90.5 mg, 0.8 mmol; 4 eq.), MBA (15.4 mg, 0.1 mmol; 10 mol%), SDS (1.15 mL of a 10 mg/mL stock solution, 4×10^{-5} mmol; 4 mM) and ABCVA (0.7 mg, 2.5×10^{-3} mmol; 0.25 mol%) in Milli-Q water (9 mL; 100 mM total monomer concentration). We purged the reaction solution with nitrogen for 30 min. Then, we started the reaction by submerging the reaction flask into an 80 °C oil bath. After 2 h, the reaction mixture remained clear. Additional initiator was added, and the mixture turned slightly turbid. We let the reaction proceed for further 4 h before letting it cool down. The glycogel was purified by dialysis against deionized water for several days and then freeze-dried. We obtained 99.7 mg of white solid (53%).

4.3.4.5 Synthesis of Lactose Glycogel LG

We dissolved LacMAm (40.9 mg, 0.1 mmol), NiPAm (45.3 mg, 0.4 mmol; 4 eq.), MBA (3.9 mg, 2.5×10^{-2} mmol; 5 mol%), SDS (288 µL of a 1 mg/mL stock solution, 1.0×10^{-6} mmol; 0.2 mM) and

ABCVA (2.8 mg, 0.01 mmol; 2 mol%) in Milli-Q water (4.712 mL; 100 mM total monomer concentration) in a 25 mL-schlenk flask. We purged the solution with nitrogen for 30 min. Then the reaction was started by submerging the reaction flask into an 80 °C oil bath. After 20 h of reaction, we let the reaction mixture cool down. We dialyzed the product against deionized water for several days and lyophilized the product to obtain a white solid (72.5 mg, 75%).

4.3.4.6 Synthesis of Fucose Glycogels FG-1 and FG-2

We dissolved FucMAm (23 1 mg, 0.1 mmol), NiPAm (45.3 mg, 0.4 mmol; 4 eq.), MBA (FG-1: 3.9 mg, 2.5×10^{-2} mmol; 5 mol%; FG-2: 7.7 mg, 5.0×10^{-2} mmol; 10 mol%), SDS (57.67 µL of a 10 mg/mL stock solution, 2.0×10^{-6} mmol; 0.4 mM) and initiator in Milli-Q water (5 mL; 100 mM total monomer concentration) in a 25 mL-schlenk flask. We purged the solution with nitrogen for 30 min, before submerging the flask into an 80 °C oil bath. The reaction was allowed to proceed for 4 h. After cooling down, we purified the glycogel by dialysis against deionized water for several days, filtered through Kimtech Science® precision wipes and lyophilized the product to obtain a white solid (FG-1: 41.5 mg, 56%: FG-2: 25.9 mg, 33%).

4.3.5 Phenol-Sulfuric Acid Assay for Determination of Total Sugar Content

The phenol-sulfuric acid assay was performed similar to a described method [62]. Two different concentrations of glycogels (1.5 and 0.75 mg/mL for lactose and melibiose nanogels, 4.0 and 2.0 mg/mL for fucose nanogels) were prepared in water. 50 µL of sample was thoroughly mixed with 150 µL sulfuric acid (95%, Th. Geyer, Renningen, Germany). Subsequently, 30 µL of 5% phenol (Sigma-Aldrich) was added, followed by mixing. The mixture was incubated at 90 °C for 5 min and let cool down in a water bath for further 5 min. After transferring the solution into a 96-well plate (Carl Roth) the absorption at 490 nm was measured.

For calculating the total sugar amount for each type of saccharide, lactose, melibiose and fucose were used separately for calibration. Control gels without sugar were also measured to prove suitability of the assay.

4.3.6 Lectin Studies

To prove the accessible sugar content of the nanogels, different sugar binding proteins (lectins) were used for binding studies. Fluorescein-labeled lectins were chosen for easy detection: ECL for lactose (β-galactose) binding, Jacalin for melibiose (α-galactose) binding and UEA I for α-fucose binding (all from Vector Laboratories, via BIOZOL Diagnostica Vertrieb GmbH, Eching, Germany).

The lectin binding to the nanogels was proven by an ELISA-type competitive inhibition assay, similar to previously described assays [63,64]. Glycogels that are bound by the lectin inhibit the lectin binding to an immobilized glycoprotein. The standard glycoprotein for ECL and Jacalin is ASF. For UEA, we found good binding to mucin from porcine stomach. The binding of the three lectins to its appropriate ligands was proven in a binding assay varying the lectin concentration.

In microtiter plates (MaxiSorp, Nunc, Wiesbaden, Germany) ASF (100 µL of 5 µg/mL bovine ASF (Sigma-Aldrich)) or mucin (100 µL of 100 µg/mL porcine stomach mucin (Sigma-Aldrich), both in sodium carbonate buffer pH 9.6) was immobilized overnight. After washing with PBS-Tween (0.05% (v/v) Tween-20) residual binding sites were blocked with 2% BSA (bovine serum albumin, Carl Roth) in PBS. Wells were washed once with PBS-Tween and twice with lectin buffer (10 mM HEPES, 150 mM NaCl, 0.1 mM CaCl2, pH 7.5). Varying concentrations of inhibitor and 5 or 10 µg/mL of lectin were incubated simultaneously for 1 h. Controls without inhibitor and without lectin were performed to indicate minimal and maximal binding, respectively. Wells were again washed with lectin buffer and residual bound lectin was detected by fluorescence read-out at 488/520 nm. Measured data were analyzed using Sigma Plot (Systat software GmbH, 11.0, Erkrath, Germany).

4.3.7 Cultivation of PA

The nanogels (4 mg) were swollen over night at 37 °C under shaking conditions in 1 mL Nutrient Broth (NB, Carl Roth).

Nutrient broth was inoculated with Pseudomonas aeruginosa and grown under shaking conditions (110 rpm) at 37 °C overnight. The overnight culture was diluted to an OD600 nm of 0.2 with NB and subsequently diluted with the nanogel suspension in a ratio of 1:2 (nanogel 2 mg/mL, PA OD 0.1). 500 µL of this mixture were plated in a 24-well plate (n = 4) (TPP, Techno Plastic Products AG, Trasadingen, Switzerland)) and cultivated under static condition overnight at 37 °C. Then the fluorescence of pyoverdine was detected using UV light (Dark Hood DH-50, BIOSTEP, FELIX 2000, Burkhardtsdorf, Germany).

All samples and the controls (PA in NB) showing fluorescence were diluted to 10^{-4}–10^{-6} with PBS (Biochrom AG, Berlin, Germany). Samples without fluorescence were diluted to 10^{-2}. Subsequently, 100 µL of each sample was plated on cetrimid agar plates (Carl Roth) and stored overnight (37 °C).

4.4 Conclusions

For the first time, we prepared melibiose, fucose and lactose containing nanogels via precipitation polymerization of NiPAm and glycomonomers. We varied the reactions conditions of the

gel production and analyzed the inhibitory potency of the gels in lectin assays. The gels showed sugar dependent inhibition of the lectin binding and a prominent multivalent effect compared to unmodified saccharides. We found that overall the inhibition strength increases with decreasing gel size. Furthermore, the monomer NiPAm and crosslinker MBA are more suitable for these lectin assays than NiPMAm and EGDMA as the latter two themselves influence the binding behaviour. The crosslinker amount influences the yield and the lectin binding differently, depending on the glycomonomer. At the same sugar content, the inhibitory potency seems to be strongly dependent on the morphology of the glycogel. Interestingly, the amount of incorporated sugar is not strongly influenced by the reaction parameters but by the type of glycomonomer. This enables a tuning of the synthesis towards yields, optimized size and morphology without decreasing sugar content in the gels. Fucose containing gels showed no inhibition due to the β-anomeric form of the glycomonomer. However, LecB is reported to bind β-fucose residues. Due to the biocompatibility of the materials a potential use of the gels in alternative treatments of Pseudomonas aeruginosa infections could be possible in the future. First trials suggest an influence of fucose gels on the secretion of pyoverdine. Work is in progress to establish biofilm formation assays with PA in the presence of the glycogels as well as a more in-depth investigation of the effect in pyoverdine secretion of β-fucose gels.

4.5 Acknowledgements

We thank Xuepu Wang, Steffi Grunst and Kathrin Geßner from Fraunhofer Institute for Applied Polymer Research for AFM analysis, SEM images and for TGA analysis, respectively.

4.6 References

1. Poole, J.; Day, C.J.; Itzstein, M. von; Paton, J.C.; Jennings, M.P. Glycointeractions in bacterial pathogenesis. *Nat. Rev. Microbiol.* **2018**, *16*, 440–452, doi:10.1038/s41579-018-0007-2.
2. Moonens, K.; Remaut, H. Evolution and structural dynamics of bacterial glycan binding adhesins. *Curr. Opin. Struct. Biol.* **2017**, *44*, 48–58, doi:10.1016/j.sbi.2016.12.003.
3. Kulkarni, A.A.; Fuller, C.; Korman, H.; Weiss, A.A.; Iyer, S.S. Glycan encapsulated gold nanoparticles selectively inhibit shiga toxins 1 and 2. *Bioconjug. Chem.* **2010**, *21*, 1486–1493, doi:10.1021/bc100095w.
4. Hartley-Tassell, L.E.; Awad, M.M.; Seib, K.L.; Scarselli, M.; Savino, S.; Tiralongo, J.; Lyras, D.; Day, C.J.; Jennings, M.P. Lectin Activity of the TcdA and TcdB Toxins of Clostridium difficile. *Infect. Immun.* **2019**, *87*, doi:10.1128/IAI.00676-18.
5. Dingle, T.; Wee, S.; Mulvey, G.L.; Greco, A.; Kitova, E.N.; Sun, J.; Lin, S.; Klassen, J.S.; Palcic, M.M.; Ng, K.K.S.; et al. Functional properties of the carboxy-terminal host cell-binding domains of the two toxins, TcdA and TcdB, expressed by Clostridium difficile. *Glycobiology* **2008**, *18*, 698–706, doi:10.1093/glycob/cwn048.

6. Turnbull, W.B.; Precious, B.L.; Homans, S.W. Dissecting the cholera toxin-ganglioside GM1 interaction by isothermal titration calorimetry. *J. Am. Chem. Soc.* **2004**, *126*, 1047–1054, doi:10.1021/ja0378207.
7. Ernst, B.; Magnani, J.L. From carbohydrate leads to glycomimetic drugs. *Nat. Rev. Drug Dis.* **2009**, *8*, 661, doi:10.1038/nrd2852.
8. Zhang, Q.; Su, L.; Collins, J.; Chen, G.; Wallis, R.; Mitchell, D.A.; Haddleton, D.M.; Becer, C.R. Dendritic cell lectin-targeting sentinel-like unimolecular glycoconjugates to release an anti-HIV drug. *J. Am. Chem. Soc.* **2014**, *136*, 4325–4332, doi:10.1021/ja4131565.
9. Spain, S.G.; Cameron, N.R. A spoonful of sugar: the application of glycopolymers in therapeutics. *Polym. Chem.* **2011**, *2*, 60–68, doi:10.1039/C0PY00149J.
10. Lee, R.T.; Lee, Y.C. Cluster glycosides. In *Complex Carbohydrates*; Ginsburg, V., Ed.; Academic Press: Orlando, FL, USA, 1987; pp. 424–429, ISBN 9780121820381.
11. Lee, R.T.; Lee, Y.C. Affinity enhancement by multivalent lectin–carbohydrate interaction. *Glycoconj. J.* **2000**, *17*, 543–551, doi:10.1023/A:1011070425430.
12. Lee, Y.C.; Lee, R.T. Carbohydrate-Protein Interactions: Basis of Glycobiology. *Acc. Chem. Res.* **1995**, *28*, 321–327, doi:10.1021/ar00056a001.
13. Lundquist, J.J.; Toone, E.J. The Cluster Glycoside Effect. *Chem. Rev.* **2002**, *102*, 555–578, doi:10.1021/cr000418f.
14. Becer, C.R. The glycopolymer code: synthesis of glycopolymers and multivalent carbohydrate-lectin interactions. *Macromol. Rapid Commun.* **2012**, *33*, 742–752, doi:10.1002/marc.201200055.
15. Eissa, A.M.; Cameron, N.R. Glycopolymer Conjugates. In *Bio-synthetic Polymer Conjugates*; Schlaad, H., Ed.; Springer Berlin Heidelberg: Berlin, Heidelberg, Germany, 2013; pp. 71–114, ISBN 978-3-642-34350-6.
16. Ehe, C. von der; Weber, C.; Gottschaldt, M.; Schubert, U.S. Immobilized glycopolymers: Synthesis, methods and applications. *Prog. Poly. Sci.* **2016**, *57*, 64–102, doi:10.1016/j.progpolymsci.2016.02.001.
17. Rosencrantz, R.R.; Nguyen, V.H.; Park, H.; Schulte, C.; Böker, A.; Schnakenberg, U.; Elling, L. Lectin binding studies on a glycopolymer brush flow-through biosensor by localized surface plasmon resonance. *Anal. Bioanal. Chem.* **2016**, *408*, 5633–5640, doi:10.1007/s00216-016-9667-9.
18. Lazar, J.; Rosencrantz, R.R.; Elling, L.; Schnakenberg, U. Simultaneous Electrochemical Impedance Spectroscopy and Localized Surface Plasmon Resonance in a Microfluidic Chip: New Insights into the Spatial Origin of the Signal. *Anal. Chem.* **2016**, *88*, 9590–9596, doi:10.1021/acs.analchem.6b02307.
19. Lazar, J.; Park, H.; Rosencrantz, R.R.; Böker, A.; Elling, L.; Schnakenberg, U. Evaluating the Thickness of Multivalent Glycopolymer Brushes for Lectin Binding. *Macromol. Rapid Commun.* **2015**, *36*, 1472–1478, doi:10.1002/marc.201500118.
20. Yan, X.; Sivignon, A.; Yamakawa, N.; Crepet, A.; Travelet, C.; Borsali, R.; Dumych, T.; Li, Z.; Bilyy, R.; Deniaud, D.; et al. Glycopolymers as Antiadhesives of E. coli Strains Inducing Inflammatory Bowel Diseases. *Biomacromolecules* **2015**, *16*, 1827–1836, doi:10.1021/acs.biomac.5b00413.
21. Arias, E.; Méndez, M.T.; Arias, E.; Moggio, I.; Ledezma, A.; Romero, J.; Margheri, G.; Giorgetti, E. Supramolecular Recognition of Escherichia coli Bacteria by Fluorescent Oligo(Phenyleneethynylene)s with Mannopyranoside Termini Groups. *Sensors* **2017**, *17*, doi:10.3390/s17051025.
22. Jacobi, F.; La Camaleño de Calle, A.; Boden, S.; Grafmüller, A.; Hartmann, L.; Schmidt, S. Multivalent Binding of Precision Glycooligomers on Soft Glycocalyx Mimicking Hydrogels. *Biomacromolecules* **2018**, *19*, 3479–3488, doi:10.1021/acs.biomac.8b00790.
23. Jans, A.; Rosencrantz, R.R.; Mandić, A.D.; Anwar, N.; Boesveld, S.; Trautwein, C.; Moeller, M.; Sellge, G.; Elling, L.; Kuehne, A.J.C. Glycan-Functionalized Microgels for Scavenging and Specific Binding of Lectins. *Biomacromolecules* **2017**, *18*, 1460–1465, doi:10.1021/acs.biomac.6b01754.
24. Saunders, B.R.; Laajam, N.; Daly, E.; Teow, S.; Hu, X.; Stepto, R. Microgels: From responsive polymer colloids to biomaterials. *Adv. Colloid Interface Sci.* **2009**, *147–148*, 251–262, doi:10.1016/j.cis.2008.08.008.

25. Plamper, F.A.; Richtering, W. Functional Microgels and Microgel Systems. *Acc. Chem. Res.* **2017**, *50*, 131–140, doi:10.1021/acs.accounts.6b00544.
26. Guan, Y.; Zhang, Y. PNIPAM microgels for biomedical applications: from dispersed particles to 3D assemblies. *Soft Matter.* **2011**, *7*, 6375, doi:10.1039/c0sm01541e.
27. Pelton, R. Poly(N-isopropylacrylamide) (PNIPAM) is never hydrophobic. *J. Colloid Interface Sci.* **2010**, *348*, 673–674, doi:10.1016/j.jcis.2010.05.034.
28. Lima, L.H.; Morales, Y.; Cabral, T. Ocular Biocompatibility of Poly-*N*-Isopropylacrylamide (pNIPAM). *J. Ophthalmol.* **2016**, *2016*, doi:10.1155/2016/5356371.
29. Cooperstein, M.A.; Canavan, H.E. Assessment of cytotoxicity of (N-isopropyl acrylamide) and poly(N-isopropyl acrylamide)-coated surfaces. *Biointerphases* **2013**, *8*, 19, doi:10.1186/1559-4106-8-19.
30. Cooperstein, M.A.; Nguyen, P.A.H.; Canavan, H.E. Poly(*N*-isopropyl acrylamide)-coated surfaces: Investigation of the mechanism of cell detachment. *Biointerphases* **2017**, *12*, doi:10.1116/1.4979920.
31. Aloush, V.; Navon-Venezia, S.; Seigman-Igra, Y.; Cabili, S.; Carmeli, Y. Multidrug-resistant Pseudomonas aeruginosa: risk factors and clinical impact. *Antimicrob. Agents Chemother.* **2006**, *50*, 43–48, doi:10.1128/AAC.50.1.43-48.2006.
32. Imberty, A.; Wimmerová, M.; Mitchell, E.P.; Gilboa-Garber, N. Structures of the lectins from Pseudomonas aeruginosa: insights into the molecular basis for host glycan recognition. *Micro. Infect.* **2004**, *6*, 221–228, doi:10.1016/j.micinf.2003.10.016.
33. Chemani, C.; Imberty, A.; de Bentzmann, S.; Pierre, M.; Wimmerová, M.; Guery, B.P.; Faure, K. Role of LecA and LecB lectins in Pseudomonas aeruginosa-induced lung injury and effect of carbohydrate ligands. *Infect. Immun.* **2009**, *77*, 2065–2075, doi:10.1128/IAI.01204-08.
34. Weichert, S.; Jennewein, S.; Hüfner, E.; Weiss, C.; Borkowski, J.; Putze, J.; Schroten, H. Bioengineered 2'-fucosyllactose and 3-fucosyllactose inhibit the adhesion of Pseudomonas aeruginosa and enteric pathogens to human intestinal and respiratory cell lines. *Nutr. Res.* **2013**, *33*, 831–838, doi:10.1016/j.nutres.2013.07.009.
35. Grishin, A. v.; Krivozubov, M.S.; Karyagina, A.S.; Gintsburg, A.L. Pseudomonas Aeruginosa Lectins As Targets for Novel Antibacterials. *Acta Nat.* **2015**, *7*, 29–41.
36. Sommer, R.; Wagner, S.; Rox, K.; Varrot, A.; Hauck, D.; Wamhoff, E.-C.; Schreiber, J.; Ryckmans, T.; Brunner, T.; Rademacher, C.; et al. Glycomimetic, Orally Bioavailable LecB Inhibitors Block Biofilm Formation of Pseudomonas aeruginosa. *J. Am. Chem. Soc.* **2018**, *140*, 2537–2545, doi:10.1021/jacs.7b11133.
37. Angeli, A.; Li, M.; Dupin, L.; Vergoten, G.; Noël, M.; Madaoui, M.; Wang, S.; Meyer, A.; Géhin, T.; Vidal, S.; et al. Design and Synthesis of Galactosylated Bifurcated Ligands with Nanomolar Affinity for Lectin LecA from Pseudomonas aeruginosa. *Chembiochem* **2017**, *18*, 1036–1047, doi:10.1002/cbic.201700154.
38. Berthet, N.; Thomas, B.; Bossu, I.; Dufour, E.; Gillon, E.; Garcia, J.; Spinelli, N.; Imberty, A.; Dumy, P.; Renaudet, O. High affinity glycodendrimers for the lectin LecB from Pseudomonas aeruginosa. *Bioconjug. Chem.* **2013**, *24*, 1598–1611, doi:10.1021/bc400239m.
39. Bücher, K.S.; Babic, N.; Freichel, T.; Kovacic, F.; Hartmann, L. Monodisperse Sequence-Controlled α-l-Fucosylated Glycooligomers and Their Multivalent Inhibitory Effects on LecB. *Macromol. Biosci.* **2018**, *18*, e1800337, doi:10.1002/mabi.201800337.
40. Johansson, E.M.V.; Crusz, S.A.; Kolomiets, E.; Buts, L.; Kadam, R.U.; Cacciarini, M.; Bartels, K.-M.; Diggle, S.P.; Cámara, M.; Williams, P.; et al. Inhibition and dispersion of Pseudomonas aeruginosa biofilms by glycopeptide dendrimers targeting the fucose-specific lectin LecB. *Chem. Biol.* **2008**, *15*, 1249–1257, doi:10.1016/j.chembiol.2008.10.009.
41. Michaud, G.; Visini, R.; Bergmann, M.; Salerno, G.; Bosco, R.; Gillon, E.; Richichi, B.; Nativi, C.; Imberty, A.; Stocker, A.; et al. Overcoming antibiotic resistance in Pseudomonas aeruginosa biofilms using glycopeptide dendrimers. *Chem. Sci.* **2016**, *7*, 166–182, doi:10.1039/c5sc03635f.
42. Blanchard, B.; Imberty, A.; Varrot, A. Secondary sugar binding site identified for LecA lectin from Pseudomonas aeruginosa. *Proteins* **2014**, *82*, 1060–1065, doi:10.1002/prot.24430.

43. Gilboa-Garber, N.; Katcoff, D.J.; Garber, N.C. Identification and characterization of pseudomonas aeruginosa PA-IIL lectin gene and protein compared to PA-IL. *FEMS Immunol. Med. Microbiol.* **2000**, *29*, 53–57, doi:10.1111/j.1574-695X.2000.tb01505.x.
44. Brun, M.A.; Disney, M.D.; Seeberger, P.H. Miniaturization of Microwave-Assisted Carbohydrate Functionalization to Create Oligosaccharide Microarrays. *Chembiochem* **2006**, *7*, 421–424, doi:10.1002/cbic.200500361.
45. Ghadban, A.; Albertin, L.; Moussavou Mounguengui, R.W.; Peruchon, A.; Heyraud, A. Synthesis of β-d-glucopyranuronosylamine in aqueous solution: kinetic study and synthetic potential. *Carbohy. Res.* **2011**, *346*, 2384–2393, doi:10.1016/j.carres.2011.08.018.
46. Vetter, D.; Gallop, M.A. Strategies for the Synthesis and Screening of Glycoconjugates. 1. A Library of Glycosylamines. *Bioconjugate Chem.* **1995**, *6*, 316–318.
47. Bejugam, M.; Flitsch, S.L. An Efficient Synthetic Route to Glycoamino Acid Building Blocks for Glycopeptide Synthesis. *Org. Lett.* **2004**, *6*, 4001–4004, doi:10.1021/ol048342n.
48. Garber, N.; Guempel, U.; Gilboa-Garber, N.; Royle, R.J. Specificity of the fucose-binding lectin of Pseudomonas aeruginosa. *FEMS Microbiol. Lett.* **1987**, *48*, 331–334, doi:10.1111/j.1574-6968.1987.tb02619.x.
49. Nessen, K. von; Karg, M.; Hellweg, T. Thermoresponsive poly-(N-isopropylmethacrylamide) microgels: Tailoring particle size by interfacial tension control. *Polymer* **2013**, *54*, 5499–5510, doi:10.1016/j.polymer.2013.08.027.
50. Rey, M.; Hou, X.; Tang, J.S.J.; Vogel, N. Interfacial arrangement and phase transitions of PNiPAm microgels with different crosslinking densities. *Soft Matter.* **2017**, *13*, 8717–8727, doi:10.1039/c7sm01558e.
51. Bourne, Y.; Astoul, C.H.; Zamboni, V.; Peumans, W.J.; Menu-Bouaouiche, L.; van Damme, E.J.M.; Barre, A.; Rougé, P. Structural basis for the unusual carbohydrate-binding specificity of jacalin towards galactose and mannose. *Biochem. J.* **2002**, *364*, 173–180.
52. Wu, A.M.; Wu, J.H.; Tsai, M.-S.; Yang, Z.; Sharon, N.; Herp, A. Differential affinities of Erythrina cristagalli lectin (ECL) toward monosaccharides and polyvalent mammalian structural units. *Glycoconj. J.* **2007**, *24*, 591–604, doi:10.1007/s10719-007-9063-y.
53. Allen, H.J.; Johnson, E.A.Z.; Matta, K.L. A Comparison of the Binding Specificities of Lectins from Ulex Europaeus and Lotus Tetragonolobus. *Immunol. Commun.* **1977**, *6*, 585–602, doi:10.3109/08820137709093469.
54. Miceli, E.; Kuropka, B.; Rosenauer, C.; Osorio Blanco, E.R.; Theune, L.E.; Kar, M.; Weise, C.; Morsbach, S.; Freund, C.; Calderón, M. Understanding the elusive protein corona of thermoresponsive nanogels. *Nanomedicine* **2018**, *13*, 2657–2668, doi:10.2217/nnm-2018-0217.
55. Kratz, K.; Lapp, A.; Eimer, W.; Hellweg, T. Volume transition and structure of triethyleneglycol dimethacrylate, ethylenglykol dimethacrylate, and *N*,*N*′-methylene bis-acrylamide cross-linked poly(*N*-isopropyl acrylamide) microgels: a small angle neutron and dynamic light scattering study. *Colloids Surf. A Physicochem. Eng. Aspects* **2002**, *197*, 55–67, doi:10.1016/S0927-7757(01)00821-4.
56. Ruffet, E.; Paquet, N.; Frutiger, S.; Hughes, G.J.; Jaton, J.C. Structural and electron-microscopic studies of jacalin from jackfruit (Artocarpus integrifolia) show that this lectin is a 65 kDa tetramer. *Biochem. J.* **1992**, *286*, 131–134.
57. Sankaranarayanan, R.; Sekar, K.; Banerjee, R.; Sharma, V.; Surolia, A.; Vijayan, M. A novel mode of carbohydrate recognition in jacalin, a Moraceae plant lectin with a β-prism fold. *Nat. Struct. Biol.* **1996**, *3*, 596, doi:10.1038/nsb0796-596.
58. Ma, B.; Simala-Grant, J.L.; Taylor, D.E. Fucosylation in prokaryotes and eukaryotes. *Glycobiology* **2006**, *16*, 158R-184R, doi:10.1093/glycob/cwl040.
59. Meyer, J.M.; Neely, A.; Stintzi, A.; Georges, C.; Holder, I.A. Pyoverdin is essential for virulence of Pseudomonas aeruginosa. *Infect. Immun.* **1996**, *64*, 518–523.
60. Kang, D.; Kirienko, D.R.; Webster, P.; Fisher, A.L.; Kirienko, N.V. Pyoverdine, a siderophore from Pseudomonas aeruginosa, translocates into C. elegans, removes iron, and activates a distinct host response. *Virulence* **2018**, *9*, 804–817, doi:10.1080/21505594.2018.1449508.

61. Lamont, I.L.; Beare, P.A.; Ochsner, U.; Vasil, A.I.; Vasil, M.L. Siderophore-mediated signaling regulates virulence factor production in Pseudomonasaeruginosa. *Proc. Natl. Acad. Sci. USA* **2002**, *99*, 7072–7077, doi:10.1073/pnas.092016999.
62. Masuko, T.; Minami, A.; Iwasaki, N.; Majima, T.; Nishimura, S.-I.; Lee, Y.C. Carbohydrate analysis by a phenol-sulfuric acid method in microplate format. *Anal. Biochem.* **2005**, *339*, 69–72, doi:10.1016/j.ab.2004.12.001.
63. Böcker, S.; Elling, L. Biotinylated N-Acetyllactosamine- and N,N-Diacetyllactosamine-Based Oligosaccharides as Novel Ligands for Human Galectin-3. *Bioengineering* **2017**, *4*, doi:10.3390/bioengineering4020031.
64. Böcker, S.; Laaf, D.; Elling, L. Galectin Binding to Neo-Glycoproteins: LacDiNAc Conjugated BSA as Ligand for Human Galectin-3. *Biomolecules* **2015**, *5*, 1671–1696, doi:10.3390/biom5031671.

5 Discussion

Carbohydrates are the most abundant natural compound on earth and are found in every living being.[1] They are responsible for numerous, essential biological processes and functions.[2] Thus, the study of carbohydrate compounds is crucial to fully understand and utilize their biological interactions and functions. For this, glycopolymers are desirable materials as they can exhibit the same or even enhanced biological properties and functionalities compared to natural saccharides.

Glycopolymers can be synthesized by direct polymerization of glycomonomers or post-polymerization glycosylation. Over the years, various synthesis strategies for glycopolymers were reported for different applications. For instance, surface immobilized glycopolymers were tested for drug delivery systems.[3,4] Another example is the modification of surface chemistry to gain highly hydrophilic and biocompatible surfaces.[5] Such properties would be profitable for biomedical applications like implant coatings or drug delivery systems. Other studies reported possible applications in the fields of biosensors and therapeutics that are based on carbohydrate-lectin interactions.[6,7]

5.1 Synthesis Strategies for Glycopolymers

In this thesis, glycosylamines, glycomonomers and glycopolymers have been synthesized from different saccharides, namely fucose (Fuc), *N*-acetylgalactosamine (GalNAc), glucuronic acid (GlcA), lactose (Lac), maltose (Mal), and melibiose (Mel). The synthesis routes are generally regioselective and protecting group free.

To prepare glycopolymers by radical polymerization, prior syntheses of glycomonomers are required. For this, glycosylamines are a practical precursor as amines enable various reactions with, e.g., carboxylic acid chlorides.[8,9] Glycosylamines were prepared by the amination according to Kochetkov (Scheme 5.1) which only requires sugar, solvent, and an excess amount of aminating reagent.[10] In detail, the reaction was originally performed with an aqueous solution of ammonium bicarbonate. Other studies demonstrated variations of the Kochetkov amination with ammonium carbonate or carbamate as amination reagent and ammonium hydroxide solution, dimethyl sulfoxide (DMSO) or methanol as solvent.[11–18] In this work, the amination of GalNAc, Lac, GlcA and Fuc was optimized by varying temperature, saccharide concentration, the aminating reagents ammonium carbonate and carbamate, and the solvents water, DMSO and methanol. Likhoshertov introduced the amination with ammonium carbamate in saturated ammonium hydroxide solution.[15] For direct comparison of ammonium carbonate and carbamate as aminating agents, the ammonium hydroxide solution was omitted. It was found that the amination of saccharides is still applicable without the

ammonium hydroxide solution and high amination yields similar to reactions with ammonium carbonate could be achieved. Water is non-toxic, environment-friendly, and readily available but could lead to hydrolysis of glycosylamines during purification.[19] DMSO is also a non-toxic solvent, though, due to its low vapor pressure, its removal can be challenging for purification. In contrast, methanol is easily removable, although many saccharides exhibit poor solubility in methanol. However, optimization results showed that the amination yield is not dependent on the solubility of tested sugars. For instance, the amination of GalNAc, Lac and Fuc in methanol resulted in higher yields than in water whereas for the synthesis of aminated GlcA, water was superior to methanol. Therefore, depending on the respective amination yield, a suitable solvent may be selected for each saccharide. The reaction leads to regioselective amination at the C1-postion without any protection groups. This enables perpetuation of biofunctionality of the carbohydrates which can be crucial for biomedical applications. Downside of this amination is the slow reaction rate and (extreme) excess amount of ammonium salts. This can be circumvented by applying microwave irradiation which decreases the reaction time of 5 days to 90 min and allows reduction of the 50-fold excess of ammonium carbonate by 90% to a 5-fold excess in methanol or DMSO.[11,20] The acceleration of the reaction results from the absorption of microwave energy by the molecules leading to homogeneous as well as rapid internal heating of the molecules, which cannot be reproduced by conventional heating.[21] Optimization results demonstrated that the microwave-assisted amination is also applicable for the amination in water as well as the method with ammonium carbamate. The complete removal of ammonium salt was not possible and coincides with the observations of previous studies.[19] To facilitate workup, the glycosylamines were not isolated as the starting material and side products like glycosylamine dimers usually do not significantly impede consecutive reactions, e.g., methacrylation.[13] The amination yield could be easily analyzed via ^{1}H NMR spectroscopy without isolation of the product. Formation of glycosylamine was further verified by ESI-MS. Previous reports about the glycosylamination at the C1-position utilized reactions such as the reduction of glycosyl azides to glycosylamines.[22,23] Contrary to the Kochetkov amination, this method requires protection groups and, therefore, several synthesis steps to yield regioselectively aminated saccharides from unmodified sugars. In summary, the presented synthesis can be a highly efficient, straightforward, and inexpensive method to generate regioselectively aminated saccharides with retained biofunctionality by employing microwave irradiation.

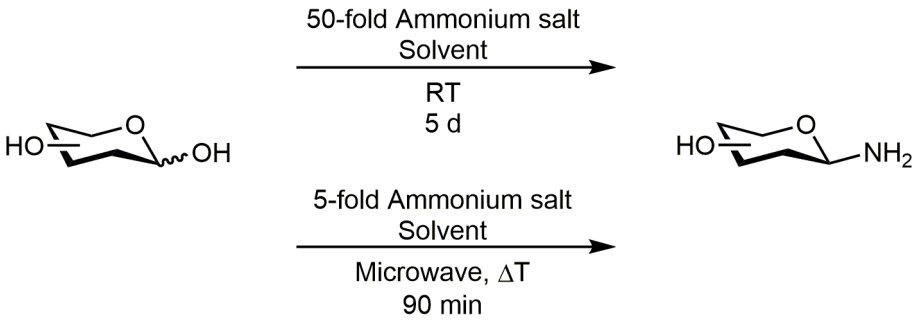

Scheme 5.1. Synthesis of glycosylamines by conventional amination reaction according to Kochetkov and microwave-assisted amination.

Glycomonomers with moieties that are polymerizable by radical polymerization were prepared. Numerous published synthesis routes employ protection groups to gain regio- and/or stereoselectivity.[24–26] However, studies of protecting group free synthesis strategies for glycomonomers have increased in recent years as they offer facile synthesis routes and compatibility with aqueous conditions reducing the use of harmful and costly organic solvents.[8,27,28] Many studies have demonstrated the (meth)acrylation of glycosylamines to be a straightforward method for synthesizing glycomonomers.[8,9,13,29] Therefore, the glycosylamines were consecutively modified with methacryloyl chloride under basic conditions to form the respective glycosylated methacrylamide (Scheme 5.2). The reaction is aqueous-based, however, methacryloyl chloride is a toxic reagent which requires precautions during synthesis. Another huge drawback is the purification of unprotected glycomonomers due to their high hydrophilicity and low solubility in organic solvents rendering it inefficient for large-scale syntheses. In this work, tedious purification via column chromatography could be facilitated for small-scale syntheses by applying preparative high performance liquid chromatography (HPLC) with a hydrophobic (C18) stationary phase. The formation of glycomonomers was verified by ^{1}H and ^{13}C NMR spectroscopy as well as ESI-MS. Other methods to synthesize glycomonomers based on (meth)acrylates or (meth)acrylamides have been reported which also employ protecting group free synthesis routes. For instance, glycosyl azides were synthesized followed by a copper catalyzed azide-alkyne cycloaddition (CuAAC) with *N*-propargyl acrylamide.[30] This reaction is a straightforward two-step synthesis. However, the use of copper is a major drawback for biomedical materials due to its cytotoxicity.[31,32] Another example is the simple reaction of sugar lactones with 2-aminoethyl methacrylate.[33] This synthesis leads to opening of the sugar ring and requires saccharides of two or more units to retain biofunctionality. Moreover, not all sugar lactones are commercially available and have to be synthesized first. In addition, lactones easily hydrolyze in water. Simple sugars were functionalized with acrylates or acrylamides by employing enzymes in water which enables a “green” route.[34,35] The disadvantages of enzymes are their temperature and pH sensitivity, as well as their high specificity since the same type of enzyme is not necessarily employable

for every saccharide.[36] Additionally, low yields due to equilibrium reactions can be a challenge. Generally, comparing (meth)acrylates and (meth)acrylamides, the latter ones are known to be less prone to hydrolysis, therefore, a wider range of reaction conditions such as high pH values are enabled with (meth)acrylamides.[37] To conclude, the methacrylation of glycosylamines is a straightforward and facile method for preparing glycomonomers as no additional synthesis steps for protection and deprotection are necessary to yield regioselectively functionalized glycosides.

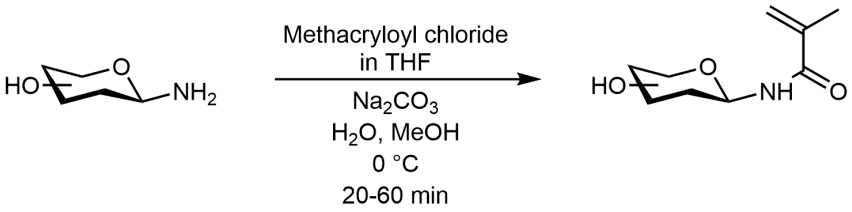

Scheme 5.2. Synthesis of glycomonomers by methacrylation of glycosylamines.

A facile and efficient method for synthesizing glycopolymers is the conventional free radical polymerization (FRP) (Scheme 5.3).[38] The reaction can be conducted in water with unprotected glycomonomers and, therefore, enables a "green" route.[39] Furthermore, the FRP technique is moderately insensitive to impurities, scalable, of low costs and the most common polymerization method used in industry.[39,40] A disadvantage is the low control of molecular weight, size distribution, structure, macromolecular architecture, and end group functionality.[40] Here, glycopolymers based on GalNAc and Lac were prepared by conventional FRP. Formation of polymer, conversion of glycomonomer as well as polymerization kinetics were investigated by ^{1}H NMR spectroscopy. The reaction rate was very similar for both glycomonomers where high conversions of 86-90% were realized after 2-4 h. Polymerizations were conducted overnight for maximum yield. The molecular weight of synthesized glycopolymers and its distribution were analyzed via SEC. It has to be noted, that the chromatographic determination of molecular weight and its accuracy depend on calibrations with suitable standards which are not available for these glycopolymers. Molecular weights of 8.9 x 10^4 g mol^{-1} and 2.8 x 10^5 g mol^{-1} with polydispersity indices (PDI) of 19 and 40 were found for the GalNAc and Lac polymer, respectively. The high PDI values indicate random formation of networks, crosslinking and/or branching which can be expected from the uncontrolled FRP method since side reactions such as chain transfer can occur, especially during the long reaction time. In comparison, previous studies investigated the FRP of maltitol- and lactitol-based vinyl alcohols. The maltitol-based homopolymer achieved a yield of 99% after 20 h and a molecular weight of 4.8 x 10^4 g mol^{-1} with a PDI of 3.2. The lactitol-based homopolymer resulted in a yield of 82% after 2.5 h with a molecular weight of 2.2 x 10^4 g mol^{-1} and a PDI of 1.7.[41] The observed monomer conversions are similar to the reported data while the reaction kinetic of the glycosylated methacrylamides appear to be relatively fast.

Overall, the molecular weight as well as the PDI increase with reaction time. Generally, the FRP technique is a simple, efficient as well as inexpensive method and suitable for the synthesis of glycopolymers whose properties do not need precise tailoring.

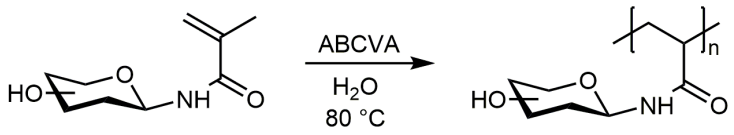

Scheme 5.3. Synthesis of glycopolymers by free radical polymerization of glycomonomers.

For the preparation of ionic glycosylated polymers, glycopolymers synthesized by FRP were subsequently sulfated (Scheme 5.4). Alternatively, commercially available ionic comonomers, such as acrylic acid, could be copolymerized. However, this could lead to copolymers with inhomogeneous distribution and low density of charges. In contrast, the one-step sulfation of carbohydrates with chlorosulfonic acid is efficient as well as regioselective since it favors hydroxy groups at C2- and C6-position.[42] This allows the synthesis of glycopolymers with homogeneous charge distribution. Furthermore, more charges can be achieved with this method than with the copolymerization of a fraction of ionic comonomers. However, the sulfation of saccharides could modify or eliminate their biofunctionality. Reports have shown that modified carbohydrates could lead to enhanced protein interaction in comparison to their unmodified analogues.[43–46] Moreover, glycans in nature also carry sulfate groups, such as heparin or chondroitin sulfate. Successful sulfation was investigated by ^{1}H NMR and IR spectroscopy. ^{1}H NMR spectra showed no hint of cleavage of saccharides and IR spectra presented new signals characteristic for sulfate groups. Due to the sulfur atoms, the sulfation degree could be easily analyzed by elemental analysis. As the disaccharide Lac offers more sulfation possibilities than the monosaccharide GalNAc, the sulfation degree of Lac polymer (1.7 sulfate groups per monomer unit) was correspondingly higher than that of the GalNAc polymer (0.9 sulfate groups per monomer unit). To facilitate handling of chemicals, solid sulfur trioxide pyridine complex was tested in place of the liquid chlorosulfonic acid. However, this resulted in a decrease of sulfation degree from 0.9 to 0.2 for the GalNAc polymer and 3.5 to 0.6 for the Lac polymer. Former studies reported the sulfation of glycopolymers bearing glucose moieties.[47] Functionalization was conducted with sulfur trioxide trimethylamine complex which yielded a sulfation degree of 0.4 sulfate groups per monomer unit. Thus, for the sulfation of glycopolymers, screening of sulfating reagents for respective glycopolymers is necessary to achieve high functionalization degrees. In summary, the direct sulfation method enables ionic charges on every or almost every monomer unit. Hence, the sulfation of glycopolymers with chlorosulfonic acid is a facile and efficient method for preparing anionic glycopolymers with homogeneous charge distributions as well as high charge densities.

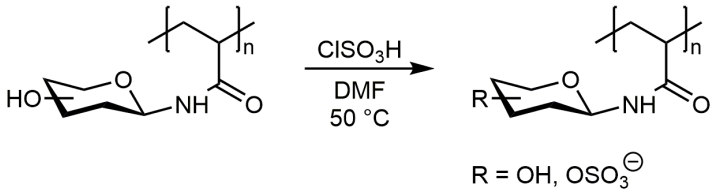

Scheme 5.4. Synthesis of anionic glycopolymers by direct sulfation.

For the preparation of cationic glycopolymers, the post-polymerization glycosylation strategy was employed. Studies presented glycopolymers prepared by copolymerization with cationic comonomers, though this could result in a inhomogeneous distribution of charges and low charge densities.[48] In contrast, the post-modification method can be very efficient and yield homogenous charge distributions as well as high charge densities.[49,50] In this work, branched poly(ethyleneimine) (PEI) was modified with disaccharides by reductive amination (Scheme 5.5). The benefits of PEI as polymer backbone are the accessibility of different molecular weights as well as the many amino groups which offer high charge densities and can undergo various reactions.[50–53] Therefore, readily available saccharides can be used without prior modification. However, PEI is known for its cytotoxicity. That said, studies have shown that its cytotoxicity is significantly reduced or removed completely when glycosylated.[53–55] A downside of the reductive amination is the use of the highly toxic reagent sodium cyanoborohydride which demands precautious handling and appropriate disposal. In addition, boron residues were found via ^{11}B NMR spectroscopy which might result from the possible formation of boronate esters. However, studies have presented the targeted use of boronate ester formation between carbohydrates.[56–58] Thus, the boron residues in the glycopolymers could be beneficial for certain applications. The reaction is regioselective but leads to the opening of the reductive saccharide. To retain biofunctionality, saccharides of two or more units can be employed.[59] Glycopolymers were verified by ^{1}H NMR and IR spectroscopy. The functionalization degree could be determined by phenol-sulfuric acid assay and elemental analysis. However, the values obtained from these methods differed significantly. This find could be attributed to possible boronate ester formations which block the saccharides from reaction with sulfuric acid and phenol. Moreover, this assay was developed for free carbohydrates and could lead to anomalous values for bound saccharides. Nevertheless, this method could still be viable if the same glycopolymers with varied functionalization degrees are compared for additional data. Here, elemental analysis is preferred for exact determination of the glycosylation degree. Many studies have reported the syntheses of glycopolymers by post-polymerization polymerization, especially by click reactions, such as the CuAAC, amine coupling or thiol-ene reactions, as they offer high efficiency.[60–64] However, these reactions require the prior syntheses of polymers with suitable functional groups like vinyl, *N*-succinimidyl or pentafluorophenyl moieties as well as modified sugars carrying thiol, azide or amino groups.

Depending on the synthesis method, protection groups and, consequently, deprotection steps are necessary. Hence, the high number of synthesis steps of these post-polymerization modifications for glycopolymers are not as efficient as the one-pot glycosylation via reductive amination. In summary, the reductive amination of branched PEI is a highly efficient synthesis method for the preparation of cationic glycopolymers.

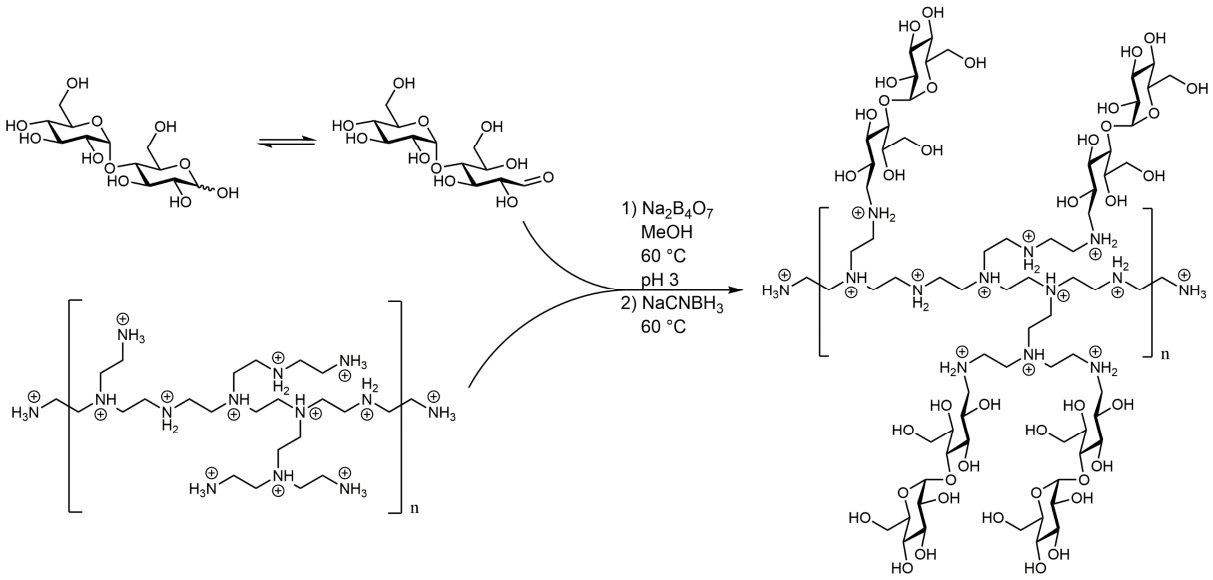

Scheme 5.5. Synthesis of cationic glycopolymers by reductive amination on the example of maltose.

Numerous synthesis strategies for glycopolymers were reported with various macromolecular architectures. However, only few reports about glycosylated colloidal hydrogels can be found even though their properties offer many benefits for glycopolymer applications.[65–67] In this work, the synthesis of glycosylated nanogels with high sugar content was established (Scheme 5.6). One of the most extensively studied hydrogel particles are based on NiPAm and MBA and prepared by free-radical precipitation polymerization.[68] The biocompatibility of PNiPAm allows utilization in biomedical fields.[69] By using regioselectively functionalized glycomonomers, the biofunctionality of the saccharides can be retained. The synthesis can be performed in water as opposed to emulsion polymerization and, thus, enables an efficient and “green” one-pot synthesis of colloidal hydrogels. By the precipitation polymerization technique, network structures of tailored sizes and low polydispersities can be fabricated. Contrary to glycosylated nanoparticles, glycosylated hydrogel colloids offer a three-dimensional network structure that can be penetrated from smaller molecules. The sugar content of glycogels were determined by phenol-sulfuric acid assay. At a constant ratio of comonomers, the analysis revealed that the sugar content was only specific to the nature of saccharide and independent of other investigated reaction parameters like concentrations of surfactant and crosslinker. Lac, Mel and Fuc glycogels exhibited a sugar content of approximately 410, 260 and

980 µmol g^{-1}, respectively. PNiPAm microgels without glycomonomers exhibited good polydispersities of 4-9% at 20 °C. In contrast, DLS, SEM and AFM measurements of glycogels revealed high polydispersities of 22-67%. Studies of similar PNiPAm-based glycogels were prepared with mannose functionalized *N*-(2-hydroxyethyl)-2-methacrylamide instead of GalNAc or Lac modified methacrylamide. Microgels with sugar contents of 12-67 µmol g^{-1} and polydispersities of 9-33% were reported while the pure PNiPAm microgel exhibited a polydispersity of 1%.[66] Hence, the polydispersity index significantly increases at the incorporation of glycomonomers. The hydrophilic character of the sugar moieties might have caused repulsion between the forming glycogel and the surfactant corona, thus, leading to scattering of the glycopolymer and increase of polydispersity. The yield, size and polydispersity could be influenced by the concentrations of surfactant and crosslinker. In TGA measurements, a water content of 5-11% was found in every freeze-dried glycogel which demonstrates the hydrophilic properties of typical hydrogels. Another typical characteristic of PNiPAm hydrogels is the thermoresponsitivity which was observed in further DLS investigations. Pure PNiPAm hydrogel particles present a phase transition at around 32 °C.[70,71] The temperature-dependent phase transition of glycogels was not as pronounced as for pure PNiPAm hydrogels but showed a gradual decrease of diameter with increasing temperature which indicates the incorporation of glycomonomers. To conclude, this synthesis route is a valuable strategy for preparing hydrogel colloids with multivalent presentations of saccharides.

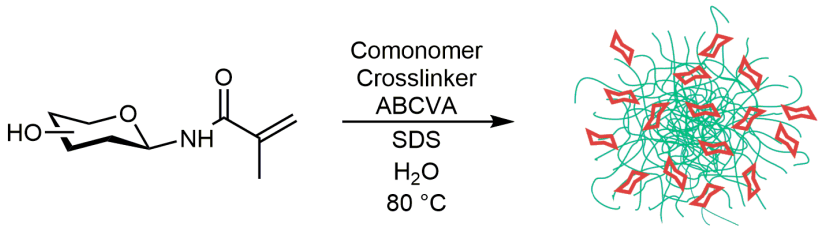

Scheme 5.6. Synthesis of glycogels by free-radical precipitation polymerization.

5.2 Glycopolymers for Medical Applications

Glycopolymers with various properties for medical applications were synthesized in this work, such as anionic homopolymers, cationic branched polymers and colloidal hydrogels. Due to the biofunctionality, biocompatibility as well as stability of glycopolymers, they have been investigated for possible drug delivery systems including drug delivery from surface coatings. For the fabrication of surface thin films, the layer-by-layer (LbL) approach emerged as an efficient and versatile method.[72,73] The LbL technique based on electrostatic interactions requires the coating materials to exhibit sufficient high charge densities and homogenous distribution of charges.[74] The formation and stability

of LbL multilayers of ionic glycopolymers were investigated via whispering gallery mode (WGM) analysis and quartz crystal microbalance with dissipation monitoring (QCM-D). The advantage of WGM and QCM-D sensoring is the extreme sensitivity, label-free detection, and real-time monitoring.[75–77] Moreover, QCM-D gives additional information about the mechanical properties of adsorbed material. To ensure suitability for medical applications, experiments were performed in physiological pH range. Coatings of glycopolymer pairs constituted of positively charged Lac- or Mal-PEI and negatively charged S-Lac (sulfated Lac polymer) or S-GalNAc (sulfated GalNAc polymer). Stable multilayer films of 8 layers were fabricated in all combinations at physiological pH range. Hence, these glycopolymers might be suitable as coating materials for biological or medical applications. Studies of LbL-coatings from maltosylated PEI and heparin reported multilayers of up to 50 bilayers in similar pH ranges.[50] This indicates that further glycopolymer layers could be added and that natural polysaccharides like heparin could be substituted with synthetic glycopolymers. No more than a total of 8 layers were tested as these thin films were sufficient to immobilize liposomes. For possible drug delivery, liposomes were incorporated as potential cargo carriers in Lac-PEI/S-Lac or Mal-PEI/S-Lac multilayers. These vesicles are known for their biocompatibility and ability to encapsulate hydrophilic as well as hydrophobic substances.[78–80] Furthermore, the slow diffusion of drugs from liposomes are beneficial for therapy where no typical burst release of high drug concentrations is wanted.[81,82] The liposomes were deposited on the thin film after three monolayers of glycopolymers. The immobilized liposome layer was stable and analysis via QCM-D measurements revealed that the adsorbed liposomes remained as intact vesicles. A second adsorption of liposomes was attempted after three additional glycopolymer layers. However, only little adsorption was observed on Lac-PEI while Mal-PEI showed no liposome adsorption at all. A possible explanation is the relatively large size of the vesicles (~100 nm) compared to the glycopolymer thin films of a few nanometers which could cause uneven glycopolymer coatings and, consequently, impede further immobilization of liposomes. This could be disadvantageous for the delivery of high drug doses if insufficient liposomes are incorporated. Nevertheless, one layer of liposomes might already encapsulate sufficient amounts of drugs depending on the surface area of the substrate and medical treatment. Many studies on liposomes embedded in LbL assembled multilayer films demonstrate the deposition of a single liposome layer on 3-20 bilayers, followed by additional coating.[83–87] Typically, commercially available polysaccharides or polyelectrolytes, such as hyaluronic acid, poly(allylamine) or poly(L-lysine), were used but, to the best of my knowledge, no coatings of solely synthetic glycopolymers with embedded liposome layers were reported. Additional coating experiments with sulfated glycopolymers and unmodified PEI revealed very thin and unstable layers. In contrast, LbL coatings with glycosylated PEI in place of unmodified PEI demonstrated stable multilayers with higher adsorbed masses. This observation could be explained by molecular interactions between the sugars as well as boronate esters. Moreover, the functionalized PEI exhibit

higher mass-to-charge ratio than unmodified PEI. Consequently, a higher amount of glycosylated PEI can be deposited on a LbL coating until charge saturation than the commercially available polymer. Hence, the glycopolymers can compete with these natural polysaccharides and polyelectrolytes as they can form stable LbL multilayer thin films with embedded liposomes. In conclusion, the ionic glycopolymers could be potentially suitable for certain drug delivery applications which require slow drug release and no extremely high drug amounts.

Another medical application, which the synthesized glycopolymers were investigated for, are therapeutics. Many glycopolymers were used to study carbohydrate-lectin interactions that mediate numerous biological processes such as disease development.[88–90] Pathogens employ lectins to bind to cell surface glycans of the host cell and to infiltrate them.[2] By competitive inhibition with ligands that show high affinity for the pathogenic lectins, the adhesion of pathogens to host cells can be prevented.[91] In this work, colloidal hydrogels with multivalent presentations of glycans were synthesized for strong multivalent binding of the lectins. The lectin inhibition potential of glycogels were studied by an ELISA-type approach with plant lectins. All Lac- and Mel-based glycogels demonstrated a very prominent multivalent effect where Lac gels exhibited a 4-fold higher inhibition than free Lac and Mel gels demonstrated a 100-fold stronger inhibition than free Mel when solely the concentration of sugar was examined. This observation demonstrates a prominent multivalent effect where a far less amount of saccharide is needed for the lectin inhibition when bound to colloidal hydrogels. Thus, low drug doses of glycogels could be sufficient for medical treatment. The three-dimensional hydrogel network might also contribute to the strong binding if lectins enter and are trapped there. No inhibition of Fuc gels could be detected as the respective plant lectin binds α-L-fucose and the glycogels bear β-L-fucose moieties. The pathogen *Pseudomonas aeruginosa* (PA) uses two lectins, namely LecA and LecB, as virulence factors which are specific for α-D-galactose and L-fucose, respectively.[92,93] As Mel carries a terminal α-D-galactose moiety, it can also be bound by LecA. Preliminary cell tests were performed with PA to study its cell growth in the presence of glycogels. For control, experiments were also conducted without glycogels or with free Mel and Fuc. The secretion of the fluorescent siderophore pyoverdine was detected by fluorescence. Pyoverdine participates in enabling the formation of biofilms which act as a protecting barrier for PA against antibiotics and consequently leads to proliferation of PA. Lac and Mel glycogels as well as the free sugars showed no difference to the control experiment without any glycogels. The fluorescence intensity was reduced in the presence of Fuc glycogels which hints at reduced secretion of pyoverdine. PA was subsequently cultivated on petri dishes and formation of colonies were observed. Thus, the reduced secretion of pyoverdine did not arise from antimicrobial activity of the Fuc glycogels but possibly from their influence on the pyoverdine biosynthesis. To sum up, these glycogels could be potential anti-adhesion

therapeutics against lectin-dependent pathogens, which moreover avert the formation of antibiotic resistance.

5.3 References

[1] H. M. I. Osborn, *Carbohydrates*, **2003**.
[2] N. Sharon, H. Lis, *Lectins*, **2007**.
[3] C. Von Der Ehe, C. Weber, M. Gottschaldt, U. S. Schubert, *Prog. Polym. Sci.* **2016**, *57*, 64.
[4] B. Torger, D. Vehlow, B. Urban, S. Salem, D. Appelhans, M. Müller, *Biointerphases* **2013**, *8*, 1.
[5] E. Bittrich, F. Mele, A. Janke, F. Simon, K.-J. Eichhorn, B. Voit, D. Appelhans, *Biointerphases* **2018**, *13*, 06D405.
[6] Z. Cai, A. Sasmal, X. Liu, S. A. Asher, *ACS Sensors* **2017**, *2*, 1474.
[7] J. Ishii, M. Chikae, M. Toyoshima, Y. Ukita, Y. Miura, Y. Takamura, *Electrochem. commun.* **2011**, *13*, 830.
[8] T. Tanaka, *Trends Glycosci. Glycotechnol.* **2016**, *28*, E101.
[9] J. Kim, Y. K. Pak, K. H. Chun, J. E. N. Shin, **2001**, *22*, 758.
[10] L. M. Likhosherstov, O. S. Novikova, V. A. Derevitskaja, N. K. Kochetkov, *Carbohydr. Res.* **1986**, *146*, 8.
[11] M. Bejugam, S. L. Flitsch, *Org. Lett.* **2004**, *6*, 4001.
[12] M. A. Brun, M. D. Disney, P. H. Seeberger, *ChemBioChem* **2006**, *7*, 421.
[13] A. Ghadban, L. Albertin, R. W. Moussavou Mounguengui, A. Peruchon, A. Heyraud, *Carbohydr. Res.* **2011**, *346*, 2384.
[14] C. Campa, I. Donati, A. Vetere, A. Gamini, S. Paoletti, *J. Carbohydr. Chem.* **2001**, *20*, 263.
[15] L. M. Likhosherstov, O. S. Novikova, V. N. Shibaev, *Dokl. Akad. Nauk* **2002**, *383*, 500.
[16] L. M. Likhosherstov, O. S. Novikova, V. N. Shibaev, *Dokl. Chem.* **2003**, *389*, 73.
[17] L. M. Likhosherstov, O. S. Novikova, A. O. Zheltova, V. N. Shibaev, *Russ. Chem. Bull.* **2004**, *53*, 709.
[18] K. Rustler, M. J. Mickert, J. Nazet, R. Merkl, H. H. Gorris, B. König, *Org. Biomol. Chem.* **2018**, *16*, 7430.
[19] D. Vetter, M. A. Gallop, *Bioconjug. Chem.* **1995**, *6*, 316.
[20] M. A. Brun, M. D. Disney, P. H. Seeberger, *Supp* **2008**.
[21] A. De La Hoz, A. Díaz-Ortiz, P. Prieto, *Microwave-assisted green organic synthesis*, Vol. 2016-Janua, The Royal Society of Chemistry, **2016**.
[22] J. Wang, W. Qi, G. Chen, *Chinese Chem. Lett.* **2019**, *30*, 587.
[23] G. Pastuch-Gawołek, K. Malarz, A. Mrozek-Wilczkiewicz, M. Musioł, M. Serda, B. Czaplinska, R. Musiol, *Eur. J. Med. Chem.* **2016**, *112*, 130.
[24] A. Ghadban, L. Albertin, *Polymers (Basel).* **2013**, *5*, 431.
[25] K. Matsuoka, H. Yamaguchi, T. Koyama, K. Hatano, D. Terunuma, *Tetrahedron Lett.* **2010**, *51*, 2529.
[26] Y. Zhao, Y. Zhang, C. Wang, G. Chen, M. Jiang, *Biomacromolecules* **2017**, *18*, 568.
[27] R. Roy, F. D. Tropper, A. Romanowska, *Bioconjug. Chem.* **1992**, *3*, 256.
[28] W. J. Zhou, M. E. Wilson, M. J. Kurth, Y. Lo Hsieh, J. M. Krochta, C. F. Shoemaker, *Macromolecules* **1997**, *30*, 7063.
[29] X. Li, M. Bao, Y. Weng, K. Yang, W. Zhang, G. Chen, *J. Mater. Chem. B* **2014**, *2*, 5569.
[30] T. Tanaka, H. Ishitani, Y. Miura, K. Oishi, T. Takahashi, T. Suzuki, S. I. Shoda, Y. Kimura, *ACS Macro Lett.* **2014**, *3*, 1074.
[31] D. C. Kennedy, C. S. McKay, M. C. B. Legault, D. C. Danielson, J. A. Blake, A. F. Pegoraro, A. Stolow, Z. Mester, J. P. Pezacki, *J. Am. Chem. Soc.* **2011**, *133*, 17993.
[32] L. Li, Z. Zhang, *Molecules* **2016**, *21*, 1.
[33] R. Narain, S. P. Armes, *Biomacromolecules* **2003**, *4*, 1746.

[34] A. Adharis, D. Vesper, N. Koning, K. Loos, *Green Chem.* **2018**, *20*, 476.
[35] L. Albertin, C. Kohlert, M. Stenzel, L. J. R. Foster, T. P. Davis, **2004**, *5*, 35.
[36] Z. Yang, Y. Liao, X. Fu, J. Zaporski, S. Peters, M. Jamison, Y. Liu, S. D. Wullschleger, D. E. Graham, B. Gu, *Sci. Total Environ.* **2019**, *686*, 1194.
[37] J. Zheng, M. Zhu, G. Ferracci, N.-J. Cho, B. H. Lee, *Macromol. Chem. Phys.* **2018**, *219*, 1800266.
[38] M. Nasiri Oskooie, M. Pooresmaeil, H. Namazi, *J. Polym. Res.* **2019**, *26*.
[39] M. Arcos-Hernandez, P. Naidjonoka, S. J. Butler, T. Nylander, H. Stålbrand, P. Jannasch, *Biomacromolecules* **2021**, *22*, 2338.
[40] J. M. G. Cowie, V. Arrighi, **2007**, 520.
[41] Y. Miura, T. Ikeda, K. Kobayashi, *Biomacromolecules* **2003**, *4*, 410.
[42] K. Zhang, E. Brendler, A. Geissler, S. Fischer, *Polymer (Guildf).* **2011**, *52*, 26.
[43] S. Böcker, L. Elling, *Bioengineering* **2017**, *4*.
[44] H. Ideo, T. Matsuzaka, T. Nonaka, A. Seko, K. Yamashita, *J. Biol. Chem.* **2011**, *286*, 11346.
[45] H. Ideo, A. Seko, T. Ohkura, K. L. Matta, K. Yamashita, *Glycobiology* **2002**, *12*, 199.
[46] M. L. Talaga, N. Fan, A. L. Fueri, R. K. Brown, P. Bandyopadhyay, T. K. Dam, *Biochemistry* **2016**, *55*, 4541.
[47] Z. Oezyuerek, K. Franke, M. Nitschke, R. Schulze, F. Simon, K. J. Eichhorn, T. Pompe, C. Werner, B. Voit, *Biomaterials* **2009**, *30*, 1026.
[48] C. Van Bruggen, J. K. Hexum, Z. Tan, R. J. Dalal, T. M. Reineke, *Acc. Chem. Res.* **2019**, *52*, 1347.
[49] P. Theato, H.-A. Klok, *Functional Polymers by Post-Polymerization Modification*, **2013**.
[50] S. Salem, M. Müller, B. Torger, A. Janke, K. J. Eichhorn, B. Voit, D. Appelhans, *Macromol. Chem. Phys.* **2015**, *216*, 182.
[51] F. Leclercq, C. Dubertret, B. Pitard, D. Scherman, J. Herscovici, *Bioorganic Med. Chem. Lett.* **2000**, *10*, 1233.
[52] J. Li, F. Wang, H. Wan, J. Liu, Z. Liu, K. Cheng, H. Zou, *J. Chromatogr. A* **2015**, *1425*, 213.
[53] S. J. Kim, H. Ise, M. Goto, K. Komura, C. S. Cho, T. Akaike, *Biomaterials* **2011**, *32*, 3471.
[54] K. Kunath, A. Von Harpe, D. Fischer, T. Kissel, *J. Control. Release* **2003**, *88*, 159.
[55] S. Grosse, Y. Aron, I. Honoré, G. Thévenot, C. Danel, A. C. Roche, M. Monsigny, I. Fajac, *J. Gene Med.* **2004**, *6*, 345.
[56] B. Wang, K. Yoshida, K. Sato, J. Anzai, *Polymers (Basel).* **2017**, 1.
[57] G. B. Sukhorukov, B. T. Levy, C. De, *Adv. Funct. Mater.* **2008**, 1586.
[58] X. Zhang, Y. Guan, Y. Zhang, *Biomacromolecules* **2012**.
[59] D. Appelhans, H. Komber, M. A. Quadir, S. Richter, S. Schwarz, J. Van Der Vlist, A. Aigner, M. Müller, K. Loos, J. Seidel, K. F. Arndt, R. Haag, B. Voit, *Biomacromolecules* **2009**, *10*, 1114.
[60] K. Neumann, A. Conde-González, M. Owens, A. Venturato, Y. Zhang, J. Geng, M. Bradley, *Macromolecules* **2017**, *50*, 6026.
[61] C. R. Becer, K. Babiuch, D. Pilz, S. Hornig, T. Heinze, M. Gottschaldt, U. S. Schubert, *Macromolecules* **2009**, *42*, 2387.
[62] E. Pedone, X. Li, N. Koseva, O. Alpar, S. Brocchini, *J. Mater. Chem.* **2003**, *13*, 2825.
[63] T. Fukuda, S. Tsuji, Y. Miura, *Polym. J.* **2019**, *51*, 617.
[64] K. Bhattacharya, S. L. Banerjee, S. Das, S. Samanta, M. Mandal, N. K. Singha, *ACS Appl. Bio Mater.* **2019**, *2*, 2587.
[65] M. Ahmed, P. Wattanaarsakit, R. Narain, *Polym. Chem.* **2013**, *4*, 3829.
[66] T. J. Paul, S. Rübel, M. Hildebrandt, A. K. Strzelczyk, C. Spormann, T. K. Lindhorst, S. Schmidt, *ACS Appl. Mater. Interfaces* **2019**, *11*, 26674.
[67] S. Quan, Y. Wang, A. Zhou, P. Kumar, R. Narain, *Biomacromolecules* **2015**, *16*, 1978.
[68] Z. Dai, T. Ngai, *J. Polym. Sci. Part A Polym. Chem.* **2013**, *51*, 2995.
[69] Y. Guan, Y. Zhang, *Soft Matter* **2011**, *7*, 6375.
[70] M. Destribats, M. Wolfs, F. Pinaud, V. Lapeyre, E. Sellier, V. Schmitt, V. Ravaine, *Langmuir* **2013**, *29*, 12367.
[71] T. Still, K. Chen, A. M. Alsayed, K. B. Aptowicz, A. G. Yodh, *J. Colloid Interface Sci.* **2013**, *405*, 96.
[72] J. Campbell, A. S. Vikulina, *Polymers (Basel).* **2020**, *12*, 1.

[73] M. Keeney, X. Y. Jiang, M. Yamane, M. Lee, S. Goodman, F. Yang, *J. Mater. Chem. B* **2015**, *3*, 8757.
[74] B. Schoeler, G. Kumaraswamy, F. Caruso, *Macromolecules* **2002**, *35*, 889.
[75] R. Bischler, M. Olszyna, M. Himmelhaus, L. Dähne, *Eur. Phys. J. Spec. Top.* **2014**, *223*, 2041.
[76] M. Olszyna, A. Debrassi, C. Üzüm, L. Dähne, *Adv. Funct. Mater.* **2019**, *29*, 1.
[77] Y. Gou, S. J. Richards, D. M. Haddleton, M. I. Gibson, *Polym. Chem.* **2012**, *3*, 1634.
[78] W. M. Merritt, Y. G. Lin, W. A. Spannuth, M. S. Fletcher, A. A. Kamat, L. Y. Han, C. N. Landen, N. Jennings, K. De Geest, R. R. Langley, G. Villares, A. Sanguino, S. K. Lutgendorf, G. Lopez-Berestein, M. M. Bar-Eli, A. K. Sood, *J. Natl. Cancer Inst.* **2008**, *100*, 359.
[79] S. Kalepu, V. Nekkanti, *Acta Pharm. Sin. B* **2015**, *5*, 442.
[80] Y. A. Brito Barrera, G. Hause, M. Menzel, C. E. H. Schmelzer, E. Lehner, K. Mäder, C. Wölk, T. Groth, *Mater. Today Bio* **2020**, *7*.
[81] R. Singh, S. P. Vyas, *J. Dermatol. Sci.* **1996**, *13*, 107.
[82] S. Bhattacharjee, *Ther. Deliv.* **2020**, *12*, 21.
[83] M. Michel, Y. Arntz, G. Fleith, J. Toquant, Y. Haikel, J. C. Voegel, P. Schaaf, V. Ball, *Langmuir* **2006**, *22*, 2358.
[84] M. Malcher, D. Volodkin, B. Heurtault, P. André, P. Schaaf, H. Möhwald, J. C. Voegel, A. Sokolowski, V. Ball, F. Boulmedais, B. Frisch, *Langmuir* **2008**, *24*, 10209.
[85] D. V. Volodkin, P. Schaaf, H. Mohwald, J. C. Voegel, V. Ball, *Soft Matter* **2009**, *5*, 1394.
[86] M. E. Lynge, M. Baekgaard Laursen, L. Hosta-Rigau, B. E. B. Jensen, R. Ogaki, A. A. A. Smith, A. N. Zelikin, B. Städler, *ACS Appl. Mater. Interfaces* **2013**, *5*, 2967.
[87] V. Domínguez-Arca, R. R. Costa, A. M. Carvalho, P. Taboada, R. L. Reis, G. Prieto, I. Pashkuleva, *Mater. Sci. Eng. C* **2021**, *121*, 111813.
[88] Y. Miura, *Polym. J.* **2012**, *44*, 679.
[89] S. G. Spain, N. R. Cameron, *Polym. Chem.* **2011**, *2*, 60.
[90] P. Kiran, S. Kumari, J. Dernedde, R. Haag, S. Bhatia, *New J. Chem.* **2019**, *43*, 16012.
[91] N. Sharon, *Biochim. Biophys. Acta - Gen. Subj.* **2006**, *1760*, 527.
[92] B. Blanchard, A. Imberty, A. Varrot, *Proteins Struct. Funct. Bioinforma.* **2014**, *82*, 1060.
[93] N. Gilboa-Garber, D. J. Katcoff, N. C. Garber, *FEMS Immunol. Med. Microbiol.* **2000**, *29*, 53.

6 Conclusion

This work presented different synthesis strategies for a variety of glycosides and glycopolymers for medical applications. The focus was on efficient, aqueous-based and protecting group free approaches. The challenging and limiting factor of most polymer synthesis was the preparation and purification of glycomonomers due to their high hydrophilicity. Thus, the discussed synthesis routes are efficient for small scales but for large scale productions of glycomonomers, synthesis routes including protection groups might be more beneficial than strategies without protecting groups. Generally, synthesis results demonstrated a strong influence of the nature of examined sugars on the reaction outcome which indicate the chemical complexity of carbohydrates. Thus, the optimization of glycoside and glycopolymer syntheses from different saccharides is greatly desired. By employing the design of experiments (DoE) approach, optimization of reactions could be facilitated. Hence, the DoE approach can be valuable tool for optimizing glycopolymer syntheses. Generally, DoE models and their predictions get more accurate with more data input. Even if the DoE approach was not used to generate experimental conditions, already achieved experimental data can still entered retrospectively. If every published data applied DoE, the data collection of glycopolymer synthesis could be greatly enhanced and forward future research about glycopolymers and their applications.

Efficient and protecting group free synthesis routes for glycopolymers that are applicable for potential drug delivery systems from surfaces were presented. The glycopolymer surface coatings were fabricated by the LbL technique. Complementary charged glycopolymers were synthesized via post-polymerization glycosylation, polymerization of glycomonomers and subsequent modification. The glycopolymers resulted in stable multilayer coatings with the ability to act as scaffolds for charged liposomes in physiological pH range. Therefore, the charge densities as well as the charge distribution of the synthesized glycopolymers are suitable for LbL thin films and for immobilizing charged liposomes. To further test the stability and applicability of the glycopolymer films for medical coatings, friction tests should be conducted. Additional investigation on the glycopolymer coating stability could be performed with glycopolymers that have been completely purified from boron residues. Furthermore, the incorporation of liposomes could be tested at different stages of the multilayers. For the drug delivery application, coating experiments with drug filled liposomes need to be performed. In addition, the drug release has to be investigated. Overall, these glycopolymers are promising materials for potential drug delivery applications where slow release of drugs from surfaces is essential.

A synthesis route for nanogels based on different sugars was established. All glycogels showed an enhanced binding potential to suitable lectins in comparison to unbound sugar due to the strong multivalency effect while certain polymer properties turned out superior for the lectin binding. This

demonstrates how the strength of this cluster glycoside effect is determined by the multivalent presentation of carbohydrates as well as the morphology of the multivalent glycopolymers. To further tailor the polymer properties like polydispersity and uniformity, synthesis parameters such as the ratio of comonomers, type and concentration of surfactant could be varied. Surfactants could be completely omitted if stabilization of gels is achieved by electrostatic repulsion of ionic initiator moieties. Monodisperse glycogels can be used to further study the size influence on their inhibition potential. A higher sugar content might further increase the lectin binding potential of such glycogels. However, a lower sugar content might already achieve the same lectin inhibition strength if spacing of glycans are appropriate to the locations of binding sites which would save resources. Investigations on the effect and possible exploitation of the thermoresponsitivity in relation to lectin binding could be conducted. Cytotoxicity assays and further cell tests with *Pseudomonas aeruginosa* need to be performed to research the potential of the glycogels as anti-adhesion therapeutics. To inhibit different pathogens, glycogels based on suitable saccharides should be synthesized. For example, mannosylated glycogels could potentially inhibit the adhesion of pathogenic *Escherichia coli* or *Salmonella typhimurium* to host cells. In summary, this material could offer an alternative to traditional antibiotics as an anti-adhesion therapeutic which does not induce antibiotic resistance.

In conclusion, this doctoral thesis provides new contribution for aqueous-based and protecting group free syntheses of glycopolymers and their precursors based on a variety of sugars that find potential application in the medical fields such as drug delivery systems or therapeutics.

7 Zusammenfassung

In dieser Arbeit wurden verschiedene Synthesestrategien für eine Auswahl an Glykosiden und Glykopolymeren für medizinische Anwendungen präsentiert. Der Fokus lag auf effizienten, wässrigen und schutzgruppenfreien Synthesen. Die Herausforderung und der limitierende Faktor der meisten Polymersynthesen war die Herstellung und Reinigung von Glykomonomeren, die aufgrund ihrer hohen Hydrophilie erschwert wurde. Daher sind die diskutierten Synthesewege für kleine Maßstäbe effizient, aber für die großtechnische Produktion von Glykomonomeren könnten Synthesewege mit Schutzgruppen vorteilhafter sein als Strategien ohne Schutzgruppen. Generell zeigten die Syntheseergebnisse einen starken Einfluss der Natur der untersuchten Zucker auf das Reaktionsergebnis, was auf die chemische Komplexität der Kohlenhydrate hindeutet. Daher ist die Optimierung von Glykosid- und Glykopolymersynthesen mit verschiedenen Sacchariden sehr erstrebenswert. Durch den Einsatz statistischer Versuchsplanung (*Design of Experiment*, DoE) konnte die Optimierung der Reaktionen erleichtert werden. Somit kann der DoE-Ansatz ein wertvolles Werkzeug für die Optimierung von Glykopolymersynthesen sein. Im Allgemeinen werden die DoE-Modelle und ihre Vorhersagen umso genauer, je mehr Daten eingegeben werden. Selbst wenn der DoE-Ansatz nicht zur Generierung experimenteller Versuchsbedingungen verwendet wurde, können bereits erzielte Versuchsdaten rückwirkend genutzt werden. Durch die Anwendung von DoE auf bisher alle veröffentliche Daten, könnte die Datensammlung zur Glykopolymersynthese erheblich verbessert werden und die zukünftige Forschung über Glykopolymere und ihre Anwendungen vorantreiben.

Es wurden effiziente und schutzgruppenfreie Synthesewege für Glykopolymere vorgestellt, die sich potenziell für *Drug-Delivery*-Applikationen von Oberflächen eignen. Die Glykopolymer-Oberflächenbeschichtungen wurden mit der Layer-by-Layer (LbL)-Technik hergestellt. Komplementär geladene Glykopolymere wurden durch Postpolymerisationsglykosylierung und Polymerisation von Glykomonomeren mit anschließender Modifikation synthetisiert. Die Glykopolymere führten zu stabilen mehrschichtigen Beschichtungen im physiologischen pH-Bereich mit der Fähigkeit, als Gerüst für geladene Liposomen zu dienen. Daher eignen sich sowohl die Ladungsdichten als auch die Ladungsverteilung der synthetisierten Glykopolymere für LbL-Dünnschichten und zum Tragen geladener Liposomen. Um die Stabilität und Anwendbarkeit der Glykopolymerfilme für medizinische Beschichtungen weiter zu testen, sollten Reibungstests durchgeführt werden. Zusätzliche Untersuchungen zur Stabilität von Glykopolymerbeschichtungen könnten mit Glykopolymeren durchgeführt werden, die vollständig von Borrückständen gereinigt wurden. Darüber hinaus könnte das Einbetten der Liposome in verschiedenen Stadien der Multilayer getestet werden. Für die Verabreichung von Medikamenten müssen Beschichtungsversuche mit medikamentengefüllten Liposomen durchgeführt werden. Zusätzlich muss die Wirkstofffreisetzung untersucht werden.

Insgesamt sind diese Glykopolymere vielversprechende Materialien für potenzielle *Drug-Delivery*-Systeme, bei denen eine langsame Freisetzung von Wirkstoffen an Oberflächen wichtig ist.

Es wurde ein Syntheseweg für Nanogele auf der Basis verschiedener Zucker (Glykogele) etabliert. Alle Glykogele zeigten im Vergleich zu ungebundenen Zuckern aufgrund des Multivalenz-Effekts ein erhöhtes Bindungspotenzial an geeignete Lektine, während sich bestimmte Polymereigenschaften als überlegen für die Lektinbindung erwiesen. Dies demonstriert, dass die Stärke des *cluster glycoside*-Effekts durch die multivalente Präsentation der Kohlenhydrate sowie die Morphologie der multivalenten Glykopolymere bestimmt wird. Um die Polymereigenschaften wie Polydispersität und Homogenität weiter zu optimieren, könnten Syntheseparameter wie das Verhältnis der Comonomere, die Art und die Konzentration des Tensids variiert werden. Auf Tenside könnte vollständig verzichtet werden, wenn die Stabilisierung der Gele durch die elektrostatische Abstoßung der ionischen Initiatorgruppen erreicht wird. Mit monodispersen Glykogelen lässt sich der Einfluss der Größe auf das Inhibitionspotenzial weiter untersuchen. Ein höherer Zuckergehalt könnte das Lektinbindungspotenzial solcher Glykogele weiter verbessern. Allerdings könnte ein geringerer Zuckergehalt bereits die gleiche Lektininhibition bewirken, wenn die Abstände der Glykane passend zu den Bindungsstellen sind, wodurch Ressourcen gespart werden könnte. Untersuchungen zur Wirkung und möglichen Ausnutzung der Thermosensitivität in Bezug auf die Lektinbindung könnten durchgeführt werden. Zytotoxizitätstests und weitere Assays mit *Pseudomonas aeruginosa* müssen durchgeführt werden, um das Potenzial der Glykogele als Anti-Adhäsions-Therapeutika zu untersuchen. Zur Hemmung verschiedener Krankheitserreger, sollten Glykogele auf der Basis geeigneter Saccharide synthetisiert werden. So könnten beispielsweise mannosylierte Glykogele die Adhäsion von pathogenen *Escherichia coli* oder *Salmonella typhimurium* an Wirtszellen hemmen. Insgesamt lässt sich sagen, dass dieses Material eine Alternative zu herkömmlichen Antibiotika darstellen könnte, die keine Antibiotikaresistenz hervorrufen.

Zusammengefasst liefert diese Doktorarbeit einen Beitrag zur Entwicklung von wässrigen und schutzgruppenfreien Synthesen von Glykopolymeren und ihren Vorläufern auf Basis von verschiedenen Zuckern, die potenzielle Anwendung im medizinischen Bereich wie Therapeutika oder *Drug-Delivery*-Systeme finden.

8 Appendix

8.1 Supporting Information to Chapter 2: Optimization of the Microwave Assisted Glycosylamines Synthesis Based on a Statistical Design of Experiments Approach

1-Amino-1-deoxy-β-D-N-acetylgalactoside (**Am-I-01**). ^{1}H-NMR (D_2O, 400 MHz): δ 5.21 (d, *J* = 3.6 Hz, 0.04H α-H1 (starting material)), 4.60 (d, *J* = 7.6 Hz, 0.05 H, β-H1 (starting material)), 4.30-3.51 (m, 6 H), 4.06 (d, *J* = 9.2 Hz, 0.64 β-H1), 2.03 (s, 3 H); ESI MS, calcd. for $C_8H_{16}N_2O_5$: $[M + H]^+$ 221.11, found 221.45 $[M + H]^+$.

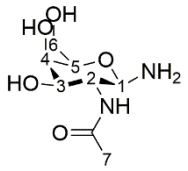

Am-I

1-Amino-1-deoxy-β-D-lactoside (**Am-II-01**). ^{1}H-NMR (D_2O, 400 MHz): δ 5.21 (d, *J* = 3.6 Hz, 0.05 H, α-H1 (starting material)), 4.65 (d, *J* = 8.0 Hz, 0.06 H, β-H1 (starting material)), 4.43 (d, *J* = 7.8 Hz, 1 H, β-H7), 4.10 (d, *J* = 8.8 Hz, 0.84 H, β-H1), 3.97-3.48 (m, 11 H), 3.19 (m, 0.82 H); ESI MS, calcd. for $C_{12}H_{24}NO_{10}$: $[M + H]^+$ 342.14, found 342.46 $[M + H]^+$.

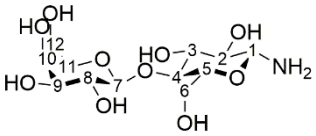

Am-II

1-Amino-1-deoxy-β-D-glucopyranuronoside (**Am-III**). ^{1}H-NMR (D_2O, 400 MHz): δ 5.24 (d, *J* = 3.7 Hz,4 H, α-H1 (starting material)), 4.64 (d, *J* = 7.9 Hz, β-H1 (starting material), 4.09 (d, *J* = 8.8 Hz, 0.82 H, β-H1), 3.12-4.34 (m, 4 H); ESI MS, calcd. for $C_6H_{12}NO_6$: $[M + H]^+$ 194.07, found 194.43 $[M + H]^+$.

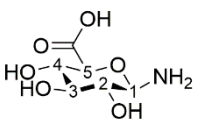

Am-III

1-Amino-1-deoxy-β-L-fucose (**Am-IV**). ^{1}H-NMR (D_2O, 400 MHz): δ 4.15-4.03 (m, 0.26 H), 3.99 (d, *J* = 8.8 Hz, 0.70 H, β-H1), 3.36-3.94 (m, 3.20 H), 3.32 (t, *J* = 8.8 Hz, 0.58 H) 1.20 (d, *J* = 6.4 Hz, 3 H); ESI MS, calcd. for $C_6H_{14}NO_4$: $[M + H]^+$ 164.09, found 164.38 $[M + H]^+$.

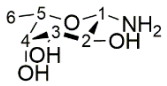

Am-IV

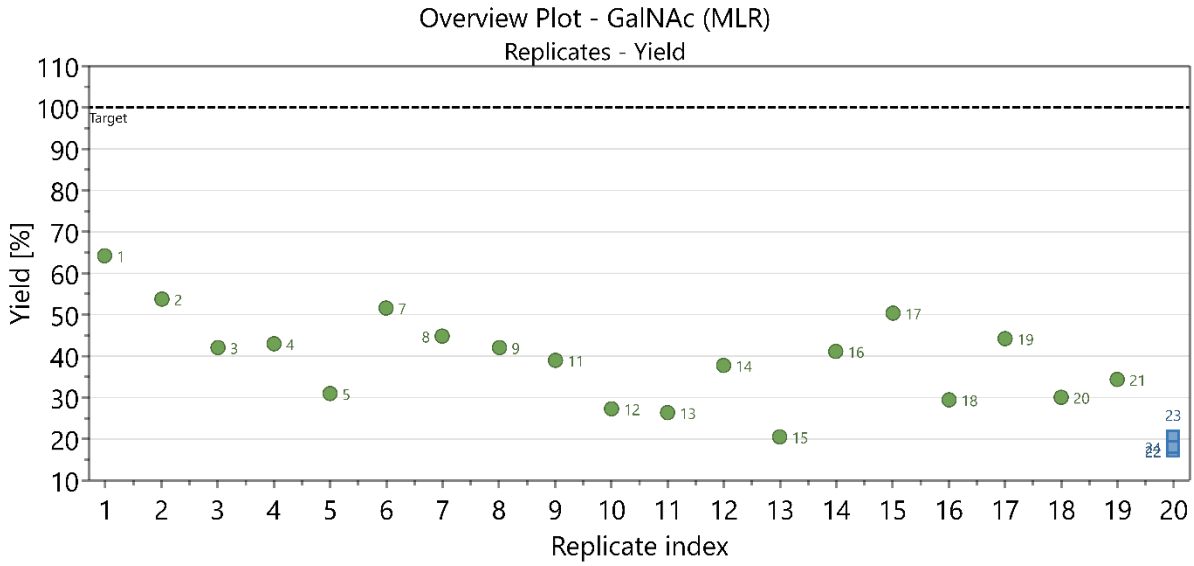

Figure 2.S1. Overview plot of yields of $GalNAcNH_2$. Replicates are indicated in blue.

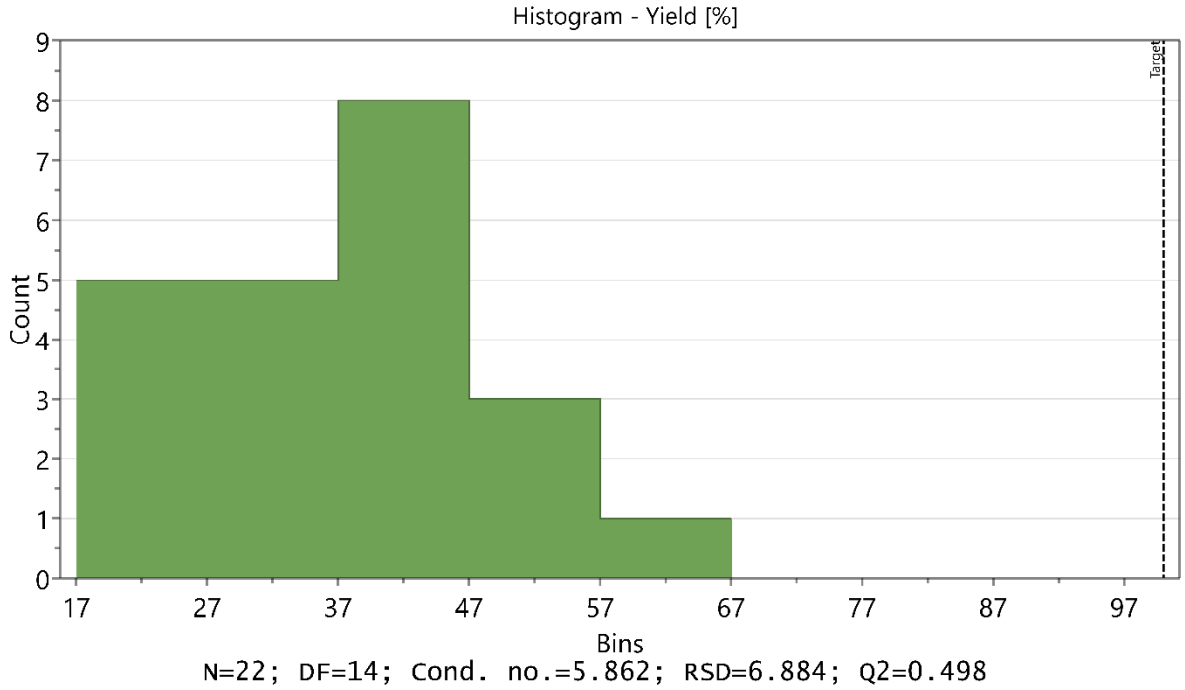

Figure 2.S2. Histogram of yields of $GalNAcNH_2$. Skewness test not triggered.

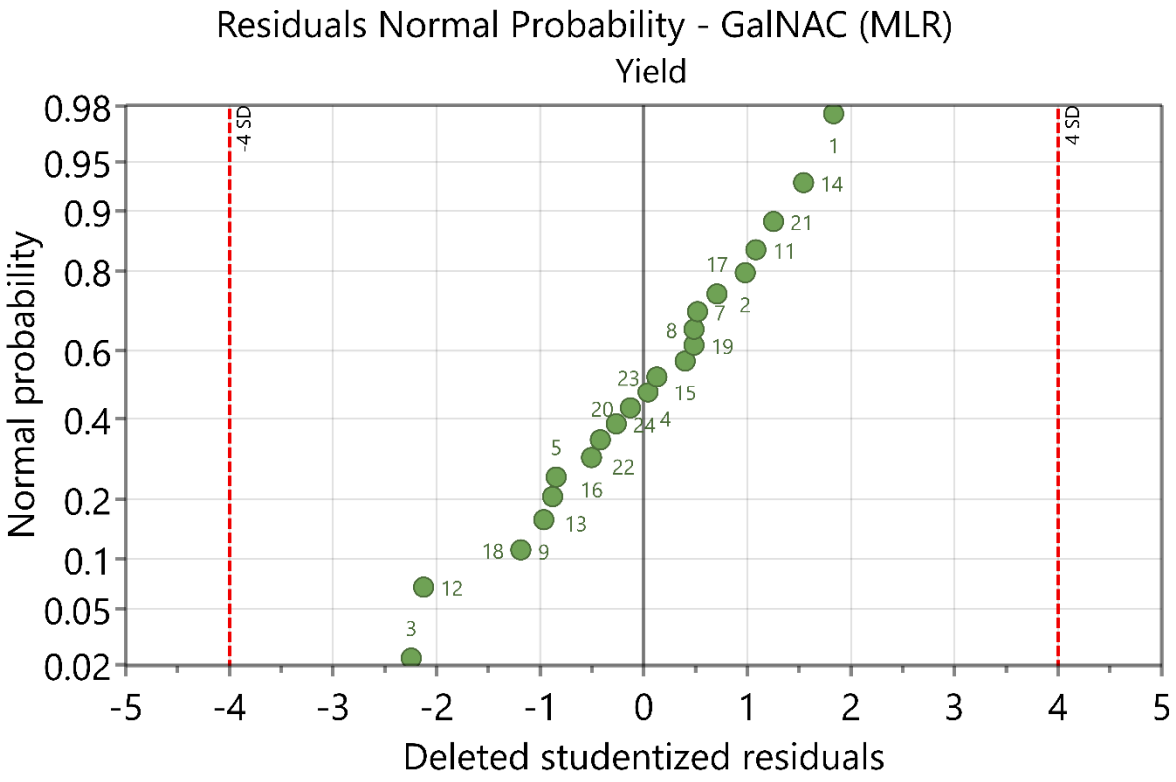

Figure 2.S3. Plot of GalNAcNH$_2$ with residuals of yields versus the normal probability of the distribution.

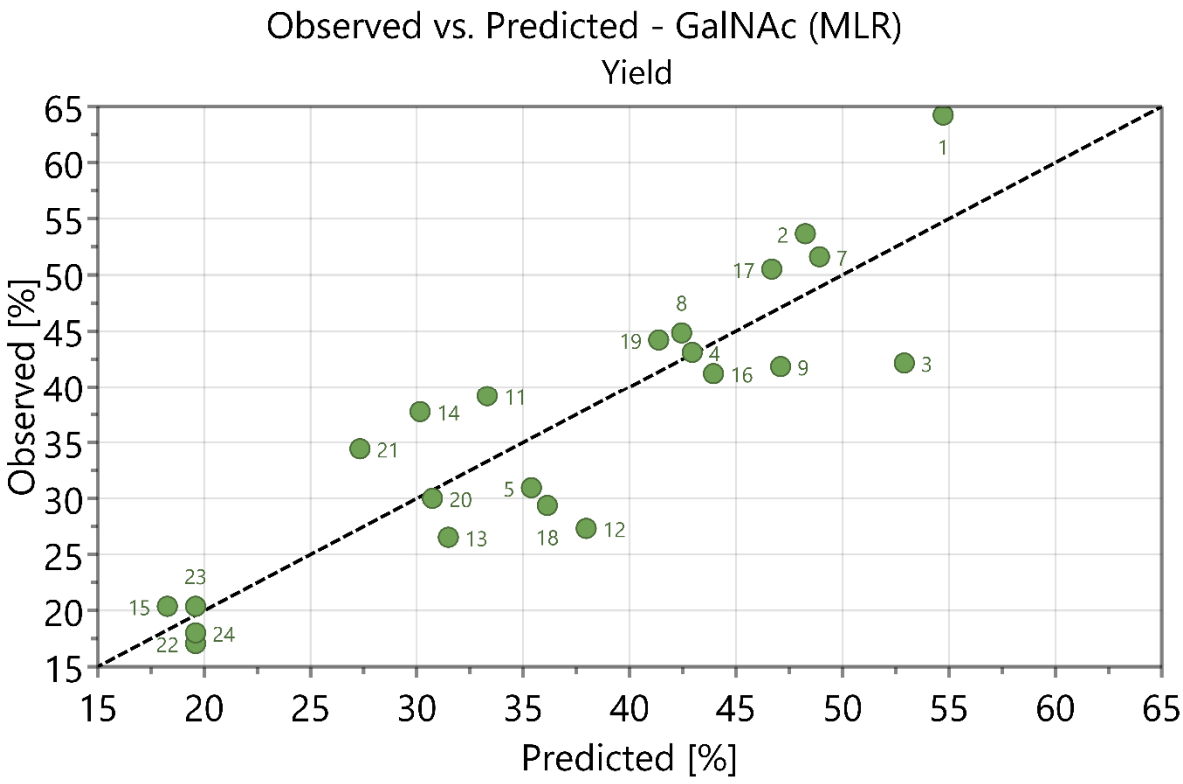

Figure 2.S4. Plot of observed values versus predicted values for yields of GalNAcNH$_2$.

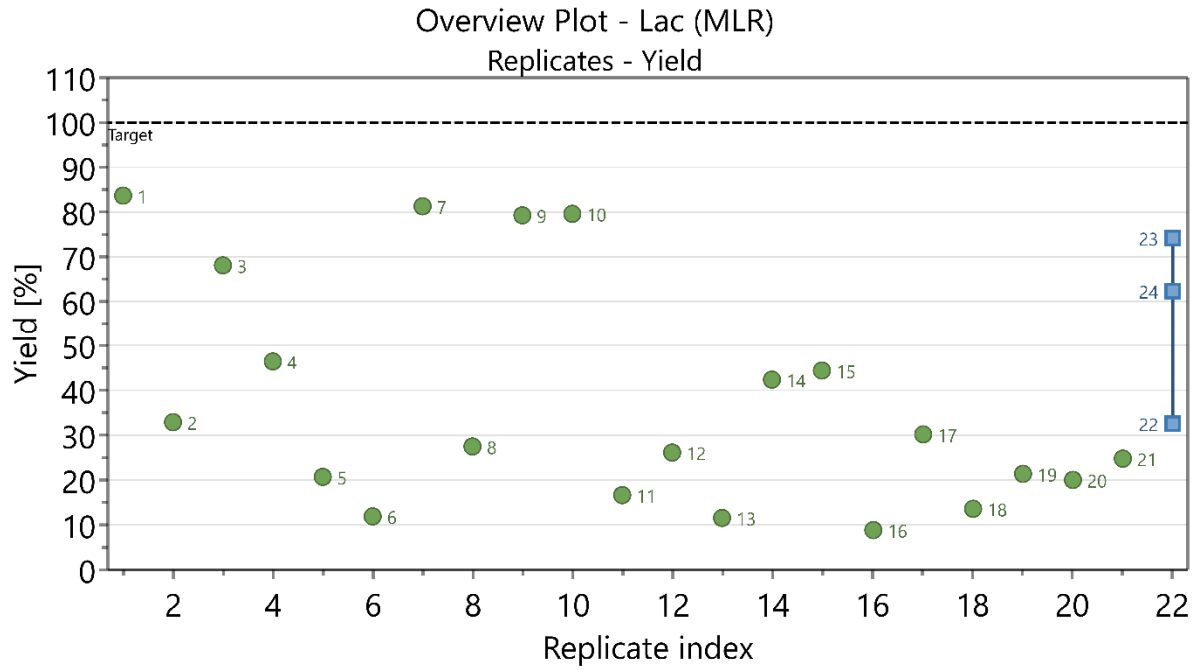

Figure 2.S5. Overview plot of yields of $LacNH_2$. Replicates are indicated in blue.

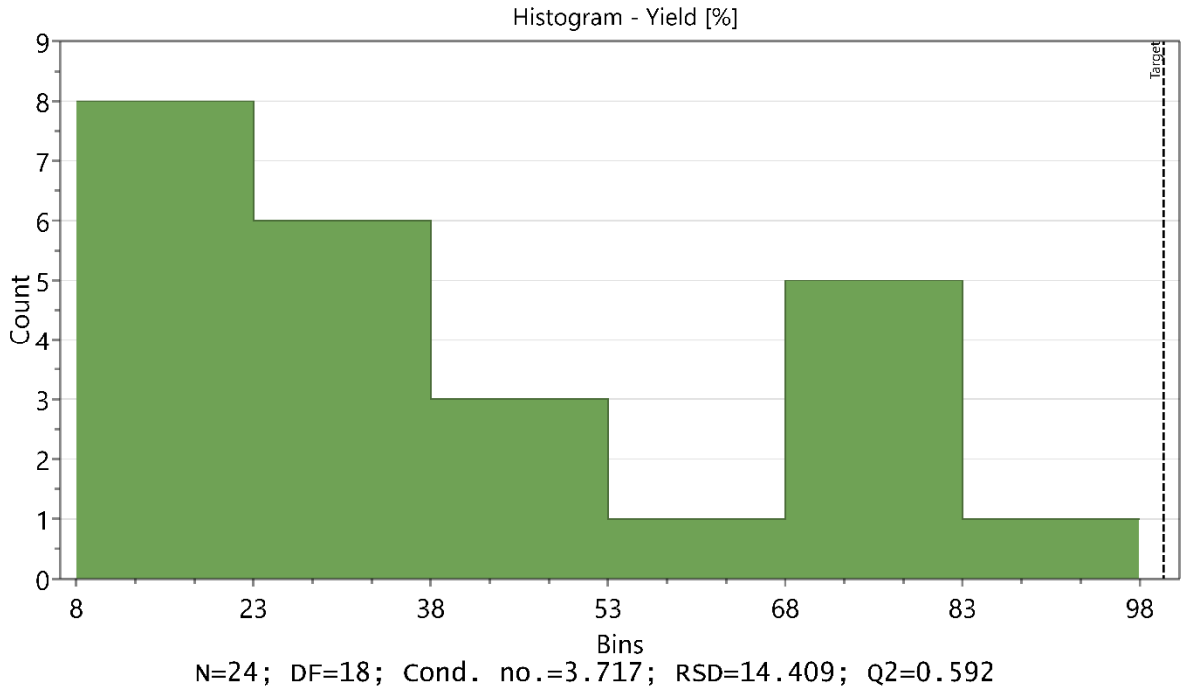

Figure 2.S6. Histogram of yields of $LacNH_2$. Skewness test not triggered.

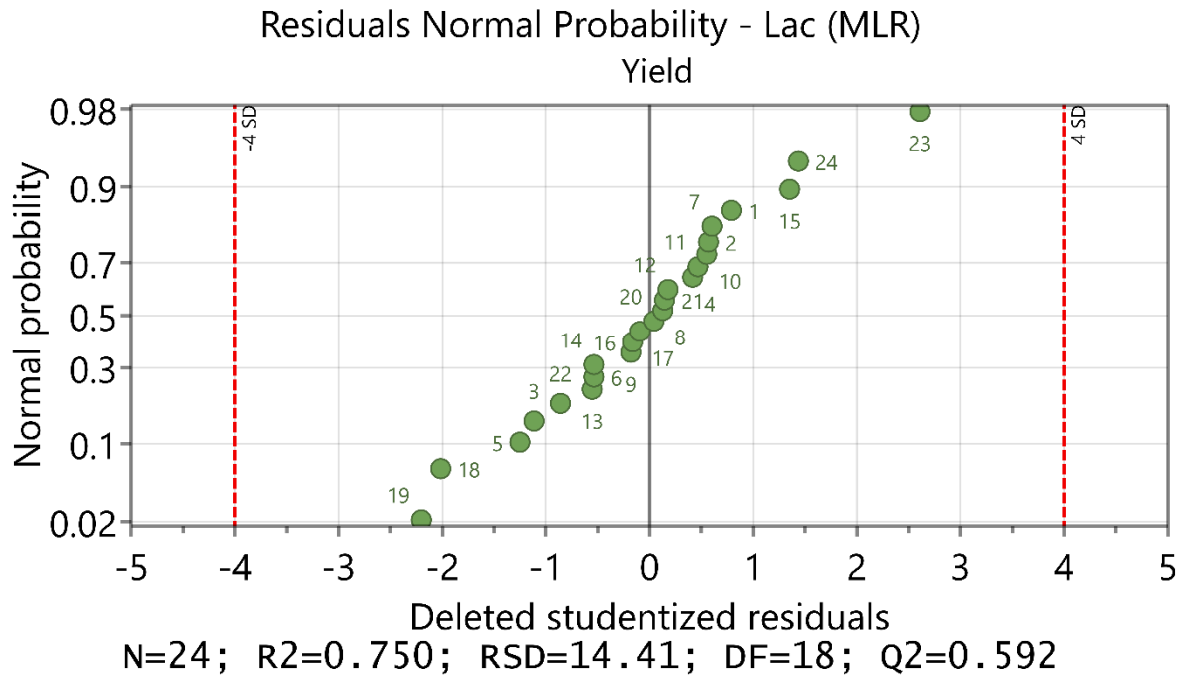

Figure 2.S7. Plot of $LacNH_2$ with residuals of yields versus the normal probability of the distribution.

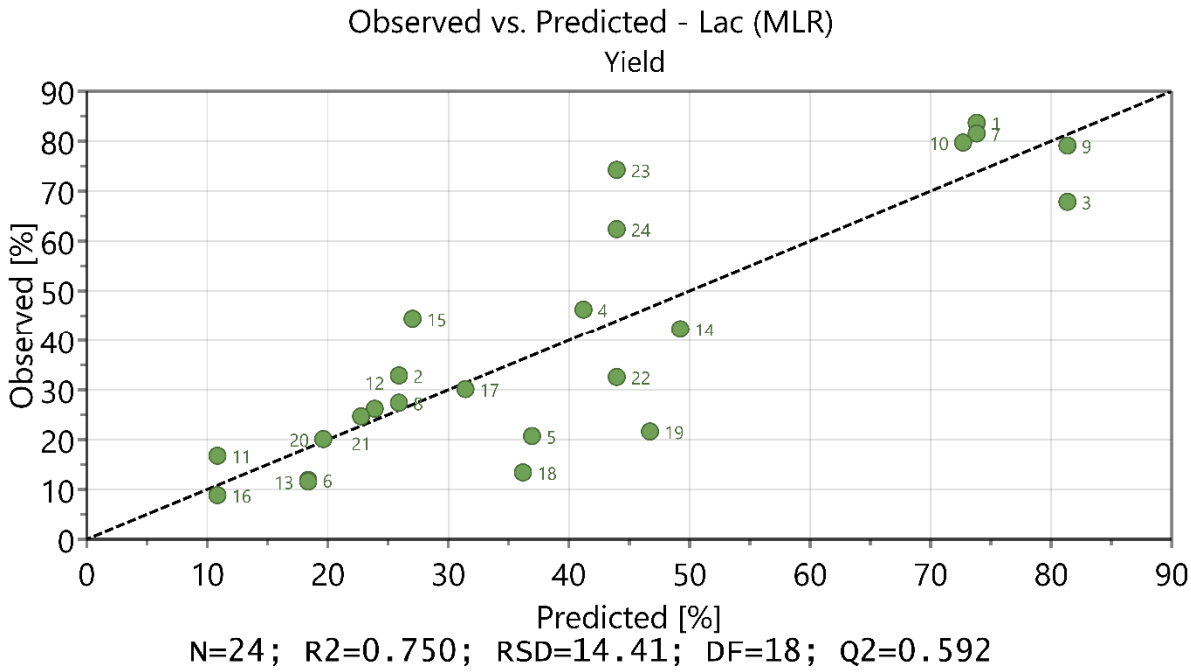

Figure 2.S8. Plot of observed values versus predicted values for yields of $LacNH_2$.

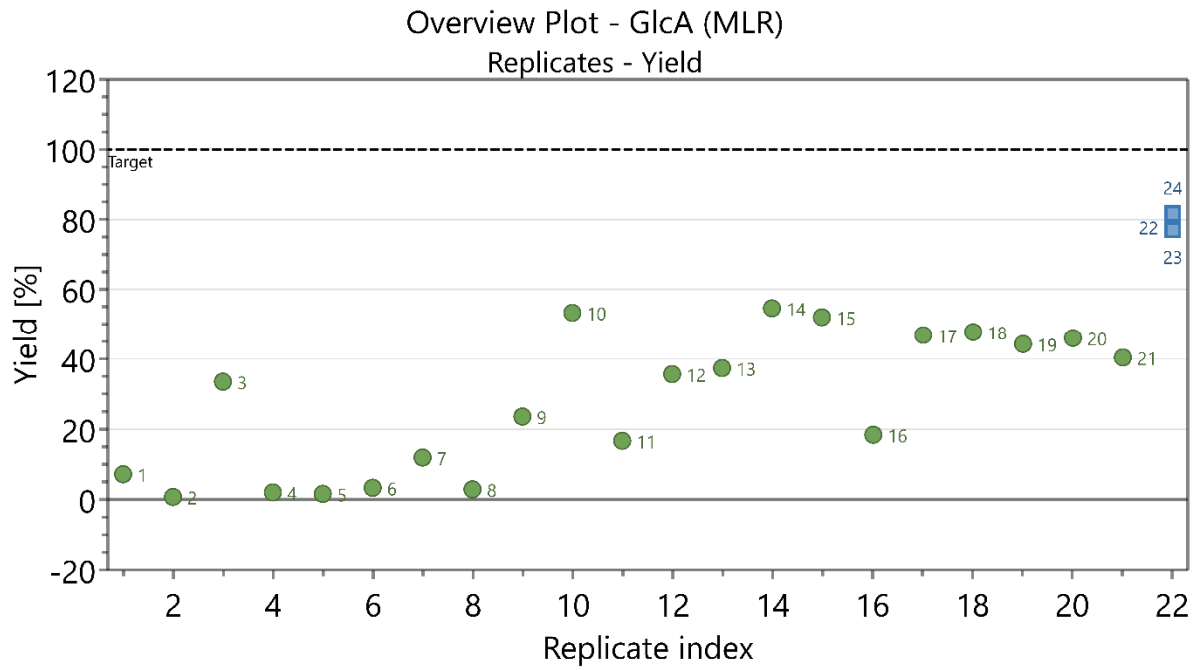

Figure 2.S9. Overview plot of yields of $GlcANH_2$. Replicates are indicated in blue.

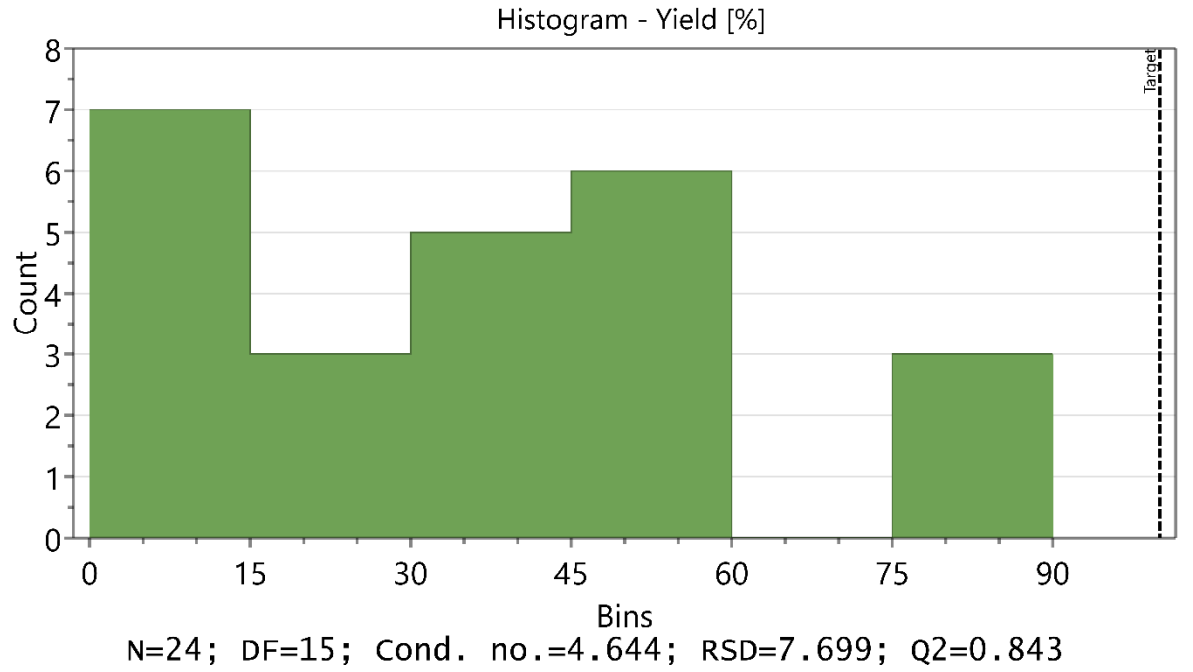

Figure 2.S10. Histogram of yields of $GlcANH_2$. Skewness test not triggered.

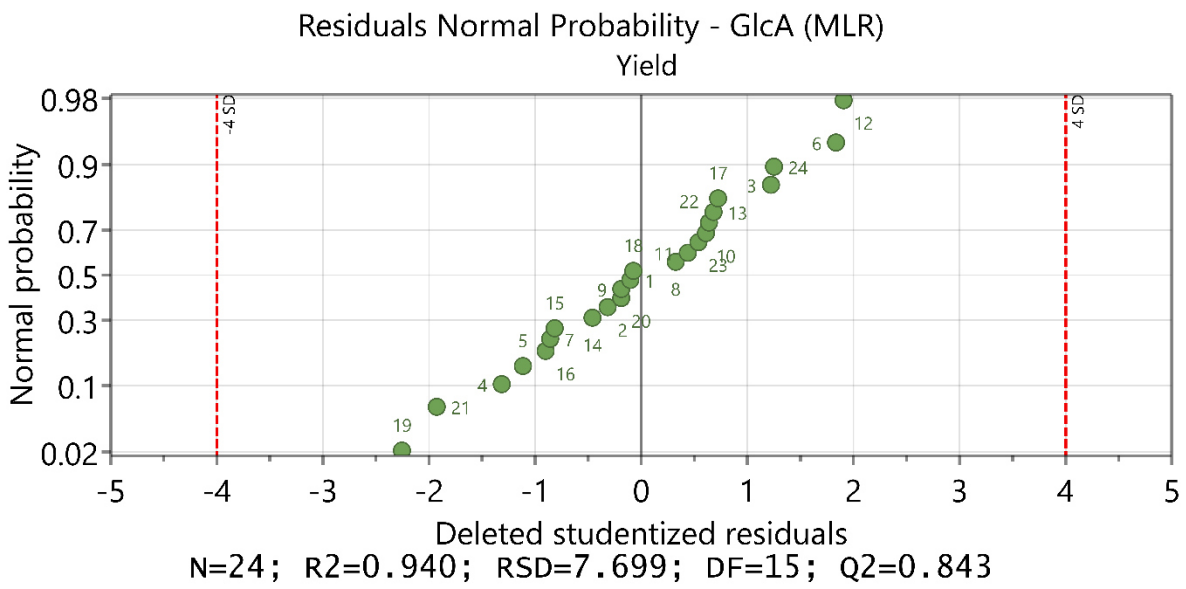

Figure 2.S11. Plot of $GlcANH_2$ with residuals of yields versus the normal probability of the distribution.

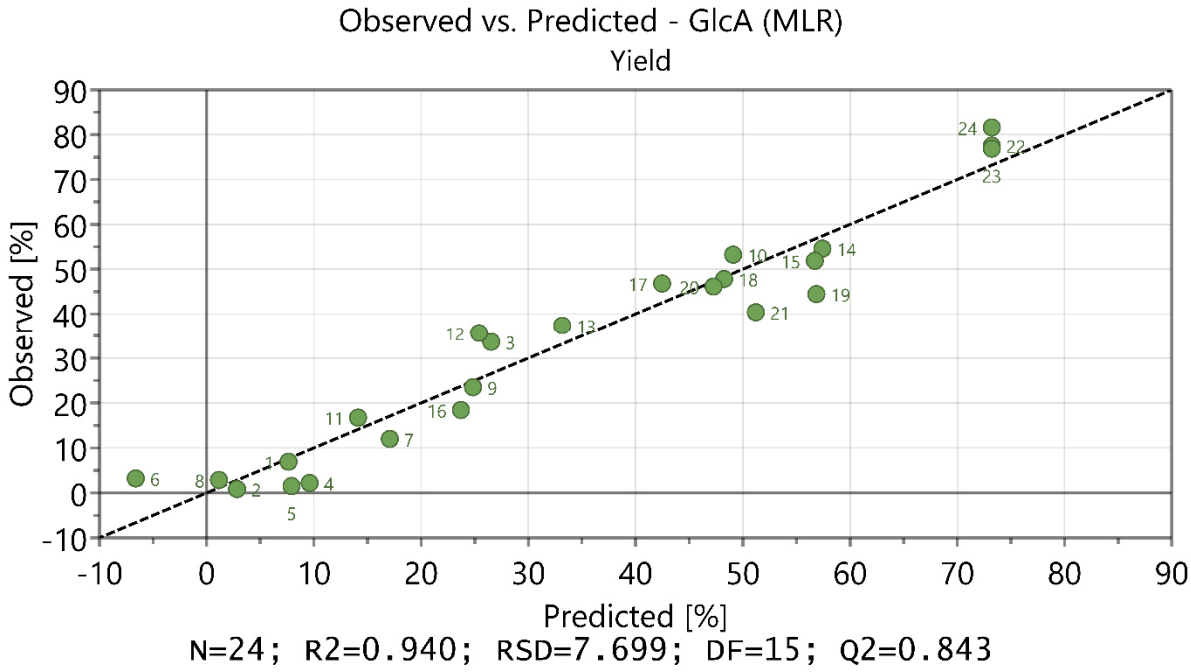

Figure 2.S12. Plot of observed values versus predicted values for yields of $GlcANH_2$.

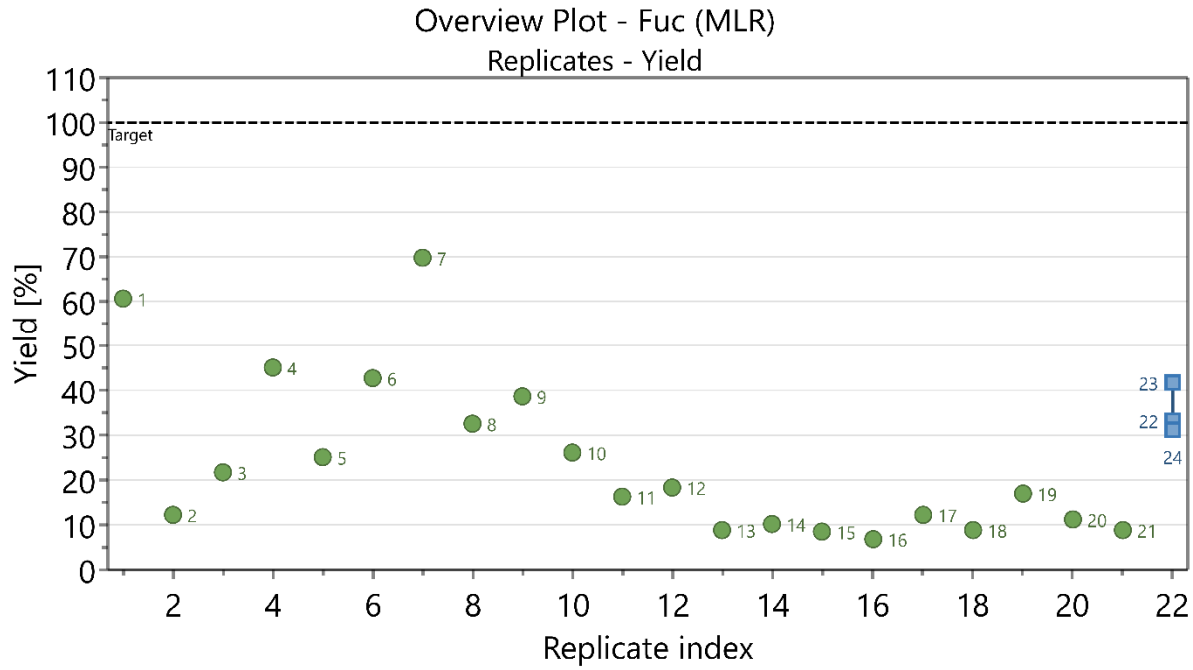

Figure 2.S13. Overview plot of yields of $FucNH_2$. Replicates are indicated in blue.

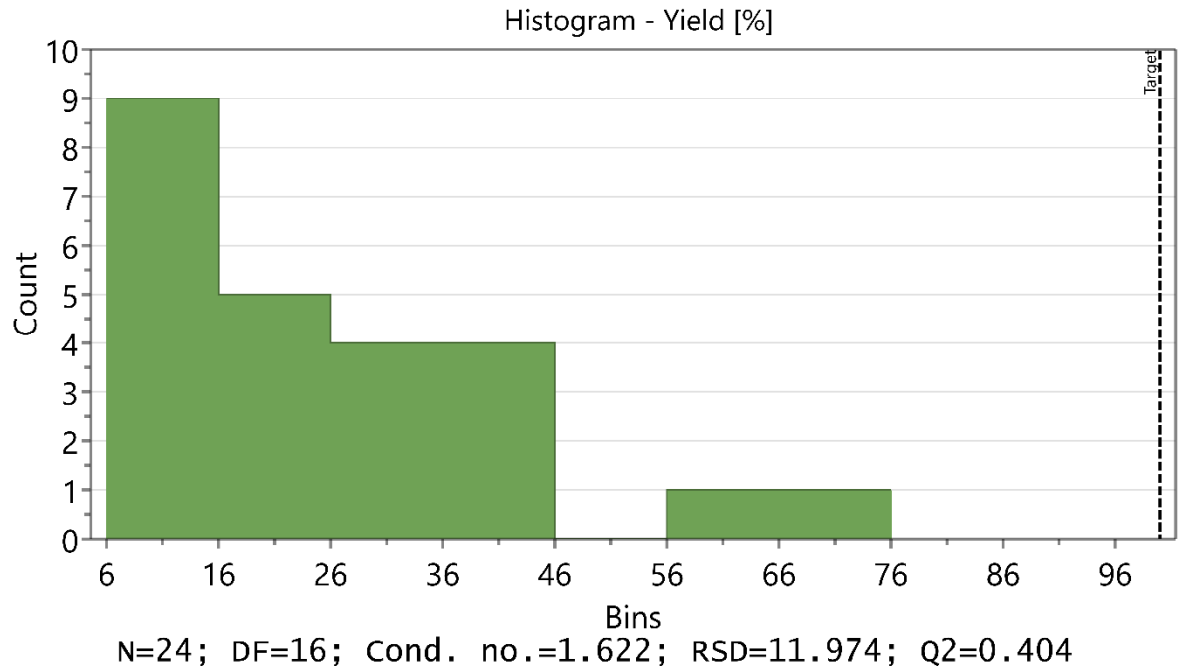

Figure 2.S14. Histogram of yields of $FucNH_2$. Skewness test triggered. No transformation performed.

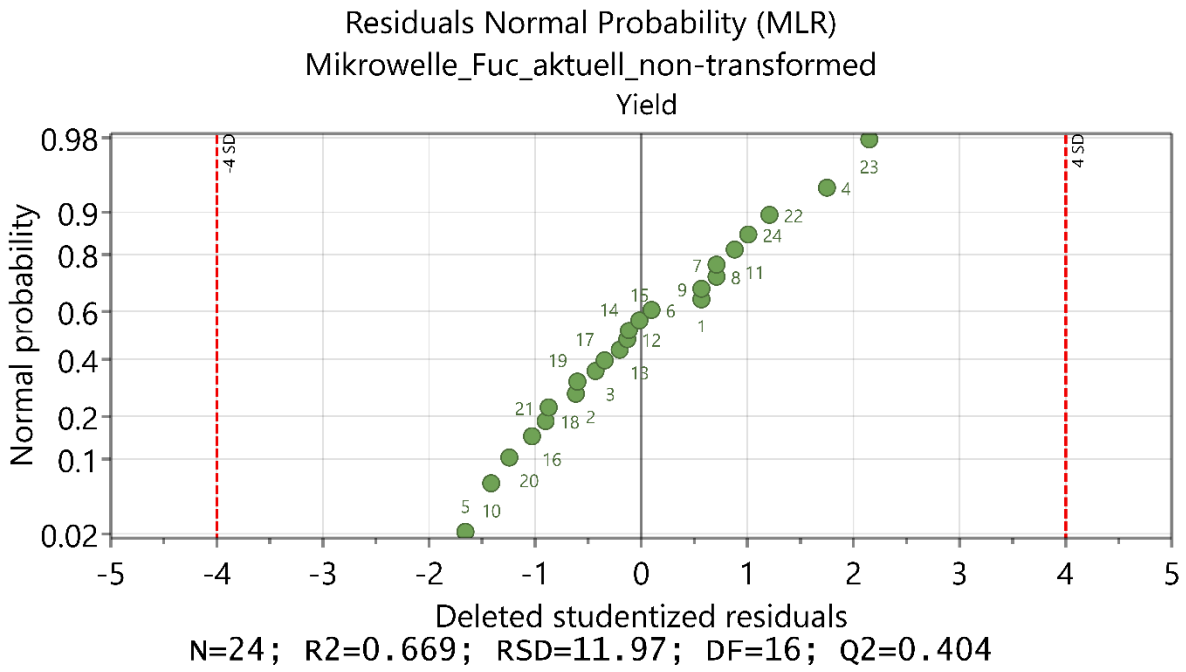

Figure 2.S15. Plot of $FucNH_2$ with residuals of yields versus the normal probability of the distribution.

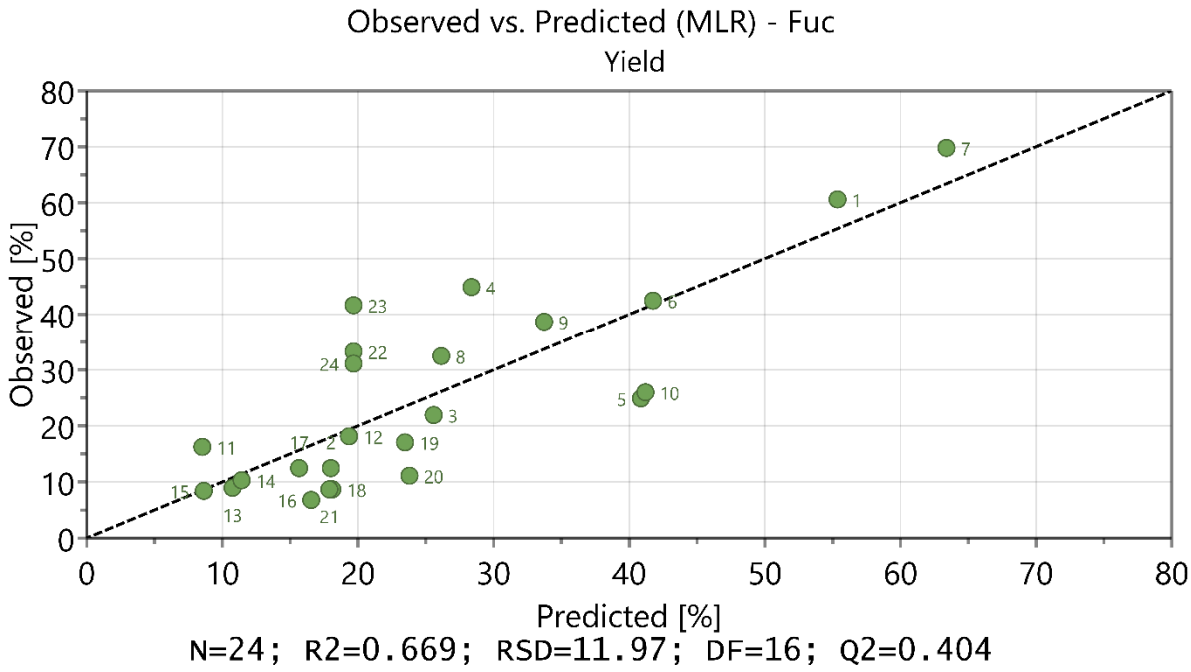

Figure 2.S16. Plot of observed values versus predicted values for yields of $FucNH_2$.

8.2 Supporting Information to Chapter 3: Glycopolymer Based LbL Multilayer Thin Films with Embedded Liposomes

Table 3.S1. GPC characterization of glycopolymers.

Sample	M_w [g/mol]	M_n [g/mol]	PDI
PGalNAcMAm	8.877×10^4	4.626×10^3	19.189
S-GalNAc	1.954×10^5	1.093×10^4	17.884
PLacMAm	2.760×10^5	6.937×10^3	39.787
S-Lac	1.990×10^5	9.534×10^3	20.874
Lac-PEI	4.828×10^6	1.996×10^4	241.873
Mal-PEI	2.437×10^3	1.105×10^3	2.205

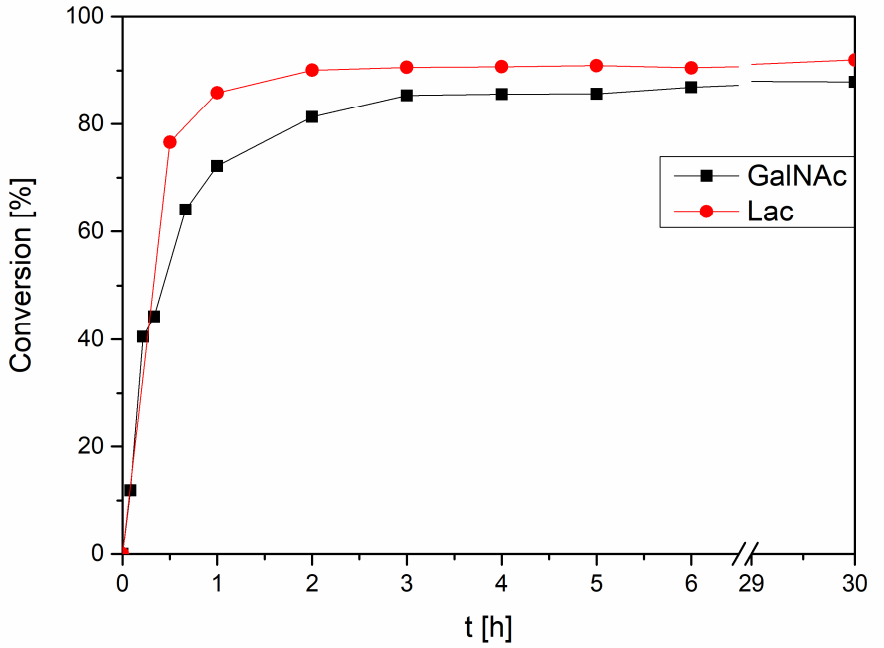

Figure 3.S1. Polymer conversion of the glycomonomers GalNAcMAm and LacMAm determined via ^{1}H NMR spectroscopy.

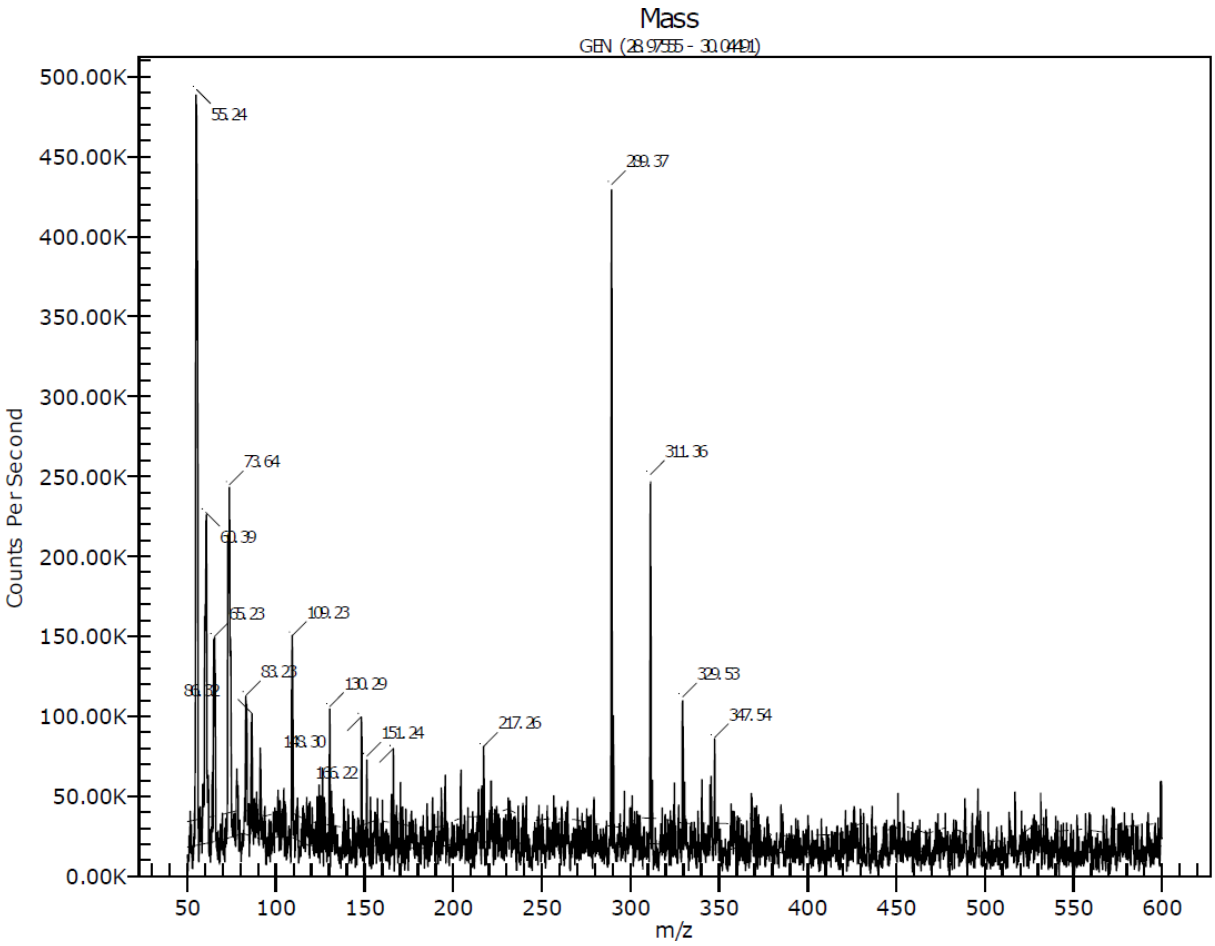

Figure 3.S2. ESI MS spectrum of GalNAcMAm.

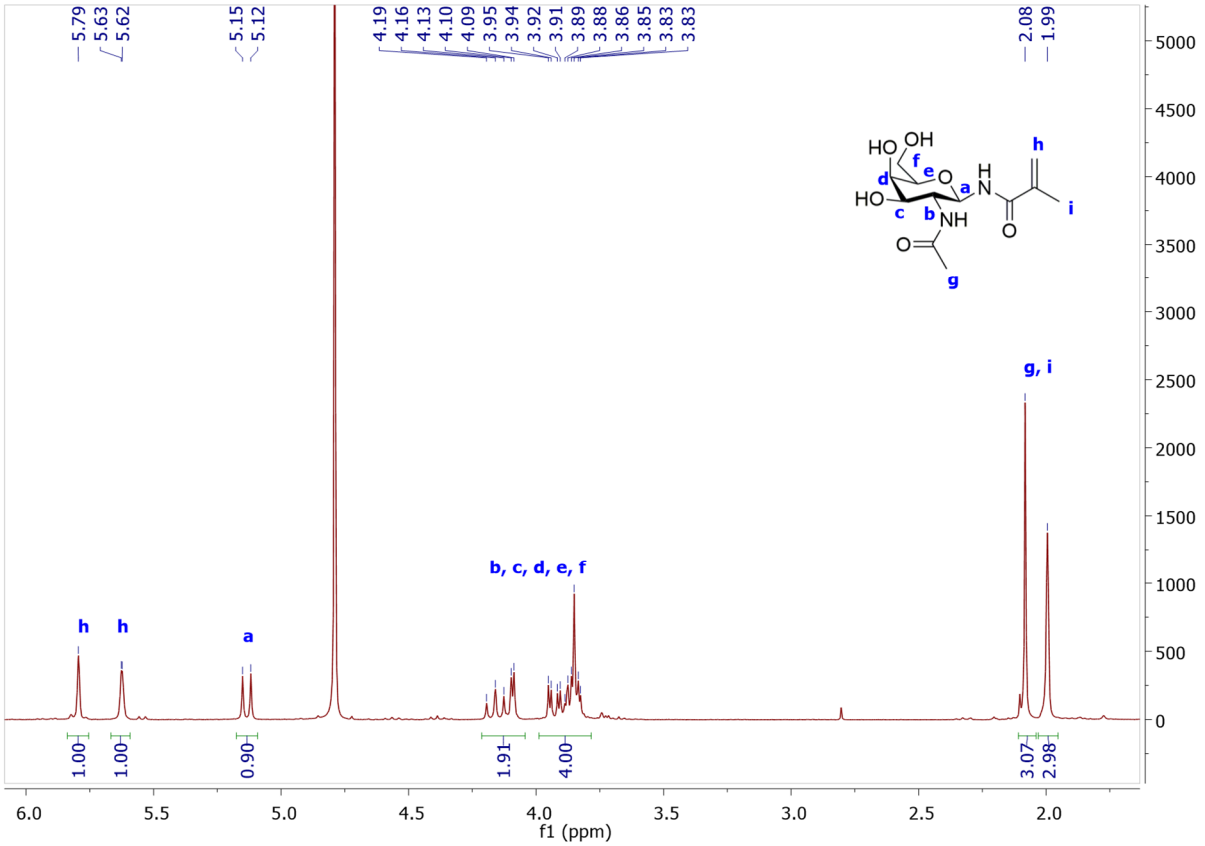

Figure 3.S3. ^{1}H NMR spectrum of GalNAcMAm.

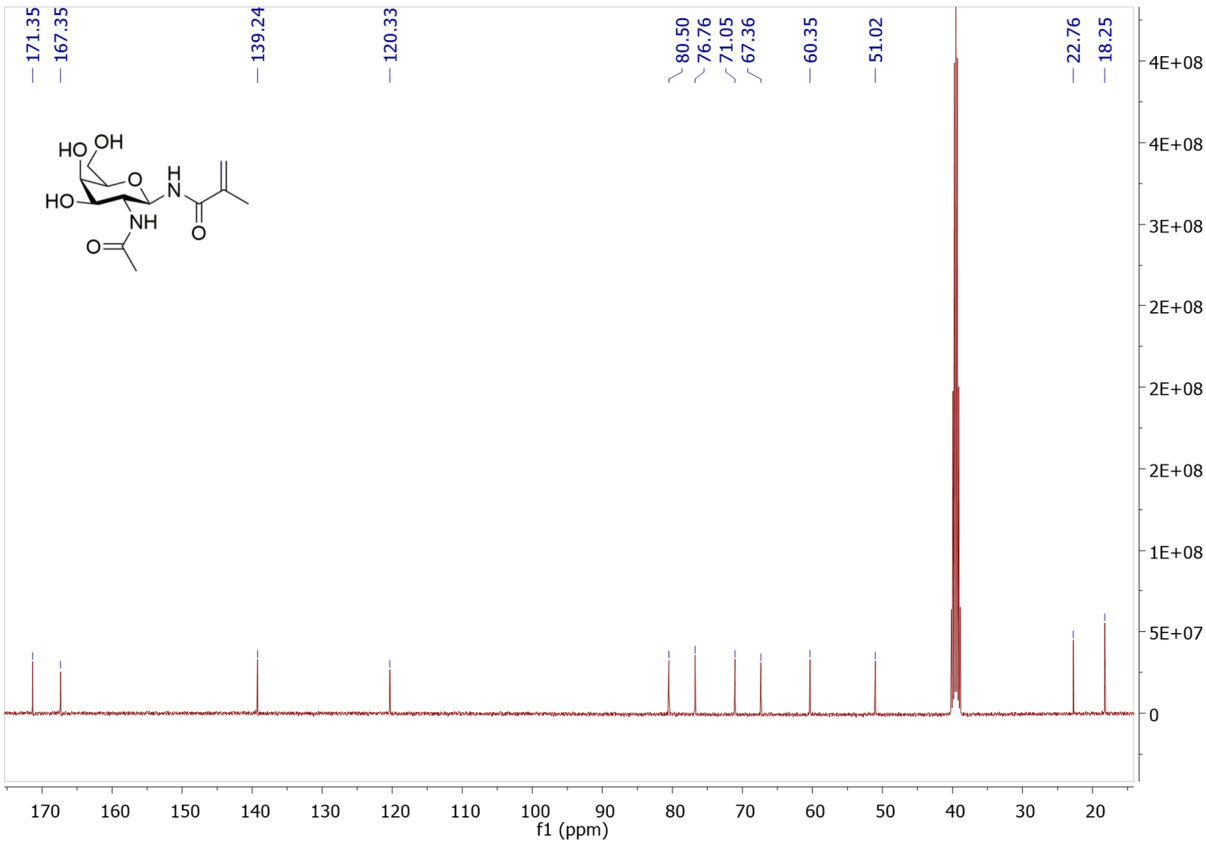

Figure 3.S4. ^{13}C NMR spectrum of GalNAcMAm.

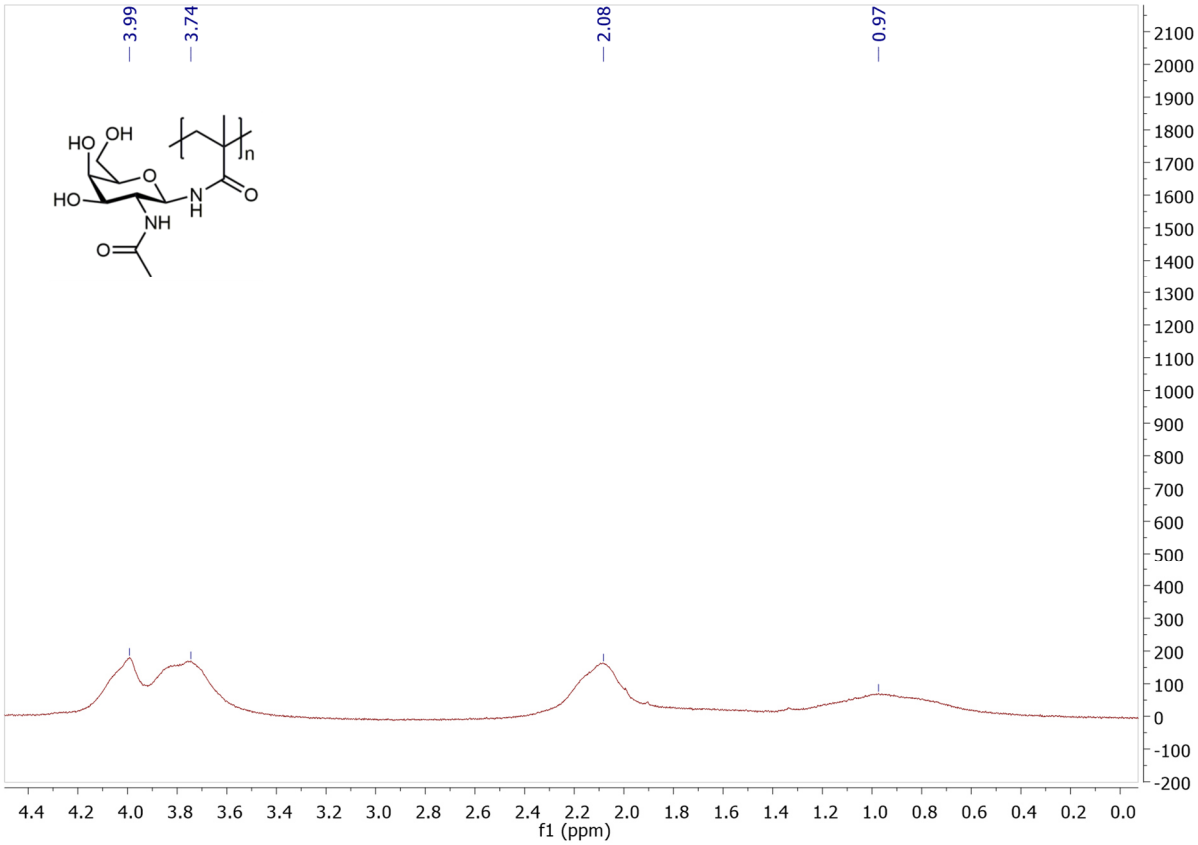

Figure 3.S5. ^{1}H NMR spectrum of PGalNAcMAm.

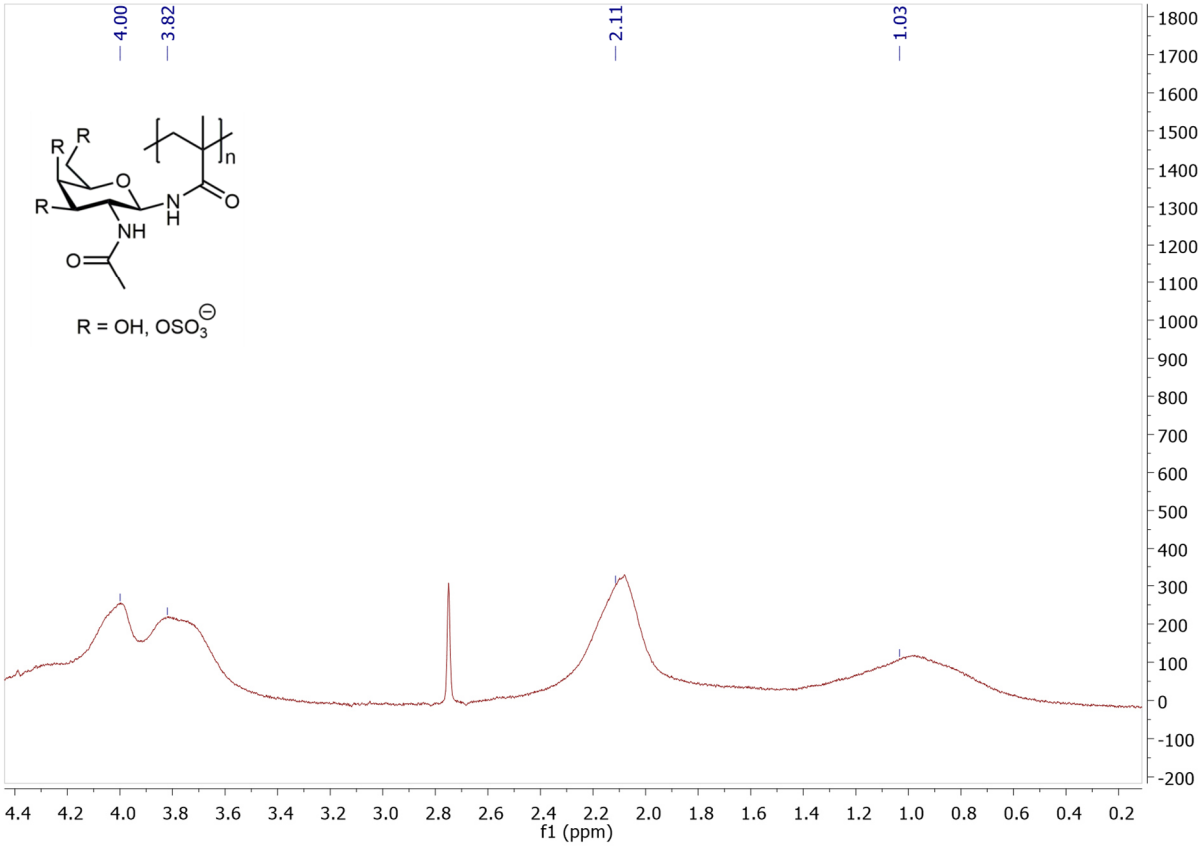

Figure 3.S6. ^{1}H NMR spectrum of S-GalNAc.

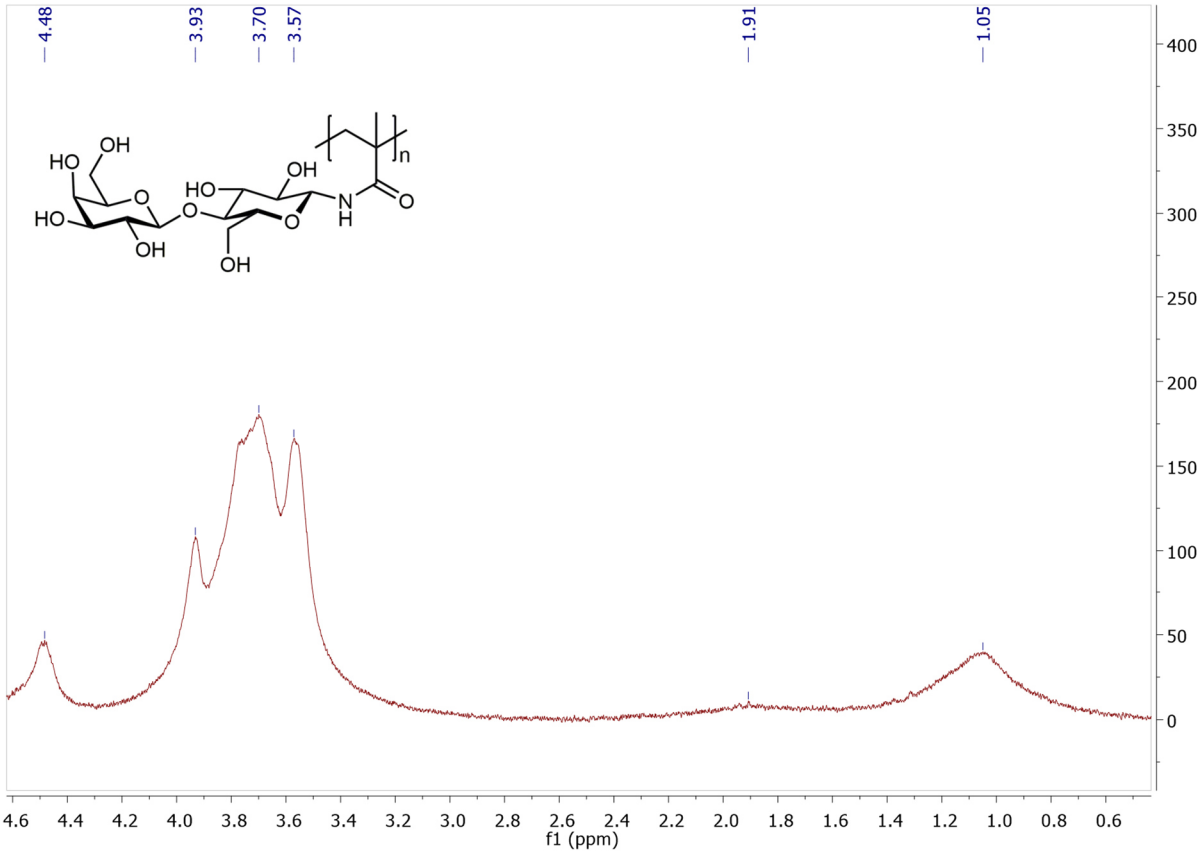

Figure 3.S7. ^{1}H NMR spectrum of PLacMAm.

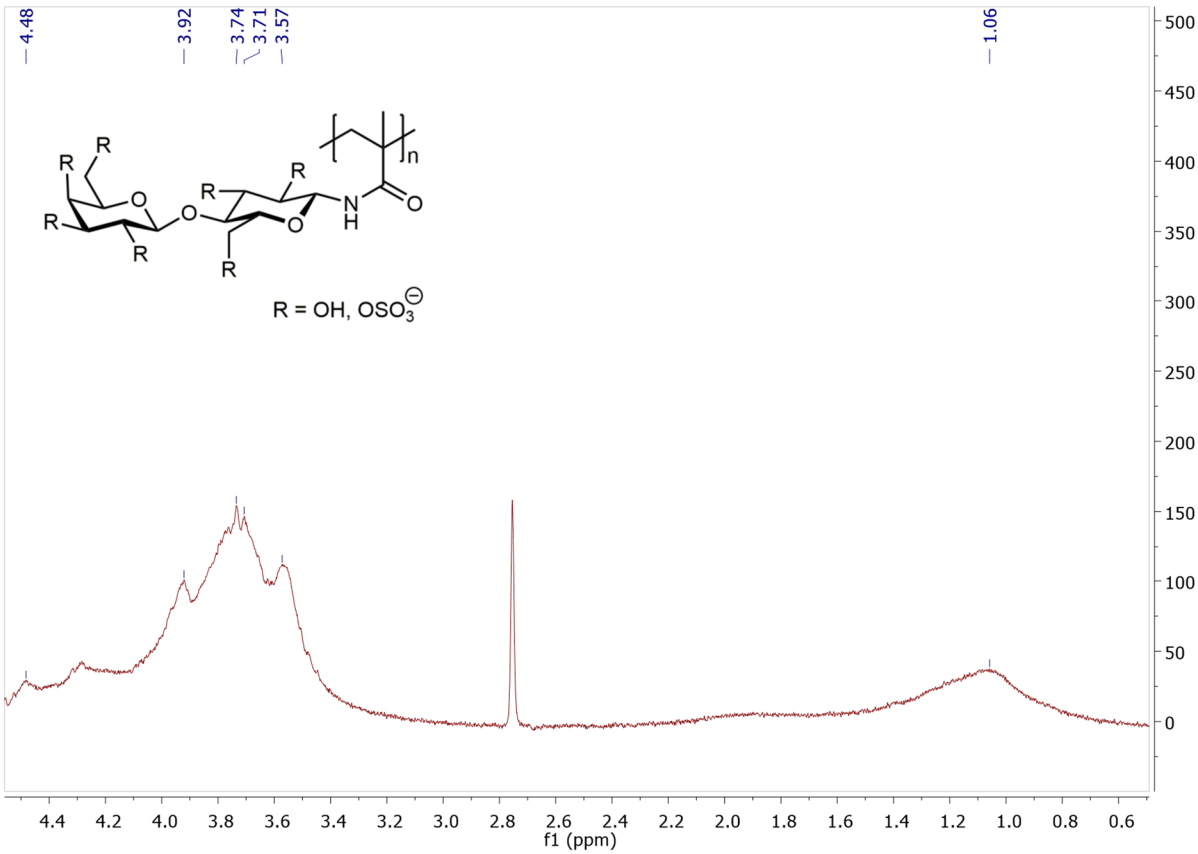

Figure 3.S8. ^{1}H NMR spectrum of S-Lac.

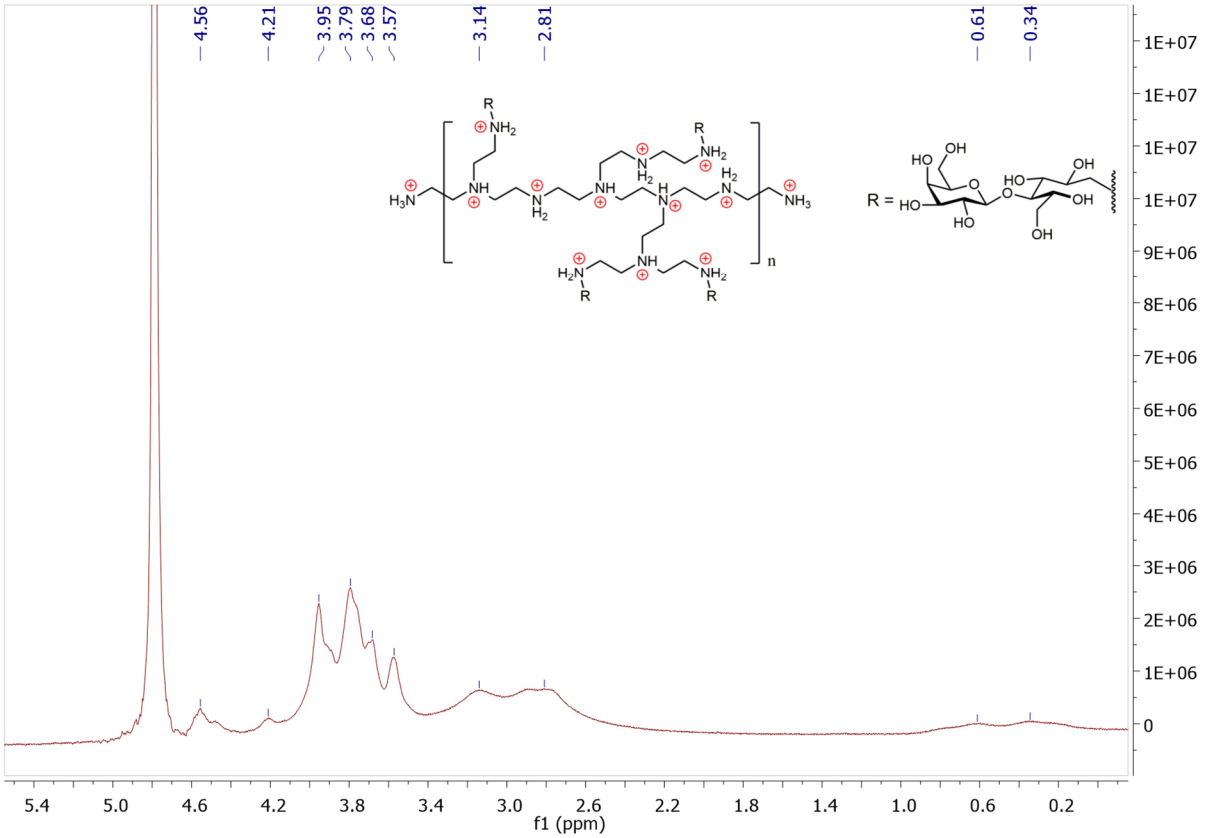

Figure 3.S9. ^{1}H NMR spectrum of Lac-PEI.

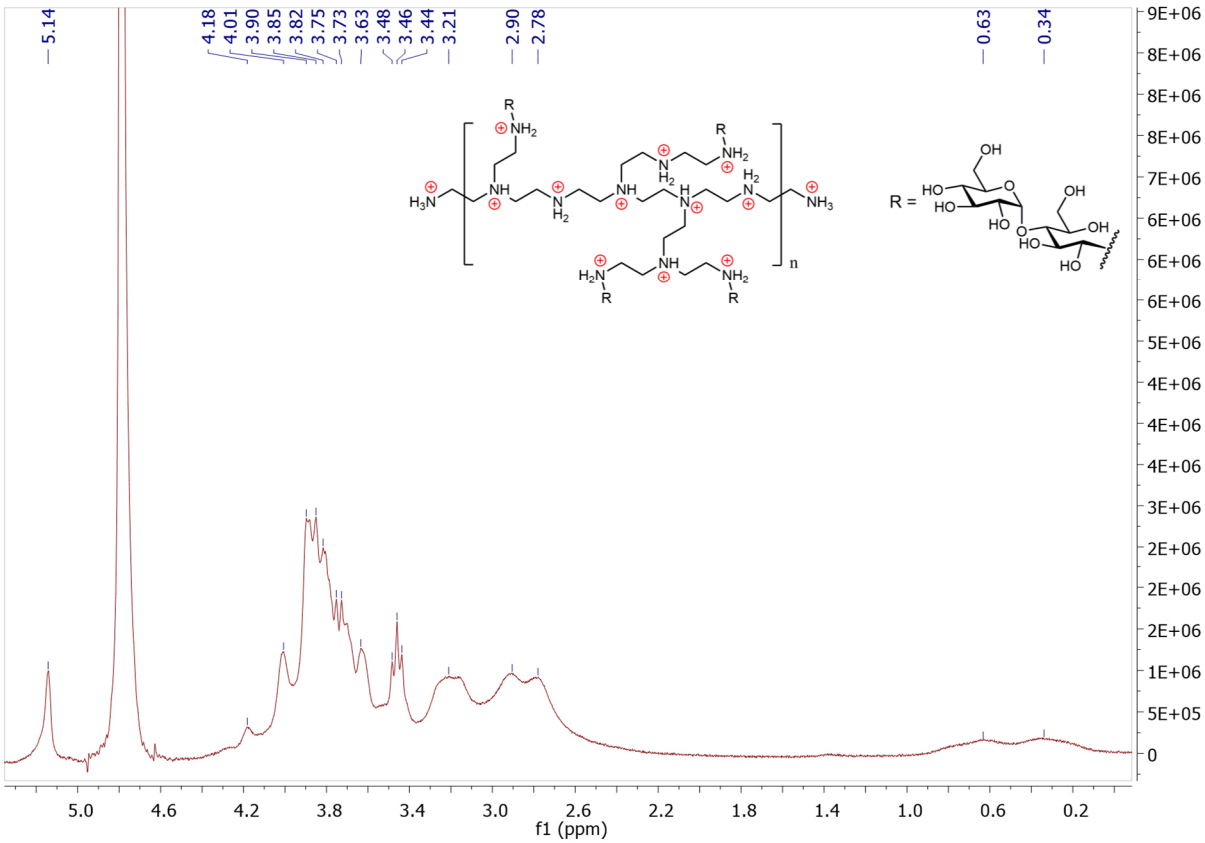

Figure 3.S10. ^{1}H NMR spectrum of Mal-PEI.

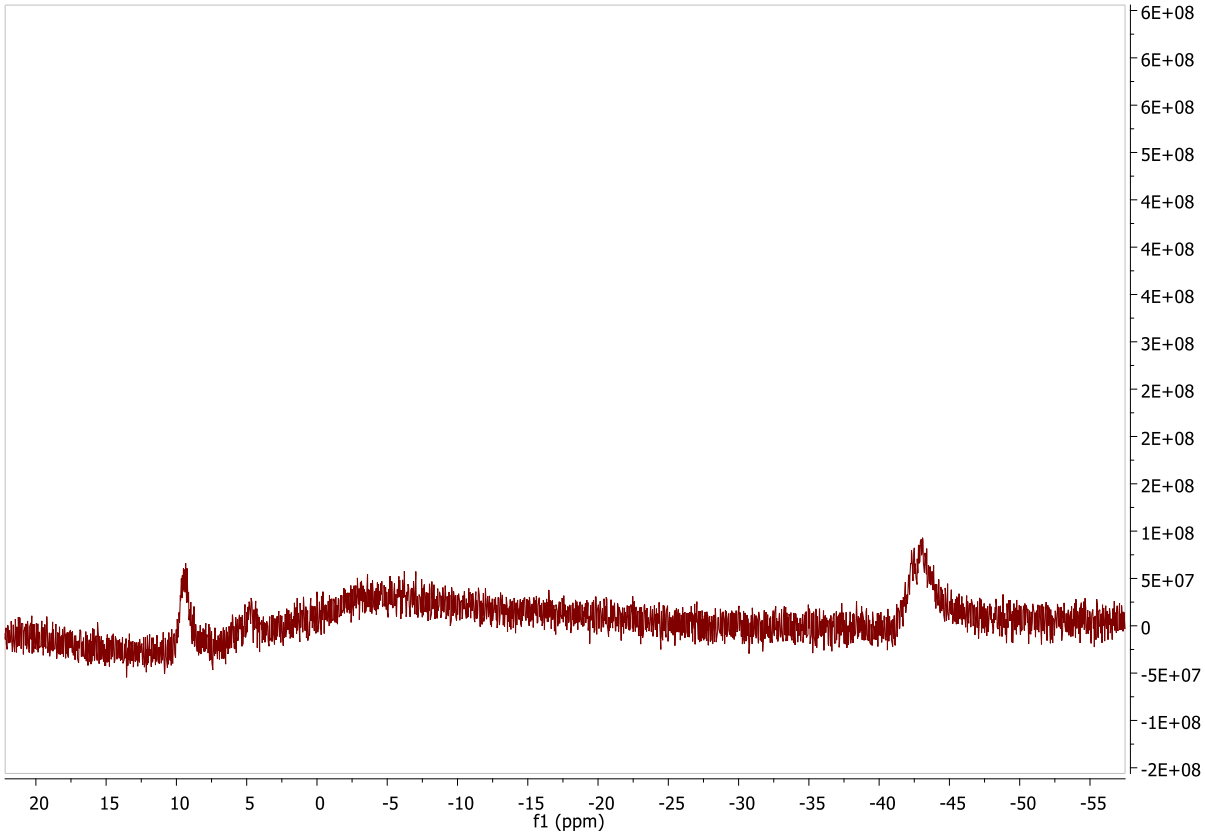

Figure 3.S11. ^{11}B NMR spectrum of Lac-PEI.

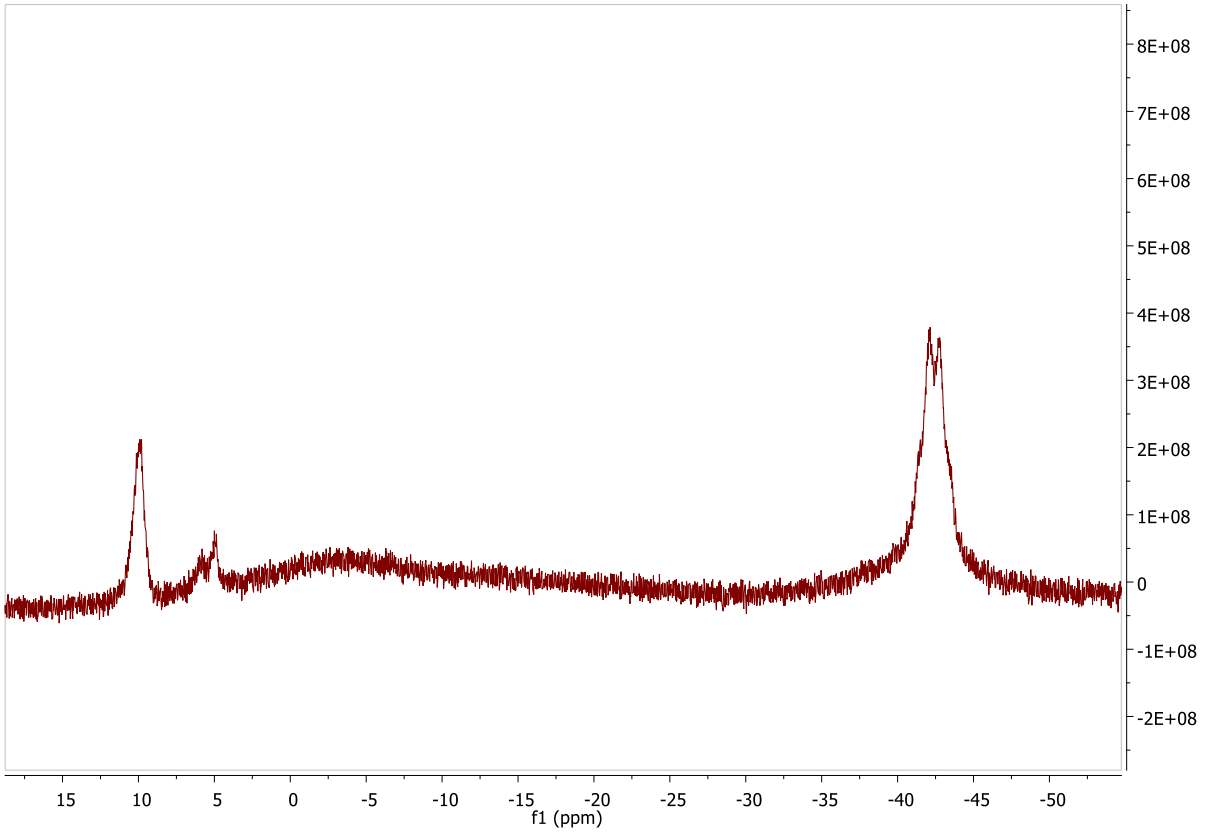

Figure 3.S12. ^{11}B NMR spectrum of Mal-PEI.

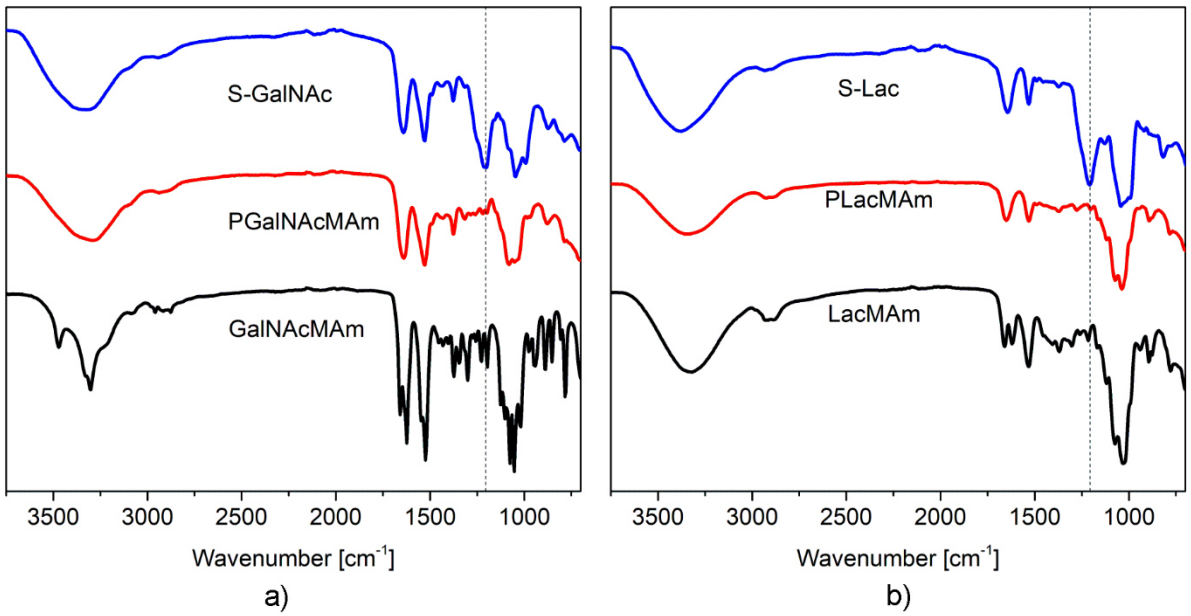

Figure 3.S13. Comparison of IR spectra of glycomonomers, glycopolymers and sulfated glycopolymers based on a) GalNAc and b) Lac.

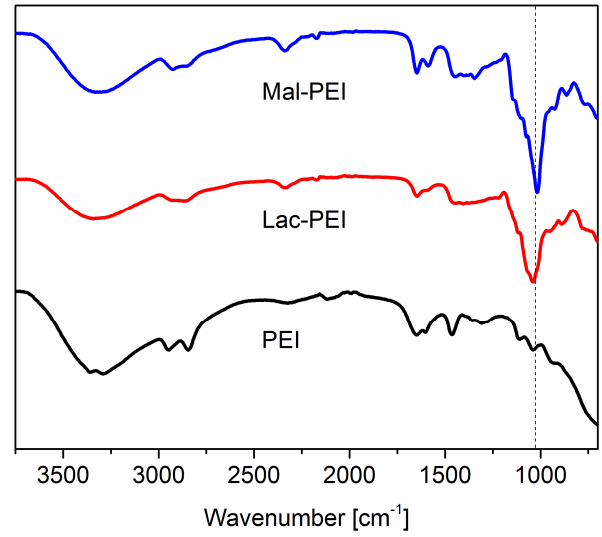

Figure 3.S14. IR spectrum of PEI and lactose and maltose functionalized PEI.

8.3 Supporting Information to Chapter 4: Functional Glyco-Nanogels for Multivalent Interaction with Lectins

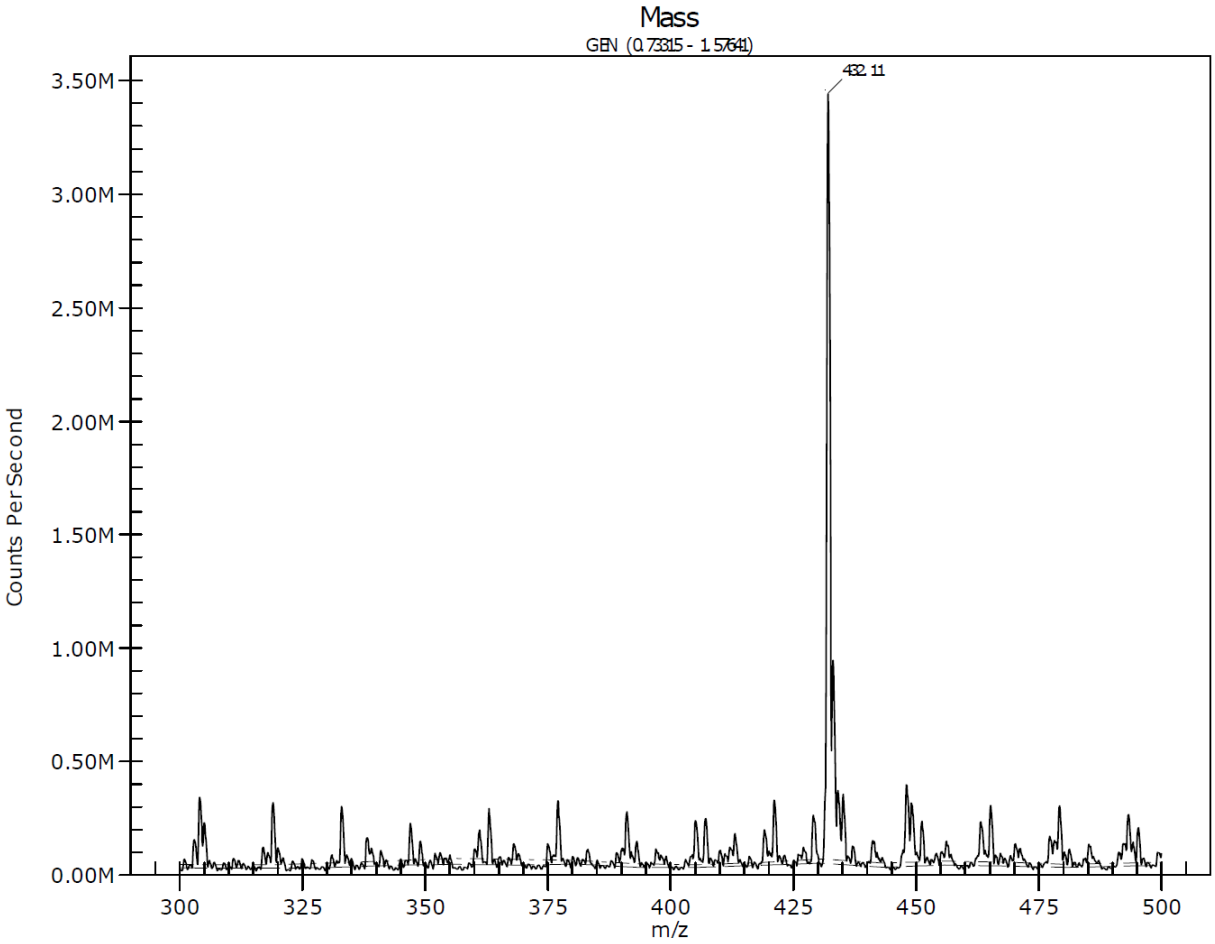

Figure 4.S1. ESI MS spectrum of LacMAm.

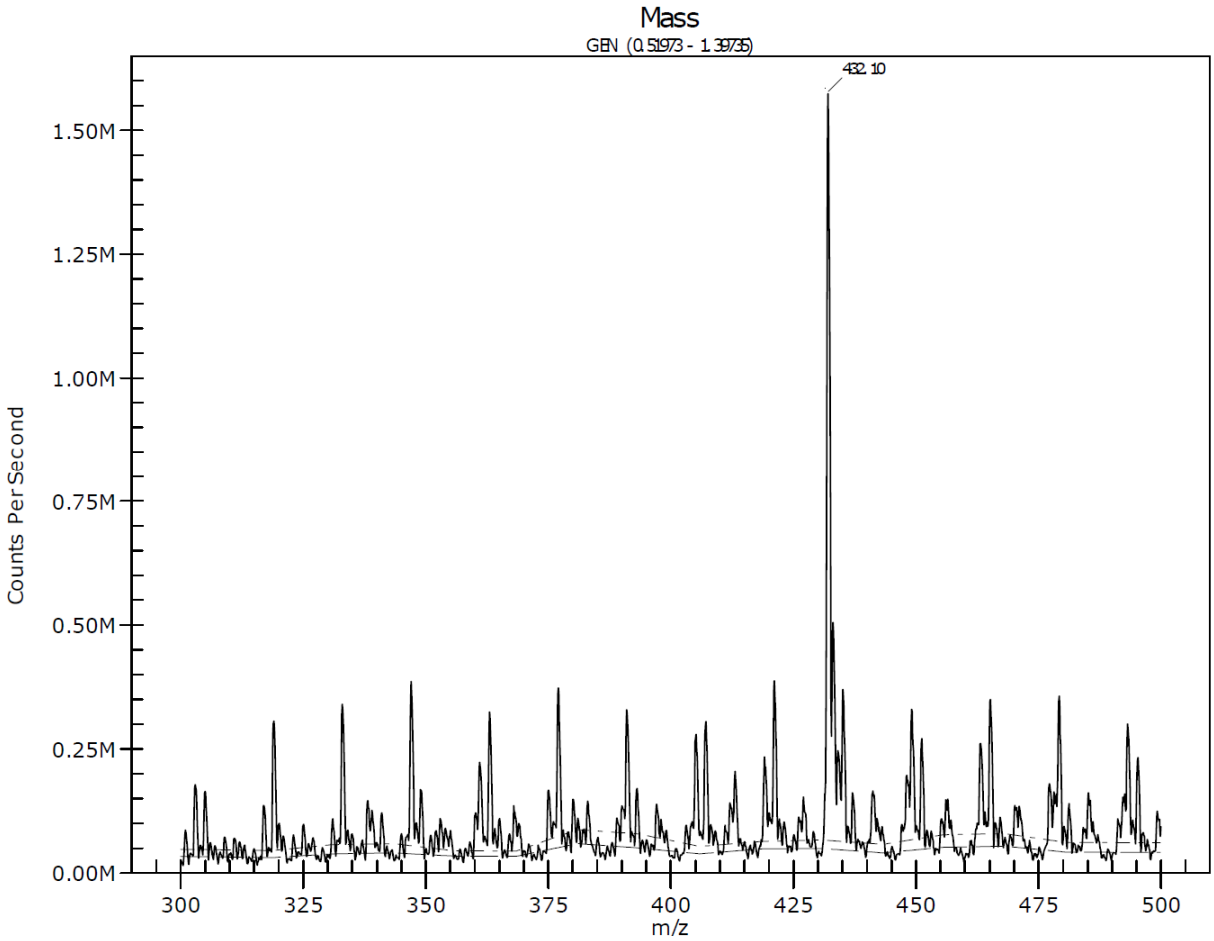

Figure 4.S2. ESI MS spectrum of MelMAm.

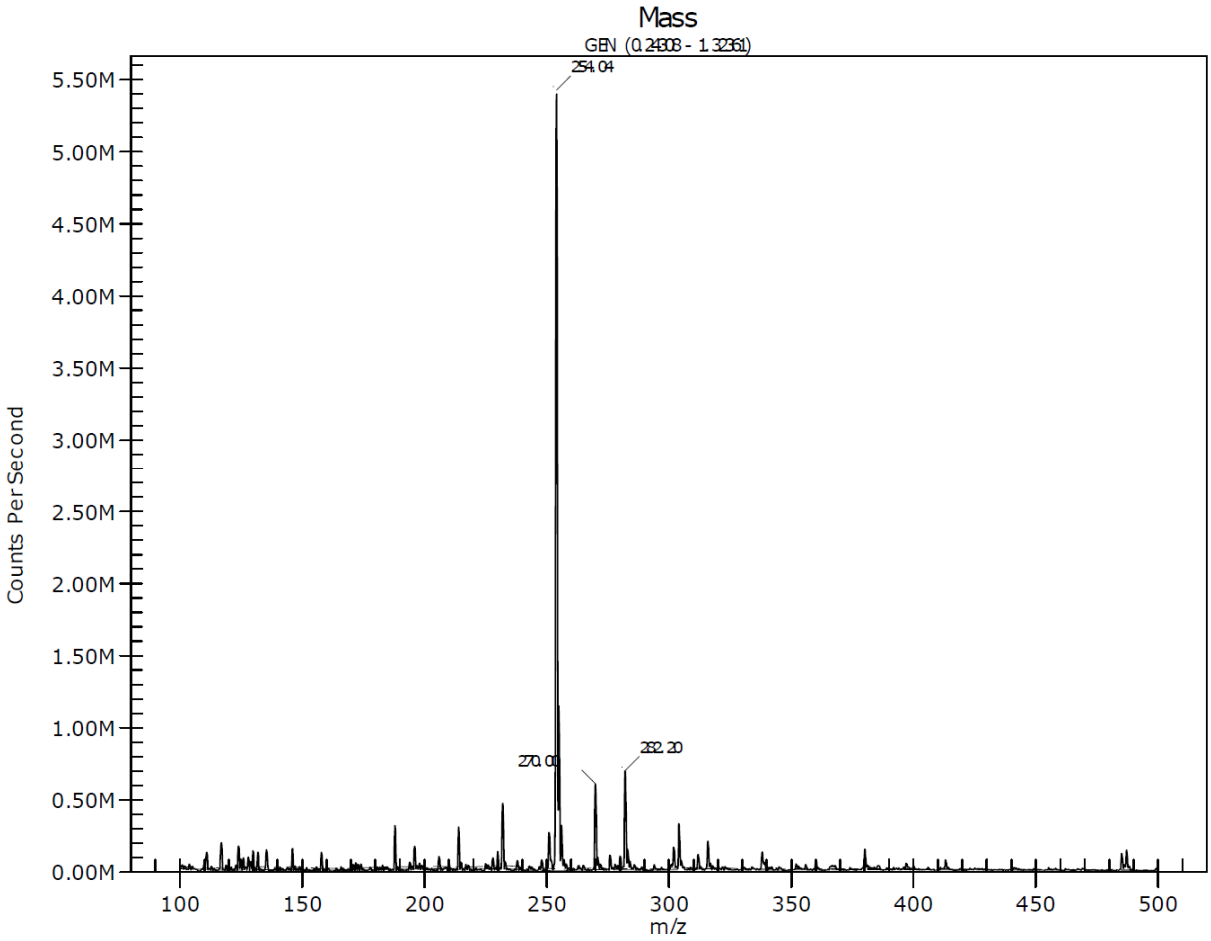

Figure 4.S3. ESI MS spectrum of FucMAm.

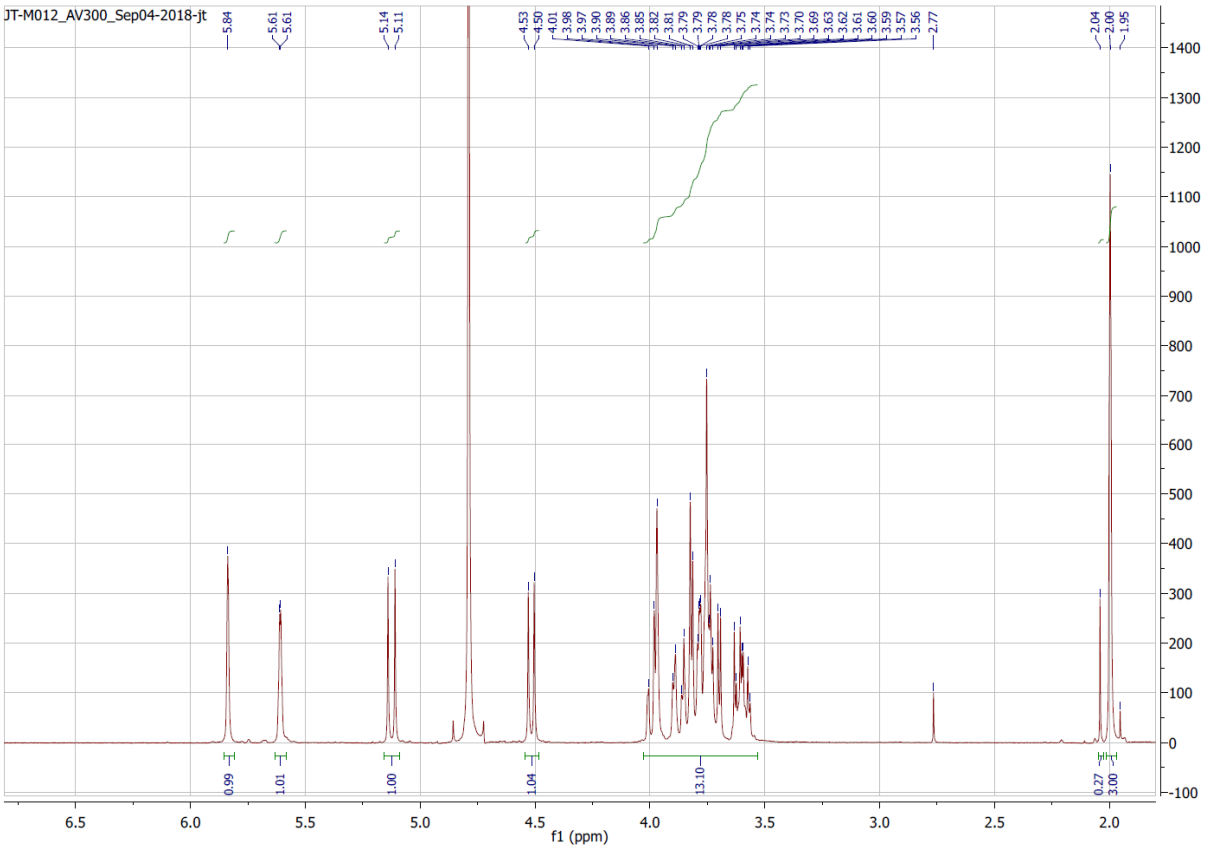

Figure 4.S4. ^{1}H NMR spectrum of LacMAm.

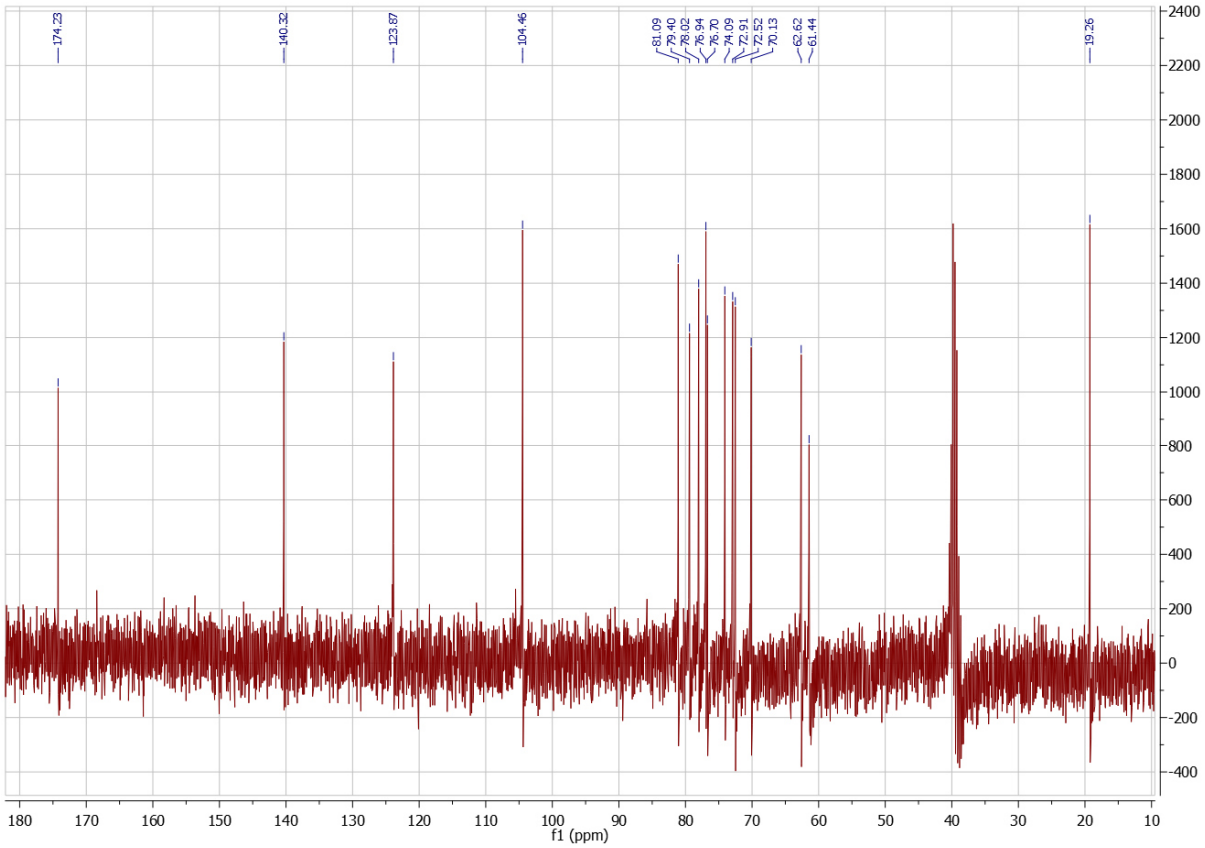

Figure 4.S5. ^{13}C NMR spectrum of LacMAm.

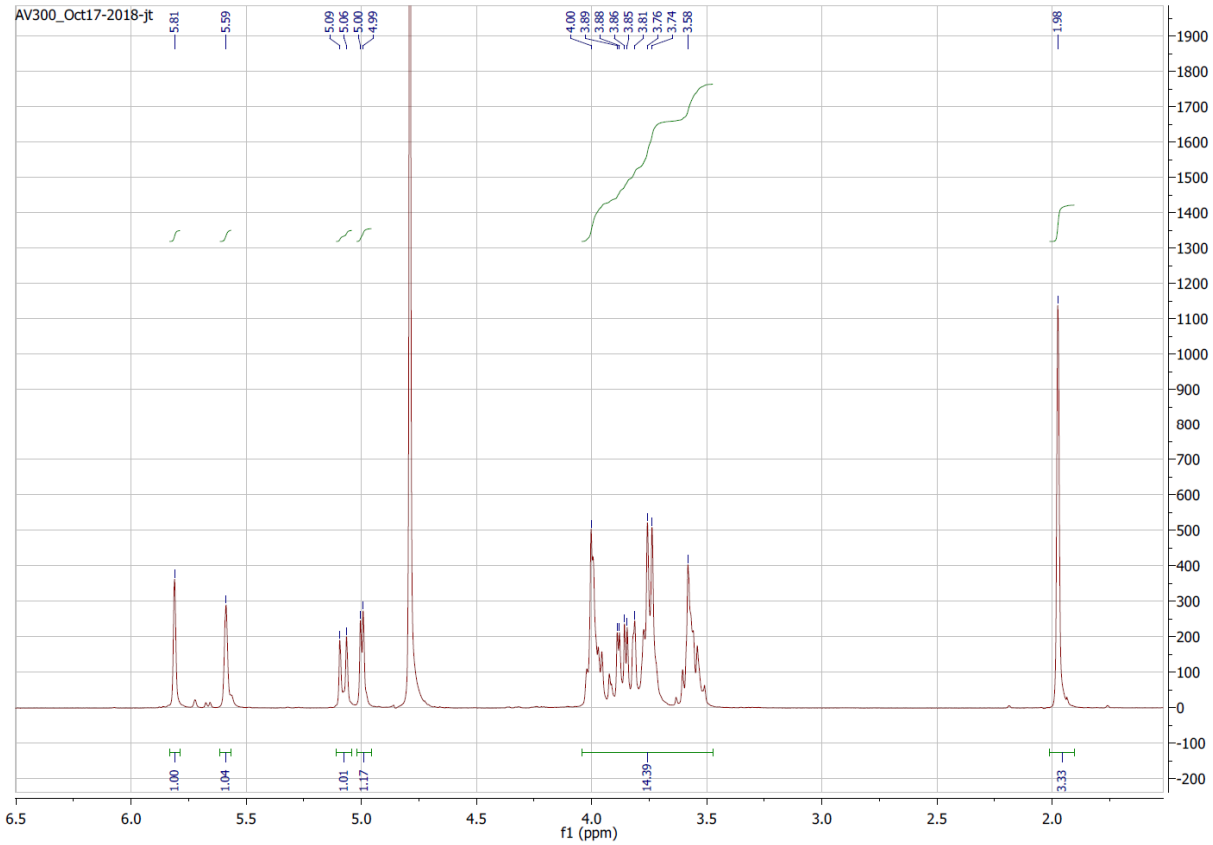

Figure 4.S6. ^{1}H NMR spectrum of MelMAm.

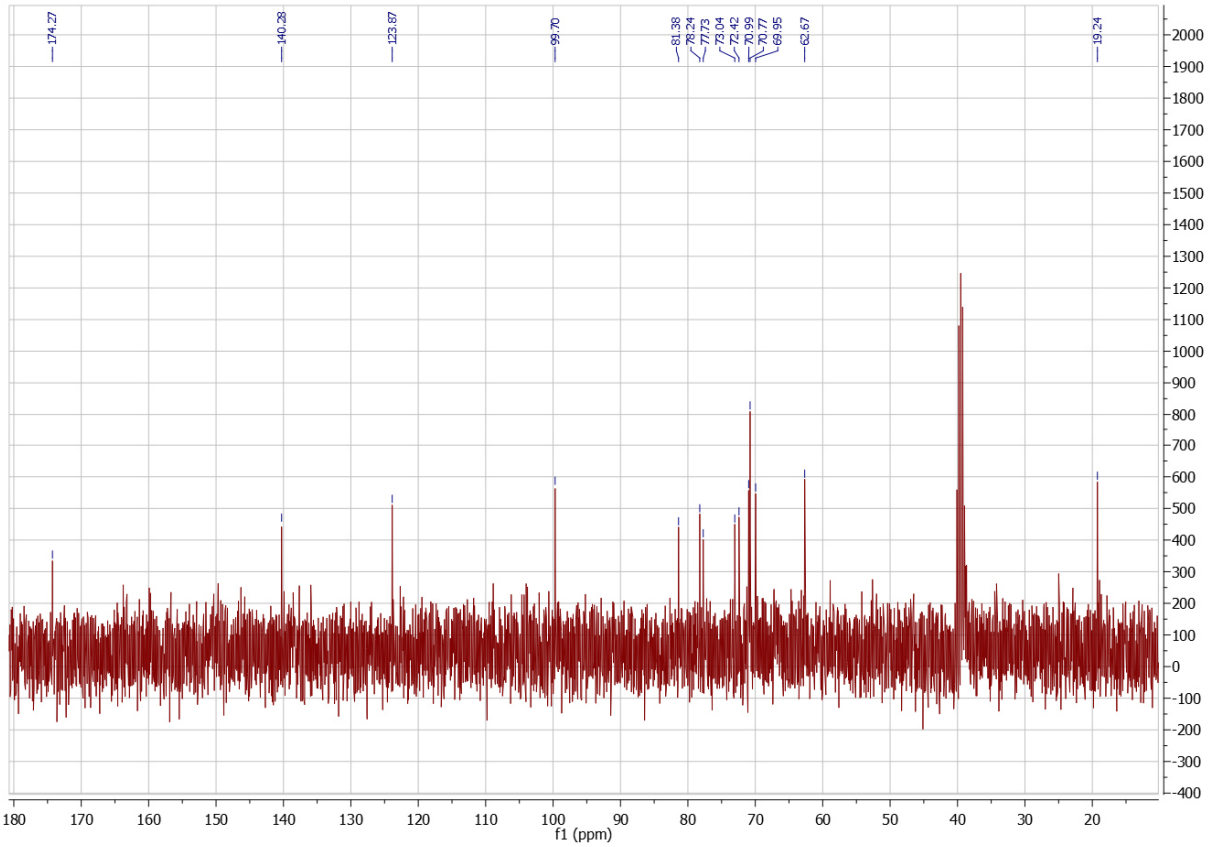

Figure 4.S7. ^{13}C NMR spectrum of MelMAm.

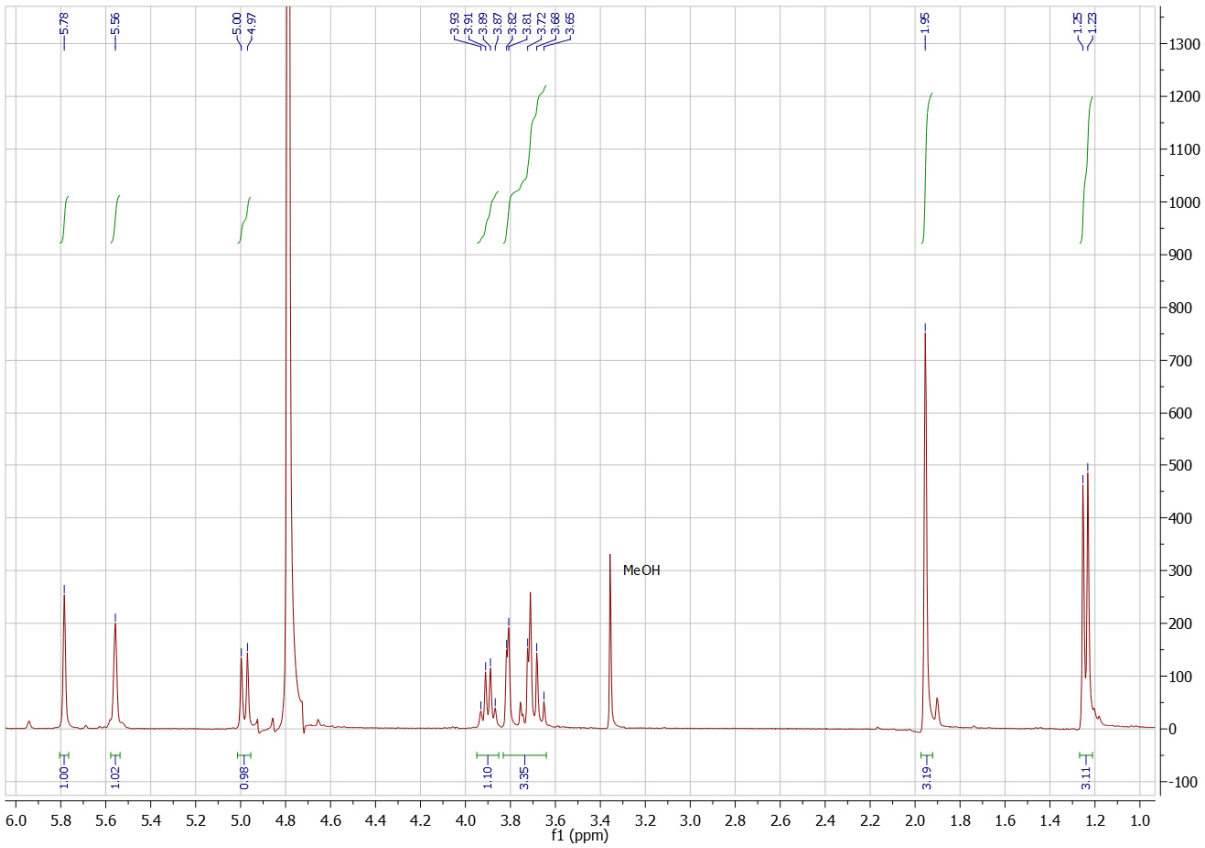

Figure 4.S8. ^{1}H NMR spectrum of FucMAm.

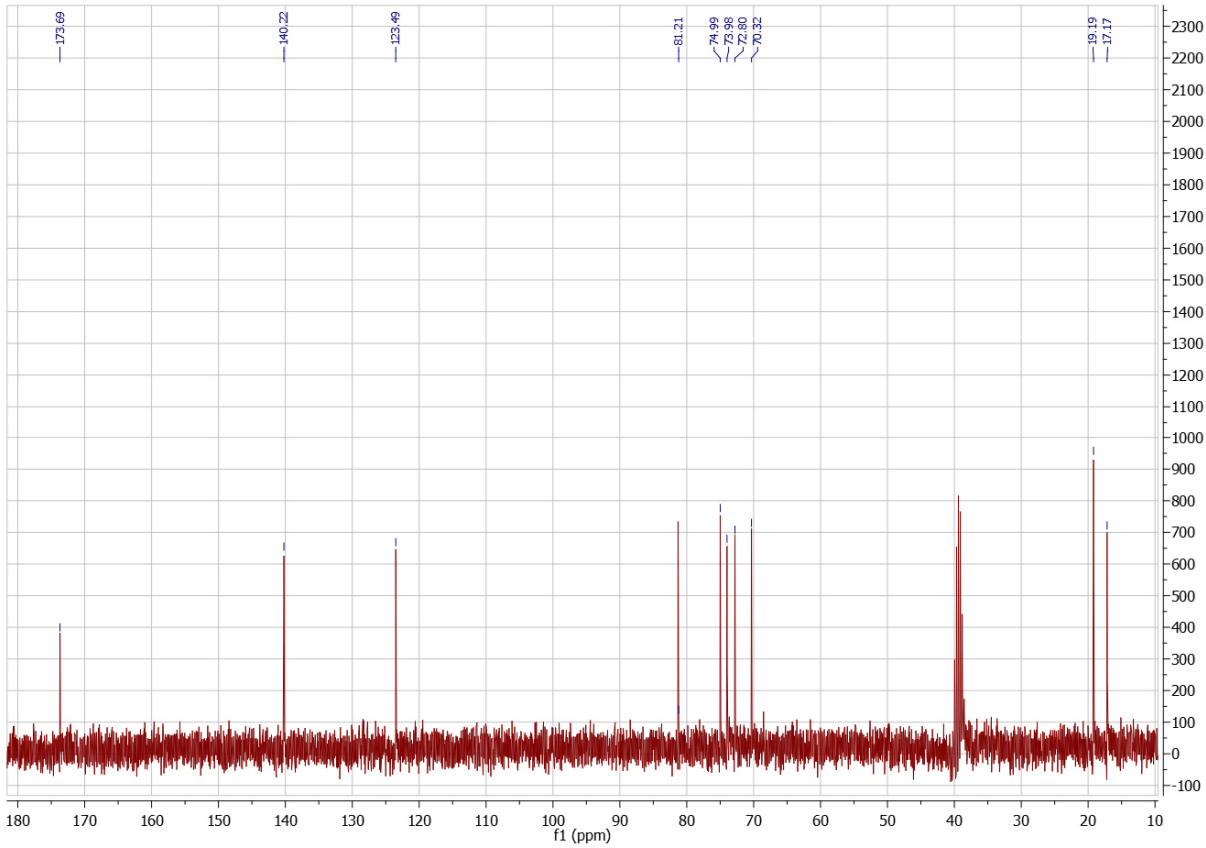

Figure 4.S9. ^{13}C NMR spectrum of FucMAm.

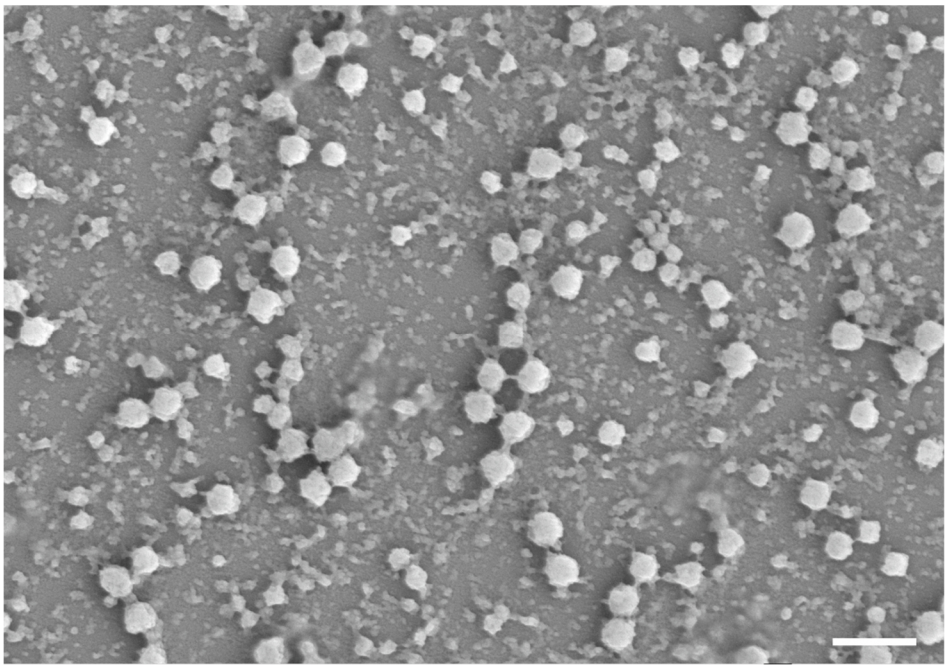

Figure 4.S10. SEM image of MG-4. Scale bar: 1 µm.

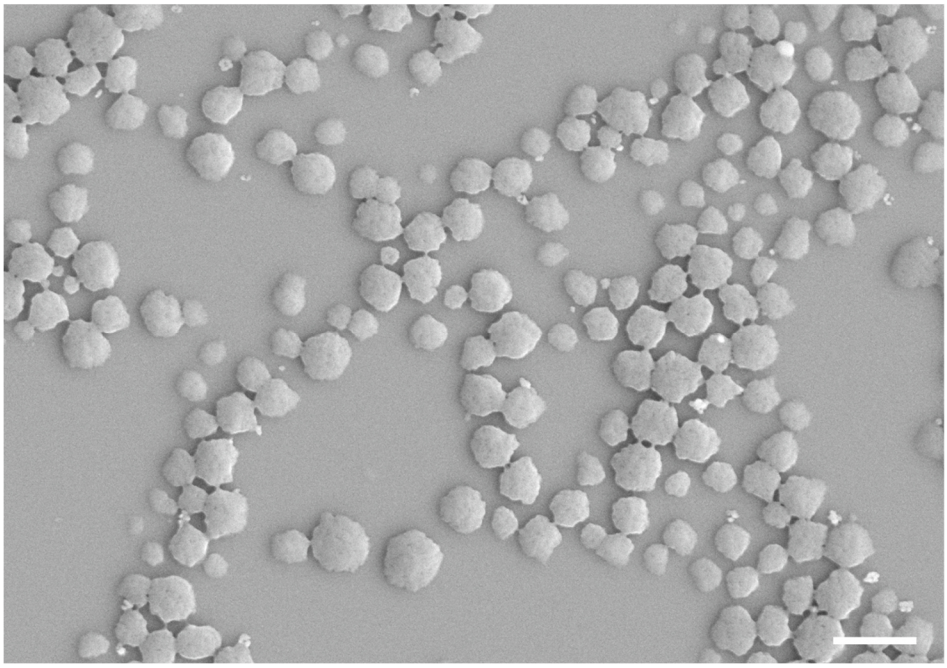

Figure 4.S11. SEM image of MG-5. Scale bar: 1 µm.

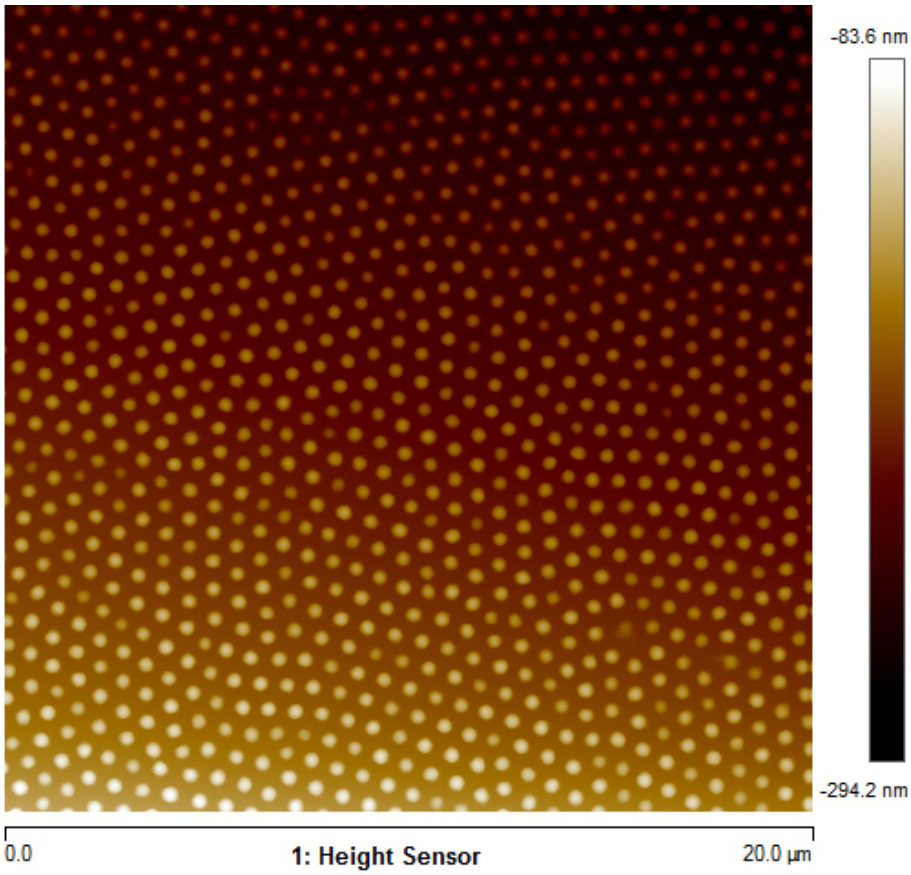

Figure 4.S12. AFM image of G-1.

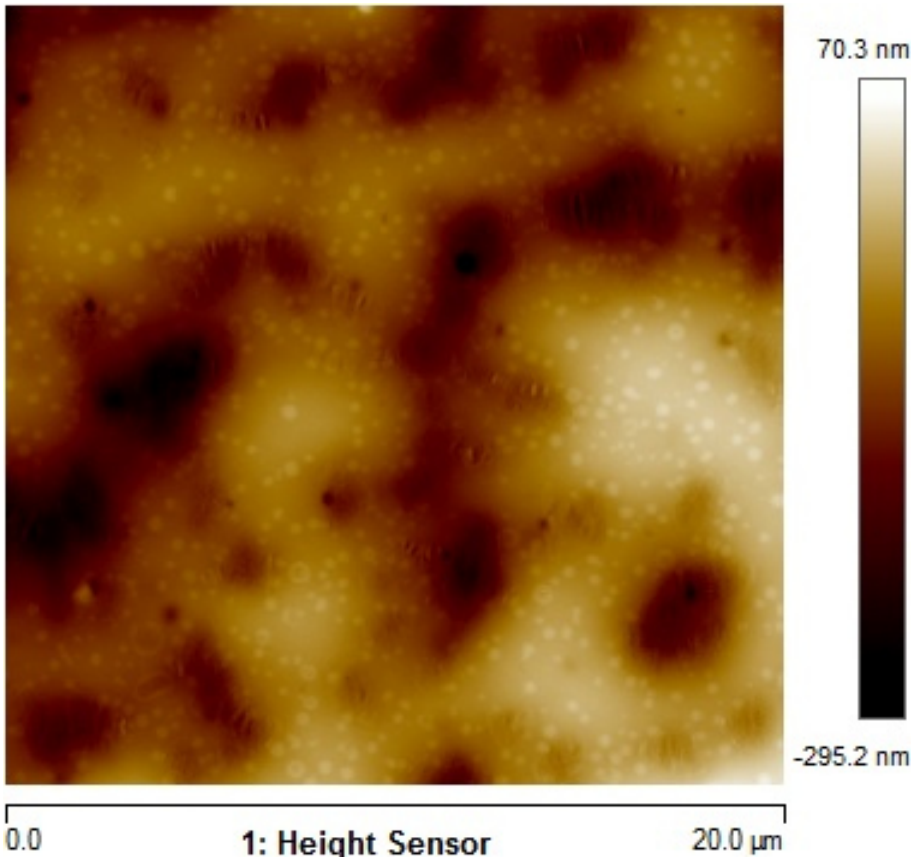

Figure 4.S13. AFM image of MG-0.

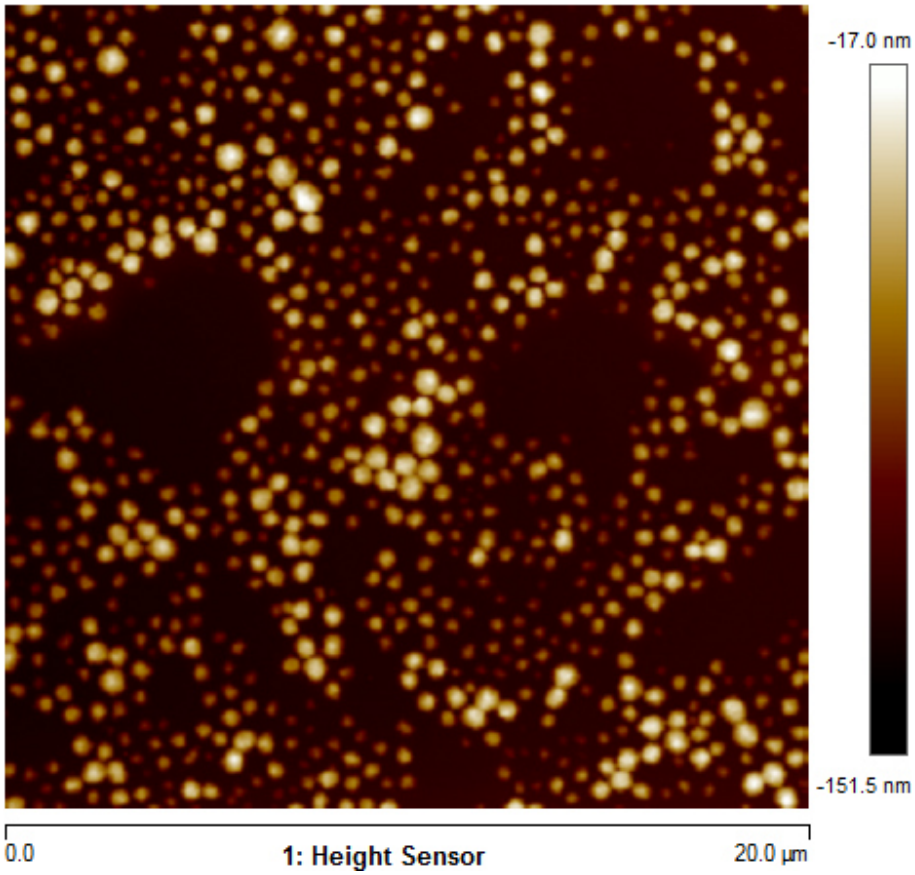

Figure 4.S14. AFM image of MG-1.

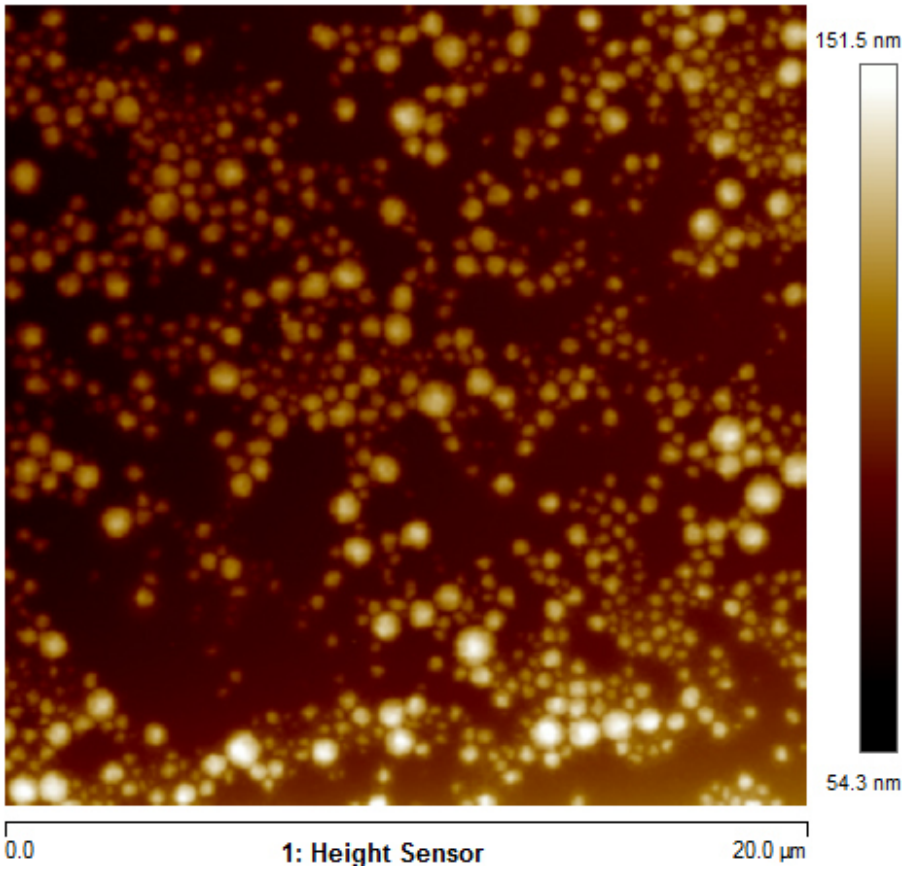

Figure 4.S15. AFM image of MG-2.

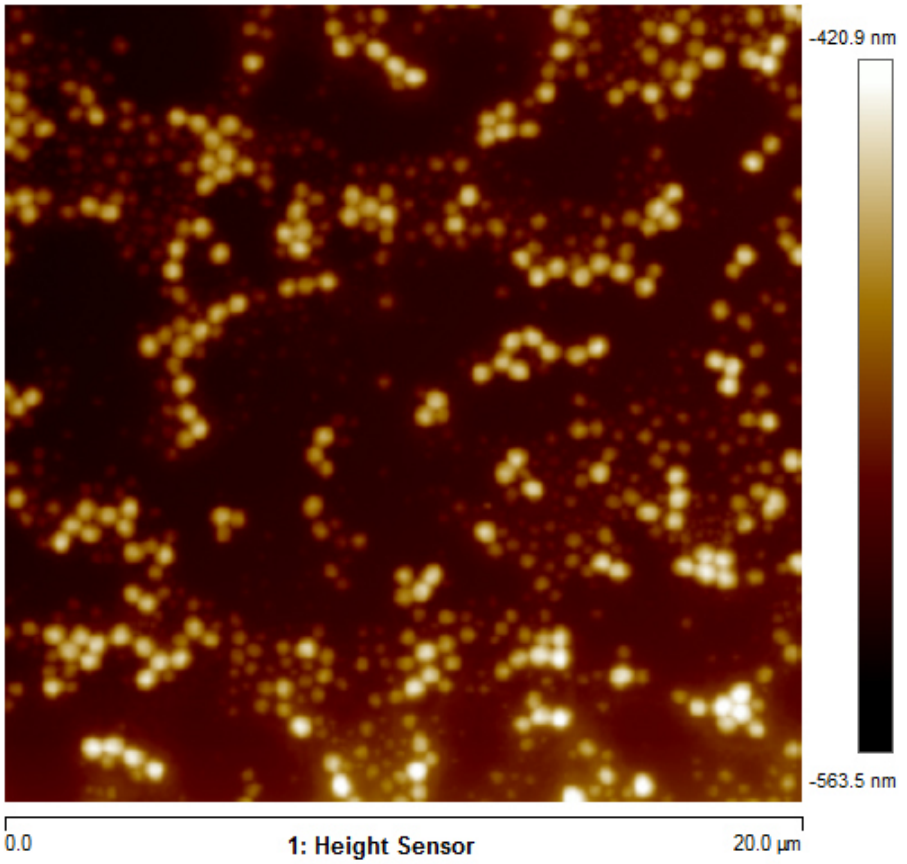

Figure 4.S16. AFM image of MG-4.

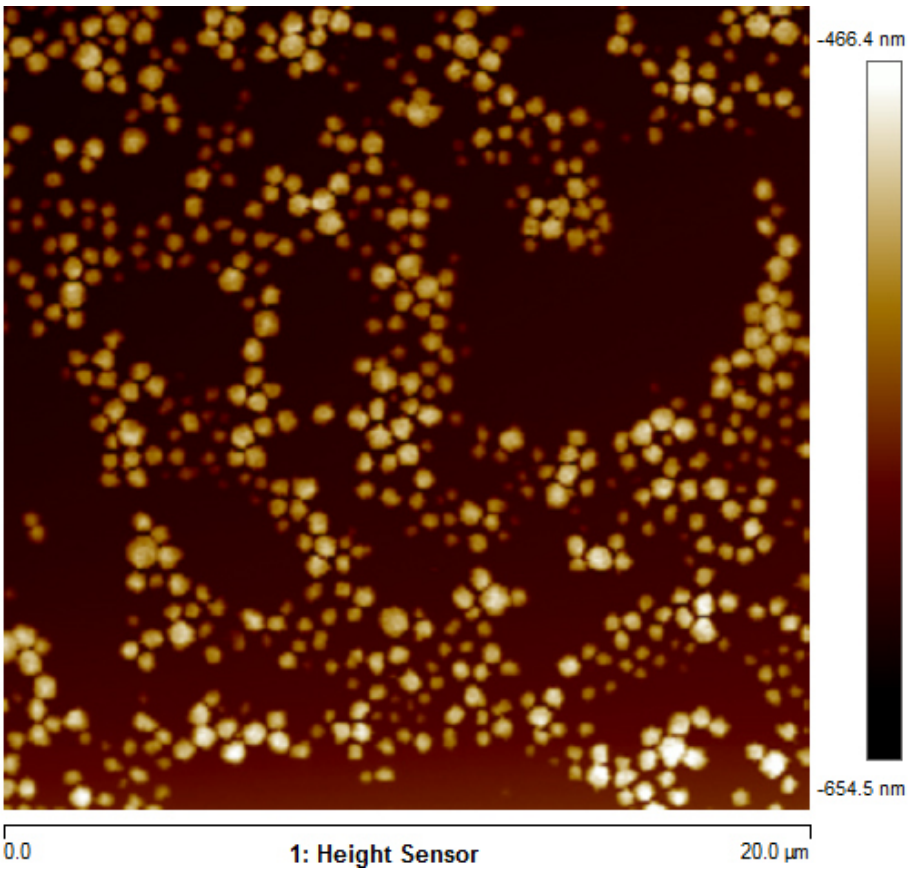

Figure 4.S17. AFM image of MG-5.

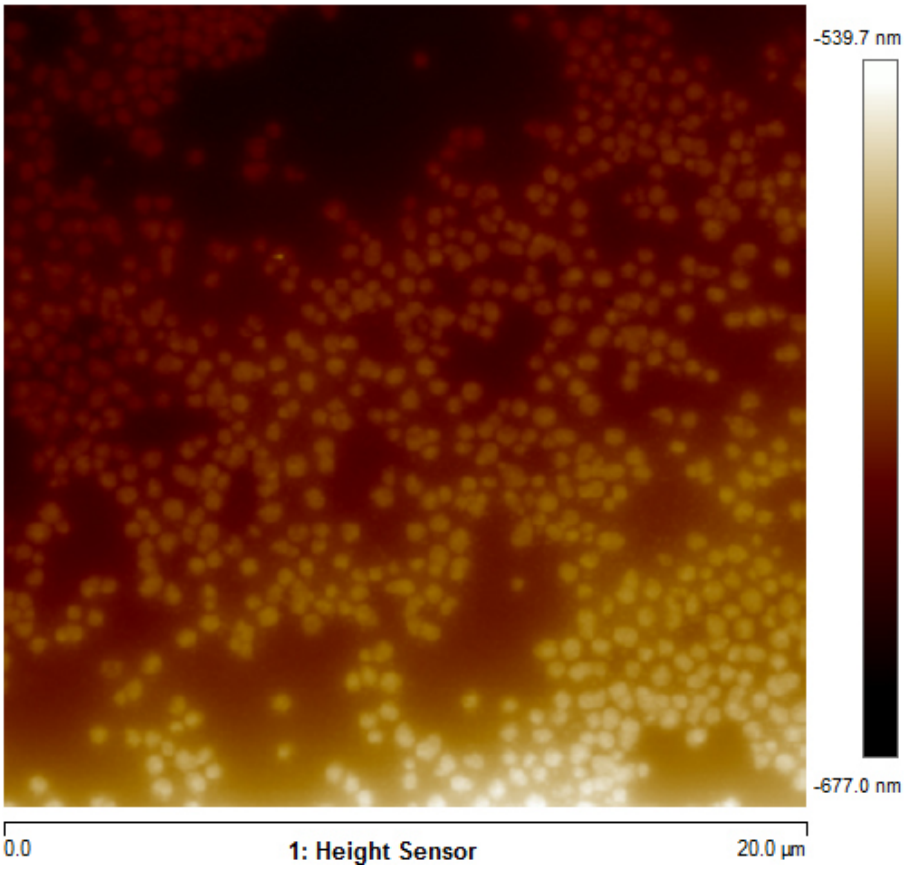

Figure 4.S18. AFM image of FG-1.

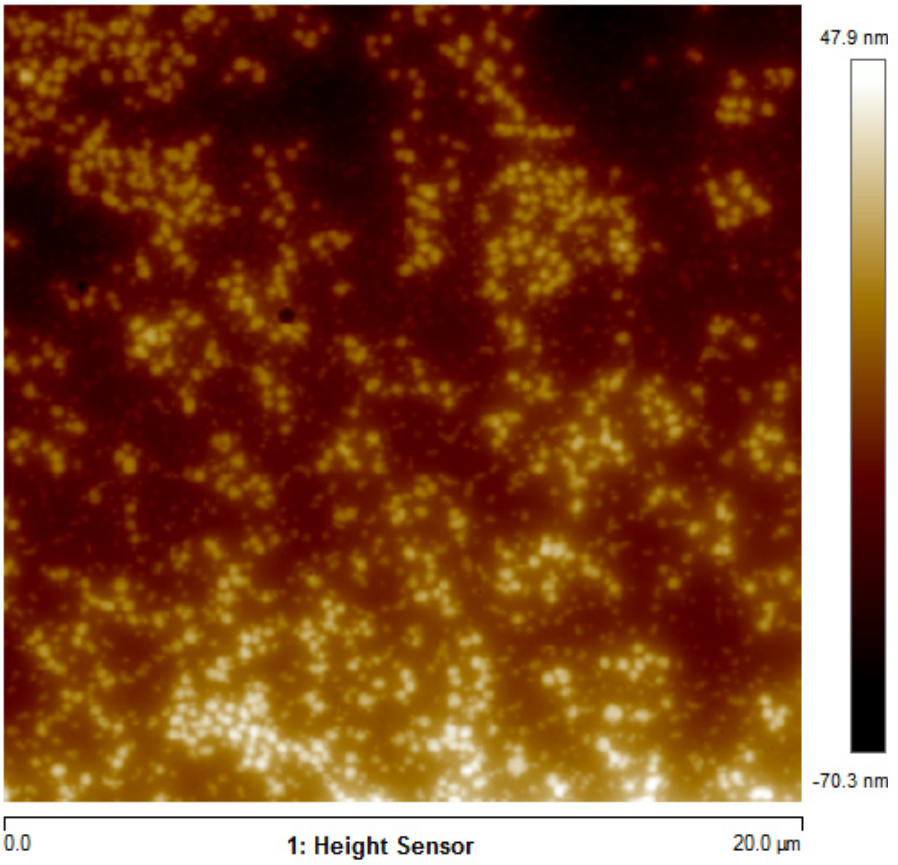

Figure 4.S19. AFM image of FG-2.

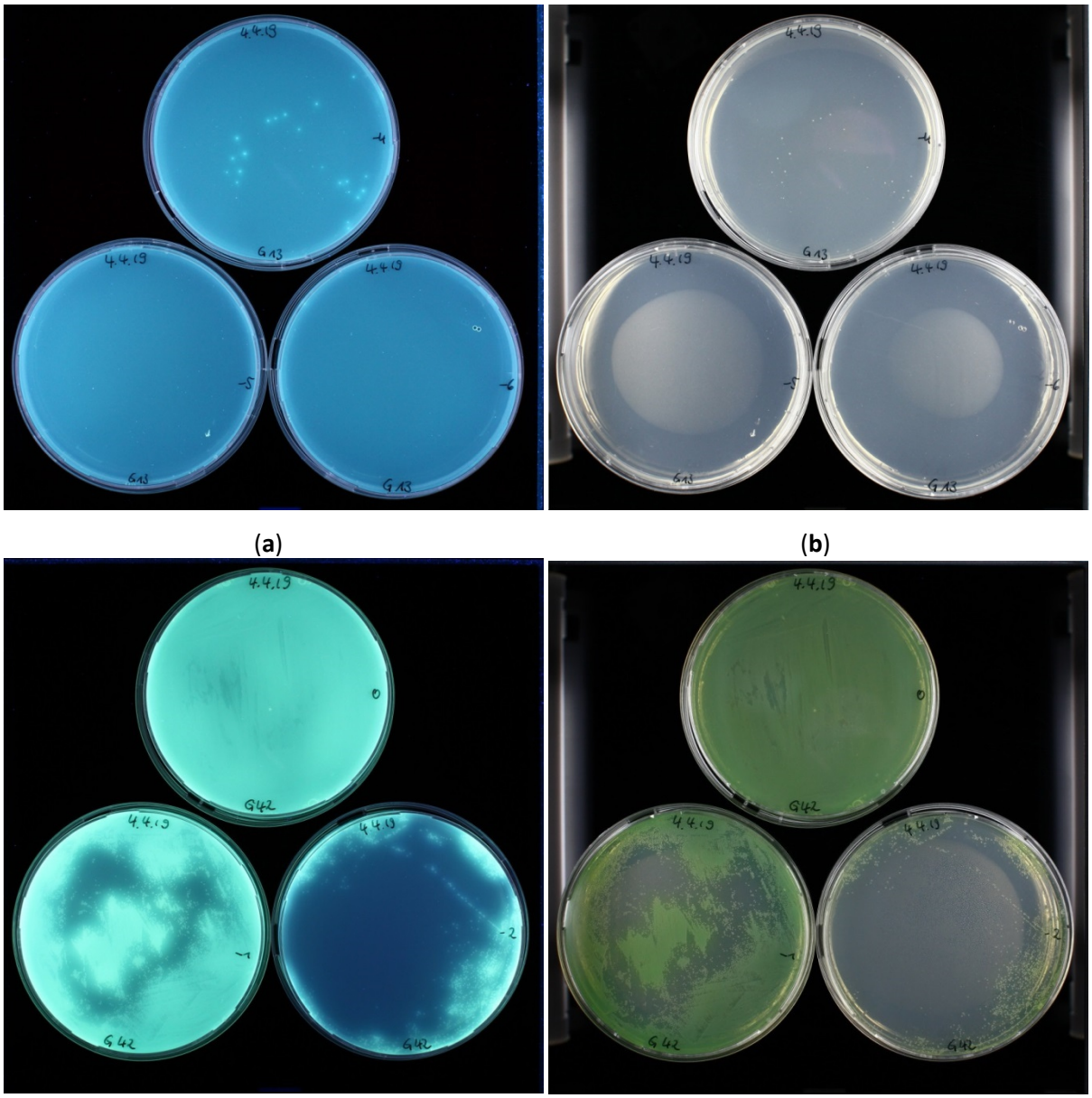

(**a**) (**b**)

(**c**) (**d**)

Figure 4.S20. Cetrimid Agar plates of PA incubated with MG-1 (**a** and **b**) FG-1 (**c** and **d**). (**a**) and (**c**) fluorescence image, (**b**) and (**d**) white light image. FG-1 inhibits pyoverdine, but is not acting antimicrobial. Less colonies are found with MG-1 due to higher dilution. 10^{-4} to 10^{-6} for MG-1 and undiluted to 10^{-2} for FG-1.

8.4 Additional Appendix to Doctoral Thesis

8.4.1 ^{1}H NMR Spectra

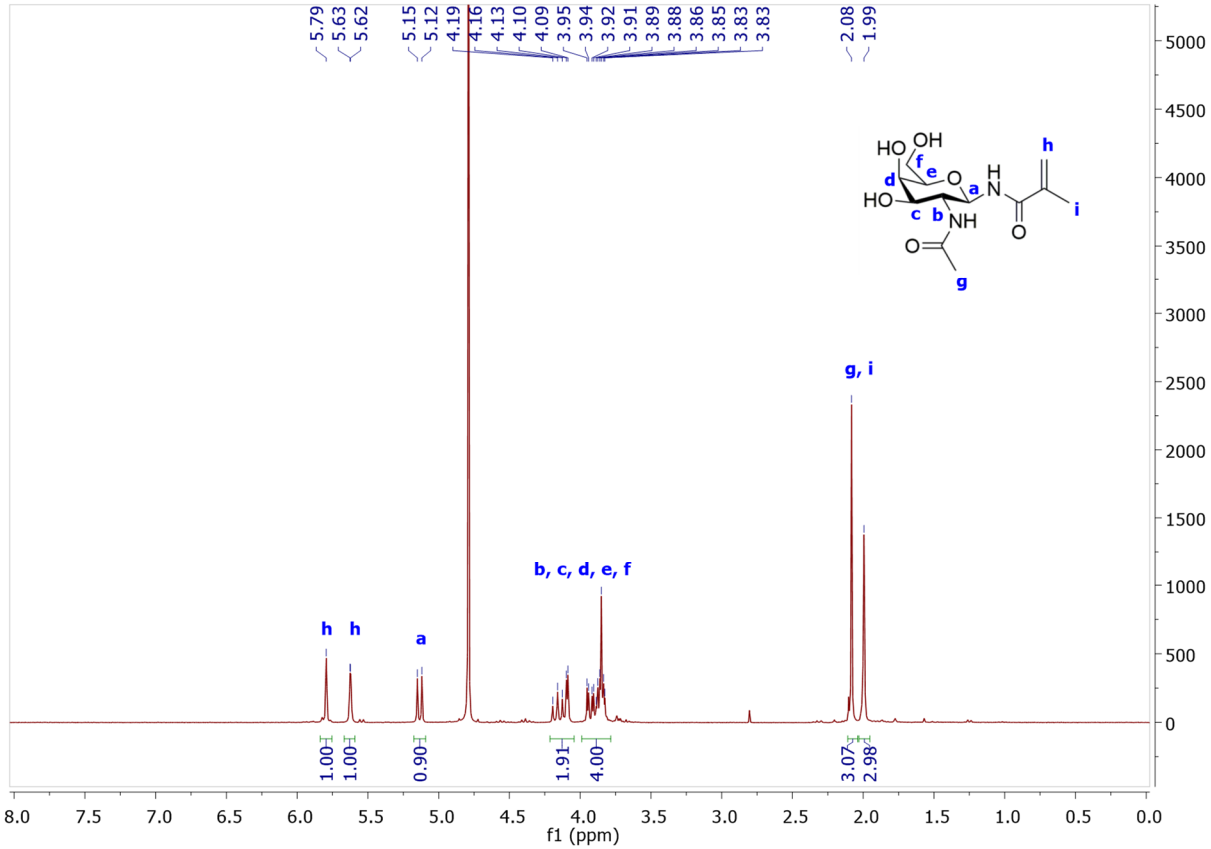

Figure S1. ^{1}H NMR spectrum of GalNAcMAm.

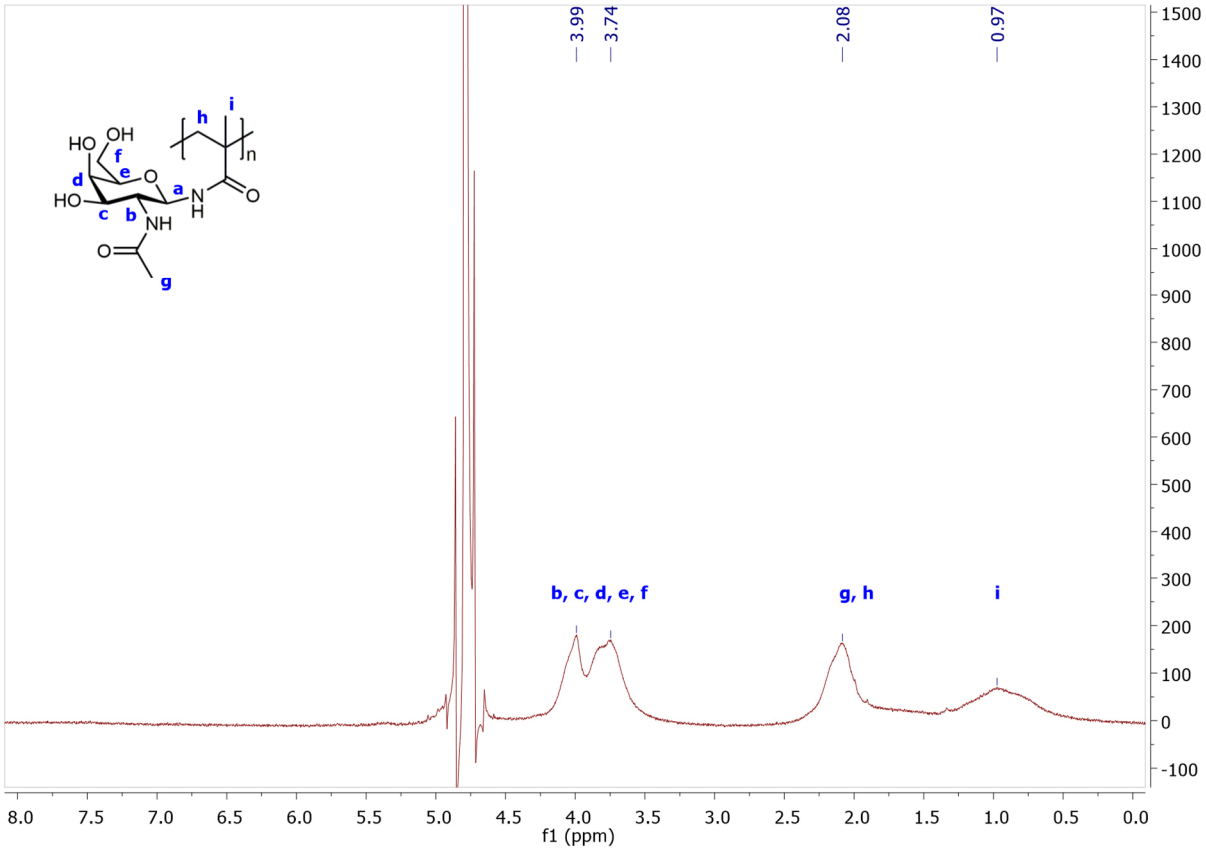

Figure S2. ^{1}H NMR spectrum of PGalNAcMAm.

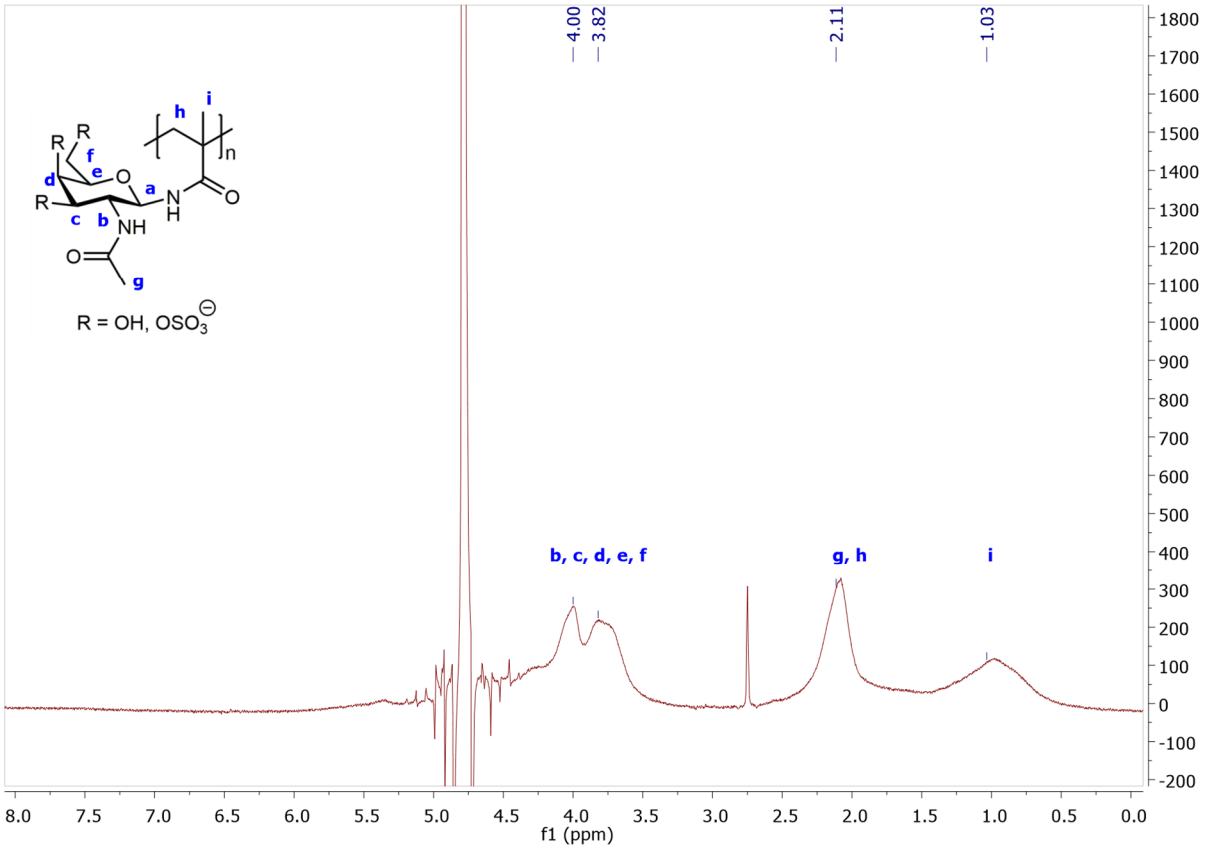

Figure S3. ^{1}H NMR spectrum of S-GalNAc.

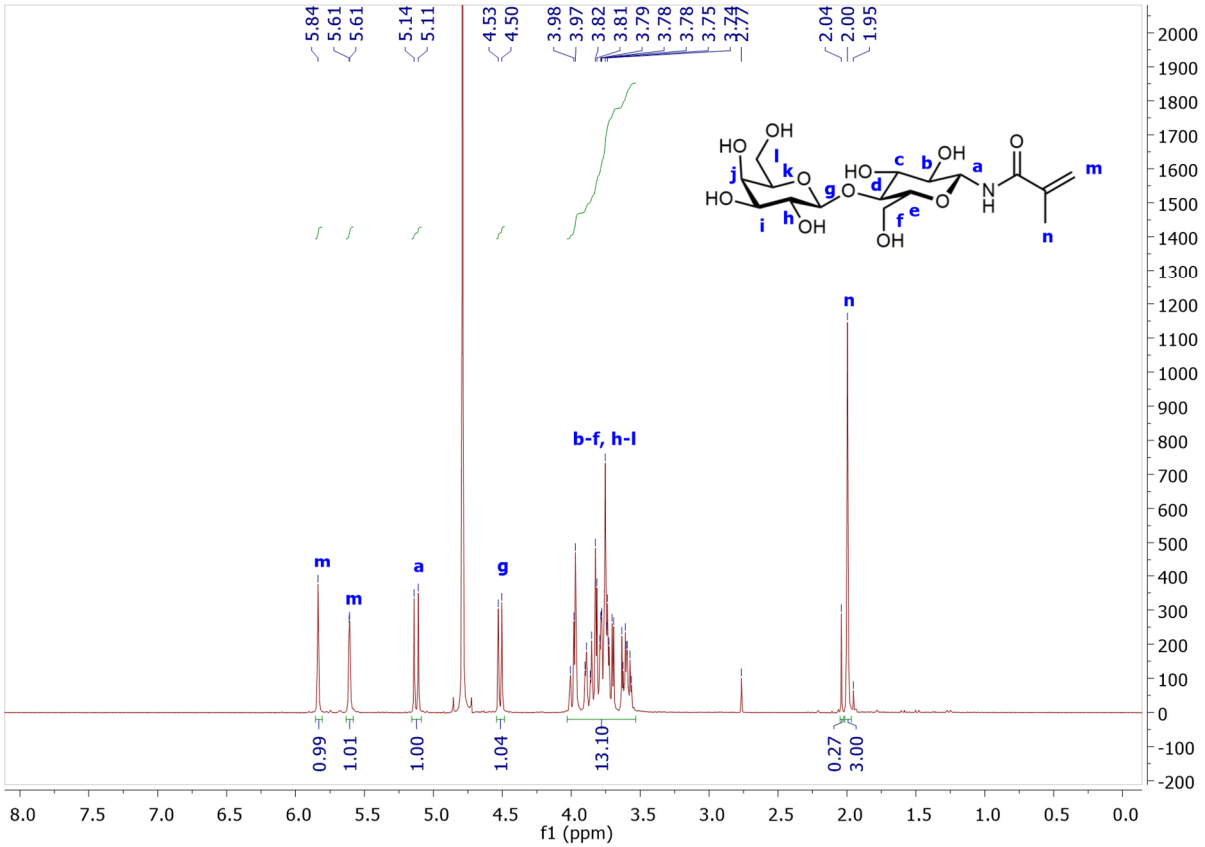

Figure S4. ^{1}H NMR spectrum of LacMAm.

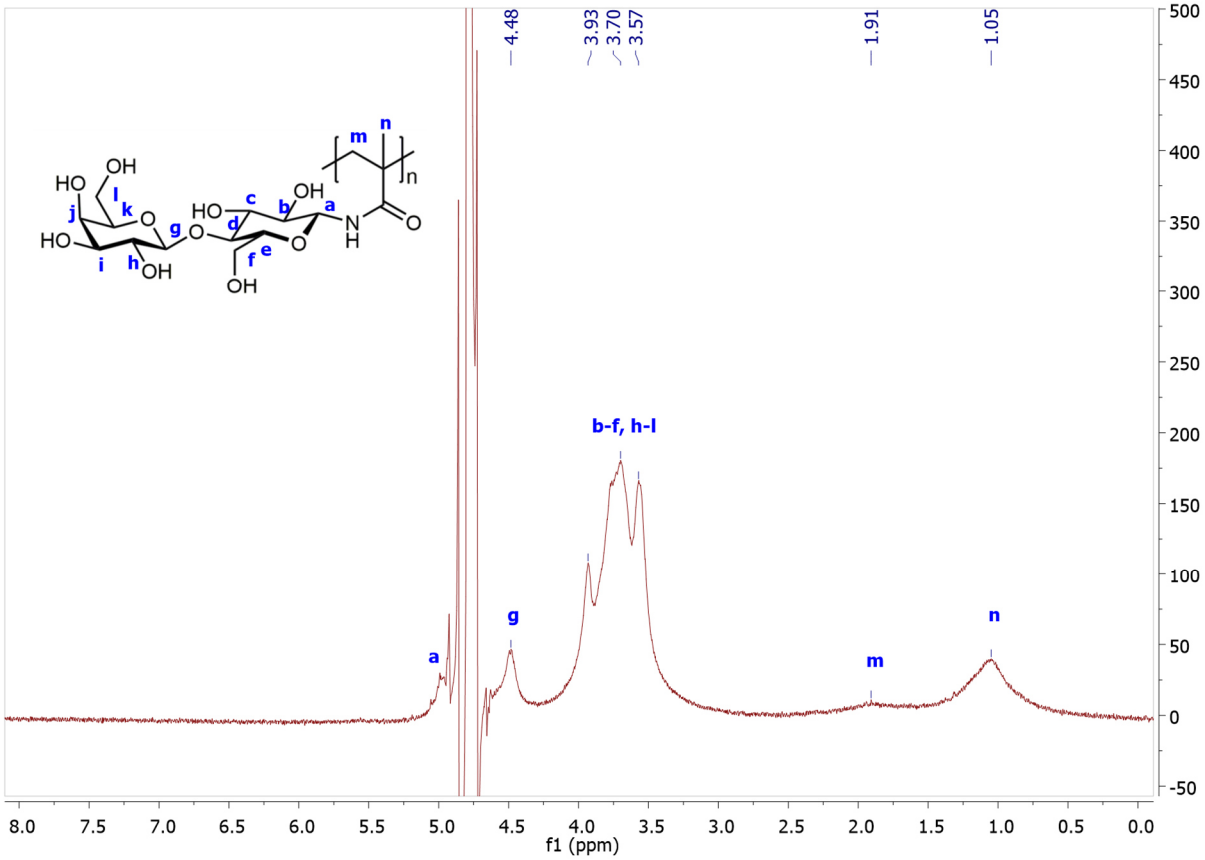

Figure S5. ^{1}H NMR spectrum of PLacMAm.

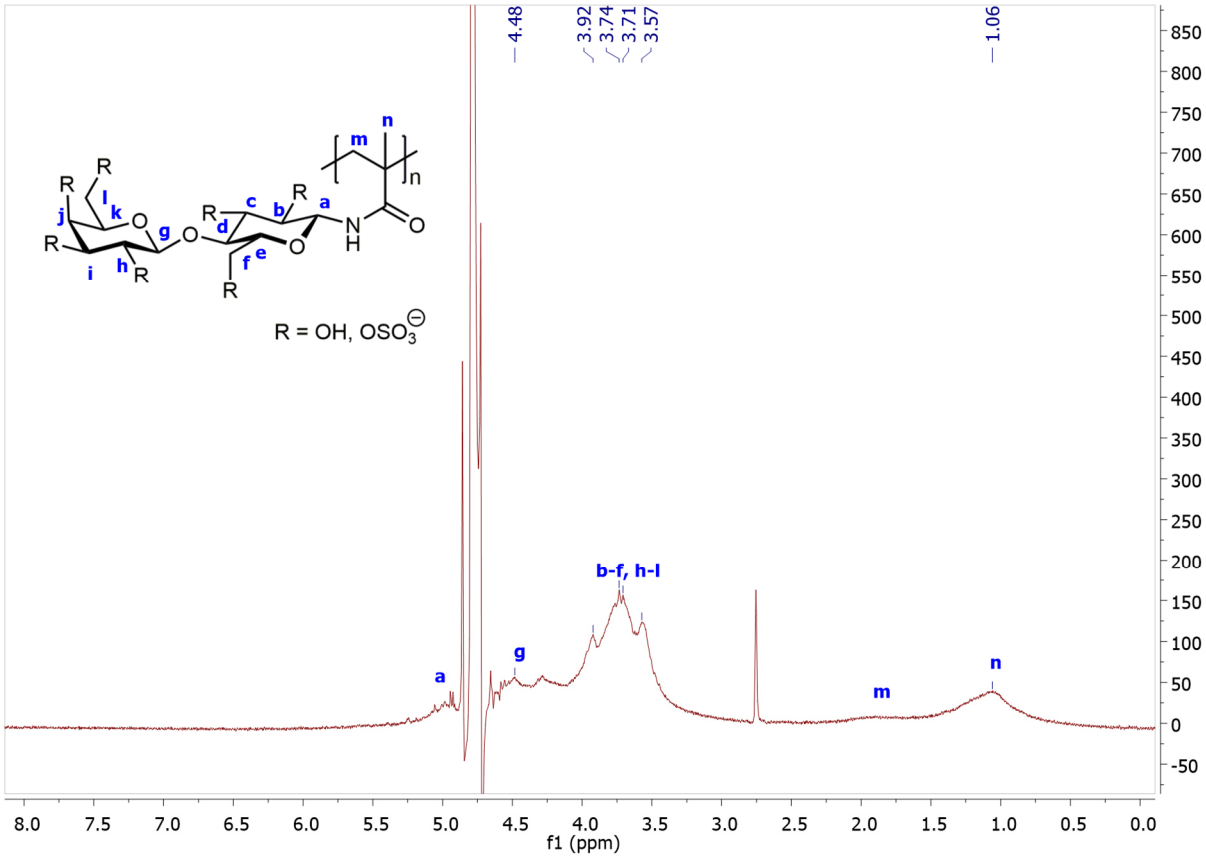

Figure S6. ^{1}H NMR spectrum of S-Lac.

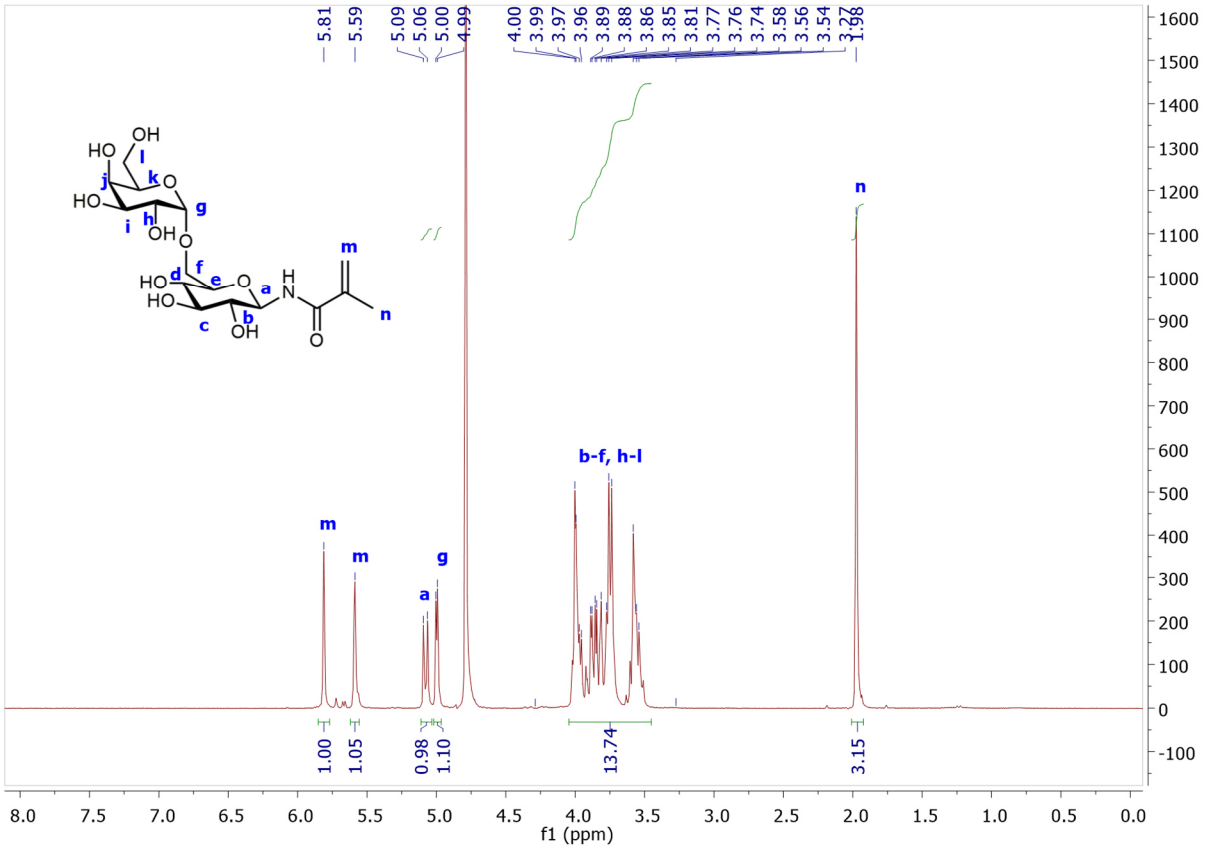

Figure S7. ^{1}H NMR spectrum of MelMAm.

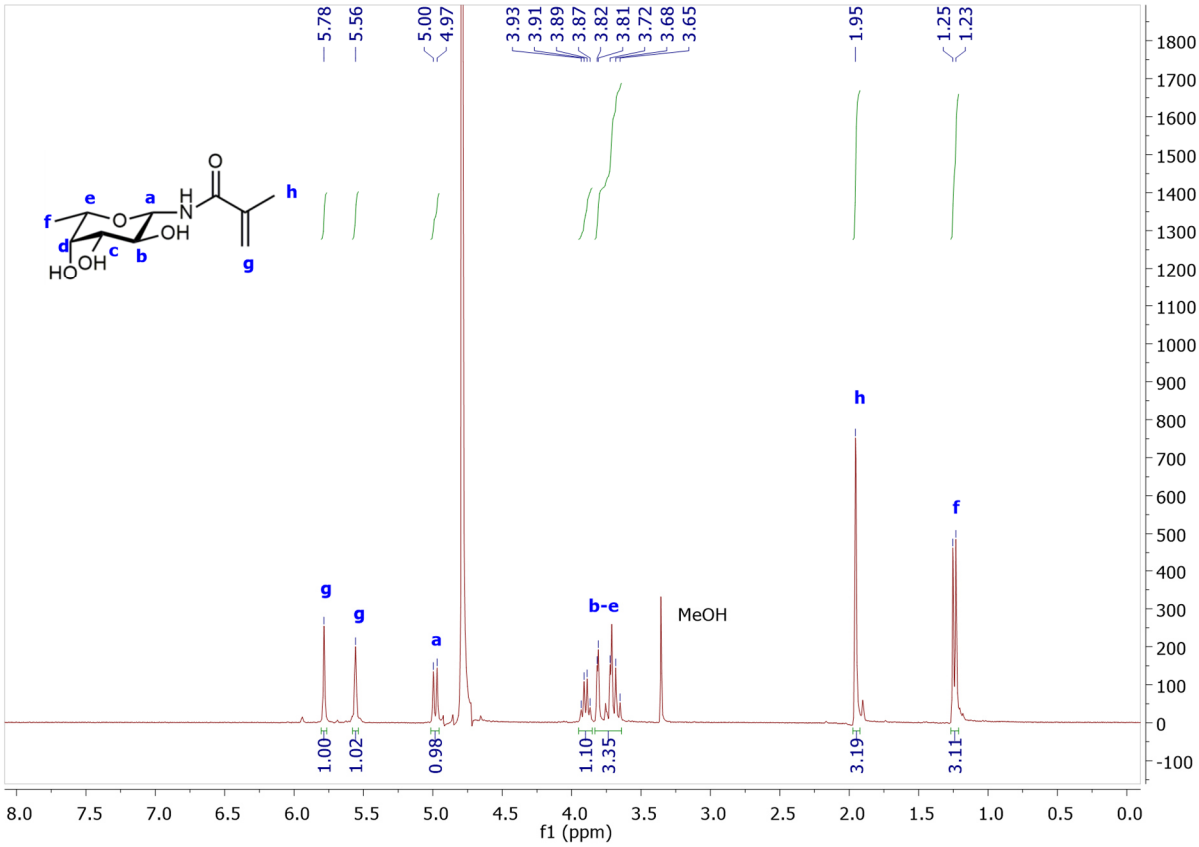

Figure S8. ^{1}H NMR spectrum of FucMAm.

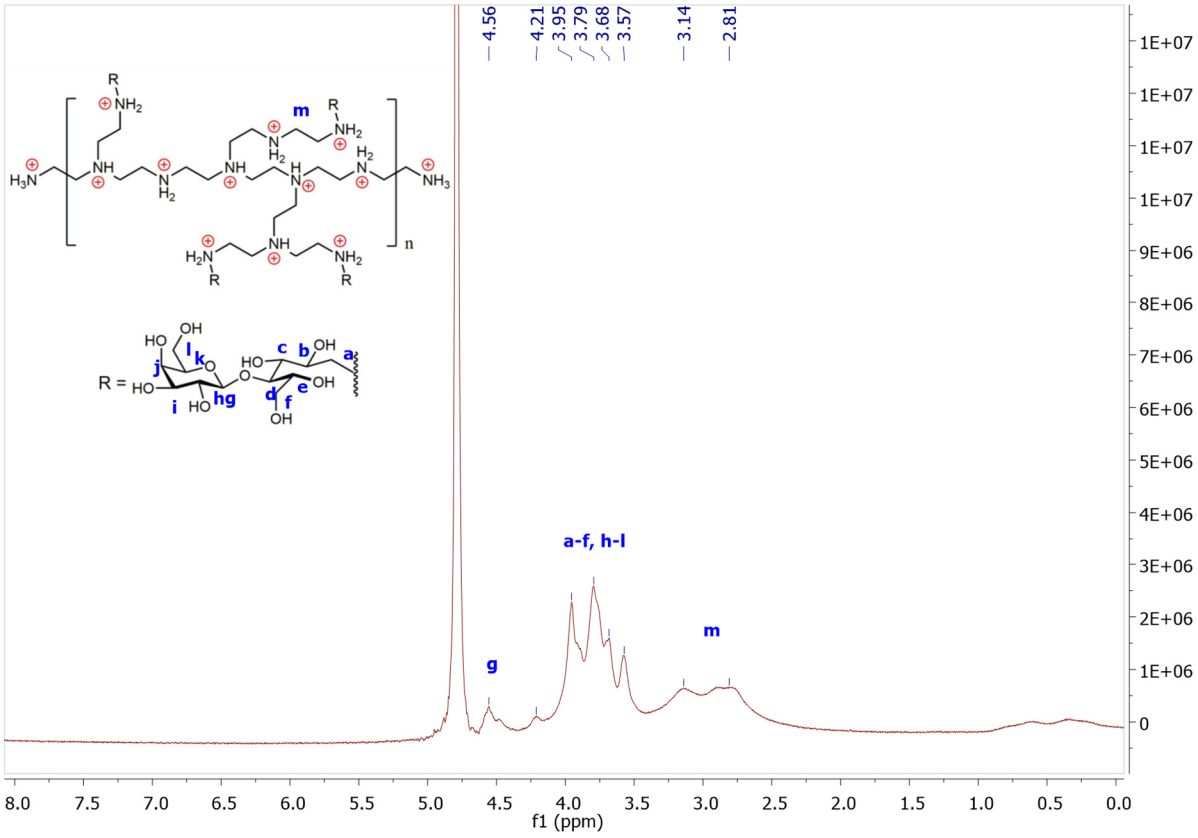

Figure S9. ^{1}H NMR spectrum of Lac-PEI.

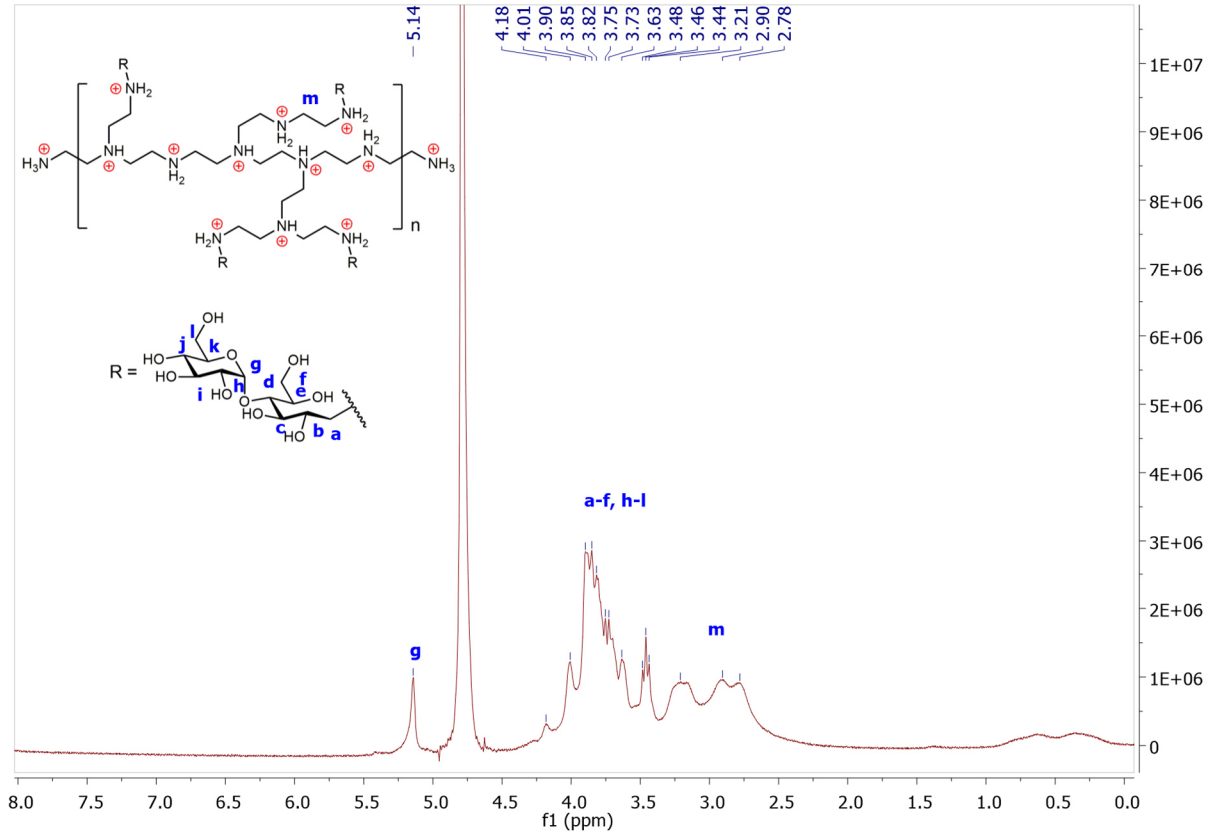

Figure S10. ^{1}H NMR spectrum of Mal-PEI.

8.4.2 Gel Permeation Chromatography Results

Table S1. Correction of **Table 3.S1.** GPC characterization of glycopolymers.

Sample	M_w [g/mol]	M_n [g/mol]	PDI
PGalNAcMAm	89,000	4,600	19
S-GalNAc	195,000	11,000	18
PLacMAm	276,000	6,900	40
S-Lac	199,000	9,500	21
Lac-PEI	4,830,000	20,000	242
Mal-PEI	2,400	1.100	2.2

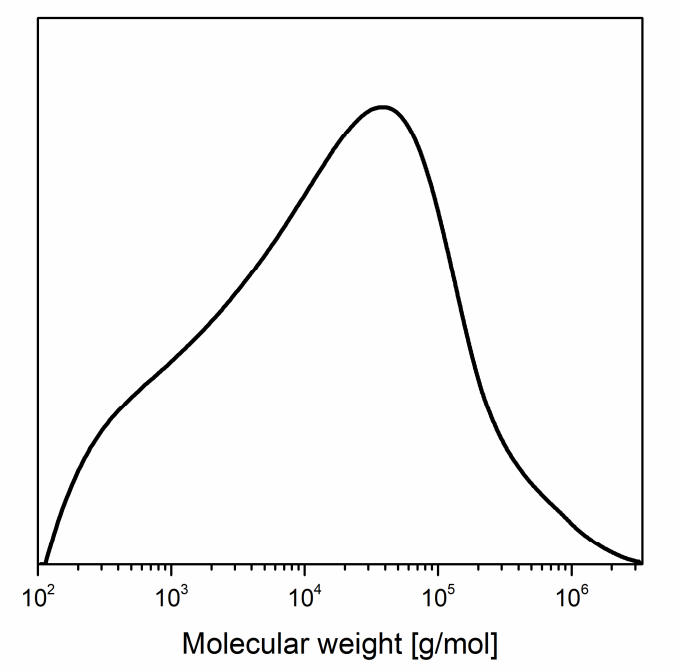

Figure S11. GPC chromatogram of PGalNAcMAm.

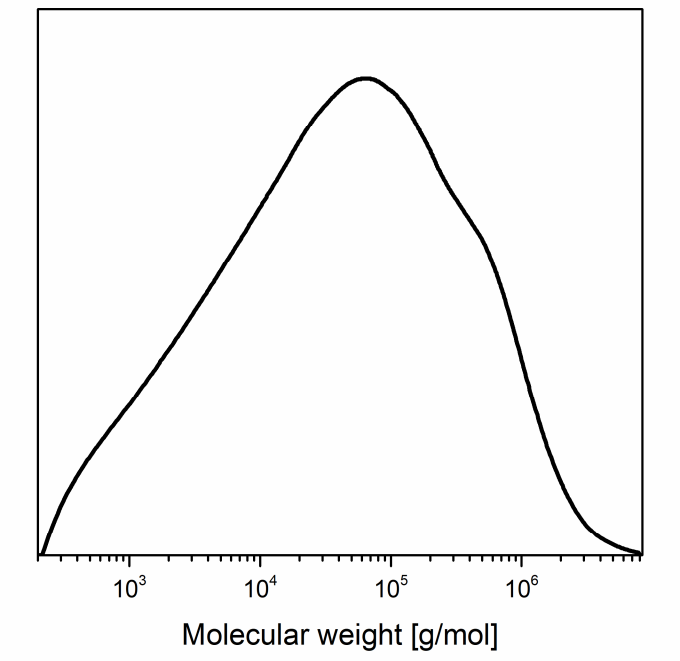

Figure S12. GPC chromatogram of S-GalNAc.

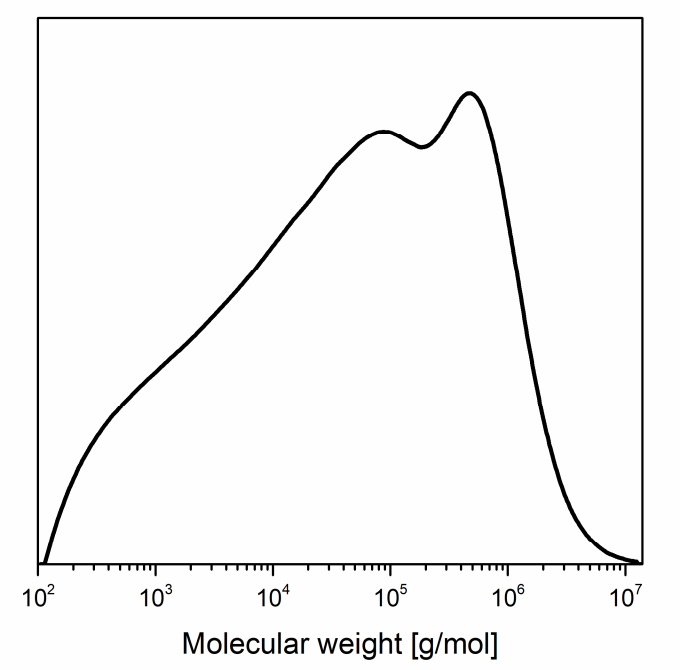

Figure S13. GPC chromatogram of PLacMAm.

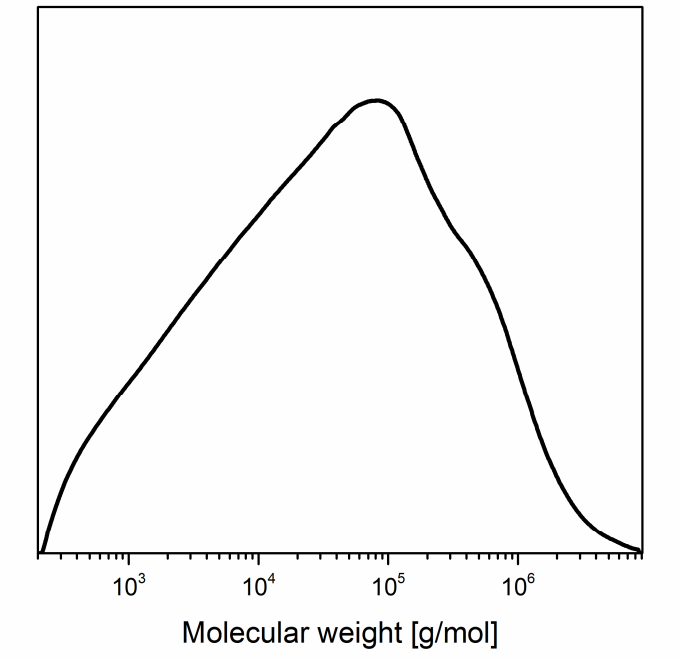

Figure S14. GPC chromatogram of S-Lac.

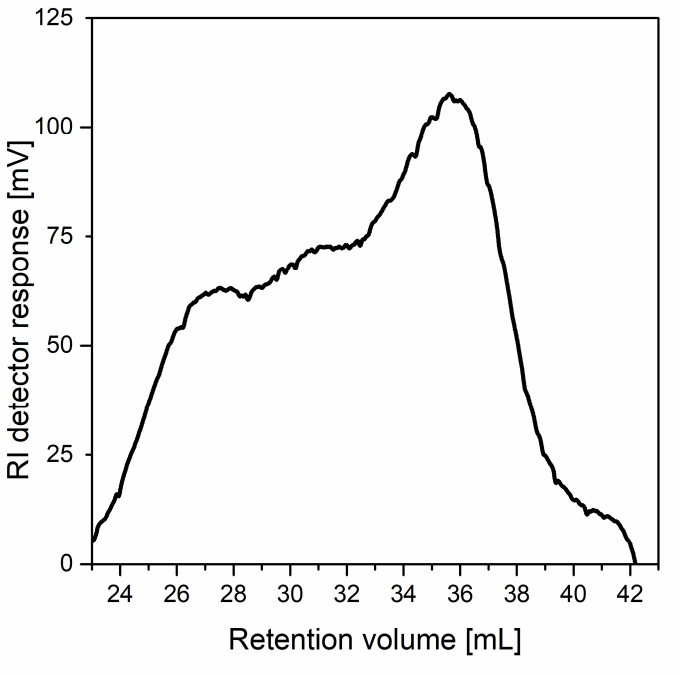

Figure S15. GPC chromatogram of Lac-PEI.

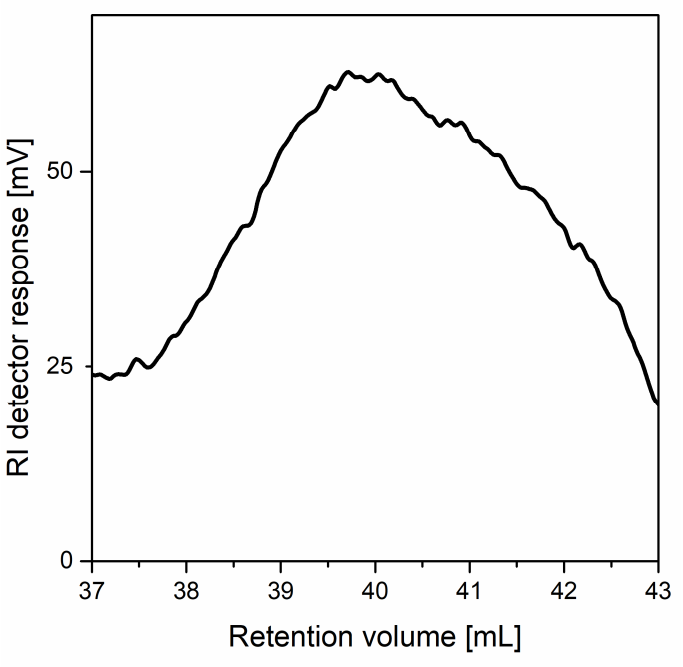

Figure S16. GPC chromatogram of Mal-PEI.

8.4.3 Analysis of Whispering Gallery Mode Measurements

The adsorbed masses in whispering gallery mode (WGM) experiments (in Chapter 3) were calculated using equation (3)

$$\sigma = \frac{\rho}{3}\frac{(r+\Delta r)^3 - r^3}{r^2} \tag{3}$$

where σ represents the surface mass density, ρ the mass density of adsorbate, r is the particle radius and Δr is the change of the particle radius. For the mass density of our glycopolymers a standard density value of 1.35 g/cm^3 was applied as the real density of the glycopolymers on the surface was not known. The thickness of adsorbate layers was calculated using equation (4)

$$\Delta\lambda = \frac{2\pi\,\Delta r n_s}{l} = \lambda\frac{\Delta r}{r} \tag{4}$$

where λ is the wavelength of the whispering gallery mode with the mode number l and n_s represents the refractive index of the particle.

8.4.4 Analysis of Quartz Crystal Microbalance Measurements with Dissipation Monitoring

In Chapter 3, the integrity of liposomes embedded in LbL glycopolymer films was analyzed by quartz crystal microbalance with dissipation monitoring (QCM-D). The shift of frequency correlates to the adsorption and desorption of substance mass. Simultaneous monitoring of the dissipation shift provides additional information about the mechanical properties of the adsorbed layer. During the liposome deposition (depicted in red in Figure 3.5), a frequency decrease and dissipation increase was observed, which displays the liposome adsorption on the sensor surface. With QCM-D measurements the mass of water in the liposomes is detected as well as the mass of the lipids. Here, the shift of frequency and dissipation is significantly larger than the shifts observed for the glycopolymers due to the high mass of water in the liposomes and indicate the intactness of the lipid vesicles. As the shift of frequency and dissipation reach an equilibrium after liposome deposition, the results confirm the adsorption and intact integrity of the liposomes on our LbL glycopolymer film. An increase of frequency and decrease of dissipation after initial liposome adsorption would indicate mass loss due to water release from the liposomes and, hence, their disintegration into lipid bilayers, whereas small shifts of frequency and dissipation upon liposome deposition would indicate the formation of lipid monolayers.

List of Publications and Presentations

Publications derived from this Doctoral Thesis

J. J. Tang, S. Rosencrantz, L. Tepper, S. Chea, S. Klöpzig, A. Krüger-Genge, J. Storsberg, and R. R. Rosencrantz, *Functional Glyco-Nanogels for Multivalent Interaction with Lectins*, *Molecules* **2019**, *24*, 1865.

S. Rosencrantz, **J. J. Tang**, C. Schulte-Osseili, A. Böker, and R. R. Rosencrantz, *Glycopolymers by RAFT Polymerization as Functional Surfaces for Galectin-3*, *Macromol. Chem. Phys.* **2019**, *220*, 1900293.

J. J. Tang, K. Schade, L. Tepper, S. Chea, G. Ziegler, and R. R. Rosencrantz, *Optimization of the Microwave Assisted Glycosylamines Synthesis Based on a Statistical Design of Experiments Approach*, *Molecules* **2020**, *25*, 5121.

J. J. Tang, A. Debrassi Smaczniak, L.ucas Tepper, S. Rosencrantz, M. Aleksanyan, L. Dähne, and R. R. Rosencrantz, *Glycopolymer Based LbL Multilayer Thin Films with Embedded Liposomes*, *Macromol. Biosci.* **2022**, 2100461.

Publications derived from Master Thesis

M. Rey, X. Hou, **J. J. Tang**, and N. Vogel, *Interfacial arrangement and phase transitions of PNiPAm microgels with different crosslinking densities*, *Soft Matter* **2017**, *13*, 8717-8727.

J. J. Tang, R. S. Bader, E. S. A. Goerlitzer, J. F. Wendisch, G. R. Bourret, M. Rey, and N. Vogel, *Surface Patterning with SiO_2@PNiPAm Core−Shell Particles*, *ACS Omega* **2018**, *3*, 12089−12098.

M. Rey, F. J. Wendisch, E. S. A. Goerlitzer, **J. J. Tang**, R. S. Bader, G. R. Bourret, and N. Vogel, *Anisotropic silicon nanowire arrays fabricated by colloidal lithography*, *Nanoscale Adv.* **2021**, **3**, 3634-3642

Presentations

“Functional Glyco-Nanogels for Multivalent Interaction with Lectins”, 4th "NanoBio Surfaces and Interfaces in Healthcare and Science Workshop" 2019, Potsdam, conference presentation.

“Functional Glyco-Nanogels for Multivalent Interaction with Lectins”, Polydays 2019, Berlin, conference presentation.

“A novel liposomal System for Drug Administration by Contact Lenses”, ProMatLeben – Polymere 2021, virtual, poster presentation.

Eigenständigkeitserklärung

Hiermit erkläre ich, Jo Sing J. Tang, dass ich die vorliegende Arbeit selbstständig und nur unter Zuhilfenahme der angegebenen Quellen und Hilfsmittel angefertigt habe. Des Weiteren versichere ich, dass diese Arbeit noch an keiner anderen Hochschule eingereicht wurde.

Potsdam, den

Danksagung

Zunächst möchte ich Herrn Univ.-Prof. Dr. rer. nat. Alexander Böker dafür danken, dass er mir die Möglichkeit gegeben hat in seinem Forschungsbereich zu promovieren und für seine stets freundliche und unterstützende Art.

Ich möchte auch Herrn Univ.-Prof. Dr. rer. nat. Helmut Schlaad und Herrn Univ.-Prof. Dr. rer. nat. Rainer Haag für die Gutachten meiner Arbeit danken. Zudem danke ich den restlichen Mitgliedern des Promotionsausschusses.

Ein großer Dank geht an meinen Betreuer Dr. Ruben R. Rosencrantz für das interessante und herausfordernde Thema, sowie für seine Betreuung und seinen Einsatz.

Ich danke meinen Kooperationspartnern, Dr. Aline Debrassi Smaczniak und Dr. Lars Dähne von Surflay Nanotec GmbH und Dr. Peter Trosan und Univ.-Prof. Dr. med. Dr. rer. nat. Thomas A. Fuchsluger aus der Universitätsmedizin Rostock, für die angenehme und produktive Zusammenarbeit.

Des Weiteren danke ich Frau Angela Krtitschka für die NMR-Messungen der Universität Potsdam.

Ich bedanke mich bei derzeitigen und ehemaligen Kolleginnen und Kollegen aus der Zuckergruppe und im gesamten IAP für eine lustige Zeit, konstruktive sowie motivierende Gespräche und die gute Zusammenarbeit.

Ich danke meinen Eltern für ihre stetige Unterstützung. Außerdem bedanke ich mich bei allen anderen lieben Menschen in meiner Familie und meinem Leben, die mich auf diesem Weg begleitet, unterstützt und motiviert haben. Vor allem danke ich Schatz für alles.